

A thesis submitted to the University of Leicester  
for the degree of Doctor of Philosophy

**Genetic Interplay between Chloroplast Protein  
Import and Thylakoid Complex Assembly in  
*Arabidopsis thaliana***

by

Raphael Mauritius Trösch

September 2013

Department of Biology,  
University of Leicester

# Abstract

## Genetic Interplay between Chloroplast Protein Import and Thylakoid Complex Assembly in *Arabidopsis thaliana*

by

Raphael Mauritius Trösch

The aim of the present thesis is to further our knowledge of chloroplast protein import regulation by identifying potential novel regulatory components using the model species *Arabidopsis thaliana*. A forward genetic screen with the pale chloroplast protein import mutant *tic40* uncovered two second-site suppressors (*stic1* and *stic2*). The *stic1* mutations map to the known thylakoid biogenesis factor ALB4, which suggest a novel genetic interaction between chloroplast protein import and thylakoid biogenesis. The genetic interaction between *TIC40* and *ALB4* is shown to be specific, and the chloroplast protein import defect of *tic40* mutants can be suppressed by *stic1/alb4* mutants. Furthermore, the ALB4 and STIC2 proteins are shown to interact in a common pathway, the abrogation of which leads to deteriorated thylakoid ultrastructure, suggesting that both ALB4 and STIC2 are involved in thylakoid biogenesis. Apart from thylakoid ultrastructural defects, the abrogation of the STIC function leads to the massive induction of an as yet uncharacterized gene, *HINAS1*, potentially mediated by a hormone signal originating from the chloroplast. How such a signal could indirectly suppress the defects of *tic40* mutants is discussed.

It is further shown that the *alb3 alb4* double mutants are smaller and accumulate less pigments than the *alb3* single mutants, and that the chloroplast ultrastructure is further deteriorated in the double mutant compared to *alb3*. Similarly, the *cpfts1* mutant and the *cpsrp54 cpsrp43* double mutants show also a more severe phenotype in the *alb4* background. These findings are backed up by the detection of weak but specific interactions of ALB4 with ALB3 and both cpSRP components, suggesting that the functions of ALB4 and its paralogue ALB3 overlap partially, and that thus both components likely contribute differentially but synergistically to the same process of protein insertion into the thylakoids via the chloroplast signal recognition particle pathway.

## Dedicated to Carina Kempf

### **Acknowledgements**

I owe many thanks to my supervisor Professor Paul Jarvis for the time he spent to assist and help with numerous aspects of this work. I'd like to thank my colleagues Dr Qihua Ling, Dr Ursula Flores-Perez, Dr Jocelyn Bedard and Alistair Haslam for discussions that often helped to solve problems. I thank Ramesh Patel for constantly caring about the every-day issues of lab work. I thank Dr Feijie Wu, Karolina Ploessl and Natalie Allcock who have helped and participated (where stated) in experiments described in this thesis. Lastly, I thank the Gatsby Charitable Foundation for their generous funding of this PhD project and for the assistance of the Gatsby mentors with scientific transferable skills throughout the time of research.

# Table of Contents

<b>Abstract</b>	<b>II</b>
<b>Acknowledgements</b>	<b>III</b>
<b>List of abbreviations used in this thesis</b>	<b>VIII</b>
<b>Chapter 1: General Introduction</b>	
<b>Chloroplast Protein Import and the Routing of Proteins to the Chloroplast Compartments</b> .....	<b>1</b>
1.1 Abstract .....	2
1.2 Plastids: Form, functions, evolution .....	3
1.2.1 Algae acquired chloroplasts through endosymbiosis .....	3
1.2.2 Plastids are not always green .....	4
1.2.3 Plastids fulfill a large variety of essential functions .....	6
1.3 Protein import into chloroplasts .....	11
1.3.1 Targeting of proteins to the chloroplast requires a transit peptide .....	11
1.3.2 Most chloroplast proteins are targeted via the general import pathway .....	13
1.3.3 Toc159 and Toc34 are the primary receptors for transit peptide binding .....	17
1.3.4 Toc75 forms the preprotein channel in the outer envelope membrane .....	19
1.3.5 The existence of an intermembrane space complex is uncertain .....	20
1.3.6 Tic110 and Tic20/21 are candidates for the inner envelope protein channel ...	22
1.3.7 Tic110, Tic40 and Hsp93 form a motor complex at the stromal side of TIC ...	25
1.3.8 Transit peptides are removed and degraded after import .....	29
1.4 Targeting of proteins to the thylakoids .....	32
1.4.1 Targeting to the thylakoid lumen occurs via the cpSec or cpTat pathway .....	32
1.4.2 Targeting to the thylakoid membranes occurs mostly via the cpSRP pathway	34
1.4.3 ALB3 and ALB4 have distinct roles in <i>Arabidopsis</i> thylakoid biogenesis .....	36
1.5 Aims.....	39
1.6 Figures.....	40
<b>Chapter 2: Results I</b>	
<b>Characterisation of <i>stic1</i> and <i>stic2</i>, Two Suppressors of the Protein Import Mutant <i>tic40</i></b> .....	<b>42</b>
2.1 Abstract .....	43
2.2 Introduction .....	44
2.3 Results .....	49

2.3.1	Identification of the <i>ALB4</i> locus .....	49
2.3.2	Confirmation of the <i>ALB4</i> locus with a T-DNA insertion line .....	50
2.3.3	Suppression of <i>tic40-4</i> by <i>stic1</i> is specific and functional .....	51
2.3.4	<i>ALB4</i> is exclusively localised in the thylakoid membrane .....	53
2.3.5	<i>ALB4</i> and <i>STIC2</i> interact directly and suppress <i>tic40</i> by a common pathway	54
2.3.6	The <i>stic1</i> and <i>stic2</i> mutants have similar defects in chloroplast ultrastructure	55
2.3.7	<i>ALB4</i> might associate with stromal chaperones .....	56
2.3.8	Chloroplast cpHsc70 is not the reason for suppression in <i>stic1 tic40</i> mutants	57
2.3.9	<i>ALB4</i> and <i>STIC2</i> are not generally involved in stress responses .....	59
2.3.10	Loss of both <i>ALB4</i> and <i>STIC2</i> leads to highly induced expression of <i>HINAS1</i> .....	60
2.4	Discussion .....	63
2.5	Materials and Methods .....	69
2.5.1	Identification of the <i>stic1</i> locus .....	69
2.5.2	Genotyping of <i>alb4</i> and <i>stic1</i> .....	70
2.5.3	<i>ALB4</i> antibody production .....	70
2.5.4	Specificity of suppression .....	71
2.5.5	Production of various constructs .....	71
2.5.6	TEM images .....	72
2.5.7	Microarray experiment .....	73
2.6	Figures and Tables.....	74
<b>Chapter 3: Results II</b>		
<b>Genetic and Physical Interaction between <i>Arabidopsis</i> <i>ALB3</i> and <i>ALB4</i> .....</b>		<b>88</b>
3.1	Abstract .....	89
3.2	Introduction .....	90
3.3	Results .....	94
3.3.1	The <i>alb3 alb4</i> double mutants are visibly paler than the <i>alb3</i> single mutants	94
3.3.2	Chlorophyll and carotenoid levels are further reduced in the double mutants	95
3.3.3	The chloroplasts of <i>alb3 alb4</i> double mutants have less thylakoid membranes than <i>alb3</i> .....	96
3.3.4	<i>ALB3</i> and <i>ALB4</i> can interact weakly, but specifically .....	97
3.3.5	<i>ALB4</i> can interact with cpHsc70 and the chloroplast SRP .....	98
3.3.6	Genetic interactions suggest functional overlap between <i>ALB4</i> and cpSRP ...	99
3.4	Discussion .....	101
3.5	Materials and Methods .....	105
3.5.1	Plant growth and genotyping .....	105

3.5.2	Total chlorophyll and carotenoid measurements and transmission electron microscopy .....	106
3.5.3	Antibody production and immunoblotting .....	107
3.5.4	Creation of ALB4-FLAG lines .....	107
3.5.5	Chloroplast isolation and crosslinking .....	108
3.5.6	FLAG- and co-immunoprecipitation .....	108
3.6	Figures and Tables .....	110
<b>Chapter 4: Results III</b>		
<b>The Stromal Processing Peptidase of Chloroplasts Is Essential in <i>Arabidopsis</i>, with Knockout Mutations Causing Embryo Arrest after the 16-Cell Stage .....</b>		<b>118</b>
4.1	Abstract .....	119
4.2	Introduction .....	120
4.3	Results .....	123
4.3.1	No homozygous <i>spp</i> mutants could be obtained .....	123
4.3.2	The <i>spp</i> mutation is embryo lethal but not gametophytic lethal .....	124
4.3.3	The <i>spp</i> mutation leads to embryo arrest at the 16-cell stage .....	124
4.3.4	Gene expression of <i>SPP</i> is more similar to <i>atTIC110</i> than to <i>atTOC75-III</i> ...	125
4.3.5	Analyses of mRNA and protein expression in the <i>toc75-III</i> , <i>tic110</i> and <i>spp</i> heterozygotes .....	126
4.4	Discussion .....	127
4.5	Materials and Methods .....	130
4.5.1	Plant growth and chlorophyll analysis .....	130
4.5.2	Identification of the <i>spp</i> mutants .....	130
4.5.3	Seed and embryo analyses .....	131
4.5.4	Quantitative RT-PCR analysis of mRNA levels .....	131
4.5.5	Immunoblot analysis of protein levels .....	132
4.6	Figures and Tables .....	134
<b>Chapter 5: General Discussion .....</b>		<b>142</b>
<b>Chapter 6: General Materials and Methods.....</b>		<b>150</b>
6.1	Growth of <i>Arabidopsis</i> plants and basic handling techniques .....	151
6.1.1	Preparation of Murashige and Skoog medium plates .....	151
6.1.2	Growth of <i>Arabidopsis thaliana</i> plants on plates .....	151
6.1.3	Growth of <i>Arabidopsis</i> plants on soil .....	152
6.1.4	Crossing of <i>Arabidopsis</i> plants .....	153
6.1.5	Transformation of <i>Arabidopsis</i> plants using <i>Agrobacterium tumefaciens</i> .....	153

6.1.5.1	Freeze-thaw transformation of <i>Agrobacterium</i> .....	154
6.1.5.2	Floral-dip transformation of <i>Arabidopsis</i> .....	154
6.1.6	Chlorophyll measurements .....	155
6.1.6.1	Chlorophyll measurements of plants grown on plates .....	155
6.1.6.2	Chlorophyll measurements of plants grown on soil .....	156
6.2	Bacterial work, cloning and DNA-related techniques .....	157
6.2.1	Preparation of LB medium .....	157
6.2.2	PCR, agarose gel and gel band purification .....	157
6.2.3	<i>E.coli</i> heat shock transformation and plasmid preparations .....	158
6.2.4	Restriction digestion and CAPS/dCAPS markers .....	159
6.2.5	Cloning of a DNA sequence using the Gateway® technology .....	160
6.2.5.1	BP reaction .....	160
6.2.5.2	LR reaction .....	161
6.2.6	Cloning for bimolecular fluorescence complementation .....	162
6.2.7	Cloning for antigen expression and antibody production .....	163
6.2.8	DNA precipitation .....	164
6.2.9	DNA extraction from plant leaves and genotyping .....	165
6.3	RNA-related techniques .....	167
6.3.1	RNA extraction and semi-quantitative RT-PCR .....	167
6.3.2	qPCR .....	168
6.4	Biochemical and protein-related techniques .....	169
6.4.1	Total protein extraction from <i>Arabidopsis</i> plants .....	169
6.4.2	Protein quantification using BioRad microassay .....	169
6.4.3	Protein precipitation .....	170
6.4.4	SDS-PAGE and Coomassie staining .....	170
6.4.5	Silver staining of SDS gels .....	172
6.4.6	Immunoblotting and amido black staining .....	172
6.4.7	Chloroplast isolation .....	174
6.4.8	Chloroplast protein import assays .....	175
6.4.9	Chloroplast subfractionation .....	177
6.4.10	Co-immunoprecipitation and anti-FLAG-immunoprecipitation .....	178
6.4.11	Protoplast isolation, transfection and microscopy .....	179
<b>7</b>	<b>Bibliography .....</b>	<b>182</b>

## List of abbreviations used in this thesis

### Units:

% (w/v)	Percentage concentration (weight per volume)
°C	Degree Celsius
bp	Base pair (nucleic acids)
Da	Dalton (proteins)
E	Einstein
g	Gram
<i>g</i>	Standard gravity
h	Hour
l	Litre
m	Metre
M	Molarity
min	Minute
mol	Mole
OD <sub>λ</sub>	Optical density at wavelength λ (in nm)
rpm	Revolution per minute
s	Second
V	Volt

### Unit prefixes:

k	Kilo (10 <sup>3</sup> )
m	Milli (10 <sup>-3</sup> )
μ	Micro (10 <sup>-6</sup> )
n	Nano (10 <sup>-9</sup> )

### Nucleic acids / nucleotides:

(T-)/(c)DNA	(Transfer-)/(complementary) deoxyribonucleic acid
APS	Adenosine phosphosulfate
dNTP (N = A, T, G, C)	Deoxyribonucleoside triphosphate
mRNA/RNAi	messenger ribonucleic acid / ribonucleic acid interference
N (A, T, G, C, U)	Nucleotides (adenine, thymine, guanine, cytosine, uracil)
NADP <sup>+</sup>	Nicotinamide adenine dinucleotide phosphate
NTP (N = A, U, G, C)	Nucleoside triphosphate
UTR	Untranslated region

## Proteins / Complexes:

(cp)Sec	(Chloroplast) secretory pathway
(cp)SRP	(Chloroplast) signal recognition particle
(cp)Tat	(Chloroplast) twin-arginine transporter pathway
(p)SSU	(Precursor of) RuBisCO small subunit
ACCase	Acetyl-coenzyme A carboxylase
ACP	Acyl carrier protein
ALB	Albino
AP	Alkaline phosphatase
BSA	Bovine serum albumin
BT5	BTB and TAZ domain protein 5
CAH1	Carbonic anhydrase 1
ceQORH	Chloroplast quinone oxidoreductase homologue
Clp	Caseinolytic protease of X kDa
cpHsc70	Chloroplast heat shock cognate 70 kDa
CpnX	Chaperonin of X kDa
DIC2	Dicarboxylate carrier 2
eIF4e	Eukaryotic initiation factor 4e
ERF4	Ethylene response factor 4
FAD	Fatty acid desaturase
FAS	Fatty acid synthase
FNR	Ferredoxin-NADP <sup>(+)</sup> reductase
Fts	Filamentous temperature-sensitive
GAP	GTP activating protein
GAPDH	Glyceraldehyde 3-phosphate dehydrogenase
GOGAT	Glutamine-oxoglutarate aminotransferase
GS	Glutamine synthetase
HcfX	High chlorophyll fluorescence, X kDa
HINAS	Highly induced in <i>Arabidopsis stic</i>
Hip	Hsp70-interacting protein
Hop	Hsp70/Hsp90-organizing proteins
HRP	Horseradish peroxidase
HspX	Heat shock protein of X kDa
IgG	Immunoglobulin G
JAZ1	Jasmonate ZIM-domain family protein 1
LHCP	Light harvesting chlorophyll <i>a/b</i> -binding protein
MFP1	MAR binding filament-like protein 1
MPP	Mitochondrial processing peptidase
NPP1	Nucleotide pyrophosphatase/phosphodiesterase 1
OEP/IEP	Outer/inner chloroplast envelope protein
OmpX	Outer membrane protein of X kDa
PIC1	Permease in chloroplasts 1
PMA2	Plasma membrane H(+)-ATPase 2

PNPase	Polynucleotide phosphorylase
PreP	Presequence protease
PRPL	Plastid ribosomal protein large subunit
PS	Photosystem (I and II)
Psa/b	Photosystem I/II subunits
RC-1/2	Reaction centres 1/2
RuBisCO	Ribulose-1,5-bisphosphate carboxylase/oxygenase
SP1	Suppressor of <i>ppi1</i> locus 1
SPP	Stromal processing peptidase
STIC	Suppressor of <i>tic40</i>
TIC	Translocon at the inner chloroplast envelope membrane
TicX	TIC component of X kDa
TOC	Translocon at the outer chloroplast envelope membrane
TocX	TOC component of X kDa
TPP	Thylakoid processing peptidase
TPR	Tetratricopeptide repeat (motif/protein family)
VIPP1	Vesicle inducing protein in plastids 1
YFP	Yellow fluorescent protein

#### Chemicals:

AP	Ammonium persulfate
BCIP	5-Bromo-4-chloro-3-indolyl phosphate
CAM	Chloramphenicol
DDM	n-Dodecyl- $\beta$ -D-maltopyranoside
DMF	Dimethylformamide
DMSO	Dimethyl sulfoxide
DSP	Dithiobis(succinimidyl propionate)
DTT	Dithiothreitol
EDTA	Ethylenediaminetetraacetic acid
EGTA	Ethylene glycol tetraacetic acid
EMS	Ethyl methanesulfonate
HEPES	4-(2-Hydroxyethyl)-1-piperazineethanesulfonic acid
IMS	Industrial methylated spirit
IPTG	Isopropyl $\beta$ -D-1-thiogalactopyranoside
LCM	Lincomycin
MES	2-(N-morpholino)ethanesulfonic acid
NBT	Nitro-blue tetrazolium chloride
PEG	Polyethylene glycol
PQ	Paraquat
SDS	Sodium dodecyl sulfate
TCA	Trichloroacetic acid
TEMED	Tetramethylethylenediamine

Tris Tris(hydroxymethyl)aminomethane

**Buffers:**

CIB Chloroplast isolation buffer  
HMS HEPES-MES-sorbitol buffer  
LB Lysogeny broth  
MMg Mannitol-magnesium buffer  
MS Murashige and Skoog medium  
TBE Tris-boric acid-EDTA buffer  
TBS(-Tween) Tris-buffered saline (with Tween-20)  
TGS Tris-glycine-SDS buffer

**Methods:**

(BN)/SDS-PAGE (Blue-native)/SDS-Polyacrylamide gel electrophoresis  
(d)CAPS (Designed) cleaved amplified polymorphic sequence  
(RT-)/(q)PCR (Reverse transcriptase)/(quantitative) polymerase chain reaction  
ANOVA Analysis of variance  
BiFC Bimolecular fluorescence complementation  
ECL Enhanced chemiluminescence  
FDR False discovery rate  
IP Immunoprecipitation  
PCA Principal component analysis  
RMA Robust multi-chip analysis  
TEM Transmission electron microscopy

**Plant-related:**

At *Arabidopsis thaliana*  
Bna *Brassica napus*  
CaMV Cauliflower mosaic virus  
Col-0 Columbia-0 (*Arabidopsis* ecotype used in this study)  
F<sub>n</sub>, T<sub>n</sub> Filial / transformant generation n  
WT Wild type

**Institutions / Programs:**

NASC	Nottingham <i>Arabidopsis</i> Stock Centre
PNACL	Protein Nucleic Acid Chemistry Laboratory
TAIR	The <i>Arabidopsis</i> Information Resource

**Other:**

CD	Chromodomain
DAG	Diacylglycerol
DGDG	Digalactosyldiacylglycerol
DUF	Domain of unknown function
ER	Endoplasmatic reticulum
MGDG	Monogalactosyldiacylglycerol
NLS	Nuclear localization signal
PTS	Peroxisome targeting signal
SQDG	Sulfoquinovosyl diacylglycerol
TPR	Tetratricopeptide repeat domain

# Chapter 1

## General Introduction

Chloroplast Protein Import and the Routing of Proteins to  
the Chloroplast Compartments

## 1.1 Abstract

Chloroplasts are cell organelles unique to plants and algae that have essential functions in these organisms. Photosynthesis provides nature's energy resources, and the chloroplast's primary metabolism delivers products that form the basis of food chains in most ecosystems. Even though chloroplasts have a small chromosome, most chloroplast proteins are encoded in the nuclear genome and need to cross the double membrane barrier that separates the chloroplast stroma from the cytosol. Similar to other cell routing systems, chloroplast proteins are synthesised with an N-terminal transit peptide that serves as a signal for chloroplast protein import. Slight differences in this signal between photosynthetic and housekeeping proteins are detected by different receptor isoforms in *Arabidopsis* and allow differential regulation of protein import for photosynthetic and metabolic processes. After binding to receptors, proteins are routed through the translocons in the outer and inner envelope membranes of the chloroplast (TOC and TIC) and then follow downstream routing systems to reach the intermembrane space, the inner envelope membrane, the stroma, the thylakoid membrane or the thylakoid lumen. Under varying environmental conditions and during plant development the plastid proteomes and sub-proteomes can change considerably, and new ways of regulation that impinge on plastid protein transport systems are currently being identified.

## **1.2 Plastids: Form, functions, evolution**

### **1.2.1 Algae acquired chloroplasts through endosymbiosis**

The first organisms to invent photosynthesis were bacteria. Heliobacteria and chloroflexi use primitive photosystems with the reaction centres RC-1 and RC-2, respectively, for a non-oxygenic photosynthesis, while cyanobacteria evolved later and combined these two photosystems for a more efficient oxygenic photosynthesis (Gupta et al., 1999; Schopf, 1993). After the evolution of eukaryotes, some protists might have engulfed and retained an ancestral cyanobacterium with mutual benefits for the host (high energy products from photosynthesis) and the endosymbiont (protection) (Margulis, 1970). This so called endosymbiotic theory was supported by the discoveries of the circular chloroplast chromosome which contains some genes organised in operons with high sequence similarity to bacterial relatives, and some metabolic pathways like non-mevalonate isoprenoid biosynthesis or nitrate and sulfate assimilation which are shared between chloroplasts and bacteria (McFadden, 2001). The first unicellular algae had to control chloroplast processes such as division and metabolite production in order to coordinate them with their own development. Therefore, gene transfer from the endosymbiont to the host's genome was evolutionarily favored, and present chloroplast genomes retained only a small fraction of the initial cyanobacterial genome (Martin et al., 2002; Timmis et al., 2004).

Endosymbiosis of eukaryotes with cyanobacteria (called primary endosymbiosis) is believed to have happened only once over a billion years ago, leading to the supergroup of archaeplastids which comprises glaucophytes, red algae, green algae and plants (Adl et al., 2005; Prihoda et al., 2012). Recently, however, such a simple origin of chlo-

roplasts has been disputed and evidence has been presented for an additional, more recent primary endosymbiotic event in the rhizarian *Paulinella chromatophora* (Dorrell and Howe, 2012; Howe et al., 2008; Marin et al., 2005). Moreover, most algal species are not archaeplastids but chromalveolates (e.g. brown algae, diatoms and dinoflagellates), chlorarachniophytes and euglenids and have gained their chloroplasts by a secondary endosymbiosis of a eukaryotic host with an equally eukaryotic green or red algal symbiont (Dorrell and Howe, 2012; Keeling, 2010). Interestingly, the possibility of serial endosymbiosis within diatoms where an original algal symbiont has been replaced with another has shown that even transient symbioses can leave a fingerprint in the host's genome and probably favour future symbioses (Dorrell and Howe, 2012; Dorrell and Smith, 2011). This could lead to the question whether endosymbiosis was not an 'event' but rather a process where early transient symbioses led to gene transfers that subsequently facilitated new symbioses which eventually led to a stable endosymbiosis (Dorrell and Howe, 2012).

### **1.2.2 Plastids are not always green**

Chloroplasts from archaeplastids have a double membrane envelope where the inner membrane derived from the cyanobacterial symbiont's plasma membrane. The outer membrane was originally thought to be derived from the host's vacuolar membrane which has been retained after engulfing the symbiont, however, the lipid composition rather reflects a homology to the symbiont's outer membrane (Block et al., 1983; Whatley et al., 1979). Like the cyanobacterial outer membrane, the outer envelope contains galactolipids and sulfolipids and lacks phosphatidylethanolamine which is otherwise typical for extraplastidic host membranes (Block et al., 1983). A third, internal membrane system, the thylakoid membrane, is homologous to cyanobacterial thylakoids

and is the site of photosynthesis. The three membrane systems enclose three aqueous compartments, namely the intermembrane space between outer and inner envelope membrane, the stroma between inner envelope membrane and thylakoid membrane, and the thylakoid lumen inside the enclosed thylakoid membrane.

Glaucophytes, such as the model species *Cyanophora paradoxa*, have the most primitive chloroplasts, termed cyanelles, which greatly resemble cyanobacteria. In fact, they are so similar to cyanobacteria that they originally have been considered endosymbiotic cyanobacteria rather than cell organelles (Jaynes and Vernon, 1982). Only after sequencing of the cyanelle genome which is greatly reduced as in other chloroplasts, and after discovering that neither cyanelles nor *Cyanophora* can grow independently, the cyanelles were found to be primitive chloroplasts (Jaynes and Vernon, 1982). Like cyanobacteria, they still have a remnant of a peptidoglycan cell wall, unstacked thylakoids, phycobilisomes containing phycocyanin (giving them a blue colour), and chlorophyll *a* but no chlorophyll *b* (Jaynes and Vernon, 1982). Red algae chloroplasts, also termed rhodoplasts, have properties between cyanelles and chloroplasts from Chloroplastida: they have unstacked thylakoids like cyanelles but lack the peptidoglycan cell wall remnant; they still have phycobilisomes (mainly with phycoerythrin, giving them a red colour), but also have light harvesting complex proteins (LHCPs) associated with their photosystem I (Grabowski et al., 2001; Wolfe et al., 1994). Finally, chloroplasts from the Chloroplastida group, which encompasses green algae and plants, have stacked thylakoids, LHCPs replace the phycobilisomes in both photosystems, they use chlorophyll *b* in addition to chlorophyll *a*, and they synthesise starch within the chloroplast (Deschamps et al., 2008; Grabowski et al., 2001).

During evolution of multicellular algae and land plants, many specialised organs arose, containing cells with altered types of chloroplasts. Non-photosynthetic

proplastids are propagated in vegetative apical meristems and germlines, ready to differentiate into chloroplasts, leucoplasts or chromoplasts depending on the type of tissue which is formed. Starch-storing leucoplasts, termed amyloplasts, occur in rhizoids and roots of green algae and plants as well as storage organs of higher plants such as cotyledons, tubers and endosperm, while oil-storing elaioplasts mainly occur in epidermal cells of some monocots and in the tapetum (Hernandez-Pinzon et al., 1999; Matilsky and Jacobs, 1983; Neuhaus and Emes, 2000). Flowering plants evolved chromoplasts as pigment-storing plastid in flower, fruit and sometimes root tissues, and etioplasts in dark-grown seedlings that contain a membranous prolamellar body which can be converted rapidly into photosynthesizing thylakoids by accumulation of chlorophyll upon illumination (Neuhaus and Emes, 2000). Collectively, these organelles are referred to as plastids and serve a variety of specialised biochemical purposes in different, also non-photosynthesizing organs, while in higher plants photosynthetic chloroplasts are predominant in specialised organs, namely leaves.

### **1.2.3 Plastids fulfill a large variety of essential functions**

The chloroplast process of primary importance is oxygenic photosynthesis. Light energy is used to split water to oxygen, protons and electrons. Oxygen is released to the atmosphere and allows eukaryotic respiration, while the energy in protons and electrons is ultimately used to assimilate carbon dioxide to high-energy compounds such as starch and sugars, which again sustains the eukaryotic heterotrophic nutrition (Nelson and Ben-Shem, 2004). Four large thylakoid membrane complexes are involved in photosynthesis, namely photosystems I (PS-I) and II (PS-II), the cytochrome  $b_6f$  complex and the F-type ATPase complex. Light quanta are absorbed by the chlorophylls of the light harvesting complex of PS-II (LHC-II) and cumulate in the reaction centre P680. There, the

luminal oxygen evolving complex which is associated with PS-II uses this energy to split water. The resulting gaseous oxygen diffuses through the thylakoid membrane, the protons accumulate in the thylakoid lumen and the electrons are shuttled to the P700 reaction centre of PS-I via the cytochrome  $b_6f$  complex, thereby pumping further protons from the stroma into the lumen. The electrons finally reduce ferredoxin on the stromal side of the thylakoid membrane, and reduced ferredoxin is either directly used for redox reactions in the chloroplast or it is used to reduce  $\text{NADP}^+$  to NADPH via the ferredoxin-NADP<sup>+</sup>-reductase (FNR). If the stroma contains abundant reduced NADPH, the electrons can also be returned to the cytochrome  $b_6f$  complex in the Q-cycle, where they power further pumping of protons from the stroma into the lumen. The proton gradient produced from both linear and cyclic electron flow is then used to generate ATP from ADP and inorganic phosphate via the F-type ATPase complex by releasing the protons through a rotating channel against the electrochemical gradient (Nelson and Ben-Shem, 2004).

The products of photosynthesis, ATP and NADPH, are mainly used for carbon assimilation inside the chloroplast. In the Calvin cycle, three molecules of carbon dioxide are joined to three molecules of ribulose-1,5-bisphosphate by the enzyme ribulose-1,5-bisphosphate carboxylase/oxygenase (RuBisCO) to form unstable products that spontaneously dissociate into six molecules of 3-phosphoglycerate (Raines, 2011). These are transformed into six molecules of glyceraldehyde-3-phosphate by two enzymes that use six molecules of ATP and six molecules of NADPH. Of the six molecules of glyceraldehyde-3-phosphate, five are recycled to three molecules of ribulose-1,5-bisphosphate in a type of reductive pentose phosphate pathway which again consumes three molecules of ATP. The remaining glyceraldehyde-3-phosphate is the net gain per cycle which costs 9 ATP and 6 NADPH (Raines, 2011). Glyceraldehyde-3-phosphate and its

isomer dihydroxyacetone phosphate are either exported into the cytosol and converted to sucrose which is distributed through the whole plant as a source of energy in sink tissues or a source of storage starch in the amyloplasts of specific storage organs, or alternatively they are directly fed into the buildup of transitory starch inside the leaf chloroplasts (Zeeman et al., 2007).

The plastid is a central compartment involved in nitrogen and sulfur assimilation and the biosynthesis of amino acids (Neuhaus and Emes, 2000). Sulfur is taken up by plastids in the form of sulfate and then assimilated via adenosine phosphosulfate (APS) to cysteine and methionine (Leustek and Saito, 1999). Imported nitrite is reduced to ammonium by the plastid nitrite reductase, and glutamine synthetase (GS) acts as a glutamate-ammonia ligase to synthesise glutamine. Together with glutamine-oxoglutarate aminotransferase (GOGAT) which produces two glutamates from glutamine and 2-oxoglutarate, glutamine synthetase takes part in the so called GS-GOGAT cycle (Lam et al., 1995; Masclaux-Daubresse et al., 2010). Glutamate can be exported or used as a substrate for aspartate aminotransferase which synthesises aspartate from glutamate and oxaloacetate in plastids and other compartments (Lam et al., 1995; Masclaux-Daubresse et al., 2010). Together with cytosol-synthesised asparagine, the three amino acids glutamate, glutamine and aspartate form more than half of the total amino acid pool in *Arabidopsis* leaves and the starting material for the synthesis of most other amino acids (Lam et al., 1995; Masclaux-Daubresse et al., 2010). Especially the biosynthesis of histidine, aromatic amino acids (tryptophane, phenylalanine and tyrosine), branched-chain amino acids (leucine and valine) and aspartate-derived amino acids (lysine, methionine, threonine and isoleucine) is localised in plastids, other amino acids can be synthesised in plastids and other compartments as well (Reyes-Prieto and Moustafa, 2012).

In plants, virtually all fatty acids are synthesised in plastids (Rawsthorne, 2002). The rate limiting step of fatty acid synthesis is performed by the plastid acetyl-coenzyme A (acetyl-CoA) carboxylase (ACCase) that forms malonyl-CoA from acetyl-CoA and bicarbonate (Harwood, 1988). The malonyl moiety is then transferred to an acyl-carrier protein (ACP). The stromal fatty acid synthase complex (FAS) consists of several subunits that perform a complex cyclic reaction in which malonyl-ACP is fused to a growing acyl-ACP chain by releasing a carbon dioxide after each cycle (Harwood, 1988). Resulting acyl-ACP can either be transformed to acyl-CoA and exported from the plastid, or ligated to a glycerol-3-phosphate by two acetyltransferases to form phosphatidic acid which is further metabolised to diacylglycerol (DAG) inside the plastid (Ohlrogge and Browse, 1995; Wang and Benning, 2012). The fatty acids of the DAGs are further desaturated by membrane-bound fatty acid desaturases (FADs), and finally the DAGs can be further metabolised to monogalactosyl-, digalactosyl- and sulfoquinovosyl diacylglycerols (MDGD, DGDG, SQDG), and phosphatidylglycerol, the typical chloroplast membrane lipids (Wang and Benning, 2012).

Apart from the characteristic plastid functions described above, these organelles take part in a wide variety of other biochemical processes as well. In *Arabidopsis*, the largest part of purine nucleotide *de-novo* biosynthesis up to xanthosine monophosphate is localised in plastids from where AMP biosynthesis continues in plastids while GMP biosynthesis takes place in the cytosol (Zrenner et al., 2006). Pyrimidine nucleotide *de-novo* biosynthesis also takes place in plastids except one single step, dihydroorotate dehydrogenation, which occurs in mitochondria (Zrenner et al., 2006). Isoprenoid synthesis is divided between the cytosol (hemi-, sesqui-, triterpenes and steroids via the mevalonate pathway) and the plastids (mono- and diterpenes via the methylerythritolphosphate pathway) (Vickers et al., 2009). In plastids, diterpenes can be

further metabolised to plastoquinone, phylloquinone and giberelline hormones while tetraterpenes ultimately form carotenoids and abscisic acid (Vickers et al., 2009). In addition, porphyrine biosynthesis for chlorophyll and heme formation takes place in chloroplasts as does synthesis of the antioxidant lipid-protecting tocopherol and of the hormones salicylic and jasmonic acid involved in plant immunity and defense (Beale, 1990; DellaPenna, 2005; Nomura et al., 2012). Thus, plastids are an essential component of all plants in most tissues and at most stages of their development and influence plant life at almost every level of functionality.

## 1.3 Protein import into chloroplasts

### 1.3.1 Targeting of proteins to the chloroplast requires a transit peptide

The large variety of different plastid functions suggests that the number of proteins in these compartments is large. Estimates of the size of the plastid proteome in the model species *Arabidopsis thaliana* range from 1900 – 2500 proteins (Abdallah et al., 2000; Leister, 2003) up to ~4000 proteins (Sun et al., 2004). As the *Arabidopsis* plastid genome encodes less than 90 proteins (Sato et al., 1999), the bulk of plastid proteins are encoded in the nuclear genome and need to be targeted to plastids after translation. In fact, most proteins encoded in the nuclear genome need to be transported to a destination compartment after translation in the cytosol. Specificity is commonly achieved by a signal sequence that is recognised by receptors and leads to the translocation of the protein across the membranes of the respective compartment. Proteins are encoded together with the signal sequence as precursors, and usually the signal sequence is removed upon import leading to the shorter mature proteins. Proteins destined for the endoplasmic reticulum are encoded with an N-terminal signal peptide of 15 to 20 amino acids length, containing a hydrophobic core which is flanked by N-terminal positive residues and C-terminal hydrophilic residues (Blobel and Dobberstein, 1975; Martoglio and Dobberstein, 1998). Nuclear precursor proteins contain a short nuclear location signal (NLS) which typically contains positive amino acids such as arginine and lysine (Kalderon et al., 1984). Peroxisomal precursors can have either C-terminal or N-terminal signal sequences, called peroxysome targeting signals (PTS), which are bound by different receptors (Gould et al., 1987; Swinkels et al., 1991). Mitochondrial precursors have either an N-terminal signal sequence called presequence, which is typically 20 to 40 amino acids long, contains an overall positive charge and can form an amphiphilic

$\alpha$ -helix, whereas many membrane proteins contain non-cleavable internal targeting information (Abe et al., 2000; Brix et al., 1997; Roise and Schatz, 1988; Wiedemann et al., 2004).

Similarly, nucleus-encoded chloroplast proteins have a targeting sequence called transit peptide, which is cleaved off after import (Chua and Schmidt, 1978; Dobberstein et al., 1977; Highfield and Ellis, 1978) (see also Section 4.2). It is located at the N-terminus, and is necessary and sufficient for chloroplast targeting since it is also able to direct chloroplast unrelated proteins to the chloroplast, and its removal leads to a block in import (Bruce, 2000, 2001; Lee et al., 2006; Lee et al., 2009). Unlike other targeting sequences, the chloroplast transit peptide is extremely variable both on the sequence and structure level. Its length varies from 20 to more than 100 amino acids, with no obvious sequence conservation (Bruce, 2000, 2001). The only trend is an excess of hydroxylated residues, especially serine, and fewer acidic residues, leading to a positive charge. But this feature is shared by mitochondrial presequences, and therefore it is not completely clear how organellar specificity is achieved (Bhushan et al., 2006; Chew and Whelan, 2004). However, while mitochondrial presequences can form an amphiphilic  $\alpha$ -helix, chloroplast transit peptides do not form a common secondary structure, which leads to the assumption that this lack of structure might be important to discriminate between chloroplast and mitochondrial targeting sequences (Krimm et al., 1999; von Heijne and Nishikawa, 1991; Wienk et al., 2000) (see also Section 4.2). Another possibility to achieve specificity would be an interaction between the transit peptide and chloroplast specific membrane lipids (Bruce, 2001; Krimm et al., 1999; Wienk et al., 2000). Indeed, a deficiency in chloroplast specific galactolipids leads to reduced chloroplast protein import (Chen and Li, 1998), and the transit peptide has the ability to interact strongly and specifically with membranes containing galactolipids (Bruce, 1998).

Recent research confirms that the intrinsically disordered transit peptide has the ability to bind to chloroplasts based on physicochemical properties rather than conserved sequence motifs, since both pro- and retro-transit peptides can bind to chloroplasts (Chotewutmontri et al., 2012). For most transit peptides, however, binding to the translocon receptor Toc34 seems to be mediated by a degenerate FGLK motif, the presence of which is necessary but not sufficient for translocation (Chotewutmontri et al., 2012; Lee et al., 2006). This FGLK motif is separated by a spacer sequence from an N-terminal uncharged domain which can interact with stromal chaperones and is equally necessary for translocation (Chotewutmontri et al., 2012). It has been speculated that transit peptides do in fact contain motifs and domains with specific physicochemical properties, but their structural organisation along the transit peptide may not be conserved which leads to a large variety in both transit peptide sequences and translocation mechanisms (Li and Teng, 2013).

### **1.3.2 Most chloroplast proteins are targeted via the general import pathway**

Isolated pea chloroplasts were found to synthesise the large but not the small RuBisCO subunit (Blair and Ellis, 1973). Therefore, even before the chloroplast transit peptide was discovered, it was postulated that some chloroplast proteins must be synthesised in the cytosol and cross the chloroplast envelope using a proteinaceous carrier, which has been termed the envelope carrier hypothesis (Blair and Ellis, 1973). Indeed, when chloroplasts were pre-treated with the protease thermolysin which removes proteins at the chloroplast surface, later added precursor proteins were not anymore able to bind to chloroplasts, proving that their binding relies on proteins on the chloroplast surface (Cline et al., 1984; Cline et al., 1985; Friedman and Keegstra, 1989). Early investigations of solubilised outer envelope membranes resulted in the finding of a protein com-

plex containing the precursor as well as Hsp70 and an unknown 86 kDa protein (Waegemann and Soll, 1991). Later it was found that precursors bind to the 86 kDa protein in the absence of ATP whereas low levels of ATP are required for binding to a newly found component of 75 kDa (Perry and Keegstra, 1994). The 86 kDa component, however, turned out to be a proteolytic fragment of a larger, relatively instable protein of 159 kDa, which seems to be a primary receptor for pre-proteins at the chloroplast surface (Bolter et al., 1998; Chen et al., 2000; Hirsch et al., 1994) (Fig. 1.1). This protein has later been named 'Toc159, for translocon at the outer chloroplast envelope membrane, 159 kDa', according to the current nomenclature of envelope membrane proteins involved in chloroplast protein import (Schnell et al., 1997). The 75 kDa component (Toc75) which was repeatedly found in association with precursors (Perry and Keegstra, 1994; Schnell et al., 1994; Tranel et al., 1995), was finally shown to be the protein conducting channel component in the outer envelope membrane (Baldwin et al., 2005; Hinnah et al., 1997; Hinnah et al., 2002) (Fig. 1.1). Toc159 and another receptor component of 34 kDa (Toc34) were discovered to be GTPases, and GTPase activity seems to be necessary for protein import since substitution of GTP with non-hydrolysable forms of GTP negatively affects protein import (Kessler et al., 1994; Seedorf et al., 1995).

In the inner envelope membrane, a large protein of 110 kDa was found to be associated with translocating precursors (Lubeck et al., 1996). This component has later been found to be an essential protein, and was suggested to form the protein conducting channel in the inner envelope membrane (Heins et al., 2002; Inaba et al., 2005; Kovacheva et al., 2005). It has been named Tic110, for 'translocon at the inner chloroplast envelope membrane, 110 kDa', in line with the current nomenclature (Schnell et al., 1997). However, another pair of proteins in the inner envelope, Tic20 and Tic21, are

both integral membrane proteins and have channel properties, similar to Tic110 (Kouranov et al., 1998; Teng et al., 2006) (Fig. 1.1). They have been found in association with precursors in a complex lacking Tic110, which is why it has been suggested that they form protein conducting channels separate from Tic110 (Kikuchi et al., 2009). On the stromal side, Tic40 and Hsp93 have been shown to interact with Tic110 and precursor proteins (Akita et al., 1997; Nielsen et al., 1997; Stahl et al., 1999; Wu et al., 1994) (Fig. 1.1). Hsp93, a molecular chaperone of the Hsp100 family, has therefore been reasoned to be part of a motor complex that binds to translocating precursors and pulls them into the stroma by an ATP consuming ratchet-type mechanism (Akita et al., 1997; Constan et al., 2004a; Nielsen et al., 1997; Schirmer et al., 1996). Tic40 also has properties of a co-chaperone and has been suggested to facilitate ATP hydrolysis by Hsp93 (Bedard et al., 2007; Stahl et al., 1999).

All the above described components form a more or less dynamic translocon complex in the chloroplast envelope membranes, composed of the two translocon subcomplexes TOC and TIC in the outer and inner chloroplast envelope membrane, respectively. At large, three functionally different entities can be distinguished; Toc159 and Toc34 are responsible for transit peptide recognition and binding, Toc75, Tic20 and Tic21 (and possibly Tic110) are channel components responsible for preprotein translocation through the envelope, and Tic40 and Hsp93 (and potentially other chaperones) form a motor complex associated with Tic110 that drives protein import by ATP hydrolysis (Jarvis, 2008; Li and Chiu, 2010). Protein import through the TOC and TIC complexes is referred to as the “general import pathway” and is the default pathway for import of nucleus-encoded chloroplast proteins.

The binding of precursors to the TIC complex is called “docking” and requires low levels of ATP (50-100  $\mu$ M) (Olsen et al., 1989). Low levels of GTP enhance the docking in the presence of ATP but cannot substitute when ATP is lacking (Olsen and Keegstra, 1992; Olsen et al., 1989; Young et al., 1999). Docking of precursors leads to the formation of early import intermediates which can be chased into the stroma by high levels of ATP (1 mM) at 25°C but not at 4°C (Leheny and Theg, 1994; Olsen et al., 1989; Rensink et al., 2000). Recently it was shown that at 100  $\mu$ M ATP and 4°C part of the precursors associate loosely with the TOC complex, likely due to energy independent binding to the receptors (stage I), and part insert into the Toc75 channel (stage II) requiring a temperature insensitive ATPase activity (Inoue and Akita, 2008a, b). By increasing the temperature to 25°C, all precursors are inserted into the Toc75 channel with their transit peptide, while some are inserted deeper than others (stage III), requiring a separate, temperature sensitive ATPase activity (Inoue and Akita, 2008a, b). However, the ATPases necessary for the binding step remain unknown (Chiu et al., 2010).

A fifth of all proteins detected in chloroplasts by mass spectrometry do not have a transit peptide (Kleffmann et al., 2004). These may include many outer envelope membrane proteins which insert spontaneously into the membrane, but likely also many proteins employing pathways different from the general import pathway (Jarvis, 2008; Li and Chiu, 2010). Some proteins, such as carbonic anhydrase 1 (CAH1) or nucleotide pyrophosphatase/phosphodiesterase 1 (NPP1), have an ER signal peptide instead of a transit peptide, are glycosylated in the Golgi apparatus and then targeted to chloroplasts via the secretion pathway (Nanjo et al., 2006; Radhamony and Theg, 2006; Villarejo et al., 2005). Some inner envelope proteins, such as chloroplast quinone oxidoreductase homologue (ceQORH) and Tic32 are targeted without a canonical transit peptide via a yet unknown mechanism (Miras et al., 2007; Nada and Soll, 2004).

### 1.3.3 Toc159 and Toc34 are the primary receptors for transit peptide binding

Both, Toc34 and Toc159 have a short C-terminal membrane anchor and a cytosolic GTP-binding domain (G-domain) (Fig. 1.1), and they can bind directly to precursor proteins which suggests a receptor role (Perry and Keegstra, 1994; Smith et al., 2004; Sveshnikova et al., 2000). In *Arabidopsis*, two isoforms of Toc34 exist, atToc33 and atToc34, which both share 61% amino acids (Jarvis et al., 1998). For Toc159 there are four isoforms in *Arabidopsis*, atToc159, atToc132, atToc120 and atToc90. All four Toc159 isoforms contain relatively conserved, large membrane domains (M-domains) and G-domains, but unlike Toc34 they also possess an acidic domain (A-domain) with unknown function, which shows considerable differences between the four isoforms (Bauer et al., 2000; Ivanova et al., 2004; Kubis et al., 2004) (Fig. 1.1). The existence of different receptor isoforms in *Arabidopsis* strongly suggests a specialised role for each isoform (Kubis et al., 2004). Indeed, the knockout of atToc33, called *ppi1* for *plastid protein import 1*, is pale and impaired in protein import of mainly photosynthetic proteins, whereas the knockout of atToc34, called *ppi3*, is green and specifically impaired in root growth (Constan et al., 2004b; Jarvis et al., 1998). While this indicates that atToc33 is rather specific for photosynthetic and atToc34 for non-photosynthetic, housekeeping precursors, their roles nevertheless overlap because the *ppi1 ppi3* double mutant is embryo lethal and the pale *ppi1* phenotype can slightly be recovered by atToc34 overexpression (Constan et al., 2004b; Jarvis et al., 1998).

Similarly, the knockout of atToc159, called *ppi2*, is albino while *attoc132*, *attoc120* and *attoc90* mutants have no obvious pale phenotypes (Bauer et al., 2000; Hiltbrunner et al., 2004; Ivanova et al., 2004; Kubis et al., 2004). atToc90 is closer related to atToc159 than to atToc132 or atToc120, its overexpression can partially complement the albino *ppi2* phenotype and its knockout slightly enhances the *ppi2* pheno-

type, leading to the conclusion that the functions of atToc90 and atToc159 partially overlap (Hiltbrunner et al., 2004; Infanger et al., 2011). However, because *attoc90* has no strong phenotype, its exact role is still unknown. atToc132 and atToc120 are closer related to each other than to atToc159 or atToc90, and the *attoc132 attoc120* double mutant is albino, suggesting that both components have overlapping roles which are separate from the atToc159/atToc90 function (Ivanova et al., 2004). Unlike *ppi2*, the *attoc132 attoc120* double mutant shows abnormal root plastids, and atToc132 and atToc120 expression is low and uniform as is typical for non-photosynthetic proteins (Kubis et al., 2004). Therefore, it was suggested that atToc33 forms a complex with atToc159/atToc90 which shows specificity for photosynthetic proteins while atToc34 forms complexes with atToc132 and atToc120 with specificity for non-photosynthetic proteins, which might prevent import exclusion of low-abundant housekeeping proteins by highly abundant photosynthetic proteins (Kubis et al., 2004). However, specificity is not complete since the *ppi2 toc132* double mutant is embryo lethal, showing that atToc159 and atToc132 are in separate complexes with partially overlapping functions (Kubis et al., 2004). Furthermore, it was shown recently that some photosynthetic chloroplast proteins can also accumulate independently of atToc159 in the *ppi2* mutant (Bischof et al., 2011).

It has been shown that atToc33 can homodimerise through their G-domains (Sun et al., 2002; Weibel et al., 2003; Yeh et al., 2007). Additionally, atToc33 might also form heterodimers with atToc159 through their homologous G-domains (Bauer et al., 2002; Rahim et al., 2009; Smith et al., 2002; Wallas et al., 2003). It has been suggested that in homodimers each atToc33 might act as a GTP activating protein (GAP) for the other interactor, and indeed a mutation in atToc33 which abolishes dimer formation leads to a significant decrease in GTPase activity (Bauer et al., 2002; Sun et al., 2002;

Yeh et al., 2007). However, another study did not report a decreased GTPase activity in the same mutant (Weibel et al., 2003). It was also suggested that GAP function is actually exerted by the transit peptide of the binding precursor (Jelic et al., 2003; Jelic et al., 2002; Reddick et al., 2007). But the stimulating properties of precursor binding on GTPase activity might be indirect in that it disrupts homodimer formation which enables more efficient nucleotide exchange and therefore increases the levels of GTP-bound, activatable atToc33 (Aronsson and Jarvis, 2011; Oreb et al., 2011).

#### **1.3.4 Toc75 forms the preprotein channel in the outer envelope membrane**

Toc75 is a member of the BamA ( $\beta$ -barrel assembly machinery A) family (Ertel et al., 2005; Gentle et al., 2005; Hsu and Inoue, 2009). It contains a C-terminal  $\beta$ -barrel domain which forms a precursor channel, and three N-terminal polypeptide transport associated (POTRA) domains which might be involved in initial precursor binding (Ertel et al., 2005; Gentle et al., 2005; Hinnah et al., 1997; Sanchez-Pulido et al., 2003; Schnell et al., 1994; Tranel et al., 1995) (Fig. 1.1). Indeed, it was shown that Toc75 can form a voltage dependent channel in artificial membranes that can directly bind to transit peptides (Hinnah et al., 2002). In *Arabidopsis*, three Toc75 isoforms exist, atToc75-III, atToc75-IV and atToc75-I, named according to their genetic location on chromosomes III, IV and I, respectively (Jackson-Constan and Keegstra, 2001). The closest homologue to pea Toc75 is atToc75-III, which is an essential gene, the knockout being embryo lethal (Baldwin et al., 2005). This component corresponds to the main precursor channel in chloroplast outer envelope membranes, where it is the most abundant protein (Eckart et al., 2002; Vojta et al., 2004). Aside its role as precursor channel, it has likely an additional role in the insertion of outer envelope membrane proteins (Huang et al.,

2011; Tu et al., 2004). Expression of the second isoform, atToc75-IV, is low and its knockout does not show a visible phenotype (Baldwin et al., 2005). However, etioplast ultrastructure is altered in the *attoc75-IV* mutant, and the reduced de-etiolation efficiency suggests a role in dark-to-light growth transition (Baldwin et al., 2005). The third isoform, atToc75-I was shown to be a pseudogene with no expression (Baldwin et al., 2005). A fourth isoform, previously named atToc75-V, was found to be in a separate protein family from the other three isoforms and was therefore renamed to OEP80 (Inoue and Potter, 2004). OEP80 is essential, with knockouts aborting at the globular stage (Patel et al., 2008). Together with Toc75, OEP80 is a member of the Omp85 superfamily of proteins which are generally involved in the insertion of  $\beta$ -barrel proteins into membranes (Gentle et al., 2004; Inoue and Potter, 2004; Patel et al., 2008). In fact, the reduced level of Toc75-III in *oep80* knockdown mutants suggest that it might be involved in the insertion of Toc75-III itself and thus be crucial for TOC assembly (Huang et al., 2011).

### **1.3.5 The existence of an intermembrane space complex is uncertain**

Studies on the energy requirement of chloroplast protein import concluded that low levels of ATP are needed for the formation of early import intermediates, and that the intermembrane space is the most likely site for this ATPase activity (Olsen and Keegstra, 1992; Olsen et al., 1989). In pea, this activity has been assigned to an Hsp70 which associates with the outer envelope membrane but is not exposed to the cytosol (Marshall et al., 1990). The discovery of Toc12, an outer envelope localised J-domain protein, which is able to stimulate Hsp70 via a soluble intermembrane space exposed domain, lead to the idea of an intermembrane space complex (Becker et al., 2004) (Fig.

1.1). This complex consists of Toc12 and its interaction partners, Toc64 and Tic22 (Becker et al., 2004; Qbadou et al., 2007) (Fig. 1.1). Toc64 is an integral outer envelope receptor with a cytosolic tetratricopeptide repeat (TPR) domain and an intermembrane space localised domain that interacts with Toc12 (Becker et al., 2004; Qbadou et al., 2007; Sohrt and Soll, 2000) (Fig. 1.1). While the cytosolic domain of Toc64 can recognise precursors which are delivered by cytosolic Hsp90 chaperones, its intermembrane space localised domain can bind translocating precursors and might therefore be involved in protein translocation (Qbadou et al., 2007).

Tic22 is a soluble protein associated with the outer surface of the inner envelope membrane and interacting with the TIC complex (Kouranov et al., 1998) (Fig. 1.1). It might be an early point of contact of precursors with the TIC machinery, however, its exact role is largely unknown (Kouranov et al., 1998). There are two isoforms of Tic22 in *Arabidopsis*, Tic22-III and Tic22-IV. The *tic22-III* mutants are slightly chlorotic, *tic22-IV* mutants are visibly normal and *tic22-III tic22-IV* double mutants are clearly chlorotic, have reduced protein import rates and reduced photosynthetic performance suggesting a non-essential and redundant role in protein import (Kasmati et al., 2013; Rudolf et al., 2013). Other studies on Tic22 show that it can act as a chaperone in apicoplasts by keeping proteins in an unfolded, import-competent state (Glaser et al., 2012) and that it can interact with Omp85 in *Anabaena* sp. PCC 7120 and participate in outer membrane biogenesis (Tripp et al., 2012). Thus, Tic22 may fulfill a general chaperoning function for protein insertion and translocation in the intermembrane space.

Recently, doubt has been cast on the existence of the intermembrane space complex. It has been found that pea Toc12 is actually a truncated form of DnaJ-J8, the homologue of which is a stromal protein in *Arabidopsis* with no essential function in protein import (Chiu et al., 2010). Furthermore, none of the *Arabidopsis* Hsp70 paralogues

which are predicted to be chloroplast localised could be found in the intermembrane space (Ratnayake et al., 2008; Su and Li, 2008). Lastly, the triple knockout mutant of all three *Arabidopsis* Toc64 paralogues does neither show a particular mutant phenotype nor decreased import efficiency, leading to the suggestion to rename Toc64 as OEP64 (Aronsson et al., 2007; Rosenbaum Hofmann and Theg, 2005). Recently, a light intensity-dependent growth defect was observed for *toc64-III* mutants, which lack the major *Arabidopsis* Toc64 isoform, and an import defect was observed in these mutants, conflicting with the previous findings (Aronsson et al., 2007; Sommer et al., 2013). Since *ppi1 toc64-III* double mutants accumulate less Toc75-III protein than either single mutant, it was suggested that both Toc33 and Toc64-III have a synergistic influence on Toc75-III accumulation (Sommer et al., 2013). However, more research on these intermembrane space components is necessary to clarify the conflicting results.

### **1.3.6 Tic110 and Tic20/21 are candidates for the inner envelope protein channel**

Recombinant Tic110 proteins from pea could be reconstituted into liposomes *in vitro* where they were shown to form  $\beta$ -barrel channels with a pore diameter of 1.7 nm (Heins et al., 2002). These data, together with the fact that *attic110* mutants abort at the globular stage of embryogenesis, suggest an essential role for Tic110, likely as a protein channel in the inner envelope membrane (Heins et al., 2002; Inaba et al., 2005; Kovacheva et al., 2005). The  $\beta$ -barrel structure, however, was disputed since another study based on circular dichroism proposed a secondary structure mainly composed of  $\alpha$ -helices (Inaba et al., 2003). The latter study suggests that Tic110 is anchored in the inner envelope membrane merely by two N-terminal transmembrane domains while the larger C-terminal domain can bind to the emerging precursor, supporting the previous

finding that Tic110 forms a scaffold for chaperone recruitment (Inaba et al., 2003; Kessler and Blobel, 1996) (Fig. 1.1, see also Section 2.2). Recent research does not seem to resolve the conflicting views as yet: While an electrophysiological study on Tic110 suggests that the large hydrophilic domain actually contains four membrane-embedded amphipathic  $\alpha$ -helices that contribute to the protein channel (Balsera et al., 2009), a very recent X-ray crystallographic analysis of *Cyanidioschyzon merolae* Tic110 suggests that the C-terminus is too flattened and elongated to be a channel but rather resembles motifs that act as scaffolds for protein-protein interactions (Tsai et al., 2013) (see Section 2.2).

Another component of the TIC complex, Tic20, was identified as a major interactor of precursor proteins during translocation through the TIC machinery (Kouranov et al., 1998; Kouranov and Schnell, 1997; Ma et al., 1996). Similar to the mitochondrial protein translocation channel components Tim22 and Tim23, it contains four  $\alpha$ -helical transmembrane domains, which lead to the idea that Tic20 might be a precursor channel in the inner envelope membrane (Kalanon and McFadden, 2008; Kouranov et al., 1998; Rassow et al., 1999) (Fig. 1.1). Indeed, in *Arabidopsis*, the double knockout of the two major Tic20 isoforms, *attic20-I attic20-IV*, is embryo lethal, which is in line with the proposed role of an essential protein translocating channel (Hirabayashi et al., 2011; Kasmati et al., 2011). The albino *attic20-I* single knockout phenotype together with its preferential expression in photosynthetic tissues suggest a specificity of atTic20-I for photosynthetic precursors, much like discussed for the TOC receptor components (Hirabayashi et al., 2011; Kikuchi et al., 2009; Teng et al., 2006). Nevertheless, atTic20-I and atTic20-IV have partially overlapping essential functions, as is proven by the embryo lethal double knockout phenotype (Hirabayashi et al., 2011; Kasmati et al., 2011). Two other Tic20 isoforms, atTic20-II and atTic20-V do not seem

to have an essential function since the *attic20-II attic20-V* double knockout does not show a phenotype different from wild type (Kasmati et al., 2011).

Since both *attic20-I attic20-IV* and *attic110* are embryo lethal, atTic20 and atTic110 have most likely non-overlapping functions, however, both have been suggested to be precursor channels (see Section 2.2). Kikuchi et al., (2009) found that Tic20 interacts with Tic21 in a large 1MD complex from which Tic110 is absent and they conclude that Tic20/21 forms the main protein translocating channel while Tic110 might have an essential function later during import, most likely as a scaffold for the assembly of the motor complex (Kikuchi et al., 2009). Since Tic110 interacts with Tic40 (Stahl et al., 1999), and Tic40 has been found to be involved in post-import protein re-insertion into the inner envelope membrane (Chiu and Li, 2008), it can be speculated that the Tic110 channel properties might allow protein export rather than import.

Tic21 was discovered in a screen for mutants which are defective in protein import (Teng et al., 2006). The *attic21* knockout is albino and accumulates precursors in the cytosol, very similar to *attic20-I* (Teng et al., 2006). The fact that the *attic21 attic20-I* double knockout does not show an additive effect and that both proteins have been identified in the same complex suggests a common function (Kikuchi et al., 2009; Teng et al., 2006). However, Tic21 has also been described as permease in chloroplasts 1 (PIC1), a potential iron channel (Duy et al., 2007). The *pic1/tic21* knockouts accumulated ferritin in the chloroplast, and ferritin expression as well as expression of other genes related to iron homeostasis and metal transport was upregulated (Duy et al., 2007). Moreover, overexpression of PIC1/Tic21 led to the accumulation of free iron in the chloroplast (Duy et al., 2007). Since it is known that a block of chloroplast iron uptake can negatively affect protein import, the *attic21* import defect phenotype could still be explained (Boij et al., 2009; Caliebe et al., 1997; Row and Gray, 2001). However, it

was shown that other pale mutants like *attic20-I* and *alb3* can also lead to an upregulation of genes related to iron homeostasis, which might be a general effect caused by impaired chloroplast development (Kikuchi et al., 2009).

Very recently, three additional components were found to interact with Tic20-I (and weakly with Tic21) in the previously reported 1 MD complex: Two nuclear encoded proteins called Tic100 and Tic56, and the large inner envelope membrane protein Tic214 which is encoded by the chloroplast gene *ycf1* (Kikuchi et al., 2013) (Fig. 1.1, see also Section 2.2). Since the complex could be reconstituted into planar lipid bilayers and showed precursor-responsive ion channel activity, it was suggested that the 1 MD complex consisting of Tic20-I, Tic214, Tic100 and Tic56 forms the actual TIC channel (Kikuchi et al., 2013). The knockout mutants *tic100* and *tic56* were seedling lethal like *tic20-I*, and the lack of additivity between these three components confirmed their common function in the complex (Kikuchi et al., 2013). Finally, Tic20-IV was found to act in parallel to Tic100 and Tic56, potentially in a complex involving different components (Kikuchi et al., 2013).

### **1.3.7 Tic110, Tic40 and Hsp93 form a motor complex at the stromal side of TIC**

The large stromal domain of Tic110 has been reported to form a scaffold for chaperones and co-chaperones which are thought to drive chloroplast protein import (Akita et al., 1997; Chou et al., 2006; Kessler and Blobel, 1996; Nielsen et al., 1997). The most abundant Tic110 interactor is cpCpn60, a subunit of the chloroplast chaperonin complex composed of cpCpn60 $\alpha$ , cpCpn60 $\beta$ , cpCpn20 and cpCpn10 which together form a hydrophobic cage in which proteins can fold properly (Kessler and Blobel, 1996; Levy-Rimler et al., 2002; Weiss et al., 2009). Consequently, this complex interacts with the

TIC complex and binds to unfolded, translocating precursors on the stromal side in order to ensure proper folding after cleavage of the transit peptide (Kessler and Blobel, 1996).

Another chaperone that interacts with the Tic110 stromal domain is Hsp93, also called ClpC, which belongs to the Hsp100 family of molecular chaperones (Akita et al., 1997; Nielsen et al., 1997). Hsp93 subunits form hexameric rings through which proteins can be pulled (Schirmer et al., 1996) (Fig. 1.1). Therefore, Hsp93 has rather unfolding than folding activity, which is used mainly to unfold misfolded proteins and thereby targeting them for degradation by the chloroplast Clp protease complex (Shanklin et al., 1995). However, this pulling action can also be used to thread unfolded proteins through an import channel, which is why it has been suggested that Hsp93 forms the main component of the import motor complex (Akita et al., 1997; Jackson-Constan and Keegstra, 2001; Nielsen et al., 1997; Schirmer et al., 1996) (see also Section 2.2). Indeed, the knockout of the highly expressed *Arabidopsis* atHsp93-V isoform leads to a pale phenotype which is impaired in protein import (Constan et al., 2004a; Kovacheva et al., 2005). While the knockout of the minor isoform, *hsp93-III* is indistinguishable from wild type, the double knockout *hsp93-III hsp93-V* is embryo lethal, showing that both isoforms are partially redundant and together essential (Kovacheva et al., 2005; Kovacheva et al., 2007).

Tic40, another component of the import motor, can be cross-linked to Tic110, Hsp93 and importing precursors, demonstrating that it acts in concert with these proteins (Chou et al., 2003) (Fig. 1.1, see also Section 2.2). Like Tic110, it is anchored in the inner envelope membrane with its N-terminus and protrudes a soluble C-terminal domain into the stroma that is able to covalently bind to Tic110 via a disulfide bridge (Chou et al., 2003; Stahl et al., 1999). Interestingly, the only cysteine in Tic40 which is

available for disulfide bridge formation lies in a Sti1 domain with high similarity to Sti1 domains in human co-chaperones Hsp70-interacting protein (Hip) and Hsp70/Hsp90-organizing proteins (Hop) (Bedard et al., 2007). Other data indicate that it is rather a tetratricopeptide repeat (TPR) domain that is responsible for Tic110 binding, and that this binding is stimulated when a precursor protein is bound to Tic110 (Chou et al., 2006; Inaba et al., 2003). Tic40 binding would then trigger the release of the precursor from Tic110 and at the same time stimulate ATPase activity of Hsp93 via its Sti1 co-chaperone domain (Bedard et al., 2007; Chou et al., 2006) (see Section 2.2).

Intriguingly, Tic40 seems to be involved in a range of other functions, as Tic40 expression in tobacco chloroplasts leads to a massive proliferation of the inner envelope membrane (Singh et al., 2008), and *tic40* mutant plants accumulate intermediate precursors that normally insert into the inner envelope membrane (Chiu and Li, 2008). These data indicate that Tic40 plays a role in the re-insertion of imported proteins into the inner envelope membrane, and that it may thus have an indirect influence on inner envelope membrane biogenesis (Chiu and Li, 2008). Recently, an essential, envelope localised secretion (Sec) system was identified (Skalitzky et al., 2011), and it may be speculated that Tic40 can act as a stimulating co-chaperone for a variety of Sec-associated chaperones or even other chaperones that are involved in many different processes. However, the relatively mild phenotype of the *tic40* knockout (Chou et al., 2003) suggests that most envelope-associated chaperones can to some extent spare the stimulatory function of Tic40, or other chaperones that rely less on co-chaperone activity or interact with other yet unidentified co-chaperones may step in.

Indeed, it was shown that stroma-localised cpHsc70-1 and cpHsc70-2 have an essential role in protein import (Su and Li, 2008, 2010) (Fig. 1.1, see also Section 2.2). The *cphsc70-1* and *cphsc70-2* knockouts are both defective in protein import, *cphsc70-1*

to a larger extent than *cphsc70-2*, and that the *cphsc70-1 cphsc70-2* double knockout is embryo lethal (Su and Li, 2008, 2010). This suggests that cpHsc70-1 is the major isoform, cpHsc70-2 can partially substitute in the *cphsc70-1* knockout, and both proteins have a partially overlapping and essential role in protein import (Su and Li, 2008, 2010). This situation is highly reminiscent to the Hsp93-V/Hsp93-III system (Kovacheva et al., 2005; Kovacheva et al., 2007), to which cpHsc70 might act in parallel. Strong support for that hypothesis comes from the fact that the *cphsc70-1 tic40* double knockout is lethal while *cphsc70-1* alone has only a mild phenotype (Su and Li, 2010). This suggests that Hsp93, from which both isoforms are present in *cphsc70-1 tic40*, cannot function in the absence of Tic40 and therefore might be strictly dependent on the co-chaperone activity of Tic40. Hence, it is rather cpHsc70-1 which accounts for the remaining protein import in the mild *tic40* background. Consequently, the *cphsc70-1 hsp93-V* double knockout is paler than either single mutant, underpinning that the two chaperone systems cpHsc70-1/2 and Hsp93-V/III/Tic40 act in parallel (Su and Li, 2010). This poses the question whether cpHsc70 makes use of another yet unidentified co-chaperone system. In *Physcomitrella patens*, knockout of a GrpE co-chaperone, which are usually associated with Hsp70, leads to a defect in protein import (Shi and Theg, 2010). A similar component in *Arabidopsis* has however not yet been identified.

Recently, the stroma localised Hsp90C, an Hsp90 chaperone family member, was also found to be involved in chloroplast protein import (Inoue et al., 2013) (Fig. 1.1). Knockout mutants of this single gene-encoded chaperone are embryo lethal, but reversible inhibition of Hsp90C ATPase activity with radicicol led already to a protein import defect (Inoue et al., 2013). Moreover, Hsp90C interacts with importing precursors, the TIC components Tic40 and Tic110 as well as with the chaperones Hsp93 and cpHsc70 (Inoue et al., 2013). Therefore, it seems that Tic40 and Tic110 interact with a

large variety of stromal chaperones which are coordinated at the stromal surface of the inner envelope for a range of different functions, from protein import propulsion and protein folding to inner envelope membrane biogenesis.

### **1.3.8 Transit peptides are removed and degraded after import**

After translocation of precursor proteins into the stroma, the stromal processing peptidase (SPP) binds to the transit peptides and cleaves them off, releasing the mature proteins (Richter and Lamppa, 1998; Teixeira and Glaser, 2013; VanderVere et al., 1995) (Fig. 1.1, see also Section 4.2). SPP belongs to the MEROPS metalloendopeptidase M16 family of peptidases which has a zinc-binding HXXEH motif in the catalytic core (Richter and Lamppa, 2003; Teixeira and Glaser, 2013). After cleavage, SPP remains bound to the transit peptide which is cleaved again C-terminally before it is released (Richter and Lamppa, 1999, 2002). The released sub-fragment is then degraded by the stromal presequence protease (PreP), a zinc-binding enzyme which belongs to the pitrilysin protease family (Moberg et al., 2003; Nilsson Cederholm et al., 2009) (see also Section 4.2).

The recognition of the transit peptide cleavage site by SPP relies mainly upon physicochemical properties, as mutational analyses revealed that SPP cleaves a large number of very different transit peptide sequences (Rudhe et al., 2004). SPP binds directly to the 10-15 C-terminal residues of the transit peptide and recognises a weak consensus motif containing valine, alanine or amino acids with similar properties (Huang et al., 2009; Richter and Lamppa, 2002). Binding to the transit peptide does not depend on catalytic activity, as mutations in the zinc-binding HXXEH motif abolish transit peptide cleavage but transit peptides still bind to SPP (Richter and Lamppa, 2003). Instead, an

N-terminal domain of SPP recognises and binds to the C-terminal part of the transit peptide (Richter and Lamppa, 2003). The same catalytic activity of the zinc-binding HXXEH motif is then used for cleavage of the transit peptide as well as for the second cleavage step which leads to the release of the sub-fragment from SPP (Richter and Lamppa, 2003).

SPP proteins are very conserved, and homologues exist in cyanobacteria, diatoms, green algae and even in the apicoplasts of malaria parasites (Richter et al., 2005). It can be assumed that all these proteases fulfill an ancient, conserved function. Indeed, *Arabidopsis* antisense knockdown lines of pea SPP show a strong, partially seedling lethal mutant phenotype (Zhong et al., 2003). Some plants were green, but grew more slowly with abnormal leaf morphology and white sectors (Zhong et al., 2003). Chloroplasts of such cells were abnormal in number and appearance, and precursors were not imported any more efficiently into these chloroplasts (Zhong et al., 2003). A later study reported leaf chlorosis of young seedlings and a persisting inhibition of root growth in a rice mutant of SPP, which has a deletion of a C-terminal glycine (Yue et al., 2010) (see Section 4.2). Given the relatively mild nature of these mutants, a knockout would be anticipated to have a more severe phenotype, which would confirm the essential role of SPP.

The presequence protease PreP is dually targeted to mitochondria and chloroplasts and thus degrades both mitochondrial presequences and the sub-fragments of chloroplast transit peptides (Bhushan et al., 2003; Moberg et al., 2003) (Fig. 1.1). In *Arabidopsis*, there are two isoforms, AtPreP1 and AtPreP2, which are both dually targeted to mitochondria and chloroplasts (Glaser et al., 2006). The crystal structure of AtPreP1 revealed that proteolysis of presequences, transit peptides but also other unstructured small peptides occurs in a large proteolytic chamber (Glaser et al., 2006). Both isoforms are expressed in all tissues, but AtPreP1 is generally expressed higher than

AtPreP2, and consequently the *atprep1* mutant has a slightly pale-green phenotype while *atprep2* mutants have a wild-type phenotype (Nilsson Cederholm et al., 2009). The *atprep1 atprep2* double mutants are chlorotic at an early developmental stage, have decreased total chlorophyll levels, abnormal morphologies of chloroplasts and mitochondria and accumulate less biomass throughout their development (Nilsson Cederholm et al., 2009). Thus, although the degradation of transit peptides is not as essential as their cleavage by SPP, their accumulation has clearly negative effects on plant development.

## 1.4 Targeting of proteins to the thylakoids

### 1.4.1 Targeting to the thylakoid lumen occurs via the cpSec or cpTat pathway

After the transit peptide has been cleaved off in the stroma, some proteins are further targeted to the thylakoid lumen and membranes (Fig. 1.2). Luminal proteins contain an additional targeting sequence immediately adjacent to the transit peptide, which directs transport across the thylakoid membrane (Ko and Cashmore, 1989; Smeekens et al., 1986). This sequence, called thylakoid signal peptide, is very similar to prokaryotic targeting sequences and is composed of an N-terminal basic region, a hydrophobic core and a C-terminal polar region (von Heijne et al., 1989). After import into the lumen it is cleaved off by the thylakoid processing peptidase (TPP) (Halpin et al., 1989). Proteins containing such a bipartite transit peptide, one for transport across each the envelope and the thylakoid membranes, can follow either one of two different pathways: the chloroplast secretory (cpSec) pathway or the chloroplast twin-arginine transporter (cpTat) pathway.

The chloroplast Sec pathway is very similar to the prokaryotic Sec pathway, involving the signal peptide binding SecA and the channel components SecY and SecE (Laidler et al., 1995; Nakai et al., 1994; Schuenemann et al., 1999a; Yuan et al., 1994) (Fig. 1.2). SecA thereby binds to unfolded precursors in the stroma, directs them to the SecYE translocons and drives translocation by cycles of membrane insertion and de-insertion via ATP hydrolysis (Economou and Wickner, 1994). However, other Sec components typically found in prokaryotes such as SecB, SecG and SecD/F have no homologues in chloroplasts. SecB is essential in prokaryotes for maintaining translocation competence of Sec precursors, SecG forms part of the prokaryotic SecYEG channel

and SecD/F might be a membrane-integrated chaperone driving translocation (Nishiyama et al., 1994; Tsukazaki et al., 2011; Weiss et al., 1988). Therefore it is feasible that, in chloroplasts, other, unrelated components might have acquired these essential functions instead.

The second pathway for luminal proteins, the cpTat pathway, depends on two adjacent arginines in the basic region of the signal peptide, hence the name (Chaddock et al., 1995). This pathway does not require ATP, instead it makes use of the thylakoid proton gradient (Cline et al., 1992; Klosgen et al., 1992; Mould and Robinson, 1991). Other studies, however, suggested that neither the proton gradient nor the transmembrane electric potential might be strictly necessary for cpTat function *in vivo* (Di Cola et al., 2005; Finazzi et al., 2003). Proteins that need to adopt a folded conformation in the stroma due to cofactor binding or oligomerisation can be translocated across the thylakoid using the cpTat but not the cpSec pathway (Creighton et al., 1995; Hynds et al., 1998; Marques et al., 2004). However, while in prokaryotes a fully folded protein conformation is a prerequisite for the Tat pathway, in chloroplast this is not required (Hynds et al., 1998).

In thylakoids, cpTatC and Hcf106 form a receptor complex, both components being able to interact with the precursor (Cline and Mori, 2001) (Fig. 1.2). While cpTatC interacts with the basic region of the signal peptide containing the twin arginine, Hcf106 interacts with the hydrophobic core and the mature part of the protein (Gerard and Cline, 2006). There is evidence, though, that cpTat substrates can first insert spontaneously into the thylakoid membrane and interact later with the receptor complex which induces release on the luminal side of the membrane (Berghofer and Klosgen, 1999; Hou et al., 2006). Translocation is believed to be mediated by Tha4 oligomers that form a pore only upon interaction with the receptor complex to which a precursor is bound

(Dabney-Smith et al., 2006; Mori and Cline, 2002) (Fig. 1.2). Tha4 has a single N-terminal transmembrane domain followed by an amphipathic helix and an unstructured C-tail (Mori and Cline, 2001). The amphipathic helix can bind to precursors which are held at the thylakoid membrane by the cpTat-Hcf106 receptor complex, and the C-tails then lead to oligomerisation of Tha4 around the precursor (Aldridge et al., 2012; Dabney-Smith and Cline, 2009; Pal et al., 2013). Recently, a model has been proposed where the amphipathic helices of the Tha4 ‘wreath’ around the precursor insert deeper into the membrane when assembled which, without changing the overall topology of Tha4 itself, creates a pore around the hinge-region between the transmembrane domains and the amphipathic helices of the Tha4 monomers through which the folded substrate is pushed (Pal et al., 2013).

#### **1.4.2 Targeting to the thylakoid membranes occurs mostly via the cpSRP pathway**

Proteins which are destined for the thylakoid membranes can either insert spontaneously without requiring proteinaceous components or energy, or they use the chloroplast signal recognition particle (cpSRP) pathway (Li et al., 1995; Michl et al., 1994) (Fig. 1.2). The central component of the cpSRP pathway is cpSRP54 which shares 44% identity with *E. coli* and 29% with mammalian SRP54 (Franklin and Hoffman, 1993). Similar to other SRP systems, it has been shown that cpSRP54 is able to bind to chloroplast 70S ribosomes and insert the plastid-encoded D1 protein co-translationally into the thylakoid membrane (Nilsson et al., 1999). However, the chloroplast cpSRP54 is unique in its functionality without a SRP-RNA component (Schuenemann et al., 1999b). The chloroplast SRP has additionally a post-translational mode which is unique to chloroplasts and is applied exclusively to insert nucleus-encoded light harvesting chlorophyll *a/b* binding proteins (LHCPs) (Schuenemann et al., 1998). For this specific role a se-

cond cpSRP component, cpSRP43, has evolved specifically in chloroplasts (Schuenemann et al., 1999b; Schuenemann et al., 1998) (Fig. 1.2). cpSRP43 contains four ankyrin repeats flanked by an N-terminal chromodomain CD1 and two C-terminal chromodomains (CD2/3) (Klimyuk et al., 1999). A region within the ankyrin repeats of cpSRP43 can bind to a characteristic internal targeting sequence of LHCPs, called L18, and the CD2 interacts with cpSRP54 forming the so called transit complex (Sivaraja et al., 2005; Tu et al., 2000) (Fig. 1.2). The transit complex interacts with the chloroplast homologue of the SRP receptor, cpFtsY, which exists in a free, soluble form in the stroma where it can interact with cpSRP54 via their highly homologous GTPase and methionine-rich domains (Kogata et al., 1999; Tu et al., 1999). A specific lipid-binding region of cpFtsY allows GTPase hydrolysis by the cpFtsY-cpSRP54 heterodimer only upon thylakoid membrane binding, which triggers dissociation of the transit complex from cpFtsY and membrane insertion of LHCP (Marty et al., 2009) (Fig. 1.2).

The single mutants of both cpSRP components, *cpsrp54* and *cpsrp43* have a surprisingly mild phenotype in *Arabidopsis* (Amin et al., 1999; Klimyuk et al., 1999; Pilgrim et al., 1998). The *cpsrp54* mutant, also called *ffc*, has been reported to have reduced levels of several LHCPs and chlorotic first true leaves which recover partially during later development (Pilgrim et al., 1998). A more recent study, however, shows that the *cpsrp54* knockout is clearly chlorotic and smaller throughout plant development, and that chlorophyll and carotenoid amounts are reduced in the mutants (Yu et al., 2012). The *cpsrp43* mutant, also called *chaos*, was shown to be slightly chlorotic and deficient in the same LHCPs than *cpsrp54* mutants (Amin et al., 1999; Klimyuk et al., 1999). The *cpsrp54 cpsrp43* double mutants were viable, but more chlorotic than either single mutant, suggesting that there is partial functional overlap between the two components, and that each component can be functional in some instances independently

from the other (Hutin et al., 2002). However, this finding also shows that the chloroplast SRP is not strictly necessary for plant survival, and that one LHCP, namely Lhcb4, accumulates normally in the double mutant, suggesting that for this protein an alternative targeting pathway exists (Hutin et al., 2002).

The *Arabidopsis cpftsY* mutant has a chlorotic phenotype which is similar in appearance and pigment-content to the *cpsrp54 cpsrp43* double mutant, but has a lower photosynthetic performance (Tzvetkova-Chevolleau et al., 2007). A similar phenotype was found for a maize *cpftsY* mutant, with a strongly chlorotic appearance and reduced levels of various LHCPs and photosynthetic enzyme complexes (Asakura et al., 2004). Interestingly, the *cpftsY cpsrp54* double mutants were recovered with respect to the more severely chlorotic *cpftsY* single mutants, suggesting that cpSRP54 function depends on cpFtsY and has a dominant negative effect in the absence of cpFtsY, presumably by binding to precursors and inhibiting their targeting via alternative pathways (Tzvetkova-Chevolleau et al., 2007). Such an alternative pathway might involve cpSRP43 and the thylakoid membrane integrase ALB3, which can interact in the absence of cpSRP54 or cpFtsY (Tzvetkova-Chevolleau et al., 2007).

#### **1.4.3 ALB3 and ALB4 have distinct roles in *Arabidopsis* thylakoid biogenesis**

In *Arabidopsis* there are two Alb3 homologues, ALB3 and ALB4, which both belong to the YidC/Oxa1/Alb3 family of membrane insertases (Kuhn et al., 2003; Yi and Dalbey, 2005) (see also Section 3.2). The bacterial YidC can insert proteins into the membrane independent from the Sec or SRP pathway (Serek et al., 2004; van der Laan et al., 2004). In addition, YidC has a Sec-dependent mode, involving the signal recognition particle and the bacterial SecYEG translocase (Samuelson et al., 2000; Scotti et al.,

2000). In mitochondria, the YidC homologue Oxa1 is mainly responsible for co-translational membrane insertion since an SRP or Sec system is absent (Glick and Von Heijne, 1996; Hell et al., 1998; Hell et al., 2001). However, Oxa1 was also proposed to work in a post-translational mode which does not involve the matrix-exposed domains of Oxa1 (Jia et al., 2007).

In *Arabidopsis*, ALB3 directly interacts with cpSRP43 via its C-terminus and is thought to stimulate GTPase activity of the cpFtsY-cpSRP54 heterodimer, thereby promoting the release of LHCP into the membrane (Dunschede et al., 2011; Falk et al., 2010; Lewis et al., 2010) (Fig. 1.2, see also Section 3.2). Consequently, the *alb3* mutant is albino, seedling lethal and severely impaired in thylakoid biogenesis (Sundberg et al., 1997). In *Chlamydomonas*, the knockout of the Alb3 homologues Alb3.1 and Alb3.2 lead both to severe reductions in photosystems I and II (PSI and PSII), but LHCP is only affected in *alb3.1* (Bellafiore et al., 2002; Gohre et al., 2006). The finding that the *Arabidopsis cpsrp54 cpsrp43* double knockout is more severely affected than the respective single mutants suggests that both cpSRP components can to some extent interact individually with cpFtsY and ALB3 (Hutin et al., 2002). The fact that *alb3* is seedling lethal in *Arabidopsis* but the *cpsrp54 cpsrp43* double mutant only pale with normal levels of Lhcb4 might indicate that ALB3 and cFtsY can insert some LHCPs without the help of other factors (Asakura et al., 2008; Hutin et al., 2002). Alternatively, chloroplast chaperones such as cpHsc70 and Hsp93 could guide LHCP to ALB3/cpFtsY in the absence of cpSRP, which might explain why the *ffc (cpsrp54) clpc (hsp93-V)* double mutant is seedling lethal under autotrophic conditions (Rutschow et al., 2008).

ALB4 was originally discovered as a larger protein called ARTEMIS, consisting of an N-terminal receptor kinase-like domain, a nucleotide binding intermediate domain and a C-terminal domain with YidC/Oxa1/Alb3 homology (Fulgosi et al., 2002). It was

detected as a 110 kDa integral inner envelope protein using antibodies against the N-terminus (Fulgosi et al., 2002). Later it was found that the *ARTEMIS* gene contains two separate open reading frames and that the previous ARTEMIS C-terminus is actually a separate protein, called ALB4 (Gerdes et al., 2006). Intriguingly, Fulgosi *et al.* (2002) ascribe the knockout of *Synechocystis* slr1471, an Alb4 homologue, the same phenotype that they could observe for the *artemis* knockout, namely impairment in cell/chloroplast division without defects in thylakoid biogenesis. A later study on *slr1471*, however, came to the opposite conclusion: *slr1471* is strongly impaired in thylakoid biogenesis but not in division (Spence et al., 2004). Similarly, the knockout of *Arabidopsis* ALB4, even though visually not distinguishable from wild type, also suggested a function of ALB4 in thylakoid biogenesis rather than division, since *alb4* has larger chloroplasts which appear more spherical and seem disturbed in thylakoid organisation (Gerdes et al., 2006).

ALB4 is encoded with a predicted transit peptide, ALB4-GFP and ALB3-GFP both produce an overlapping chloroplast signal, and ALB4 could exclusively be detected in the thylakoid membrane with an anti-ALB4 antibody (Gerdes et al., 2006) (see also Section 3.2). Recently, it was shown that *alb4* has a slight growth defect and is impaired in photophosphorylation (Benz et al., 2009). ALB4 but not ALB3 interacts with nucleus and plastid encoded ATP synthase subunits and promotes assembly and stabilisation of the ATP synthase complex (Benz et al., 2009). Moreover, ALB4 can functionally substitute for an *E. coli* *yidC* mutant, suggesting that it has a conserved function. In contrast, the ALB3 C-terminus evolved a specific chromodomain-binding domain which is absent in YidC, Oxa1 and ALB4, and which is necessary to interact specifically with cpSRP43 for LHCP membrane insertion (Benz et al., 2009; Falk et al., 2010).

## 1.5 Aims

In this thesis, a genetic interaction between the protein import motor component Tic40 and the thylakoid targeting factor ALB4 is uncovered. Knockout mutations in the *ALB4* gene and another, yet uncharacterised gene were identified to suppress pale *tic40* mutants, and have been called *stic1* and *stic2*, respectively, for suppressors of t*ic40* locus 1 and 2. Recently, a similar second-site suppressor screen of pale *ppi1* mutants has very successfully uncovered SP1, a novel regulator of chloroplast protein import (Ling et al., 2012). SP1 is a ubiquitin E3 ligase that regulates the degradation and thus the turnover of major TOC components during developmental transitions between plastid types and potentially during stress responses (Ling et al., 2012). Lack of SP1 protein leads to an over-accumulation of atToc75-III, which in the *ppi1* background leads to an increased protein import rate and thus suppression (Ling et al., 2012). The newly identified STIC proteins might similarly regulate protein import, albeit rather indirectly. A co-regulation of protein import, inner envelope membrane biogenesis and thylakoid biogenesis seems possible, and a novel signaling network that communicates thylakoid assembly status to protein import and inner envelope membrane biogenesis factors might potentially be emerging from this study. Furthermore, the relationship between ALB4 and ALB3 is assessed for the first time by analyzing double mutants, and conclusions from this study help to further clarify the role of ALB4 in thylakoid biogenesis.

## 1.6 Figures

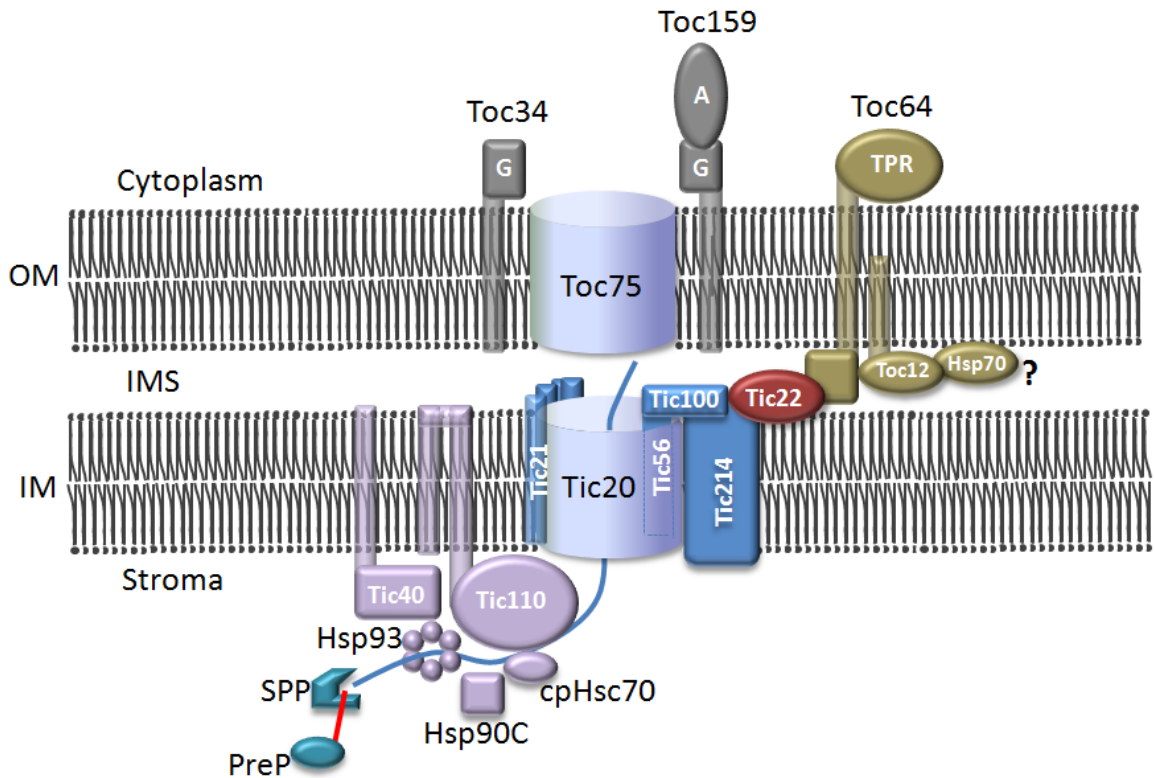


**Figure 1.1.** Components of the chloroplast protein import translocon.

In the outer chloroplast envelope membrane (OM) there are the pre-protein receptor components Toc34 and Toc159 (in *Arabidopsis thaliana* each represented by a small gene family), and the channel component Toc75. Both Toc34 and Toc159 have a membrane and a GTPase domain (G) which are necessary for membrane anchoring and dimerisation. Toc159 has in addition an acidic (A) domain with unknown function. After translocation of the pre-protein through the Toc75 channel, it reaches the channel in the inner chloroplast envelope membrane (IM) which presumably consists of the components Tic214, Tic20, Tic21, Tic100 and Tic56. Tic214 and Tic20 have 6 and 4 transmembrane helices, respectively, while Tic21 is only loosely associated with the channel complex. Tic56 is deeply buried inside the complex. Tic100 is on the surface of the complex in the intermembrane space (IMS) and together with Tic22 is thus probably a first point of contact of the pre-protein with the TIC complex. On the stromal side, Tic40, Tic110 and the chaperones Hsp93, cpHsc70 and Hsp90C (and potentially others) form a motor complex that drives pre-protein translocation by ATP hydrolysis. Stromal processing peptidase (SPP) and presequence protease (PreP) are required for the cleavage and degradation of the transit peptide (red) that guides the pre-protein (blue line) through the import complex. The existence of Toc12 and intermembrane space Hsp70 are disputed, but these components were suggested to form an intermembrane space complex together with Toc64 that guides pre-proteins through the IMS. Toc64 has a cytosolic tetratricopeptide repeat (TPR) domain, which has been suggested to bind pre-proteins that are delivered by cytosolic Hsp90 proteins. Data used from references discussed in the text and from Kikuchi et al., (2013).

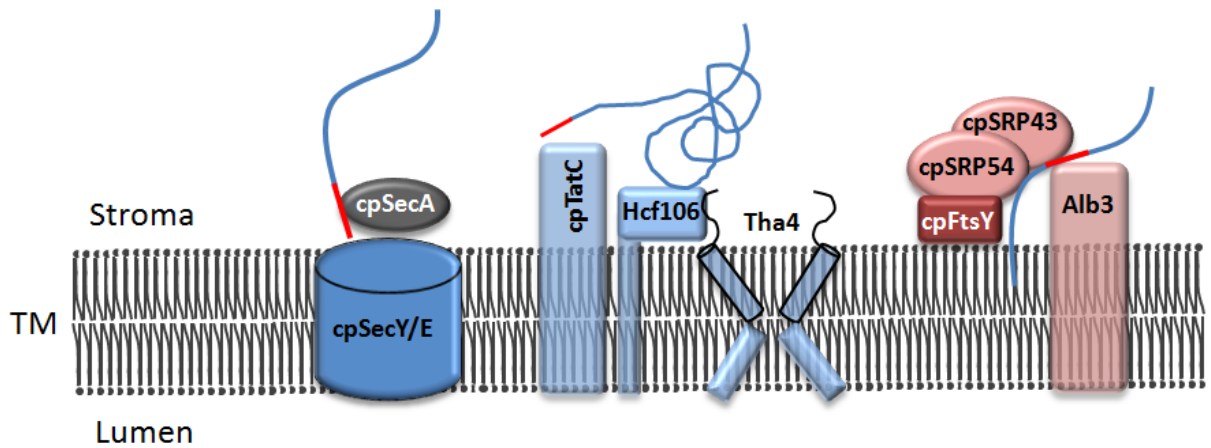


**Figure 1.2.** Pathways for thylakoid targeting.

The targeting of proteins to the thylakoid membranes and lumen can occur via four different pathways. For targeting of luminal proteins, unfolded precursors (blue) can bind to cpSecA in the stroma via an N-terminal targeting sequence (red). cpSecA then guides the precursor to the cpSecY/E channel (composed of the cpSecY and cpSecE components) and drives translocation by ATP-dependent membrane insertion. Folded precursors reach the lumen via the twin arginine translocase (Tat) pathway: precursors interact with a receptor complex composed of cpTatC and Hcf106, then Tha4 monomers assemble spontaneously around the captured precursor, forming a pore in the thylakoid membrane (TM) to allow translocation. For the targeting of membrane proteins, especially light harvesting complex proteins (LHCPs), the precursors bind to the chloroplast signal recognition particle (cpSRP) composed of the two components cpSRP43 and cpSRP54. LHCPs can interact with cpSRP43 via an internal targeting sequence. After precursor binding to the cpSRP, the cpSRP54 component interacts with stromal cpFtsY, which then attaches the complex to the thylakoid membrane. This complex can interact with the insertase Alb3 via a cpSRP43-Alb3 interaction, which leads to membrane insertion of the precursor. A fourth pathway for the targeting of thylakoid membrane proteins occurs spontaneously and thus does not require any proteinaceous components. Data used from references discussed in the text.

# Chapter 2

## Results I

Characterisation of *stic1* and *stic2*, Two Suppressors of the Protein Import Mutant *tic40*

## 2.1 Abstract

In a screen for extragenic suppressors of a mutant of the chloroplast protein import component Tic40, two loci have been previously identified to suppress *tic40* to a similar extent. These loci have been called *stic1* and *stic2*, for suppressor of *tic40* locus 1 and 2, respectively. In this chapter, the identification of the *stic1* locus affecting the *ALB4* gene, the specificity of the suppression for *tic40*, and the effect *stic1* has on suppressing the protein import defect of *tic40* are described. Furthermore, the ALB4 protein was confirmed to be localised exclusively in the thylakoid membranes and to directly interact with the stromal STIC2. Both *stic1* and *stic2* have common defects in the chloroplast ultrastructure, and *stic1 stic2* double mutants as well as *stic1 stic2 tic40* triple mutants show non-additive phenotypes, suggesting that ALB4 and STIC2 act in the same pathway. In an attempt to find this common function, a microarray experiment uncovered the as yet functionally unknown gene *HINAS1* (highly induced in *A*rabidopsis *s*tic) which is more than 20-fold up-regulated in both *stic1* and *stic2*. A hypothesis is suggested which explains suppression in an indirect way, where the *stic1* and *stic2* mutations induce hormone signalling to induce expression of *HINAS1* which, directly or indirectly, leads to a specific replacement of Tic40 function in the *tic40* mutant and therefore to suppression.

## 2.2 Introduction

Chloroplasts may contain an estimated number of over 4000 proteins (Sun et al., 2004) (see also Section 1.3.1), most of which are encoded in the nuclear genome and imported into the chloroplast post-translationally through the translocons at the outer (TOC) and inner (TIC) chloroplast envelope membranes (Jarvis, 2008). These proteins are synthesised with an N-terminal transit peptide which can interact with TOC receptors of the Toc34 and Toc159 families at the chloroplast outer envelope membrane, and thus confers targeting specificity (Kubis et al., 2003; Kubis et al., 2004) (see Section 1.3.1). After the pre-protein (containing the transit peptide) is threaded through the TOC channel formed by Toc75 and the adjacent TIC channel, the transit peptide is cleaved off by the stromal processing peptidase (see Section 1.3.8) and the protein either folds into its native structure or continues in downstream targeting pathways to its proper sub-organelle location (Jarvis, 2008). The identity of the TIC channel is subject to controversial discussions and current research.

Several TIC components have been suggested to fulfil TIC channel functions, namely Tic110 (Heins et al., 2002), Tic20 (Chen et al., 2002), and Tic21 (Teng et al., 2006). Tic110 has two N-terminal transmembrane domains and an C-terminal domain whose structure is disputed. Tic110 channel activity is based on the assumption that the Tic110 C-terminus forms four more transmembrane domains (Balsera et al., 2009; Heins et al., 2002), but other reports suggest that this domain is more likely to be entirely stromal (Jackson et al., 1998) and to form a scaffold for the binding of stromal chaperones (Inaba et al., 2005; Inaba et al., 2003) (see also Section 1.3.6). Recent in-depth structural analyses of the Tic110 C-terminus seem to support the latter model, arguing

against TIC channel function for Tic110 (Tsai et al., 2013). Nevertheless, homozygous *tic110* knockout mutants are embryo lethal at the globular stage, heterozygous *tic110* mutants with reduced Tic110 protein level show chlorosis and impaired protein import capacity, and Tic110 associates with various TOC proteins, confirming its important role in chloroplast protein import (Akita et al., 1997; Kovacheva et al., 2005).

Tic20 was proposed to be part of the TIC channel based on its four predicted transmembrane domains, the severe chlorosis and protein import defects of antisense lines, and the fact that pre-proteins can be efficiently crosslinked to Tic20 during the later stages of protein import (Chen et al., 2002; Kouranov et al., 1998; Kouranov and Schnell, 1997) (see also Section 1.3.6). Knockout mutants of the major Tic20 isoform in *Arabidopsis*, *tic20-I*, are albino and seedling lethal while *tic20-I tic20-IV* double mutants are embryo lethal, suggesting an essential function for Tic20 (Hirabayashi et al., 2011; Kasmati et al., 2011). Similarly, Tic21 has four predicted transmembrane domains and localises to the inner envelope membrane; the *tic21* mutants are albino and defective in protein import, and Tic21 has therefore been suggested to form part of the TIC channel (Teng et al., 2006). Further evidence for Tic20 and Tic21 as TIC channels components came from the discoveries that both are part of a 1-megadalton complex in the inner envelope membrane, and that Tic20 can form functional channels *in vitro* (Kikuchi et al., 2009; Kovacs-Bogdan et al., 2011) (see also Section 1.3.6). Recent research proposes that this 1-megadalton complex consists of Tic20 and three novel TIC components, Tic214, Tic100 and Tic56, with Tic21 loosely associated, and forms the actual TIC channel (Kikuchi et al., 2013). Tic214, encoded on the chloroplast genome by the *ycf1* gene, is a large protein with six predicted transmembrane domains and is exposed on both sides of the inner envelope membrane, while Tic100 is an intermembrane space protein and Tic56 buried inside the complex (Kikuchi et al., 2013).

All components of the 1-megadalton complex, and TOC proteins, could be efficiently pulled down with tagged pre-proteins during import, and purified 1-megadalton complexes reconstituted into lipid bilayers had pre-protein dependent channel activity (Kikuchi et al., 2013).

Most importantly, Tic110 and the co-chaperone Tic40, which has been shown previously to interact with Tic110 (Stahl et al., 1999), are not part of the novel 1-megadalton complex and could not be pulled down with importing precursors, and thus their involvement in protein import is challenged (Kikuchi et al., 2013). However, earlier studies showed that Tic110 can directly bind pre-proteins via their transit peptides (Inaba et al., 2003), and that binding of Tic40 to Tic110 is necessary to release the transit peptide from Tic110 and thus free it for processing (Chou et al., 2006) (see also Section 1.3.7). Kikuchi et al. (2013) used an ATP concentration of 0.5 mM for the protein import reactions which was presumably high enough for the pre-proteins to contact TOC components and the 1-megadalton complex, but not high enough for the later steps of protein import which might require binding to Tic110. In summary, it seems that Tic110 is unlikely the pre-protein conducting channel but most likely plays a role during the late stages of protein import.

Even though Tic40, like Tic110, is encoded by a single gene in *Arabidopsis*, the *tic40* knockouts have a surprisingly mild phenotype (Chou et al., 2003). They are pale but viable and have swollen chloroplasts with a reduced protein import rate, although precursor binding is not impaired (Chou et al., 2003). This is in stark contrast to the embryo lethal *tic110* knockout mutants (Kovacheva et al., 2005), which suggests that Tic40 plays an auxiliary role while Tic110 is essential for plant development. Tic40 inserts into the inner envelope membrane with a single transmembrane span and has a large C-terminal stromal domain that can interact with Tic110 and the Hsp100-family

chaperone Hsp93 (Chou et al., 2003; Stahl et al., 1999) (see also Section 1.3.7). This stromal domain contains a tetratricopeptide repeat (TPR) domain and a domain with similarity to the human co-chaperones Hsp70-interacting protein (Hip) and Hsp70/Hsp90 organizing protein (Hop) (Chou et al., 2003). The Sti1 domain from the human Hip co-chaperone can functionally replace the Tic40 Hip-like Sti1 domain, suggesting a high functional conservation of this domain and thus a co-chaperone function for Tic40 (Bedard et al., 2007). The TPR domain is necessary for binding to Tic110 (Chou et al., 2006) and, interestingly, plants overexpressing Tic40 which lacks the TPR domain show a strong dominant negative effect with a phenotype more severe than the *tic40* mutants, suggesting that impaired binding of Tic40 to Tic110 may titrate away Tic40-interacting factors from Tic110 which are necessary for Tic110 function (Bedard et al., 2007).

Hsp93 which, like Tic110 and Tic40, associates with pre-proteins late during import (Chou et al., 2003), and whose ATPase activity could be stimulated by the Tic40 C-terminus (Chou et al., 2006), might represent such a factor (see Section 1.3.7). However, *tic40 hsp93-V* double mutants, where Hsp93-V represents the major isoform of two in *Arabidopsis*, are even slightly suppressed (Kovacheva et al., 2005), arguing against an important function of Hsp93-V together with Tic110 in the absence of Tic40 (although compensation by the second isoform Hsp93-III has not been examined). Even though the *hsp93-V hsp93-III* double mutants are embryo lethal (Kovacheva et al., 2007), the situation is further complicated by the fact that Hsp93 (also known as ClpC) has a second function as part of the stromal Clp protease (Shanklin et al., 1995), and lethality of the double mutant can therefore not be attributed exclusively to its role in protein import. Recent reports show that in addition to Hsp93 also stromal cpHsc70 and Hsp90C can interact with the TIC apparatus (Inoue et al., 2013; Su and Li, 2010) and

that Tic40 plays an additional role in the post-import re-insertion of intermediate precursors into the inner envelope membrane (Chiu and Li, 2008) (see also Section 1.3.7). But despite these recent advances, the function of the Tic110-Tic40-chaperone complex and its role in protein import remain unclear.

Since *tic40* mutants are viable, a screen for extragenic suppressors of *tic40* (in Col-0) has been performed using ethyl methanesulfonate (EMS) as a chemical mutagen. Eight suppressors of *tic40* were crossed by pairs and found to group into two complementation groups: five alleles of a locus called *stic1* (for suppressor of t*ic40* locus 1) and three alleles of a locus called *stic2* (for suppressor of t*ic40* locus 2). Both *stic1* and *stic2* were found to be semi-dominant mutations, meaning that the level of STIC proteins influences the phenotype in the *tic40* background. While *stic2* was mapped and preliminarily characterised by Dr Feijie Wu, this work focused on the identification and characterisation of *stic1*, and also continued with further in-depth studies on both *stic1* and *stic2*.

## 2.3 Results

### 2.3.1 Identification of the *ALB4* locus

The EMS screen of *tic40* mutants revealed five alleles of the suppressor locus *stic1*. These alleles are named *stic1-1*, *stic1-2*, *stic1-3*, *stic1-4* and *stic1-5*. Before the start of the project, the position of the *stic1* mutation has already been localised on chromosome 1 between the annotation units F3I6 and F2J7. Using a new marker on F3I6, the interval could be further reduced and then contained 120 genes of which only five were known to encode chloroplast-localised products based on the TAIR 8 database. Therefore, an *ad hoc* sequencing approach was taken and, using the *stic1-4* line as a template, a G-to-A mutation in the gene *ATIG24490* (*ALB4*) at position 920 relative to the start codon was identified. Because this mutation was exactly in the junction of intron 3 and exon 4, a splice defect was suspected, and then confirmed by RT-PCR with primers that flanked the mutation site (Fig. 2.1 A). The RT-PCR product was a mixture of five fragments of the sizes 704 bp, 619 bp, 375 bp, 364 bp and 315 bp. The identity of the individual fragments was uncovered by cloning the complete RT-PCR products into the pGEM<sup>®</sup>-T Easy vector and isolating clones by colony PCR that included individual fragments which could be sequenced. Thus, it was found that the 704 bp fragment contained the third and fourth introns, the 619 bp fragment contained the third intron, the 375 bp fragment had a deletion of the first base of exon 4, the 364 bp fragment had a deletion of the first 12 bases of exon 4, and the 315 bp fragment completely lacked exon 4 (Fig. 2.1 A).

The four other alleles were subsequently sequenced, and this confirmed the locus to be *ALB4*: *stic1-1* has a nonsense mutation at position 639 creating a premature stop

codon in the third exon; *stic1-2* has a missense mutation at position 2213 creating an amino acid change of glycine to serine in the ninth exon; *stic1-3* has a nonsense mutation at position 930 creating a premature stop codon in the fourth exon; *stic1-5* has a nonsense mutation at position 2102 creating a premature stop codon in the ninth exon (Fig. 2.1 B). Using semi-quantitative RT-PCR, it could be shown that the *ALB4* mRNA level is reduced in *stic1-1*, *stic1-3* and *stic1-5*; this is presumably because in each case there is at least one downstream exon-junction complex left after termination of translation, which leads to a decapping of the 5' cap and hence nonsense-mediated decay of the mRNA (Fig. 2.1 B). Interestingly, in *stic1-2* the *ALB4* mRNA level is increased, suggesting feedback up-regulation of *ALB4* expression in the mutant (Fig. 2.1 B).

### **2.3.2 Confirmation of the *ALB4* locus with a T-DNA insertion line**

In order to confirm that the *ALB4* locus is responsible for the suppression in the *stic1* mutants, the T-DNA insertion line Salk\_136199/N636199, which was described earlier (Benz et al., 2009; Gerdes et al., 2006), was ordered from the Nottingham *Arabidopsis* Stock Centre (NASC) and named *alb4-1*. This line contains a T-DNA insertion in the sixth intron (Fig. 2.2 A) which leads to two transcript variants, one of which corresponds to the wild-type transcript and so accounts for the residual (less than 10% of the normal level) ALB4 protein in the homozygous mutant (Gerdes et al., 2006). This mutant has been crossed to the Tic40 knockout line *tic40-4* (Kovacheva et al., 2005), and suppression of the pale *tic40-4* phenotype in the *alb4-1 tic40-4* double mutant was verified (Fig. 2.2 B). In parallel, for each of the five *stic1* point mutation lines, a set of dCAPS primers was designed that allowed the distinction between lines which were homozygous, heterozygous or wild type for the corresponding mutation by a simple restriction digestion. All *stic1 tic40-4* suppressor lines were then backcrossed six times

to *tic40-4* in order to remove potential background mutations introduced by EMS during the suppressor screen before they were analysed (Fig. 2.2 B). All the backcrossed *stic1 tic40-4* suppressor lines, and *alb4-1 tic40-4*, show a similar increase in the total chlorophyll level compared to *tic40-4* (Fig. 2.2 C).

An antibody against the soluble C-terminus (last 155 amino acids) of ALB4 was created and it was verified that *stic1-1*, *stic1-3*, *stic1-4* and *stic1-5* are ALB4 null mutants and that *alb4-1*, as described previously, is an ALB4 knockdown mutant (Fig. 2.2 D). As expected for *stic1-2*, which has a missense mutation and accumulates high levels of ALB4 message, the protein level was not affected (Fig. 2.2 D). Interestingly, the similar extent of suppression in *stic1-2 tic40-4* compared the other suppressors suggest that *stic2-1* is nevertheless a loss of function mutant and that the particular glycine (G397) which is affected in *stic1-2* is essential for ALB4's function.

### **2.3.3 Suppression of *tic40-4* by *stic1* is specific and functional**

In order to identify whether the suppression of *tic40-4* by the *stic1* mutations is specific, two *stic1* alleles, *stic1-1* and *stic1-4*, were crossed to a variety of other pale protein import mutants. The *ppi1* mutant is an atToc33 knockout and severely impaired in the import of photosynthetic proteins (Jarvis et al., 1998; Kubis et al., 2003). The *hsp93-V* knockout mutant (also known as *clpC1*) and the heterozygous *tic110* mutant are, like *tic40*, defective in the import of both photosynthetic and non-photosynthetic proteins (Kovacheva et al., 2005). Finally, the hypomorphic *toc75-III-3* allele (previously called *mar1*) accumulates less chlorophyll than wild type due to a missense mutation, and analogous *toc75-III* RNAi lines are severely impaired in the import of both photosynthetic and non-photosynthetic proteins (Huang et al., 2011; Stanga et al., 2009). None of

these pale import mutants, not even the TIC-related mutants, could be suppressed by either *stic1-1* or *stic1-4* (Fig. 2.3 A). Quantification of the total amount of chlorophyll in the double mutants showed no significant difference compared to the single mutants (Fig. 2.3 B). Interestingly, work on the second suppressor locus *stic2* by Dr Feijie Wu yielded virtually identical results (not shown).

In order to extend the analysis of the specificity of suppression, *stic1-1* has also been crossed to chlorotic mutants with defects not directly related to chloroplast protein import. The *rif1* mutant (also called *noa1*) was suggested to play a role in chloroplast ribosome assembly and, indirectly, in the production of nitric oxide (Flores-Perez et al., 2008; Van Ree et al., 2011). The *rif10* mutant is affected in the chloroplast polynucleotide phosphorylase (PNPase), a component necessary for 3' maturation of chloroplast RNAs (Sauret-Gueto et al., 2006). The *prp111* mutant affects the plastid ribosomal protein L11, a component of the large subunit of the plastid 70S ribosome and causes a reduced ribosome activity (Pesaresi et al., 2001). Again, *stic1-1* was not able to suppress any of these chlorotic phenotypes neither at the seedling stage (Fig. 2.4 A and B) nor during later development (not shown).

As *tic40* seems to be suppressed very specifically by *stic1* (and also *stic2*), and since *tic40* mutants have a pronounced protein import defect (Kovacheva et al., 2005), it was investigated whether *stic1-1* can also suppress this import defect. The import experiments were performed as described by Kovacheva et al. (2005) using the precursor of RuBisCO small subunit (pSSU), and the reported import defect of *tic40-4* could be repeated (Fig. 2.4 C). More importantly, import efficiency of pSSU in chloroplasts isolated from the *stic1-1 tic40-4* suppressors was increased compared with *tic40-4*, suggesting that *stic1* suppresses *tic40* at least partly by an increased efficiency of chloroplast protein import (Fig. 2.4 C). Almost identical results were obtained for *stic2* by Dr Feijie

Wu (not shown). The import experiments were performed in collaboration with Karolina Ploessl, a graduate student from the University of Regensburg.

#### **2.3.4 ALB4 is exclusively localised in the thylakoid membrane**

ALB4 has to been described as a protein that, similar to its paralogue ALB3, localises the stromal lamellae of thylakoids (Benz et al., 2009). The fact that *stic1/alb4* mutants suppress *tic40* posed the question of whether a fraction of ALB4 is localised to the inner envelope; this was also suggested because ALB3 is known to interact with the thylakoid Sec component cpSecY/SCY1 and a novel Sec system composed of SCY2 and SECA2 localised to the inner envelope (Klostermann et al., 2002; Skalitzky et al., 2011). A ALB4-YFP fusion construct which was transiently expressed in isolated wild-type protoplasts showed a clear fluorescence signal which coincided with the chlorophyll autofluorescence signal, proving chloroplast localisation (Fig. 2.5 A). Compared to the envelope control Tic110-YFP, ALB4-YFP showed a clear signal inside chloroplasts which likely corresponds to thylakoid localisation (Fig. 2.5 A). However, a potential envelope signal corresponding to a fraction of ALB4-YFP could not be unequivocally disproved with this method, since a minority of ring-like fluorescence patterns were observed (not shown); these could equally have been caused by reduced import efficiency of the large ALB4-YFP fusion protein, or transient localisation of ALB4-YFP in the envelopes while in transit to the thylakoids after import. Therefore, a chloroplast sub-fractionation approach followed by immunodetection of ALB4 in the sub-fractions was taken in order to determine its localisation. Chloroplasts from 5-day-old seedlings or 5-week-old rosette leaves of a line stably expressing FLAG-tagged ALB4 were isolated and sub-fractionated into envelope, stroma and thylakoid fractions. Using anti-FLAG antibody, ALB4-FLAG could exclusively be detected in the thylakoid fractions

both in 5-day-old and 5-week-old plants (Fig. 2.5 B), confirming the previous localisation study on ALB4 (Benz et al., 2009). In parallel, the 14 kDa STIC2 protein has been localised in the stroma by Dr Feijie Wu (not shown).

### **2.3.5 ALB4 and STIC2 interact directly and suppress *tic40* by a common pathway**

The similar phenotypes of *stic1 tic40* and *stic2 tic40*, the shared specificity for suppression of *tic40*, and the recovery of the *tic40* import defect in each case already suggested that ALB4 and STIC2 might act in a common pathway. Further evidence for this hypothesis came from the analysis of *stic1 stic2* double mutants and *stic1 stic2 tic40* triple mutants. The *stic2-1* allele has a point mutation in the junction of the third exon with the third intron (Fig. 2.6 A) which leads to a splice defect and the absence of measurable STIC2 protein (not shown, data from Dr Feijie Wu). Neither *stic1-1*, *stic2-1* nor *stic1-1 stic2-1* had a phenotype visibly different from wild type (Fig. 2.6 B). More importantly, the *stic1-1 stic2-1 tic40-4* triple mutant did not lead to an increased suppression, indicating non-additivity of *stic1* and *stic2* with respect to suppression (Fig. 2.6 B). These observations were supported by chlorophyll measurements (Fig. 2.6 C). It should be mentioned that the previously reported growth phenotype of *alb4* knockout mutants (Benz et al., 2009) could never be observed for any of our *stic1* knockout mutants, or even for the *alb4-1* T-DNA insertion allele which was identical with the one used in the previous study.

In order to assess the possibility of an interaction between ALB4 and STIC2, an immunoprecipitation (IP) assay using the ALB4-FLAG-expressing transgenic line was performed. Chloroplasts from 2-week-old seedlings of the ALB4-FLAG line and a wild-type control were cross-linked with 0.5 mM dithiobis(succinimidyl propionate)

(DSP) before IP with anti-FLAG beads, and the eluate was probed with anti-STIC2 and anti-LHCP as a control. A clear and specific interaction of STIC2 with ALB4-FLAG could be observed (Fig. 2.7 A), while such an interaction could not be observed with non-crosslinked chloroplasts (not shown), suggesting a relatively transient (or weak) but specific interaction. Because ALB4-FLAG is overexpressed and leads to unnaturally high ALB4 protein levels, the interaction was confirmed with a co-IP approach using anti-ALB4 antibody. Chloroplasts from 2-week-old seedlings of wild-type plants were cross-linked with 0.5 mM DSP before co-IP with anti-ALB4 antibody and ALB4 pre-immune serum, and the eluate was again probed with anti-STIC2 and anti-LHCP as a control. ALB4 could not be detected itself because it migrates at the size of the IgG heavy chain, but STIC2 could be clearly and specifically detected (Fig. 2.7 B).

To assess if the observed interaction is likely to be direct, a bimolecular fluorescence complementation (BiFC) approach was taken. Either ALB4-nYFP together with STIC2-cYFP, or ALB4-cYFP together with STIC2-nYFP, were transiently expressed in double-transfected wild-type protoplasts and analysed for a complemented fluorescence signal. Both combinations resulted in a signal, sometimes appearing slightly granular, which clearly resided inside the chloroplasts, suggesting a direct interaction of ALB4 and STIC2 at the thylakoid surface (Fig. 2.7 C). BiFC was conducted in collaboration with Dr Feijie Wu who also cloned STIC2-cYFP and STIC2-nYFP.

### **2.3.6 The *stic1* and *stic2* mutants have similar defects in chloroplast ultrastructure**

For the *alb4-1* knockdown mutant, a swollen chloroplast ultrastructure and a disorganised thylakoid ultrastructure were reported previously (Gerdes et al., 2006). Here, the chloroplast and thylakoid ultrastructures of the *stic1-1* and *stic2-1* knockouts were ana-

lysed and compared. Both the swollen chloroplast and the disorganised thylakoid ultrastructure could not only be verified for *stic1-1* but was also shown for *stic2-1*, further underlining the similar behaviour of the two mutations (Fig. 2.8 A). The disorganised thylakoid ultrastructure is not caused by defects in thylakoid grana, as quantification of the ratio between granal lamellae and attached stromal lamellae (Fig. 2.8 B) as well as the number of stromal lamellae attached per granum (Fig. 2.8 C), did not vary significantly between wild type and the mutants. However, the distance between the thylakoid lamellae is greater in the mutants; they were generally less parallel and frequently seemed disrupted (Fig. 2.8 A, bottom row). The swollen appearance of the mutant chloroplasts (Fig. 2.8 A, top row) was quantified by determining the length-width ratio of the chloroplasts in the cross-sectional plane of the image for a large number of chloroplasts. This ratio was closer to 1 (a sphere would have a ratio of exactly 1) for the mutant chloroplasts (Fig. 2.8 D), confirming the overall swollen appearance of the chloroplasts. A significantly increased number of plastoglobules was seen in the mutant chloroplasts (Fig. 2.8 E), and might indicate a higher lipid turnover, possibly caused by oxidative stress in the mutants (Austin et al., 2006).

### **2.3.7 ALB4 might associate with stromal chaperones**

In order to identify interaction partners of ALB4, IP experiments were performed using the ALB4-FLAG expressing line. Chloroplasts were crosslinked with 0.5 mM DSP before IP with anti-FLAG beads, and the efficiency of the IP was confirmed by detecting ALB4-FLAG with the anti-ALB4 antibody in the eluate (Fig. 2.9). As expected, no interaction between ALB4 and the TIC components Tic110 or Tic40 was observed, confirming the physical separation of the thylakoid-localised ALB4 from the envelope-localised TIC complex. Also, thylakoid-localised LHCPs were not detected as interac-

tion partners of ALB4 which serves as a control to prove that the proteins were not over-crosslinked. On the other hand, stromal chaperones like Hsp93, cpHsc70 and Cpn60 could be crosslinked to ALB4, although Hsp93 and Cpn60 appear also in the wild-type control and might therefore bind non-specifically to the anti-FLAG beads. The interaction between ALB4 and cpHsc70, however, was considered to be specific (Fig. 2.9), also because Dr Feijie Wu could verify a strong interaction between STIC2 and cpHsc70 such that cpHsc70 could be even detected in the eluate on a Coomassie-stained gel (not shown). As STIC2 interacts with ALB4 (Fig. 2.9), the relatively weak interaction of ALB4 with cpHsc70 might be indirect and bridged by STIC2. Another weak but more or less specific interaction might occur with ferredoxin-NADP reductase (FNR), while no interaction could be observed with the ribosomal proteins PRPL2 and PRPL35 (Fig. 2.9). Therefore, this experiment does not provide evidence for a direct participation of ALB4 in co-translational protein insertion, as has been shown for Oxa1 of mitochondria (Szyrach et al., 2003), but rather suggests that it might play a role in chaperoning and redox-regulating protein insertion.

### **2.3.8 Chloroplast cpHsc70 is not the reason for suppression in *stic1 tic40* mutants**

The weak but specific interaction of cpHsc70 with ALB4 and its very strong interaction with STIC2 led to the speculation that cpHsc70 could play a role in the suppression of the *tic40* phenotype. A recent publication showed that cpHsc70 could bind to importing precursors, that *cphsc70* mutants were impaired in protein import, that the *cphsc70-1 tic40* double-mutant genotype is lethal, and that *cphsc70 hsp93-V* double mutants have a much more severe phenotype than either single mutant (Su and Li, 2010). This all suggests that cpHsc70 plays a crucial role in chloroplast protein import in parallel to the Tic40-Hsp93 system. If this is the case, and if indeed cpHsc70 should be limiting for

protein import in the absence of Tic40, then either an increase in the amount of cpHsc70 or an increase in cpHsc70 interacting with the TIC translocon could be the reason for the suppression of the *tic40* defect in the *stic* mutants. Therefore, the total amounts of cpHsc70 were determined and quantified in total protein extracts from isolated chloroplasts of 2-week-old seedlings from wild type, *stic1-1 tic40-4* and *tic40-4*, using the same anti-cpHsc70 antibody as published previously (Su and Li, 2010). The higher abundance of cpHsc70 in *tic40* mutants compared to wild type (Fig. 2.10 A,B) was in line with the findings of Su and Li, (2010). However, the total amount of cpHsc70 was consistently lower in the *stic1-1 tic40-4* suppressor than in *tic40-4* when normalised to either Tic110 or Hsp93 (Fig. 2.10 A,B). Therefore, increased total amounts of cpHsc70 could not be the reason for suppression; suppression might rather lead to a lower requirement for cpHsc70 and therefore, as a secondary effect, to a reduced amount in the suppressors.

To find out if the *stic1* mutation leads to an increased association of cpHsc70 with the envelopes and therefore, irrespective of the total amount of cpHsc70, to an increased efficiency in protein import, wild-type and *stic1* mutant chloroplasts were sub-fractionated into stroma and envelope fractions and the amount of cpHsc70 in each sub-fraction was visualised by immunoblotting. The low amount of cpHsc70 in the envelope fraction was not due to stroma contamination since GAPDH was absent from the envelope fraction (Fig. 2.11 A). However, significantly more cpHsc70 was not associated with the envelopes in the *stic1* mutants compared to wild type (Fig. 2.11 A), suggesting that *stic1* leads neither to an increase in the cpHsc70 level nor to an increased association of cpHsc70 with the envelopes, and hence the TIC translocon.

If cpHsc70 participates in chloroplast protein import and *cphsc70-1 tic40* double mutants are non-viable (Su and Li, 2010), the question remains if cpHsc70 is limiting

for protein import in the *tic40* mutant. Therefore, cpHsc70 was overexpressed in the *tic40-4* background (35S:cpHsc70>*tic40-4*) in order to study the resulting phenotype. Two T<sub>1</sub> plants, #1 and #2, with a single insertion of the construct were identified by analysing the segregation of the T<sub>2</sub> progeny on selective medium. Homozygous T<sub>3</sub> progeny from #1 and #2 were shown to have greatly increased cpHsc70 amounts, proving that the construct was functioning as expected (Fig. 2.11 B). When the phenotypes were compared to *tic40-4*, *stic1-1 tic40-4* and wild type, it was found that 35S:cpHsc70>*tic40-4* is not capable of suppressing *tic40-4* but rather leads to a phenotype paler than *tic40-4* (Fig. 2.11 C). Therefore, it seems that cpHsc70 is not limiting for protein import in the *tic40* mutant, and that protein import cannot be enhanced by simply increasing the amount cpHsc70 in the *tic40* background. Interestingly, another consequence of these results is that the amount of cpHsc70 needs to be well-balanced in chloroplasts as reduced (Su and Li, 2010) and increased (Fig. 2.11 C) amounts of cpHsc70 in the *tic40* background lead to a phenotype more severe than *tic40* itself.

Interestingly, cpHsc70 could also not be detected in the eluates of co-IPs with either anti-Tic110 or anti-Tic40 antibodies while the interactions between Tic110, Tic40 and Hsp93 could be confirmed in the same experiments (Fig. 2.10 C). This partly conflicts with previous results from Su and Li (2010), which show an interaction between cpHsc70 and Tic110.

### **2.3.9 ALB4 and STIC2 are not generally involved in stress responses**

Because neither *stic1* nor *stic2* single mutants had a visible phenotype different from wild type (Fig. 2.6 B), the question remained as to which general purpose the two proteins share *in vivo*. Previous experiments showed that ALB4 and STIC2 are likely func-

tionally related, and that the mutants share at least a common defect in the chloroplast ultrastructure (Fig. 2.8). The significantly higher number of plastoglobules in both mutants might suggest a role in protection from oxidative stress, as high numbers of plastoglobules have been associated with oxidative stress previously (Austin et al., 2006; Eugeni Piller et al., 2012). Therefore, both *stic1* and *stic2* mutants have been subjected to a variety of different stresses, with a main focus on oxidative stress (Fig. 2.12). High light stress (2000  $\mu\text{E}/\text{m}^2/\text{s}$  for 4 hours per day for one week) was performed on the rosettes of 3-week-old mutants, drought stress has been achieved by dehydration of 3-week-old mutants for a further 2 weeks. Direct oxidative stress was performed in various different ways by transferring 2-week-old mutant seedlings to either 250  $\mu\text{M}$  lincomycin, 1  $\mu\text{M}$  Paraquat (methyl viologen), or 60  $\mu\text{M}$  chloramphenicol, followed by growth for a further one or two weeks. Finally senescence-inducing dark stress was performed by wrapping individual 3-week-old rosette leaves in aluminium foil for 3 or 5 days. However, none of the stress treatments resulted in significant differences between either mutant and the wild type (Fig. 2.12 A, B, C), suggesting that the mutants can cope perfectly well with oxidative stress, and that the accumulation of plastoglobules in the mutants has different reasons.

### **2.3.10 Loss of both ALB4 and STIC2 leads to highly induced expression of**

#### ***HINASI***

Since a common function for ALB4 and STIC2 related to the suppression of *tic40* could not be deduced from any of the previous results, a microarray experiment was performed on the *stic* mutants and their transcriptomes were compared to that of wild type. In order to maximise the reliability of the results, RNA was extracted from two *stic1*

alleles (*stic1-1* and *stic1-4*) and two *stic2* alleles (*stic2-1* and *stic2-3*) as well as wild type, and in triplicate for each genotype. The twelve mutant samples and the three wild-type samples were sent to NASC's International Affymetrix Service, and the samples were hybridised onto an AraGene-1-1-ST *Arabidopsis* Gene 16 ArrayPlate and fluorescence intensities representing gene expression levels were measured and provided by NASC.

Using Partek® software, a principal component analysis (PCA) of the complete dataset was performed, and it was found that while the six *stic2* samples cluster together relatively well, the six *stic1* samples have a broader distribution and a higher overlap with the wild-type samples (Fig. 2.13 A). This result already predicted correctly that the list of significantly differentially regulated genes compared to wild type would be longer for *stic2* than for *stic1*. Raw expression data were imported and normalised using the standard Partek® method Robust Multi-Chip Analysis (RMA), and then the *stic1* and *stic2* samples were compared to wild type using the analysis of variance (ANOVA) method. The output was ranked according to the *p*-value and the threshold was set at 0.05 according to the conventions. A Venn diagram comparing the numbers of differentially regulated genes for *stic1* versus wild type and *stic2* versus wild type shows that there is a considerable overlap of 88 genes that are differentially regulated in both mutants (Fig. 2.13 B). The volcano plot showing the fold-changes compared to the corresponding *p*-values of genes from the whole '*stic1* plus *stic2* versus wild type' dataset shows that slightly more genes are up-regulated (right side) than down-regulated (left side) in the *stic* mutants, and that one gene (top right corner) is highly upregulated with a very low *p*-value (Fig. 2.13 C).

The false discovery rate (FDR)-corrected  $p$ -values allow a more stringent analysis by reducing the false discovery rate drastically at the expense of numbers of significantly differentially regulated genes. Using this method, three significant hits were found for *stic1* compared to wild type, and 11 for *stic2* compared to wild type (Table 2.1). The most striking observation is that the top hit for both *stic1* and *stic2* is the same gene, *AT1G35780*. This as yet functionally unknown gene is up-regulated more than 20-fold in both *stic1* and *stic2*, and has therefore been termed *HINAS1* for highly induced in *Arabidopsis stic*, locus 1 (Fig. 2.13 D). This gene is identical with the outlier in the top right corner of the volcano plot (Fig. 2.13 C). It has a similarly unknown paralogue in *Arabidopsis*, *AT1G78150*, which consequently has been termed *HINAS2* but is not differentially regulated in *stic1* or *stic2*. As expected, the second hits for *stic1* and *stic2* compared to wild type are *ALB4* and *STIC2*, respectively, with a drastically reduced expression level of each gene in the corresponding mutant (Table 2.1). The remaining annotated hits are only significant for *stic2* versus wild type, but the trend of expression is still the same in *stic1* versus wild type for each of these genes, again suggesting that *ALB4* and *STIC2* participate in the same pathway. These genes are mostly related to plant hormone signalling, pointing to the possibility that a hormonal signal could rescue the *tic40* phenotype in the *stic* mutants (Table 2.1). A heat map of all the significantly differentially regulated genes shows two genes (*AT4G29200* and the un-annotated Affymetrix ID 13390441) to be down-regulated (blue) and all others to be up-regulated (red) compared to wild type, while *ALB4* is down-regulated only in the *stic1* alleles and *STIC2* (*AT2G24020*) only in the *stic2* alleles (Fig. 2.13 E).

## 2.4 Discussion

Tic40, Tic110, Hsp93 and possibly a range of other chaperones and co-chaperones interact with each other at the inner envelope membrane and exert a function most likely during the late stages of protein import (Chou et al., 2006; Kikuchi et al., 2013). The nature of this function is not yet fully understood, and therefore a forward genetic screen was applied in order to identify genetic interactors of Tic40 which might shed light on Tic40 function and ultimately on the function of this TIC subsystem. Intriguingly, one of two suppressors of *tic40* mutants was mapped to the *ALB4* gene which encodes the thylakoid-localised ALB4 paralogue of the LHCP membrane insertase ALB3. ALB3 interacts with the stromal signal recognition particle (cpSRP) and the cpSRP receptor cpFtsY, which use GTP to target LHCP proteins to the thylakoid membrane (Moore et al., 2000; Tu et al., 1999). ALB3 is essential for LHCP insertion and *alb3* mutants are albino and seedling lethal (Moore et al., 2000; Sundberg et al., 1997). In contrast, *alb4* knockdown mutants are indistinguishable from wild type but have a subtle defect in the thylakoid ultrastructure and swollen chloroplasts, suggesting a non-essential function or a function which is partially redundant with other factors (Gerdes et al., 2006). A growth defect phenotype of the *alb4-1* knockdown line reported later (Benz et al., 2009) could be confirmed neither for the same line nor for the protein null *stic1* mutants in this study. However, the reported defect in the *alb4* thylakoid ultrastructure could be verified for *stic1*, and it appears to affect the stromal lamellae but not the grana; note that Benz et al. (2006) reported a defect for both stromal lamellae and grana. A structural defect of *alb4* in the stromal lamellae would be in line with the previous findings that ALB4 is localised in stromal lamellae but not grana, and is not involved in LHCP insertion (Benz et al., 2009; Falk et al., 2010). In addition, the present

study revealed that chloroplasts of *stic1* mutants contain a significantly higher number of plastoglobules, which suggests a higher thylakoid lipid turnover.

Interestingly, the *stic2* mutant possesses almost identical properties to *stic1* (see also Chapter 5). Dr Feijie Wu showed that *stic2* suppresses *tic40* to a similar extent as *stic1*, that this suppression is also specific, and that it alleviates the *tic40* protein import defect. Furthermore, the present study revealed that the chloroplast ultrastructural defects are very similar for *stic1* and *stic2*, that the two suppressors behave in non-additive ways in double mutants and in triple mutants with *tic40*, and that the ALB4 and STIC2 proteins can interact, possibly even directly. This shows that ALB4 and STIC2 most likely share a common function or pathway, abrogation of which causes the relatively subtle thylakoid ultrastructural phenotype and the swollen chloroplasts in the wild-type *TIC40* background, and the clear suppression of the *tic40* phenotype in the *tic40* background (see also Chapter 5). This leads to the question of what the function or common pathway of ALB4 and STIC2 might be.

While STIC2 is a small 14 kDa stromal protein of unknown function which is related to a ubiquitous family of bacterial proteins of unknown function, more is known about ALB4. Like ALB3, it has a conserved N-terminal domain containing five transmembrane domains, and a C-terminal domain which is less conserved and contains four distinct motifs (Falk et al., 2010). Of these, motifs I and III are conserved between ALB4 and ALB3 while motifs II and IV, which are necessary for the interaction of ALB3 with the cpSRP subunit cpSRP43, are not present in ALB4 (Falk et al., 2010). As it was shown that ALB3 can also interact with the thylakoid-localised SCY1, it was speculated that the C-terminal motifs I and III could be required for this interaction and, thus, that both ALB3 and ALB4 may interact with SCY1 (Falk et al., 2010; Klostermann et al., 2002). Interaction of ALB3 with SCY1 was not necessary for LHCP

insertion, and so ALB3 might play an additional role, *e.g.* in co-translational protein targeting together with SCY1 and cpSRP54 (Moore et al., 2003; Zhang and Aro, 2002). Recently, an envelope-localised Sec system composed of SCY2 and SECA2 was discovered (Skalitzky et al., 2011), and since *stic1/alb4* mutants suppress *tic40* we hypothesised that a portion of ALB4 might be localised in envelopes, possibly interacting with the envelope Sec system in analogous fashion to the ALB3-SCY1 interaction in the thylakoids. However, ALB4 appears to be exclusively localised in the thylakoid membranes, and thus the suppression of *tic40* in *stic1/alb4* mutants is likely indirect. Moreover, it was shown that, in gel filtration experiments, ALB4 does not co-elute with ALB3 or SCY1 but rather with the ATP synthase, and that ALB4 is necessary for correct assembly of the ATP synthase (Benz et al., 2009).

The minor defects that the *stic1/alb4* and *stic2* single mutants (and even the double mutants) have suggest that both ALB4 and STIC2 might play auxiliary roles, and potentially have chaperoning function during membrane protein insertion and thylakoid complex assembly (see also Chapter 5). Indeed, Dr Feijie Wu could observe a strong interaction between STIC2 and cpHsc70 in IP studies, such that cpHsc70 was even clearly visible on Coomassie stained polyacrylamide gels and could be verified by mass spectrometry. In this study, interaction of cpHsc70 with ALB4 was revealed, albeit weaker than with STIC2, and additional chaperones and FNR were shown to associate with ALB4 with a lower specificity than cpHsc70. Thus, ALB4 and STIC2 might guide chaperones and redox-active components to the forming thylakoid complexes, and generally perform regulatory functions. Interestingly, a recent report suggested that cpHsc70 also plays an important role in protein import in parallel to Tic40 and Hsp93 (Shi and Theg, 2010; Su and Li, 2010). We hypothesised that, if *tic40 cpHsc70-1* double mutants are lethal as reported, a general increase of cpHsc70 levels in the chloroplasts

of the *stic* mutants, or an increased interaction of cpHsc70 with Tic110, might suppress the *tic40* phenotype. However, it was clearly shown that cpHsc70 levels are not generally increased in *stic1*, that more cpHsc70 does not bind to the envelopes in *stic1* than in wild type, and that artificial overexpression of cpHsc70 in *tic40* does not lead to suppression but instead to a more severe phenotype than *tic40* (see also Chapter 5). This rather suggests that cpHsc70 levels need to be precisely balanced in chloroplasts, and that both lack and excess of cpHsc70 might have adverse effects on development, a finding that has been previously described for Hsp70 in *Drosophila* (Krebs and Feder, 1997). Strangely, cpHsc70 could be immunoprecipitated neither with anti-Tic110 nor with anti-Tic40 antibodies, whereas Su and Li (2010) showed that both Tic110 and Tic40 could be immunoprecipitated with anti-cpHsc70 antibodies. Thus, the role of cpHsc70 in protein import remains unclear, and it is likely not directly responsible for the suppression of *tic40* by the *stic* mutants.

The weak phenotypes of *stic* single mutants prompted the question: Is the function of the STIC proteins generally dispensable for development and survival, or does it become necessary under certain conditions which could explain the retention of these genes during evolution? The decreased integrity of the thylakoid network of the *stic* mutants might lead to a higher sensitivity of the mutants to certain stress conditions that may occur naturally, and therefore plants containing the functional STIC proteins might have an evolutionary advantage. However, various stresses applied to the *stic* single mutants, including high-light stress, drought stress, oxidative stress, and dark-induced senescence, did not affect the *stic* mutants more than the wild-type control. This shows that the mutants, despite their slightly disorganised thylakoid network, can perfectly cope with a variety of stresses and, therefore, that the STIC proteins are unlikely to be required to confer a general stress tolerance (see also Chapter 5). This does not exclude

the possibility, though, that the STIC proteins are required in a very specific stress situation which has not been tested yet.

As ALB4 resides exclusively in the thylakoid membranes, the suppression of *tic40* by *stic1* and possibly also *stic2* might be indirect. The *stic* mutants might induce a signal, *e.g.*, a hormonal response, which leads to a change in nuclear gene expression. How such a response could specifically suppress *tic40* but not any other pale chloroplast mutants is difficult to understand, unless one assumes that a component is induced in the *stic* mutants which can specifically replace Tic40 function in the *tic40* background. Therefore, it is fascinating that one single component is induced more than 20-fold in both *stic1* and *stic2* in a microarray experiment, whereas the global gene expression levels in the *stic* mutants are generally not very different from wild type. This gene, termed *HINAS1* for highly induced in Arabidopsis stic, is completely unknown and encodes a protein of 286 amino acids with a predicted molecular weight of 31 kDa and a domain of unknown function, DUF 4057. Although it is not predicted to have a transit peptide by TargetP (Emanuelsson et al., 2000), it is predicted to be chloroplast localised by PCLR (Schein et al., 2001) and SLPFA (Tamura and Akutsu, 2007); nuclear localisation is predicted by a few other prediction programs summarised in SUBA3 (Tanz et al., 2013). However, its paralogue HINAS2 is predicted to be localised in chloroplasts by a variety of prediction tools including TargetP and ChloroP (Emanuelsson et al., 1999), other tools listed in SUBA3 predict nuclear localisation. It would be fascinating to find out if HINAS proteins belong to a group of proteins which are dually localised in both plastids and the nucleus, as was previously shown for MFP1 (Samaniego et al., 2006) and Whirly1 (Grabowski et al., 2008).

The 20-fold up-regulation of *HINAS1* in both *stic1* and *stic2* mutants indicates that this is a very specific response to the loss of STIC proteins (see also Chapter 5).

Assuming that the same response occurs in the *tic40* background of the suppressor mutants, it is tempting to speculate that HINAS1 itself, directly or indirectly, leads to the suppression of Tic40. But under which natural conditions is *HINAS1* activated? Apart from *HINAS1*, most of the other genes which are significantly up-regulated in *stic2*, and to a lesser extent also in *stic1*, are related to hormone signalling, mainly involving jasmonate, abscisic acid and ethylene. At least for jasmonate and abscisic acid, it is known that the first steps of biosynthesis occur at the thylakoid membranes in chloroplasts (Bannenberget al., 2009; Nambara and Marion-Poll, 2005). Therefore, the *stic* mutants may lead to a thylakoid defect which is accompanied by a specific hormone signal that in turn leads to an induction of *HINAS1* (see also Chapter 5). Interestingly, based on ATTED-II data (Obayashi et al., 2007) *HINAS1* is co-expressed with two hypothetical glycosyl hydrolases, a group of enzymes that can be induced by sugar starvation (Lee et al., 2007). Moreover, one of the significantly induced genes in *stic2* encodes DIC2, a mitochondrial dicarboxylate carrier which may be involved in gluconeogenesis in the mitochondria (Palmieri et al., 2008). Hence, it may be speculated that the *stic* mutants suffer sugar starvation which leads to a specific response which firstly frees bound sugars by glycosyl hydrolases, secondly increases mitochondrial activity, and thirdly increases the protein import capacity of the chloroplasts by complementing Tic40 function.

## 2.5 Materials and Methods

### 2.5.1 Identification of the *stic1* locus

The candidate gene *ALB4* (*AT1G24490*) was amplified with the four primer pairs seqALB4-1-F (5'-CATTCGGAGCCATAGTTTATG-3'), seqALB4-1-R (5'-TATTTCCAGGTACCTCATCTG-3'), seqALB4-2-F (5'-CCTTGCAGGTACAGTATGTTA-3'), seqALB4-2-R (5'-CTGTTGCATAGAAGGATTTTCG-3'), seqALB4-3-F (5'-AAATGTGTACCACATTGGTGC-3'), seqALB4-3-R (5'-ATTAGATAGAGVTGCTTCAGC-3'), seqALB4-4-F (5'-AAATACCAAGAGAGAAGGGTG-3'), seqALB4-4-R (5'-ACGATATGAGGGAGCAAAATG-3') using high fidelity Taq polymerase and genomic DNA isolated from the *stic1-4* suppressor line. The fragments were gel-purified and sent for sequencing (see Section 6.2.2). After identification of the *stic1-4* point mutation, the process was repeated with genomic DNA from the other four alleles. The *stic1-4* splice defect was confirmed by RT-PCR using the primers RTF (5'-CCTTATTCCTATGGTTTTCGCT-3') and RTR2 (5'-ATGAGATTCCACTGCCAT-TCT-3'), and the PCR products were cloned into pGEM®-T Easy (Promega) and individual clones from each size class were identified by colony PCR with the RTF/RTR2 primer pair. The corresponding plasmids were sent for sequencing. RT-PCR on *stic1-1*, *stic1-2*, *stic1-3* and *stic1-5* was performed using the RTF/RTR2 primer pair and using the control primers eIF4e-F (5'-AAACAATGGCGGTAGAAGACACTC-3'), eIF4e-R (5'-AAGATTTGAGAGGTTT-CAAGCGGTGTAAG-3') (see Section 6.3.1).

### 2.5.2 Genotyping of *alb4* and *stic1*

The *alb4-1* T-DNA line Salk\_136199/N636199 was ordered from NASC and genotyped using the genomic primer pair seqALB4-2-F / seqALB4-2-R and the T-DNA-specific primer pair seqALB4-2-F / SALK LBb1 (5'-GCGTGGACCGCTTGCTGCAACT-3') (see Section 6.2.2). The *stic1* alleles were genotyped using the following dCAPS primers: *stic1-1* with STIC1-1-F (5'-GGTTTATTCTCTACAGGTTGA-3') and STIC1-1-R (5'-CCATGTGTACAGTATAGAAGA-3'); *stic1-2* with STIC1-2-F (5'-GGTGACC-CCAGAATGCCACAAACCT-3') and STIC1-2-R (5'-GTACTAACACGTCCATGTGAT-3'); *stic1-3* with STIC1-3-F (5'-TTGTTTATCTTTGCAGGAGAGAATT-3') and STIC1-3-R (5'-TAACATACTFTACCTGCAAGG-3'); *stic1-4* with STIC1-4-F (5'-TTCTTTATTTTTGTTTATCTCTGCA-3') and STIC1-4-R (5'-TAACATACTGTACTGCAAGG-3'); *stic1-5* with STIC1-5-F (5'-TTGGTCACTAAGGAAGATAAGTCA-3') and STIC1-5-R (5'-CACCTTCTCTCTTGGTATTT-3'). The resulting PCR products were incubated with MnlI (*stic1-1*), BstXI (*stic1-2*), EcoRI (*stic1-3*), PstI (*stic1-4*) and MaeIII (*stic1-5*), respectively. In each case, the restriction enzyme cut the wild-type allele but not the mutant allele (see Section 6.2.4). The *tic40-4* mutant was genotyped as described previously (Kovacheva et al., 2005).

### 2.5.3 ALB4 antibody production

For anti-ALB4 antibody production (see also Section 6.2.7), wild-type cDNA was amplified with ALB4-His-F (5'-GGGGGATCCCCAGTGGAGAAATTCCTAA-3') and ALB4-His-R (5'-GGCCTGCAGGTTACCTCTTCTCTGTTTCAT-3') using high-fidelity Taq polymerase. The PCR product was cloned into pGEM®-T Easy (Promega) and sequenced. Plasmid containing the ALB4 insert and pQE-30 vector (Qiagen) were

both digested with BamHI and PstI, gel-extracted and ligated. XL1-blue cells were transformed with the ligation and grown in the presence of 1% glucose and ampicillin (pQE-30 resistance). Positive clones containing the ALB4 insert were amplified and induced with 1 mM IPTG and then the recombinant protein was extracted and purified. Pure His-tagged ALB4 C-terminus was sent to Harlan Laboratories for antibody production.

#### **2.5.4 Specificity of suppression**

The mutants used to test specificity of suppression have been described before: *ppi1* (Jarvis et al., 1998; Kubis et al., 2003), *hsp93-V-1* and heterozygous *tic110-1* (Kovacheva et al., 2005), *toc75-III-3* (Huang et al., 2011), *rif1-1* (Flores-Perez et al., 2008), *rif10-1* (Sauret-Gueto et al., 2006), *prp111-1* (Pesaresi et al., 2001).

#### **2.5.5 Production of various constructs**

First-strand cDNA prepared from total wild-type RNA was amplified with the primers ALB4-pENTR-F (5'-AAAAAGCAGGCTCCCAAAGCAAGAACACAACAACA-3') and ALB4-pENTR-R (5'-AGAAAGCTGGGTTTCCTCTTCTCTGTTTCATGAGA-3') using high-fidelity Taq polymerase. The PCR product was further amplified with the AttB1/B2 primer pair, and the product was cloned into pDONR 207 vectors using the Gateway® technology (Invitrogen). Positive clones were further sub-cloned into the C-terminal YFP vector p2GWY7 and the C-terminal FLAG vector pH2GW7-FLAG (Karimi et al., 2005; Karimi et al., 2002) (see also Section 6.2.5). The ALB4-YFP construct was used for transient expression in protoplasts, and the ALB4-FLAG construct was used for stable, *Agrobacterium* mediated transformation of wild-type plants.

For the BiFC constructs (see Section 6.2.6), first-strand cDNA prepared from total wild-type RNA was amplified with the primers ALB4-BiFC-F (5'-AAGAGATCTCAAAGCAAGAA-CACAACAACA-3'), ALB4-BiFC-R (5'-AAGGTCGACTCCTCCTCTCTGTTTCAT-GAGA-3') using high-fidelity Taq polymerase; the PCR product was gel purified and digested with BglII and Sall. The vectors pSAT4(A)-nEYFP-N1 and pSAT4(A)-cEYFP-N1 (Tzfira et al., 2005) were digested similarly, and the PCR product was ligated into the vectors using T4 DNA ligase and ligation buffer (NEB). The STIC2-BiFC constructs were prepared by Dr Feijie Wu.

For overexpression of cpHsc70, wild-type cDNA was amplified with the primers cpHsc70-F (5'-AAAAAGCAGGCTCCTTCAAACCCTCCTTGCACTCT-3') and cpHsc70-R (5'-AGAAAGCTGGGTTTCATTGGCTGTCTGTGAAGTC-3') using high-fidelity Taq polymerase. The PCR product was further amplified with the AttB1/B2 primer pair, and the product was cloned into pDONR 207 vector (see Section 6.2.5). Positive clones were further sub-cloned into the pB2GW7 vector, which places cpHsc70 under the CaMV 35S promoter (Karimi et al., 2002). The 35S:cpHsc70 construct was used for stable, *Agrobacterium*-mediated transformation of *tic40* mutant plants.

### **2.5.6 TEM images**

Seedlings of 10 days age grown *in vitro* were brought to the departmental Electron Microscopy Laboratory, University of Leicester. Cotyledons were used for the analysis. All samples were processed and photographed by Natalie Allcock. Images were analysed using Photoshop® software.

### **2.5.7 Microarray experiment**

Total RNA was isolated from 10-day-old seedlings grown *in vitro* using the Spectrum™ Plant Total RNA Kit (Sigma) and then purified using the RNeasy® MinElute™ Cleanup Kit (Qiagen). The samples were sent to the NASC's International Affymetrix Service. Raw data returned from the service was analysed using Partek® software.

## 2.6 Figures and Tables

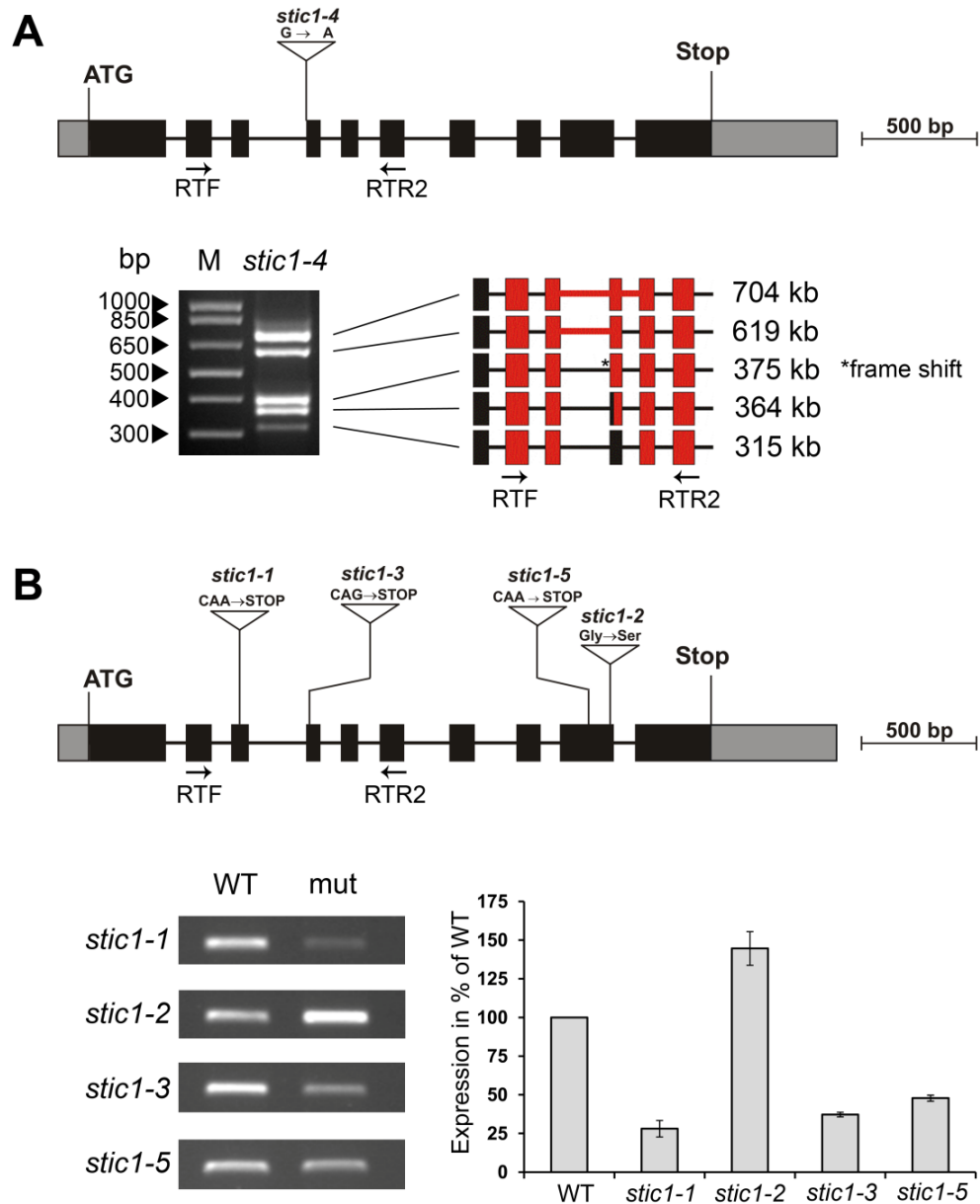


**Figure 2.1.** Analysis of *ALB4* expression in *stic1 tic40* suppressor mutants.

Gene expression was determined for all five *stic1* suppressor alleles by semi-quantitative RT-PCR using the RTF/RTR2 primer pair. The position and nature of the point mutation of each allele is marked in the gene model of *ALB4*. (A) The *stic1-4* mutation leads to a splice defect with five different fragments of the sizes marked on the right, which were cloned and sequenced. The sequences are shown in red; no fragment corresponds to wild type as even the third fragment has a deletion of one nucleotide leading to a frame-shift. M: 1 kb marker. (B) The *ALB4* transcript abundance of *stic1* mutants (mut) compared to wild type (WT) is reduced in *stic1-1*, *stic1-3* and *stic1-4* but increased in *stic1-2*. Quantification shown as percentage of wild-type expression, measurements in triplicates normalised to expression of an *eIF4e* control. Error bars denote the standard errors.

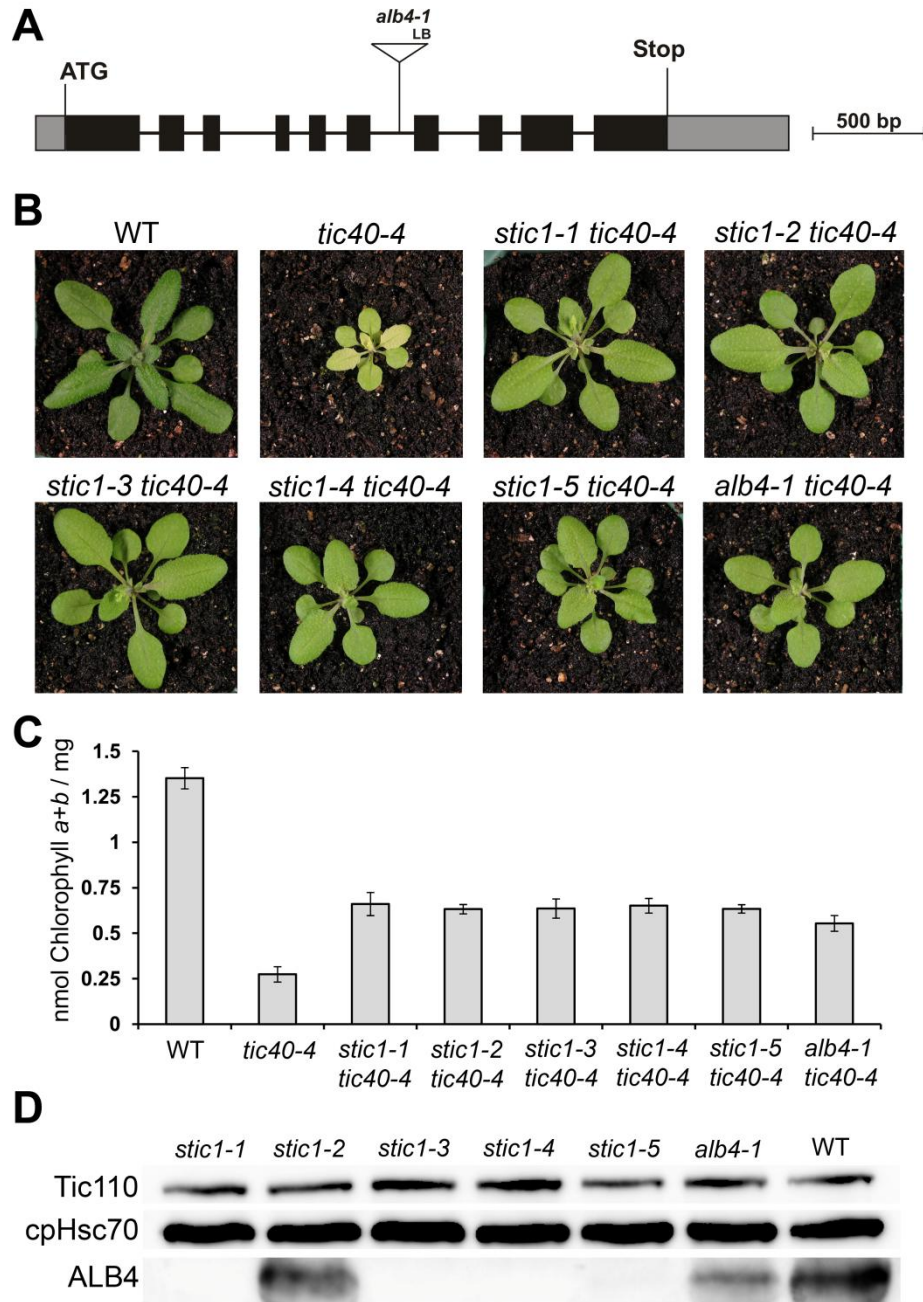


**Figure 2.2.** Analysis of the visible, chlorophyll and protein level phenotypes of *stic1 tic40*. (A) The position of the T-DNA insertion in *alb4-1* (Salk\_136199) is shown in the gene model of ALB4. (B) The five *stic1 tic40* suppressor alleles from the EMS screen are compared to *alb4-1 tic40-4*, wild type and *tic40-4*. Plants are 4 weeks old and directly grown on soil. (C) Quantification of the total chlorophyll amount per mg fresh weight in each line (age: 4 weeks) using the SPAD-502 chlorophyll meter (n=6). Error bars denote the standard errors. (D) Immunoblot with total protein from 2-weeks-old seedlings using anti-ALB4 antibody. The blot shows that *stic1-1*, *stic1-3*, *stic1-4* and *stic1-5* are knockout mutants (protein null), that *alb4-1* is a knock-down allele, and that *stic1-2* accumulates normal levels of ALB4 (which is likely non-functional, see text). Tic110 and cpHsc70 are shown as loading controls.

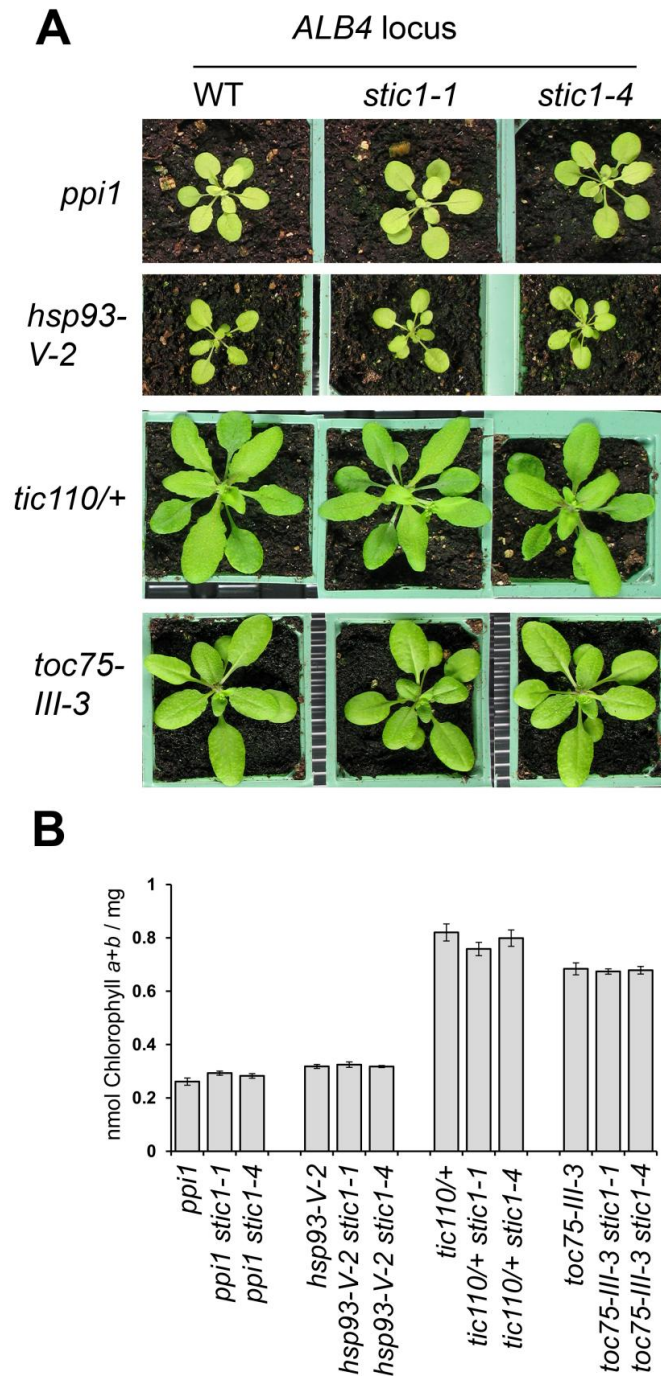


**Figure 2.3.** No suppression of other protein import mutants by *stic1*.

(A) Two alleles of *stic1*, *stic1-1* and *stic1-4*, were crossed to pale/pale-green protein import mutants: *ppi1* (= *attoc33*), *hsp93-V* (= *clpC1*), heterozygous *tic110*, and the hypomorphic allele *toc75-III-3*. Double mutants were grown directly on soil and compared to the single mutants (wild type at the *ALB4* locus) at the age of 4 weeks. (B) Quantification of the total chlorophyll amount per mg fresh weight in each line from (A) (age: 4 weeks) using the SPAD-502 chlorophyll meter (n=6). Error bars denote the standard errors.

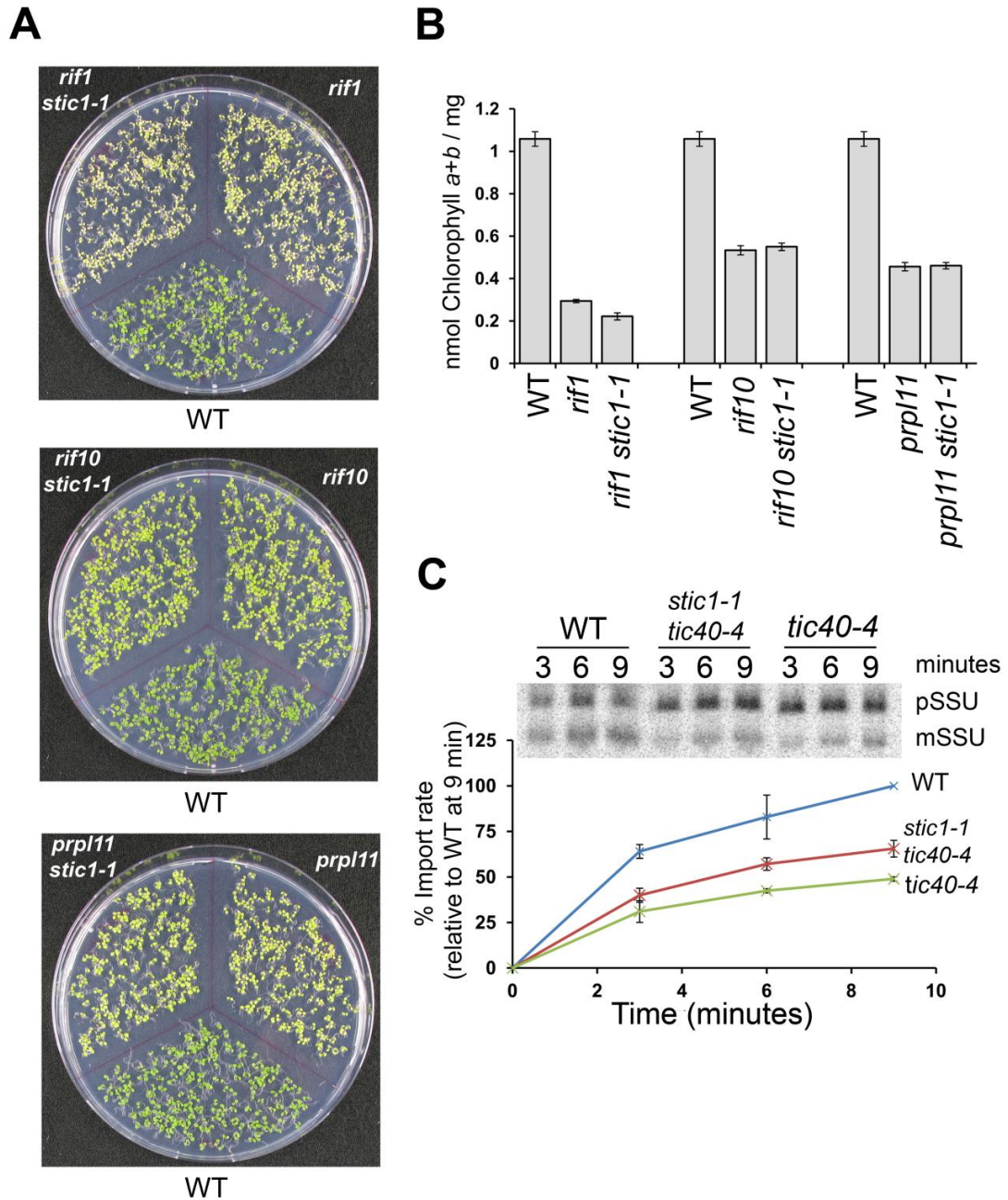


**Figure 2.4.** Specificity and functionality of the suppression.

(A) The allele *stic1-1* was crossed to the pale mutants *rif1*, *rif10* and *prpl11* which are defective in functions different from protein import. Double mutants were compared to single mutants and wild type at 1 week post-germination on half-strength MS plates containing 0.6% sucrose. (B) Spectrophotometric quantification of the total chlorophyll amount per mg fresh weight in each line from (A) using DMF extraction (n=6). Error bars denote the standard errors. (C) Import experiments using radiolabeled precursor of RuBisCO small subunit (pSSU) and chloroplasts from wild type, the *stic1-1 tic40-4* suppressor and *tic40-4*. Mature RuBisCO small subunit (mSSU) was quantified in samples from 3, 6 and 9 minutes incubation time, respectively, for each genotype. Values are averages from three independent experiments, given as percentages of wild type after 9 minutes incubation. Error bars denote the standard errors. Import experiments were performed in collaboration with Karolina Ploessl.

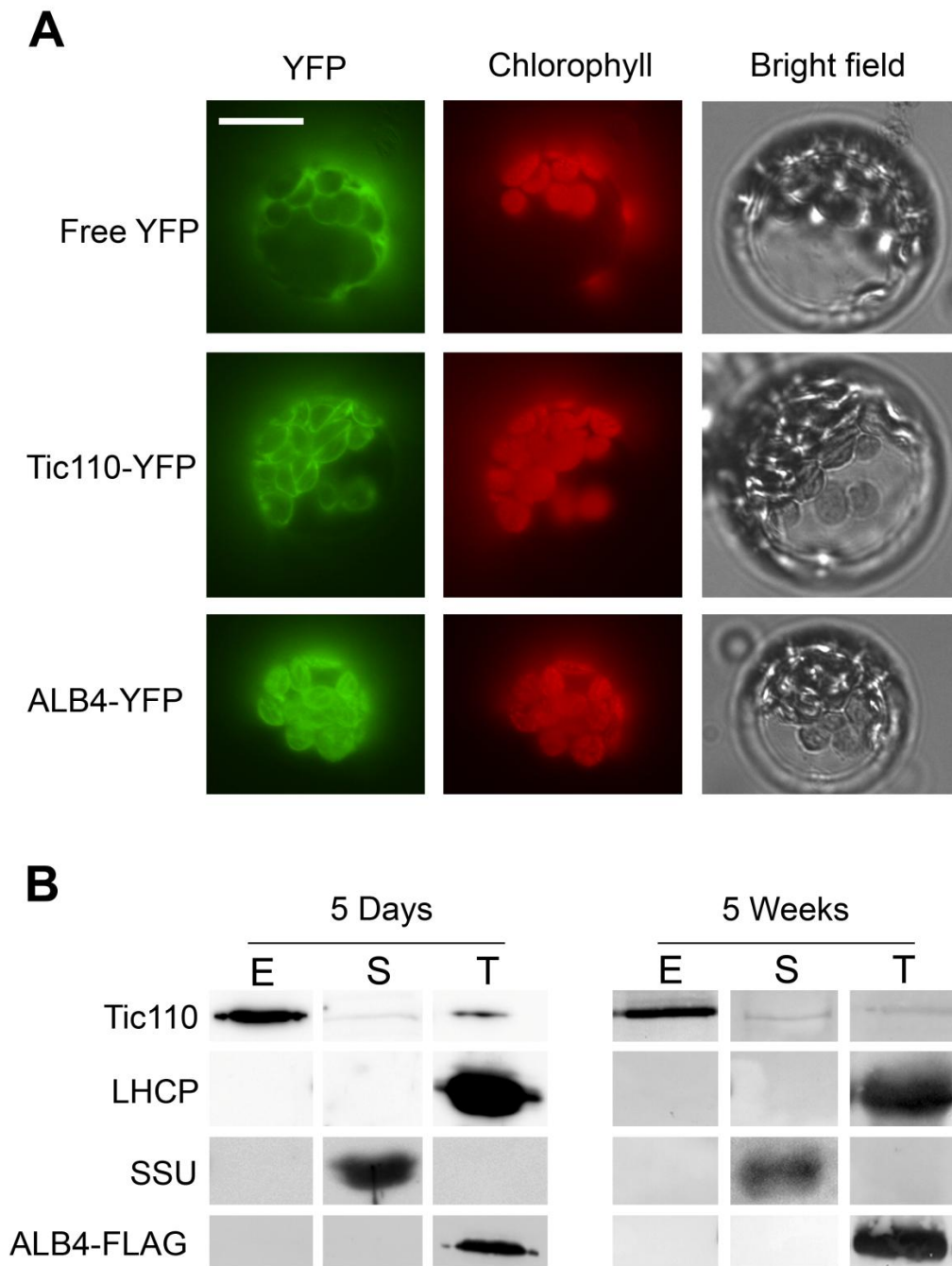


**Figure 2.5.** Subcellular localisation of ALB4.

(A) Fluorescence microscopy with isolated wild-type protoplasts transfected with YFP constructs. An ALB4-YFP construct shows a clear YFP signal (green) that co-localises with chloroplasts (red due to auto-fluorescence of chlorophyll), while free YFP accumulates in the cytosol in the gaps between the chloroplasts. Tic110-YFP is used as a control for chloroplast envelope localisation. The top left scale bar is  $\sim 12.68 \mu\text{m}$  long. (B) Sub-fractionation of chloroplasts from ALB4-FLAG expressing plants of different ages (5 days and 5 weeks) into envelope (E), stroma (S) and thylakoid (T) fractions. Controls are Tic110 (envelope protein), LHCP (thylakoid protein), and RuBisCO small subunit (SSU, stromal protein). ALB4-FLAG can be detected exclusively in the thylakoid fractions in immunoblots using the anti-FLAG antibody.

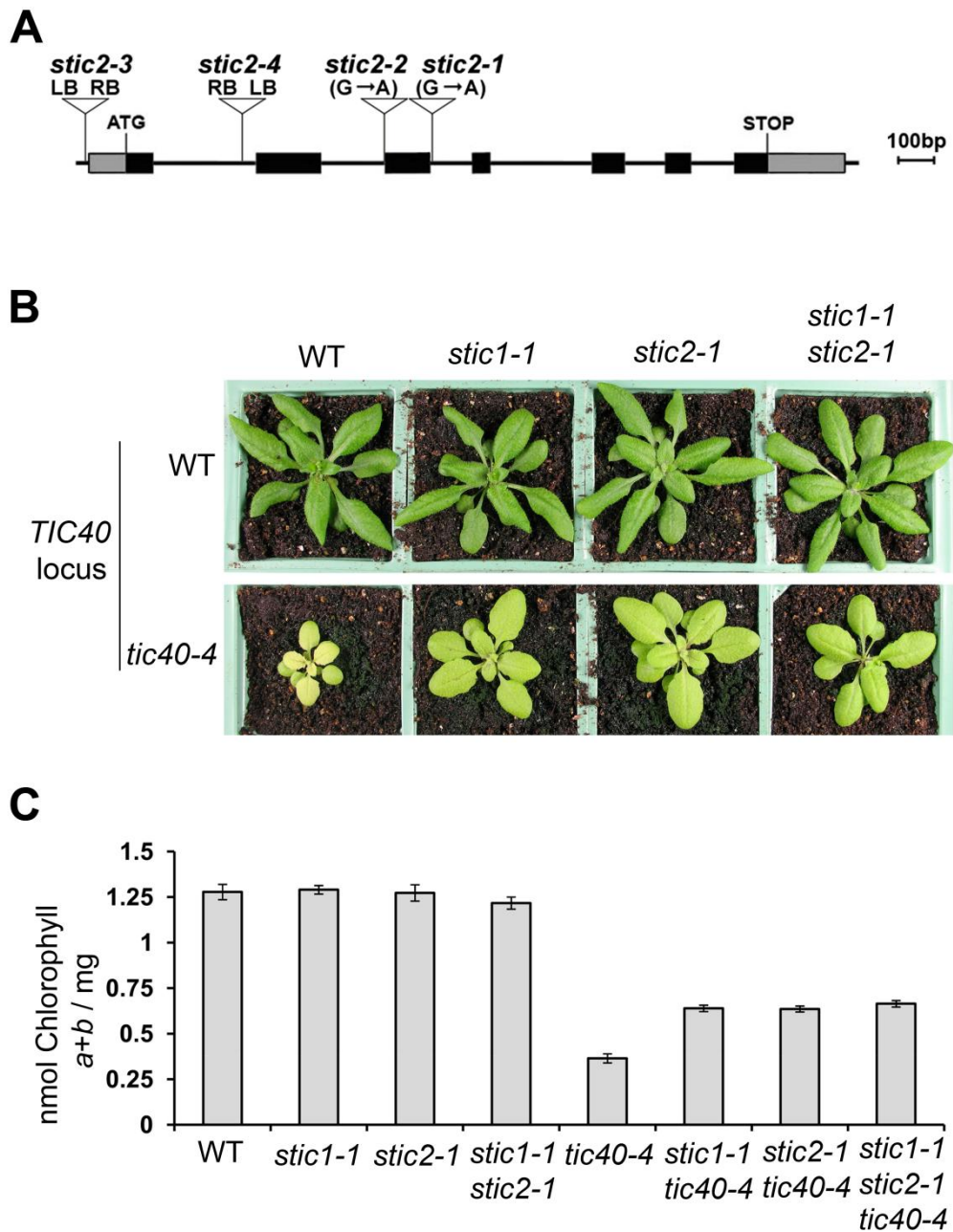


**Figure 2.6.** Genetic interaction between ALB4 and STIC2.

(A) Gene model of *STIC2* showing the mutant alleles (*stic2-1*, *stic2-2*: nonsense alleles; *stic2-3*, *stic2-4*: T-DNA insertion alleles). (B) Phenotypes of 4-week-old mutants directly grown on soil. Top row: *stic* mutants compared to wild type (WT). Bottom row: *stic tic40* mutants compared to *tic40*. (C) Quantification of the total chlorophyll amount per mg fresh weight in each line from (B) (age: 4 weeks) using the SPAD-502 chlorophyll meter (n=6). Error bars denote the standard errors.

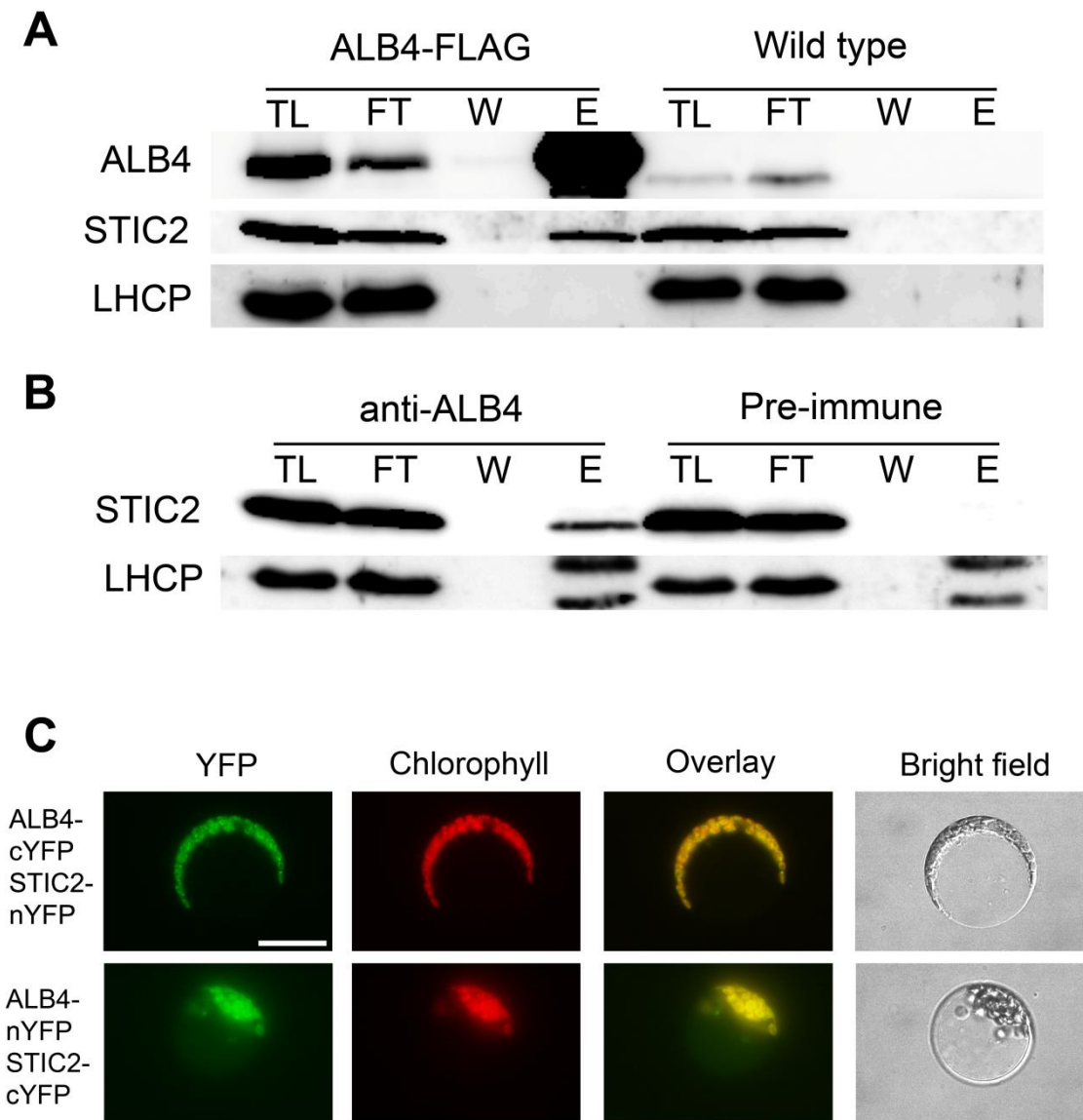


**Figure 2.7.** Physical interaction between ALB4 and STIC2.

(A) Immunoprecipitation with anti-FLAG beads using 100 million chloroplasts isolated from 2-weeks-old seedlings of a ALB4-FLAG overexpressing line cross-linked with 0.5 mM DSP. TL: total lysate, FT: flow-through, W: wash, E: elute. Loading: 0.45% of TL, 0.45% of FT, ~4.5% of W, 36% of E. Detection of HRP-linked secondary antibodies with ECL method. (B) Co-immunoprecipitation using 100 million wild-type chloroplasts cross-linked with 0.5 mM DSP; Pull-down with anti-ALB4 antibody and protein A sepharose beads. TL: total lysate, FT: flow-through, W: wash, E: elute. The proteins were eluted in 50  $\mu$ l of 2 $\times$  protein loading buffer, the loading and detection is the same as in (A). Note that ALB4 cannot be detected because it runs at the size of the IgG heavy chain which masks the ALB4 band in the elute. (C) BiFC by double transfection of wild-type protoplasts with either ALB4-cYFP and STIC2-nYFP or ALB4-nYFP and STIC2-cYFP. The complemented YFP fluorescence signal was visible in the chloroplasts (their location is indicated by the red chlorophyll autofluorescence), as shown in the overlay. The top left scale bar is ~12.68  $\mu$ m long.

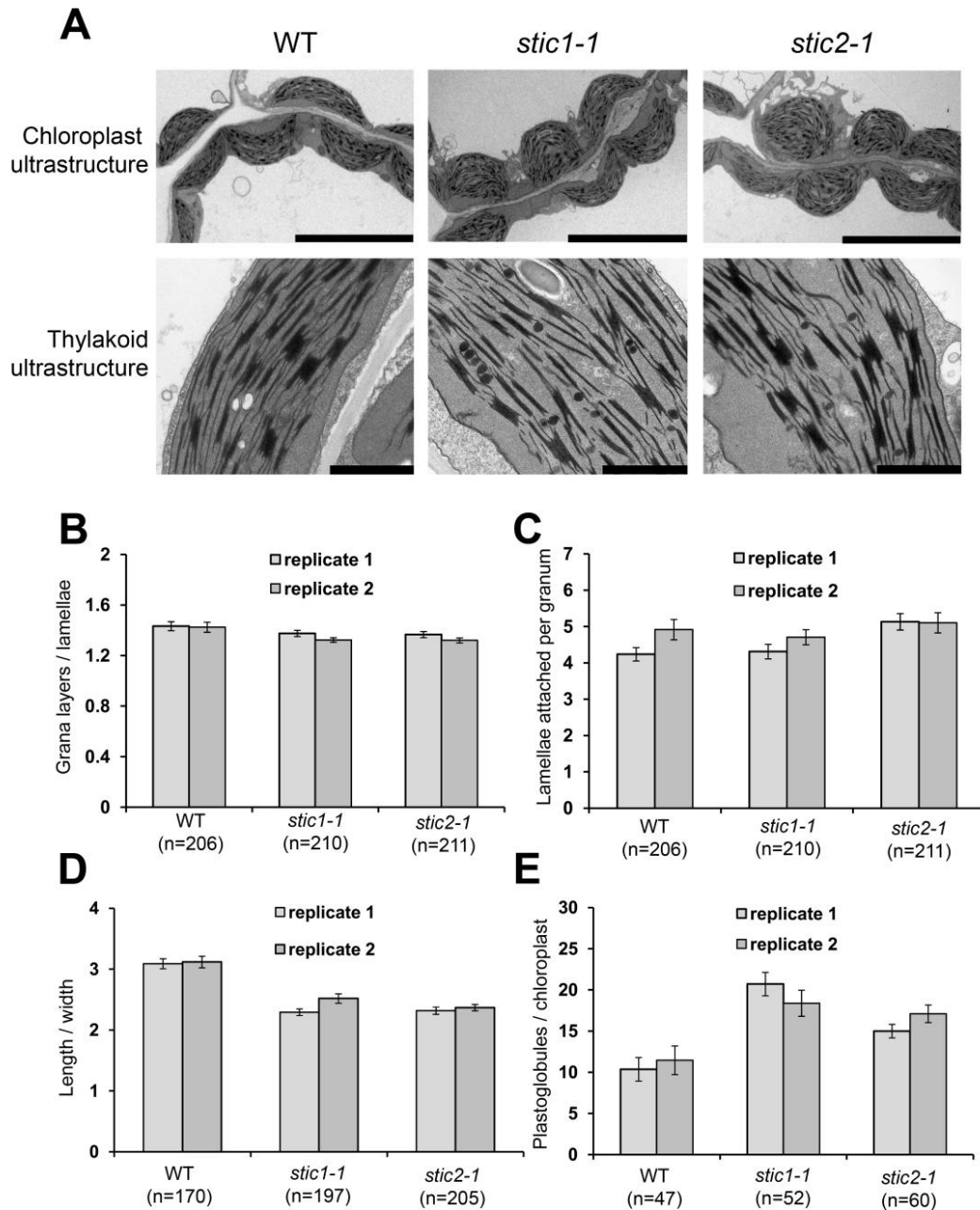


**Figure 2.8.** Chloroplast ultrastructure in the *stic1-1* and *stic2-1* single mutants.

(A) Chloroplast ultrastructure in the top row showing the slightly swollen phenotype of *stic1-1* and *stic2-1* mutant chloroplasts compared to wild type. Scale bar at the bottom right is 10  $\mu\text{m}$ . Thylakoid ultrastructure in the bottom row showing the disorganised stromal lamellae in *stic1-1* and *stic2-1* mutant chloroplasts compared to wild type. Scale bar at the bottom right is 1.5  $\mu\text{m}$ . (B) Quantification of the ratio between the numbers of granal lamellae and stromal lamellae attached per granum for n grana (numbers shown in brackets) in two biological replicates (TEM images from two separate seedlings of the same plate). (C) Quantification of the numbers of stromal lamellae per granum for n grana (numbers shown in brackets) in two biological replicates. (D) Quantification of the ratio between the length and the width of a chloroplast (in the cross-sectional plane) for n chloroplasts (numbers shown in brackets) in two biological replicates. (E) Quantification of the numbers of plastoglobules per chloroplast for n chloroplasts (numbers shown in brackets) in two biological replicates. The error bars in (B), (C), (D) and (E) denote the standard errors.

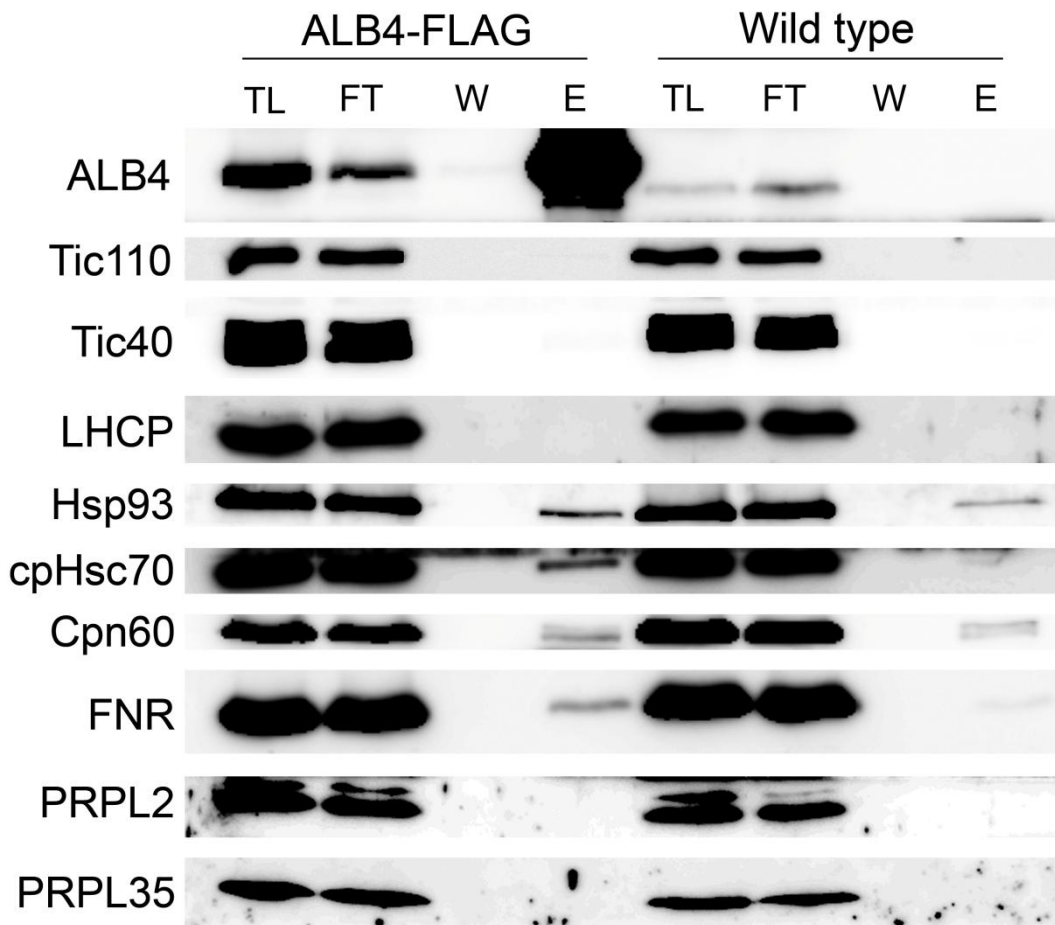


**Figure 2.9.** Analysis of ALB4-FLAG protein interactions.

Chloroplasts (100 million) from ALB4-FLAG overexpressing plants or wild type were cross-linked with 0.5 mM DSP (15 minutes) and quenched with 50 mM glycine (15 minutes). The chloroplast pellet was lysed in a volume of 2 ml lysis buffer and immunoprecipitation was performed using anti-FLAG beads. The total lysate (TL) was collected directly after lysis and 9  $\mu$ l was loaded (0.45%). The flow-through (FT) was collected from the supernatant after incubation with the beads and 9  $\mu$ l was loaded (0.45%). The wash (W) was collected after the sixth wash of the beads with wash buffer (~4.5% was loaded). For elution, the beads were directly incubated in 50  $\mu$ l of 2 $\times$  protein sample buffer and 18  $\mu$ l of the elute (E) was loaded (36%). ALB4 was detected with the anti-ALB4 antibody (note the shift in the ALB4-FLAG band caused by the FLAG tag) using the enhanced chemiluminescence (ECL) technique. Envelope controls are Tic110 and Tic40; the thylakoid control is LHCP. Interactions (but not necessarily specific ones) can be seen for the stromal proteins Hsp93, cpHsc70, Cpn60 and FNR but not for the ribosomal proteins PRPL2 and PRPL35. Blots have been repeated twice.

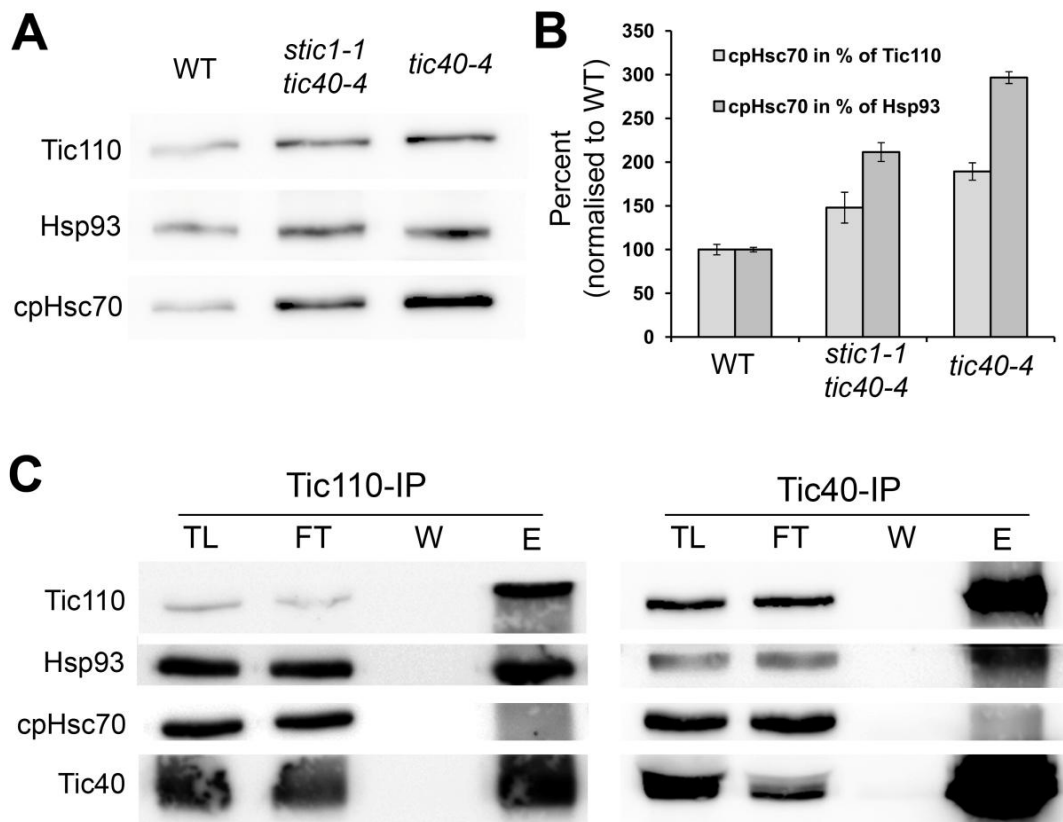


**Figure 2.10.** Chloroplast cpHsc70 is not more abundant in suppressor mutants than in *tic40*.

(A) Immunoblots with total protein samples from 2-week-old wild-type (WT), *stic1-1 tic40-4* and *tic40-4* seedlings grown *in vitro*. Total protein was quantified by a Bradford assay and loading was normalised to equal amounts of total protein. Detection of HRP-linked secondary antibodies with ECL method. (B) Quantification of the intensities of the cpHsc70 bands in (A) relative to the band intensities of Tic110 or Hsp93 given in percentage of Tic110 and Hsp93, respectively, and normalised to wild type. (C) Co-immunoprecipitation with anti-Tic110 (left) and anti-Tic40 antibody (right) using 100 million wild-type chloroplasts cross-linked with 0.5 mM DSP. TL: total lysate, FT: flow-through, W: wash, E: elute. Loading: 0.45% of TL, 0.45% of FT, ~4.5% of W, 36% of E. Detection of HRP-linked secondary antibodies with ECL method.

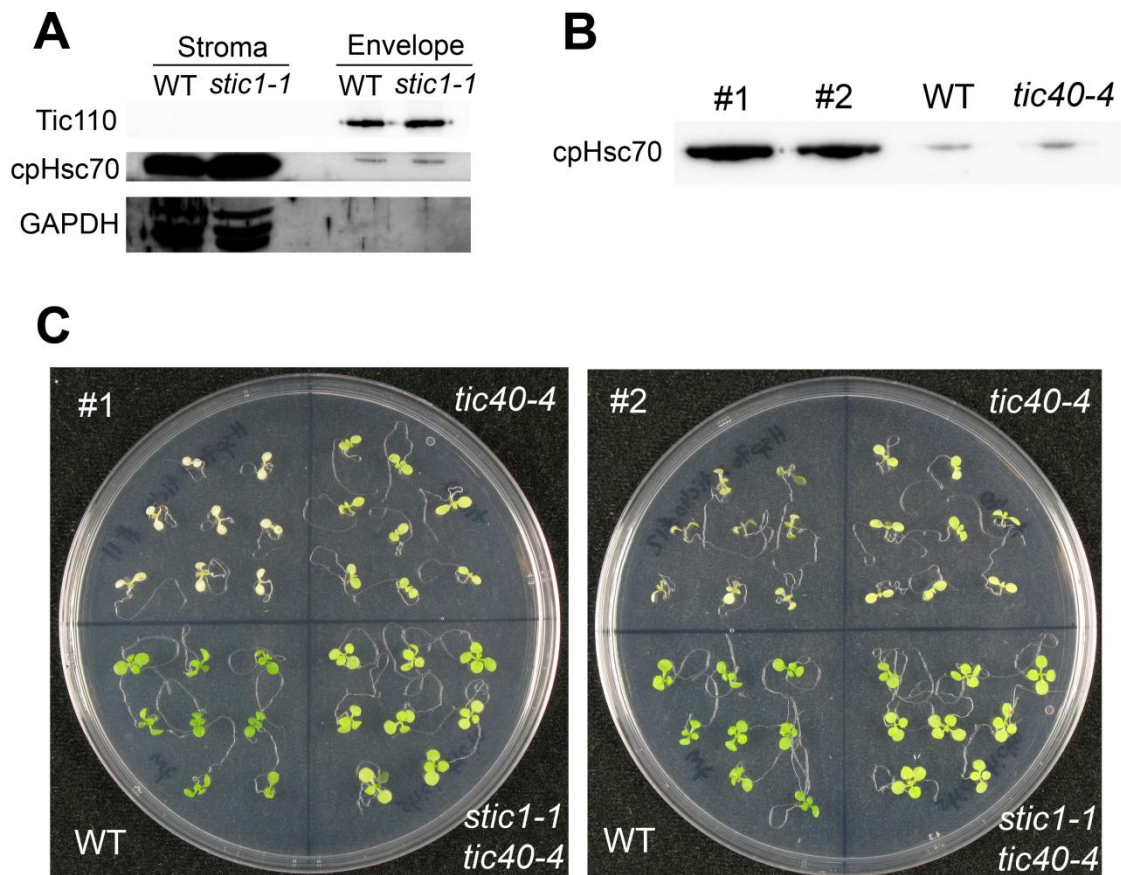


**Figure 2.11.** Chloroplast cpHsc70 is not responsible for suppression.

(A) Sub-fractionation of chloroplasts from 2-week-old seedlings into stroma and envelope fractions. Equal proportions of sample were loaded for wild type (WT) and *stic1-1*. Tic110 and GAPDH antibodies were used to show purity of envelope and stroma fractions, respectively. Detection of HRP-linked secondary antibodies with ECL method. (B) Overexpression of *cpHsc70* under the control of the 35S promoter in the *tic40-4* background (35S:*cpHsc70*>*tic40-4*). Total protein was extracted from 2 weeks old seedlings of wild type (WT), *tic40-4* and homozygous T<sub>3</sub> progeny of two T<sub>1</sub> plants, #1 and #2, that contain the construct. Total protein was quantified by a Bradford assay and loading was normalised to equal amounts of total protein (10 µg). Detection of immunoblot using HRP-linked secondary antibodies with ECL method. (C) Phenotypes of 2-week-old seedlings of the homozygous T<sub>3</sub> progeny of #1 and #2 overexpressing cpHsc70 in the *tic40-4* background, compared to wild type (WT), *tic40-4* and *stic1-1 tic40-4*.

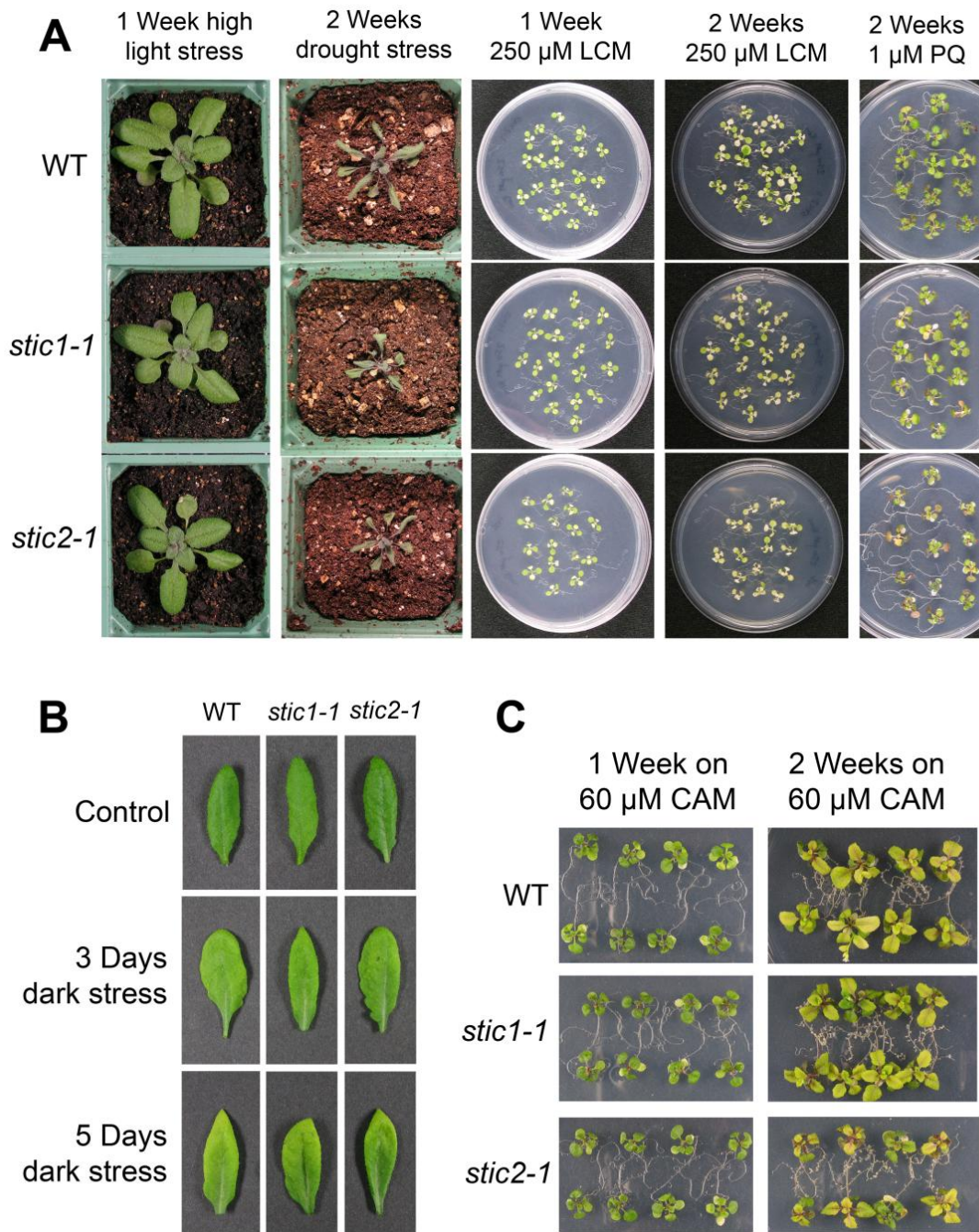


**Figure 2.12.** Stress experiments with the *stic1-1* and *stic2-1* single mutants.

(A) Three-week-old plants were treated with 4 hours of 2000  $\mu$ E/m<sup>2</sup>/s high light per day for one week (first column); 3-week-old plants were withdrawn from watering for two weeks (second column); 2-week-old seedlings grown *in vitro* were transferred on half-strength MS containing 250  $\mu$ M lincomycin (LCM) and photographed after one week (third column) and two weeks (fourth column); two weeks old seedlings grown *in vitro* were transferred to half-strength MS containing 1  $\mu$ M Paraquat (PQ) and photographed after 2 weeks (fifth column). (B) Individual rosette leaves of 4-week-old plants were wrapped in aluminium foil to induce senescence for 3 and 5 days. (C) Two-week-old seedlings grown *in vitro* were transferred to half-strength MS containing 60  $\mu$ M chloramphenicol (CAM) and photographed after one and two weeks, as indicated.

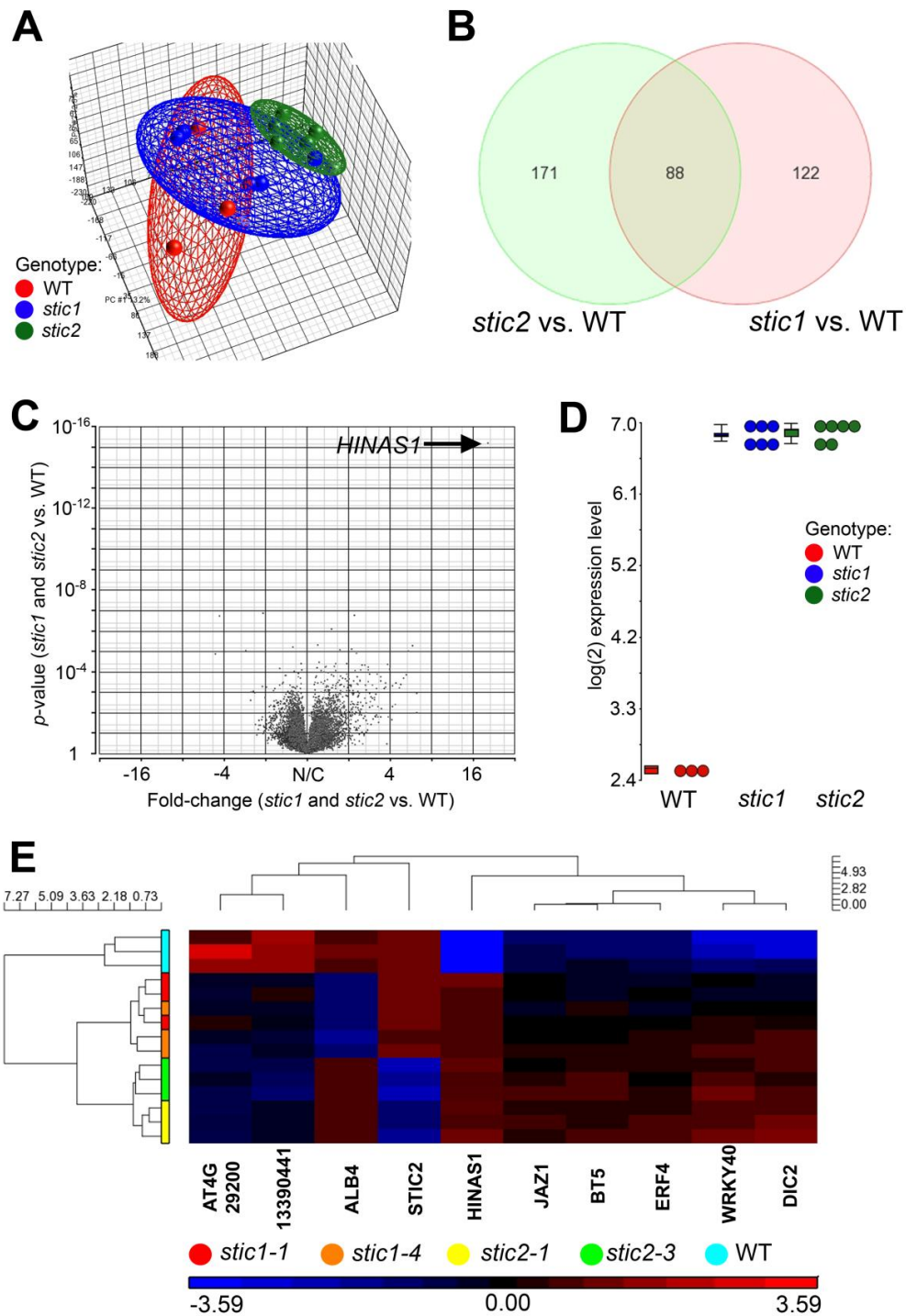


**Figure 2.13:** Microarray analysis of the *stic* mutants compared to wild type. (A) PCA plot of three biological replicates of *stic1-1* and *stic1-4* (blue), *stic2-1* and *stic2-3* (green) and wild type (red). (B) Venn diagram showing the numbers of significantly differentially regulated genes (uncorrected  $p$ -value < 0.05) for *stic1* vs. wild type and *stic2* vs. wild type (WT). (C) Volcano plot showing the fold-change of *stic1* and *stic2* vs. wild type (WT) against the corresponding  $p$ -value for the complete dataset. *HINAS1* is indicated by the black arrow. (D) Log<sub>2</sub> expression level of *HINAS1* (*ATIG35780*) in the three wild-type replicates and the six *stic1* and *stic2* replicates. (E) Heat map of genes which are significantly differentially regulated in either *stic1* or *stic2* compared to wild type (FDR-corrected  $p$ -value < 0.05).

Gene Symbol	p-value ( <i>stic1</i> vs. WT)	Ratio ( <i>stic1</i> vs. WT)	Fold-Change ( <i>stic1</i> vs. WT)	p-value ( <i>stic2</i> vs. WT)	Ratio ( <i>stic2</i> vs. WT)	Fold-Change ( <i>stic2</i> vs. WT)
<i>HINAS1</i>	1.91225E-15	20.0887	20.0887	1.81686E-15	20.349	20.349
<i>ALB4</i>	1.84617E-10	0.236422	-4.22972	0.727861	0.974033	-1.02666
<i>STIC2</i>	0.901168	0.980737	-1.01964	1.6587E-08	0.132064	-7.57211
<i>JAZ1</i>	3.83599E-06	1.89613	1.89613	7.3037E-08	2.52585	2.52585
13390441	1.17429E-06	0.25836	-3.87057	2.32245E-07	0.207171	-4.82692
<i>BT5</i>	0.000238407	1.74867	1.74867	2.16936E-06	2.49555	2.49555
<i>WRKY40</i>	3.95181E-05	4.76687	4.76687	4.81478E-06	6.9297	6.9297
<i>DIC2</i>	0.000112954	4.16824	4.16824	5.88612E-06	6.99563	6.99563
<i>ERF4</i>	0.000137247	2.00748	2.00748	7.86302E-06	2.56815	2.56815
<i>AT2G37030</i>	0.0483907	1.26685	1.26685	2.19439E-05	2.05723	2.05723
<i>AT4G29200</i>	5.51963E-05	0.235307	-4.24976	1.91148E-05	0.198286	-5.04321
<i>AT1G80440</i>	0.000466836	1.72714	1.72714	0.000021792	2.16052	2.16052

**Table 2.1:** Transcript IDs and gene symbols of genes which are significantly up- or down-regulated in either *stic1* or *stic2* mutants compared to wild type (WT). The *p*-values (for either *stic1* or *stic2* vs. WT) are the uncorrected *p*-values. The expression ratios and fold-changes compared to WT are shown for each gene; negative numbers denote down-regulation. *HINAS1* is up-regulated more than 20-fold in both *stic1* and *stic2* mutants compared to WT. *ALB4* is significantly down-regulated only in *stic1* mutants, and *STIC2* in *stic2* mutants. *JAZ1* encodes a member of the jasmonate ZIM-domain family of proteins which are negative regulators of gene expression and are degraded by the 26S proteasome upon binding of isoleucine-bound jasmonic acid (JA-Ile) as a response of a jasmonate signal (Chini et al., 2007; Thines et al., 2007). The ID 13390441 is an un-annotated sequence on chromosome 2. *BT5* is an auxin-responsive gene and encodes a member of the BTB and TAZ domain proteins which are involved in gametophyte development (Robert et al., 2009). *WRKY40* encodes a repressor of abscisic acid (ABA)-responsive gene expression which is sequestered at the chloroplast envelope by interacting with the cytosolic C-terminus of the envelope membrane-spanning magnesium-protoporphyrin IX chelatase H subunit (CHLH/ABAR) upon an ABA signal (Shang et al., 2010). *DIC2* encodes a mitochondrial dicarboxylate carrier (Palmieri et al., 2008). *ERF4* is induced by ethylene, jasmonic acid and abscisic acid and encodes an ethylene-responsive element binding factor that acts as a repressor to modulate hormone-induced gene expression (Yang et al., 2005). *AT2G37030* encodes an as yet uncharacterised SAUR-like auxin-responsive protein family, *AT4G29200* a  $\beta$ -galactosidase related protein and *AT1G80440* a RING/U-box superfamily protein.

# Chapter 3

## Results II

Genetic and Physical Interaction between *Arabidopsis*  
ALB3 and ALB4

### 3.1 Abstract

ALB3 is a well-known component of a thylakoid protein targeting complex that interacts with the chloroplast signal recognition particle (cpSRP) and the cpSRP receptor, cpFtsY. Its protein-inserting function has been mainly established for light harvesting complex proteins (LHCPs) which first interact with the unique chloroplast cpSRP43 component and then are delivered to the ALB3 integrase by a GTP-dependent cpSRP-cpFtsY interaction. In *Arabidopsis*, a recently discovered ALB3 homologue, ALB4, has been proposed not to be involved in LHCP targeting but instead in the stabilisation of the ATP synthase complex. Here it is shown that there is some functional overlap between ALB3 and ALB4 which is probably due to the targeting of pigment-bearing proteins. Genetic and physical interactions between ALB4 and ALB3, and between ALB4 and cpSRP suggest that both proteins might use a similar subset of interactors for their specific functions.

## 3.2 Introduction

The albino *alb3* mutant was originally isolated in *Arabidopsis thaliana* using a *Ds* insertion screen which was adapted from maize (Long et al., 1993). It was reported to have white to light yellow cotyledons and leaves, abnormal chloroplasts and reduced levels of chlorophyll (Sundberg et al., 1997). ALB3, being homologous to the bacterial membrane protein YidC and the mitochondrial cytochrome c oxidase complex assembly factor OXA1, was shown to be chloroplast thylakoid localised and therefore it was suggested to play a similar role to OXA1 in the assembly of thylakoid membrane complexes (Sundberg et al., 1997). Since ALB3 antibodies could inhibit the insertion of LHCP proteins, the affected thylakoid membrane complexes were identified to be the light harvesting complexes (Moore et al., 2000) (see also Section 1.4.3).

For the *in vitro* reconstitution of LHCP proteins into thylakoid membranes it was previously found that the stroma could be replaced by the chloroplast signal recognition particle (cpSRP), the cpSRP receptor cpFtsY and GTP (Tu et al., 1999). The necessity of ALB3 for LHCP insertion suggested that these stromal factors can deliver LHCPs to the thylakoids via an interaction with ALB3 at the thylakoid membrane (Moore et al., 2000) (see also Section 1.4.3). The chloroplast SRP is composed of cpSRP54 and a homodimer of cpSRP43 in *Arabidopsis* (Jonas-Straube et al., 2001; Schuenemann et al., 1998). These components interact with each other and with their LHCP cargo in the stroma (Jonas-Straube et al., 2001; Tu et al., 2000), while cpFtsY enables thylakoid docking of the cpSRP-LHCP complex via ALB3 and GTP-dependent interaction with cpSRP54 (Moore et al., 2003). A conserved membrane insertase function was con-

firmed for ALB3 by showing that it could complement a bacterial deletion mutant of YidC and restore the ability to insert membrane proteins (Jiang et al., 2002).

Mutants of ALB3 homologues have been isolated from several distantly related species and a very similar defect in the accumulation of pigments and in thylakoid organisation has been reported in every case. In *Chlamydomonas reinhardtii*, the knock-out of Alb3.1, one of two paralogues, causes a drastic reduction in both chlorophyll and LHCPs, similar to *Arabidopsis* (Bellafiore et al., 2002). In the cyanobacterium *Synechocystis* sp. PCC6803, the knockout of the ALB3 homologue slr1471 leads also to impaired thylakoid organisation, reduced levels of photosynthetic pigments, and consequently reduced photosynthetic performance (Spence et al., 2004) (see also Section 1.4.3).

While the importance of ALB3 for the insertion and assembly of pigment-bearing LHCPs in an evolutionary conserved way seems well established, the contribution of ALB3 to the insertion or assembly of other photosystem proteins or components of other thylakoid complexes is less well understood. In *Arabidopsis*, the insertion of PsbS, PsbX, PsbW and PsbY was unaffected by the blocking of ALB3 with anti-ALB3 antibodies, while in *Chlamydomonas* the knockout of Alb3.1 led to a general reduction of photosystem II (PSII) but left PSI, the cytochrome  $b_6f$ -complex and the ATP synthase complex unaffected (Bellafiore et al., 2002; Woolhead et al., 2001). Interaction studies showed that ALB3 is able to bind to PSII core components and that it is likely involved in the assembly of the PSII core (Ossenbuhl et al., 2004; Pasch et al., 2005), which would explain the reduced level of PSII in the *Chlamydomonas* Alb3.1 knockout (Bellafiore et al., 2002). ALB3 was also shown to interact with the chloroplast cpSecY translocase, and it was suggested that these components act together as a cpSRP-specific translocase (Klostermann et al., 2002); however, as removal of cpSecY (SCY1)

did not inhibit ALB3 function, the relevance of this interaction for protein insertion via ALB3 was disputed (Moore et al., 2003; Mori et al., 1999).

In *Arabidopsis*, a homologue of ALB3 exists which is called ALB4 (Gerdes et al., 2006) (see also Section 1.4.3). A knockdown mutant of ALB4 was reported to be visibly normal under standard growth conditions, but to have altered chloroplast ultrastructure; the organelles were more spherical in shape and had deteriorated thylakoid structure (Gerdes et al., 2006). A later study reported a slightly reduced growth rate of the *alb4* knockdown line (Benz et al., 2009). Knockout mutants of *alb4* were shown to have reduced amounts of ATP synthase subunits while transcription of those components is not reduced (Benz et al., 2009). Moreover, larger ATP synthase complexes were decreased in favour of smaller intermediate complexes, and the photophosphorylation capacity of the mutant is consequently reduced, pointing to a role of ALB4 in the stabilisation of ATP synthase intermediates during complex assembly (Benz et al., 2009). Although both ALB4 and ALB3 were localised to the same subfraction of stromal lamellae, gel filtration and co-immunoprecipitation showed no interaction between ALB3 and ALB4, while ALB4 clearly interacted with ATP synthase subunits and ALB3 with cpSecY (Benz et al., 2009). Given the strong difference between the phenotypes of the *Arabidopsis alb3* and *alb4* mutants, only a minor overlap in function seems likely, and a preference of ALB3 for LHC and PSII assembly and ALB4 for ATP synthase assembly as was proposed is therefore a reasonable assumption (see also Section 1.4.3).

However, the consequences of the loss of both ALB3 and ALB4 have not been investigated yet. The different phenotypes of the *alb3* and *alb4* single mutants suggest minimal overlap of functions. However, it is possible that both ALB3 and ALB4 have additional targets to the already reported ones, and that the mode of insertion of those targets may involve ALB3 and ALB4. Therefore, to address the possibility that ALB3

and ALB4 share some functions, the double mutant *alb3 alb4* was analysed, and the genetic and physical interactions of ALB4 with ALB3 and with other components of the cpSRP-targeting pathway were further investigated.

### 3.3 Results

#### 3.3.1 The *alb3 alb4* double mutants are visibly paler than the *alb3* single mutants

For the analysis of *alb4* mutants, the line Salk\_136199 was chosen, which has a T-DNA insertion in the sixth intron (Fig. 3.1 A) and was described previously (Benz et al., 2009; Gerdes et al., 2006). This line has been reported to accumulate less than 10% of wild-type ALB4 (Gerdes et al., 2006), which results in a growth retardation defect of the mutants (Benz et al., 2009). In order to investigate such a potential growth retardation defect, homozygous *alb4* mutants were grown alongside wild type directly on soil. However, under neither long nor short day conditions could a growth retardation defect of *alb4* mutant plants be detected, which is in contrast with the results of Benz et al. (2009) (Fig. 3.1 B). This confirms the previous finding that this *alb4* mutant line does not have a visual phenotype under normal growth conditions (Gerdes et al., 2006).

To assess the functional relationship between ALB3 and ALB4, *alb3 alb4* double mutants were identified and analysed. To this end, *alb4* was crossed to heterozygous *alb3* mutants (as the homozygous *alb3* genotype is seedling lethal). An *alb3* line containing a T-DNA insertion in the eighth intron was chosen (Fig. 3.1 A), which contains a greatly reduced amount of ALB3 protein (Fig. 3.1 D) and is, like *alb4*, in the Col-0 background. In the resulting F<sub>2</sub> generation, plants that were homozygous for *alb4* and heterozygous for *alb3* were selected (Fig. 3.1 C). The F<sub>3</sub> progeny of these plants segregated a quarter of albino *alb3 alb4* double mutants (Fig. 3.3 A). These double mutants have a reduced amount of ALB4 protein as was described earlier for this *alb4* line (Gerdes et al., 2006) and at the same time a greatly reduced amount of ALB3 protein (Fig. 3.1 D).

Interestingly, when the double mutants were grown carefully alongside control *alb3* single-mutant plants, it became clear that the *alb3 alb4* double mutants are visibly paler than the *alb3* single mutants (Fig. 3.2). After two weeks growth on medium supplemented with 0.6% sucrose, the first true leaves that emerged from the *alb3* mutant seedlings were considerably more yellowish than those emerging from the *alb3 alb4* double mutant seedlings, while the cotyledons did not appear to be significantly different between the two genotypes. The 2-weeks-old seedlings were then transferred onto medium supplemented with 3% sucrose to support further growth for another week, and the resulting 3-weeks-old *alb3* seedlings were considerably larger and more yellowish than the *alb3 alb4* double-mutant seedlings (Fig. 3.2). This implies that *alb3* mutants are able to accumulate photosynthetic pigments more effectively than the *alb3 alb4* double mutants.

### **3.3.2 Chlorophyll and carotenoid levels are further reduced in the double mutants**

In order to test the hypothesis that *alb3* mutants accumulate more photosynthetic pigments than the *alb3 alb4* double mutants, chlorophyll and carotenoids from both genotypes were extracted and quantified. Significantly, especially chlorophyll *a* was reduced in the double mutant compared to *alb3* while the reduction in chlorophyll *b* was minor (Fig. 3.3 B). The ratio of chlorophyll *a* to chlorophyll *b* (Chl *a* / Chl *b*) is larger than 2 for *alb3* mutants but smaller than 1 for *alb3 alb4* double mutants, showing that *alb3* mutants contain more chlorophyll *a* than *b* while the *alb3 alb4* double mutants contain more chlorophyll *b* than *a*. This is intriguing since chlorophyll *a* binds mainly to photosynthetic core proteins, suggesting that the predominant loss of chlorophyll *a* in the *alb3 alb4* double mutants could be caused by a loss of photosynthetic core proteins. In addition to chlorophyll, the amount of total carotenoids (including carotenes and

xanthophylls) was measured and found to be reduced to approximately a third in the *alb3 alb4* double mutants compared to *alb3* single mutants (Fig. 3.3 C). The reduction in both, chlorophylls and carotenoids, implies that ALB4 is responsible for the accumulation of some pigment-bearing proteins in the *alb3* background. The apparent lack of such proteins in the *alb3 alb4* double mutants could also have a profound effect on the accumulation of thylakoid membranes, which is examined in detail in the next section.

### **3.3.3 The chloroplasts of *alb3 alb4* double mutants have less thylakoid membranes than *alb3***

Plastids lacking ALB3 have been shown previously to accumulate significantly fewer thylakoid membranes than wild type (Sundberg et al., 1997). Here, the mesophyll cell plastids of the first true leaves of 17-day-old seedlings of both *alb3* and *alb3 alb4* double mutants were analysed by transmission electron microscopy. Consistent with the previous report (Sundberg et al., 1997), it was found that *alb3* plastids contain considerably fewer thylakoid membranes and no grana stacks could be observed (Fig. 3.4 A). Interestingly, the *alb3 alb4* double mutant plastids are almost completely devoid of thylakoids with many instead accumulating large vesicles (Fig. 3.4 A). In the *alb3 alb4* double mutant, large, round plastids containing large vesicles occur roughly at the same frequency as rather flat plastids without vesicles, although intermediate forms occur. Generally, the plastids of the *alb3 alb4* double mutant are larger than those of the *alb3* single mutants. Quantification of thylakoid membranes and vesicles of a large number of plastids from both *alb3* single and *alb3 alb4* double mutants show that *alb3* mutant plastids contain on average 6-7 thylakoids while thylakoids are virtually absent from *alb3 alb4* double mutants (Fig. 3.4 B). Similarly, *alb3 alb4* double mutants accumulate on average 3-4 large vesicles, while vesicles do not accumulate in *alb3* single mutants.

Although it was shown previously that starch grains are absent from *alb3* mutant chloroplasts (Sundberg et al., 1997), some starch grains could be found in a low number of *alb3* mutant chloroplasts (Fig. 3.4 B and Fig. 3.4 A top left). However, no starch grains could be observed in the *alb3 alb4* double mutants. This further indicates that the *alb3 alb4* double mutants have a more severe phenotype than the *alb3* single mutants, with reduced photosynthetic capacity, and that therefore there is some functional overlap between ALB3 and ALB4.

### **3.3.4 ALB3 and ALB4 can interact weakly, but specifically**

Given that the genetic analysis revealed significant functional overlap between ALB3 and ALB4, it is conceivable that the two proteins interact physically with each other or with the same partners *in vivo*. An interaction between ALB3 and ALB4 could not be found in uncrosslinked chloroplasts neither in a previous study (Benz et al., 2009) nor in the present study (data not shown). However, by using chloroplasts expressing a FLAG-tagged ALB4, a weak interaction of ALB3 with ALB4-FLAG could be detected after crosslinking with 0.5 mM DSP (Fig 3.5 A). Several control proteins, all of which are thylakoid membrane-associated proteins, did not interact with ALB4-FLAG, indicating that the detected ALB3-ALB4 interaction is specific. Such a weak interaction suggests that the ALB3-ALB4 interaction is not stable but rather transient and possibly mediated by other factors that bridge the interaction *in vivo*.

Because the ALB4-FLAG lines contain an overexpressed and tagged form of ALB4, one could argue that the observed interaction is an artefact caused by the artificial nature of the experimental system. To exclude this possibility, co-IP was performed with anti-ALB4 antibody and wild-type chloroplasts (Fig 3.5 B). Again, a weak but

specific interaction between ALB3 and ALB4 could be observed, confirming the finding described above. It is particularly interesting that the ATP synthase subunit CF<sub>1</sub>γ could neither be crosslinked to ALB4 nor to overexpressed ALB4-FLAG, even though it was shown previously that ALB4 co-migrates with CF<sub>1</sub>γ in 2D BN/SDS-PAGE experiments (Benz et al., 2009). This finding argues against a non-specific interaction caused by over-crosslinking the proteins and therefore increases the relevance of the ALB3-ALB4 interaction detected in this study.

### **3.3.5 ALB4 can interact with cpHsc70 and the chloroplast SRP**

In an attempt to identify further interactors of ALB4 using the ALB4-FLAG lines, it was found that, in addition to ALB3, cpHsc70 could be crosslinked to ALB4-FLAG (Fig. 3.6 A). LHCP which could not be crosslinked to ALB4-FLAG was used as a control. Again, the interaction was rather weak and therefore probably of a transient nature. Because it has been reported before that OXA1, a mitochondrial homologue of ALB3 and ALB4, can interact with components of the large ribosomal subunit in mitochondria (Jia et al., 2003; Szyrach et al., 2003), the interaction of ALB4-FLAG with two plastid ribosomal large-subunit proteins (PRPLs) was also investigated. However, neither PRPL2 nor PRPL35 could be cross-linked to ALB4-FLAG, arguing against a similar role of ALB4 similar to OXA1 (Fig. 3.6 A).

Since ALB4 could be crosslinked specifically to ALB3, the question arises whether it could also be crosslinked to the cpSRP components and cpFtsY (which are well known to act in the same pathway as ALB3). Because anti-FLAG and anti-ALB4 immunoprecipitations (IP) gave comparable results for the interactions of ALB3 and ALB4 (Fig. 3.5), further interaction studies were performed by anti-FLAG IP using

ALB4-FLAG expressing lines. Using these ALB4-FLAG expressing lines, an interaction between ALB4 and both cpSRP components but not cpFtsY could be observed (Fig. 3.6 B). Since a previous study reported an interaction between *Chlamydomonas* Alb3.2 and VIPP1 (Gohre et al., 2006), the interaction between ALB4 and VIPP1 in *Arabidopsis* was also examined. Indeed, a clear interaction between ALB4-FLAG and VIPP1 could be observed. The interactions seem to be specific, since ALB4-FLAG could not be crosslinked to other thylakoid components, which were used as negative controls in this experiment.

### **3.3.6 Genetic interactions suggest functional overlap between ALB4 and cpSRP**

Since ALB4 interacts physically and genetically with ALB3, and physically with the cpSRP components, the question arises: Does ALB4 interact genetically with cpSRP components? To investigate this possibility, the ALB4 protein-null line *stic1-1* (described in results I of this thesis) was crossed to the *cpsrp54 cpsrp43* double mutants, to *cpftsy* and as a control to the mutants of the TAT component Hcf106 and the Sec component SecA1. The *cpsrp54 cpsrp43* double-mutant line and the *cpftsy* line were identical to the lines described previously (Hutin et al., 2002; Tzvetkova-Chevolleau et al., 2007). The *cpsrp54 cpsrp43* double-mutant line had a late flowering phenotype when grown under standard long-day conditions, probably due to background mutations. The *seca1* line (SALK\_063371) and the *hcf106* line (SALK\_020680) have also been described previously (Kugelman, 2010; Liu et al., 2010). The *hcf106 stic1-1* and the *seca1 stic1-1* double mutants were albino like the *hcf106* and *seca1* single mutants, respectively, but a more severe phenotype as for the *alb3 alb4* double mutant was not observed (Fig. 3.7). However, both the *cpsrp54 cpsrp43 stic1-1* triple mutant and the *cpftsy stic1-1* double mutant were much smaller and more affected in development than

the *cpsrp54 cpsrp43* double mutants and *cpftsy* single mutants, respectively (Fig. 3.8 A, B,C). Interestingly, *cpftsy stic1-1/+* (heterozygous for *stic1-1*) showed a clear intermediate phenotype (Fig. 3.8 C) between *cpftsy* and *cpftsy stic1-1* which is reminiscent of the semi-dominant behavior of *stic1* in *tic40* suppression. Since *stic1/alb4* mutants have a very weak phenotype by themselves, the more severe phenotypes of *alb3*, *cpftsy* and *cpsrp54 cpsrp43* in the *stic1-1* background are considered to be more than additive and suggest functional overlap between ALB4 and the cpSRP pathway.

### 3.4 Discussion

This study shows that the *Arabidopsis alb3 alb4* double mutants have a lower chlorophyll and carotenoid content than *alb3* single mutants, and that the chloroplast ultrastructure of the double mutant is further deteriorated. Therefore, one role of ALB4 in the *alb3* mutant background is likely to be the insertion of some pigment-bearing proteins into the thylakoid membrane. It is known that both PSI and PSII core proteins mainly bind chlorophyll *a* and  $\beta$ -carotene molecules, while the LHCI and LHCII antenna proteins bind chlorophylls *a* and *b* as well as xanthophylls (Croce et al., 2002; Ferreira et al., 2004; Jordan et al., 2001; Liu et al., 2004). Therefore, the greater reduction of chlorophyll *a* than chlorophyll *b* in the *alb3 alb4* double mutant compared to *alb3* suggests a role for ALB4 in the insertion of photosystem core components.

In the absence of crosslinker, ALB3 and ALB4 could not be co-immunoprecipitated from isolated thylakoid membranes (Benz et al., 2009). Likewise, an interaction between ALB3 and ALB4 could not be detected in the present study using uncrosslinked isolated chloroplasts. This suggests that any interaction between these components may be rather weak. Indeed, by using crosslinked chloroplasts a weak but specific interaction between ALB3 and ALB4 could be detected. Therefore, the interaction between ALB3 and ALB4 is likely not stable but rather transient and potentially bridged by a pool of common interactors. In *Chlamydomonas reinhardtii*, both paralogous ALB3 proteins, Alb3.1 and Alb3.2, could also interact with each other and with reaction centre polypeptides, suggesting that both play a role in the assembly of reaction centres (Gohre et al., 2006).

The weak phenotype of *alb4* single mutants suggest that thylakoid protein targeting can be largely managed by ALB3 alone. However, as ALB4 is able to interact with ALB3 it may normally perform regulatory or chaperoning functions in conjunction with ALB3 and other components involved in thylakoid protein insertion. Since *alb4* mutants were shown to reduce the stability of ATP synthase complexes and to have a deteriorated thylakoid ultrastructure (Benz et al., 2009; Gerdes et al., 2006), one may speculate that ALB4 generally fine tunes the protein insertion process of the cpSRP-ALB3 system and that other thylakoid protein complexes might be similarly destabilised in the *alb4* mutants. The interactions of ALB4 with cpHsc70 might support this idea, since such a chaperoning function of ALB4 may involve the transient binding of other chaperones.

As it is well known that proteins from the YidC/OXA1/ALB3 family can function in both post- and co-translational membrane protein insertion, a role for ALB3 in co-translational membrane protein insertion that might involve SCY1 and cpSRP54 has been suggested previously (Moore et al., 2003; Zhang and Aro, 2002). In fact, the ALB3 and ALB4 C-termini contain two motifs, motif I and motif III, which are conserved between the two paralogues and have been suggested to be involved in SCY1 binding (Falk et al., 2010). Therefore, the question arises as to whether ALB3 and ALB4 are involved in co-translational protein targeting. The C-terminus of OXA1, the mitochondrial homologue of ALB3 and ALB4, is known to interact with the ribosomal large subunit during co-translational protein insertion, albeit independently from SRP or Sec translocon, both of which are absent in mitochondria (Glick and Von Heijne, 1996; Szyrach et al., 2003). Here it is shown that ALB4-FLAG could not be crosslinked to two plastid ribosomal proteins of the large subunit, PRPL2 and PRPL35. This does not exclude that ALB4 could transiently interact with other ribosomal proteins or translating

proteins, but it suggests that an active participation of ALB4 in co-translational membrane protein insertion is rather unlikely.

It was shown *in vitro* that the C-terminus of ALB3 can interact with cpSRP43 based on motifs which are absent in the C-terminus of ALB4, which consequently cannot interact with cpSRP43 (Falk et al., 2010). Surprisingly, in the present study it could be found that both cpSRP43 and cpSRP54 can be crosslinked to ALB4 *in vivo*, suggesting either an indirect, bridged interaction of ALB4 with cpSRP43, or an interaction not involving the ALB4 C-terminus. The fact that ALB4 can interact with ALB3, cpSRP43 and cpSRP54 would fit to a function of ALB4 in fine-tuning the protein insertion process of the ALB3-cpSRP system as stated above. cpFtsY was not observed to be crosslinked to ALB4 which is in line with the earlier finding that cpFtsY does not form significant interactions with cpSRP components and ALB3 (Tu et al., 2000). Possibly the GTP-dependent interaction of cpSRP54 with cpFtsY is too transient to be caught with the conditions used here, even by crosslinking. The finding that *cpsrp54 cpsrp43 stic1-1* triple mutants and *cpftsy stic1-1* double mutants have a more severe phenotype than the respective *cpsrp54 cpsrp43* double and *cpftsy* single mutants further supports the results of the protein interaction studies. Like in the case of the *alb3 alb4* double mutant, these genetic interactions are considered to be more than additive because of the weak *stic1-1/alb4* phenotype. Thus, genetic and interaction studies both suggest that ALB4 participates in the ALB3-cpSRP pathway (see also Chapter 5). As expected, the *hcf106 stic1-1* and *secal1 stic1-1* double mutants do not show genetic interaction, which is in line with the previous finding that the Sec and Tat components are not affected in *alb3* and *cpftsy* mutants and that there is likely little functional overlap between the ALB3-cpSRP pathway for thylakoid targeting and the Sec and Tat pathways for luminal targeting (Asakura et al., 2008).

In short, it is suggested that ALB4 can insert pigment-bearing components (likely reaction centre core components) in the *alb3* background while in the wild-type background ALB4 might rather have an auxiliary, possibly chaperoning function in the insertion of those proteins. While ALB3 is certainly crucial for the insertion of LHC components, and ALB4 might influence the stability of non-photosynthetic thylakoid complexes, it seems that a sharp separation of the functions of the two paralogues is not supported by the data. Both genetic and interaction studies suggest some functional overlap between ALB3 and ALB4, but they may have evolved such that ALB3 plays key roles during protein membrane insertion while ALB4 assists and fine-tunes this process. Thus, ALB3 and ALB4 likely contribute differentially but synergistically to the same process of protein insertion into the thylakoids via the ALB3-cpSRP pathway.

## 3.5 Materials and Methods

### 3.5.1 Plant growth and genotyping

Mutant seeds were ordered from NASC (*alb3*: GABI\_293B08/N324478 and *alb4*: Salk\_136199/N636199). They were grown directly on soil (*alb4*, kanamycin resistance marker silenced), or *in vitro* on half-strength Murashige and Skoog plates containing 0.5% (w/v) sucrose and 11.25 µg/ml sulfadiazine (for *alb3* selection) after surface sterilisation of the seeds and two days stratification at 4°C as described previously (Aronsson and Jarvis, 2002) (see also Sections 6.1.2 and 6.1.3). Albino seedlings (homozygous *alb3* mutants and *alb3 alb4* double mutants) were grown *in vitro* on half-strength Murashige and Skoog plates containing 3% (w/v) sucrose. Plants were grown under long-day cycles (16 h light, 8 h dark) except where indicated as short day (8 h light, 16 h dark).

For genotyping, the following primers were used: *alb4* forward, 5'-CCTTGCA-GGTACAGTATGTTA-3'; *alb4* reverse, 5'-CTGTTGCATAGAAGGATTTTCG-3'; *alb3* forward, 5'-CGCTTCGTATTGAGAGATATA-3'; *alb3* reverse, 5'-GAGAGGA-TACAACTAGAGACA-3'. For T-DNA specific PCRs the *alb4* forward primer was combined with SALK LBb1, 5'-GCGTGGACCGCTTGCTGCAACT-3' and the *alb3* reverse primer was combined with GK-LB, 5'-CCCATTTGGACGTGAATGTAGACAC-3'. For the other mutants, the following primers were used: *hcf106* forward, 5'-TGTCTTTTGTTTTAGGATGTTTCA-3'; *hcf106* reverse, 5'-GAGGAGATGCAG-CTGTTGTTTC-3'; *secal1* forward, 5'-TTTTAATCTATGTTGTTCTTGTGG-3'; *secal1* reverse, 5'-CATCTTCTTTGCTCGTTGTG-3'; *cpsrp43* forward, 5'-CTGGGGTTCGG-ACAAGTGCGTAAG-3'; *cpsrp43* reverse, 5'-CTCCAGCCCATCCTCGTAGTCCT-3'; *cpsrp54* forward, 5'-ATGGCTCCTGTAATTCCTATCTCT-3'; *cpsrp54* reverse, 5'-

AGCAGGGACTGATGTAAAACCT-3’; insertion specific combinations were *hcf106*-R with LBa1, *secal*-F with LBa1, *cpsrp43*-F with Ds5-4 (5’-TACGATAACGG-TCGGTACGG-3’). No insertion specific primer was available for *cpsrp54* due to the nature of the mutation. The *cpftsy* mutants were selected without genotyping based on their very clearly visible phenotype.

### **3.5.2 Total chlorophyll and carotenoid measurements and transmission electron microscopy**

Pigment extraction and measurement was based on a method described previously (Czarnecki et al., 2011). Approximately 50 mg of 3-week-old seedlings were frozen in liquid nitrogen, ground and then covered with 300 µl of 80% acetone containing 10 µM KOH. The samples were vortexed for at least one minute and then centrifuged at 10,000 *g* for 10 minutes in a microcentrifuge. Absorbances of the supernatant were measured at 663 nm, 647 nm and 470 nm, and the amounts of total chlorophyll per mg fresh weight were calculated as follows (Czarnecki et al., 2011):

$$\text{Chl } a = ((12.25 \times A_{663}) - (2.79 \times A_{647})) / (0.3 \times \text{fresh weight}).$$

$$\text{Chl } b = ((21.5 \times A_{647}) - (5.1 \times A_{663})) / (0.3 \times \text{fresh weight}).$$

$$\text{Car} = [1000 \times A_{470} - 1.82 (\text{Chl } a) - 85.02 (\text{Chl } b)] / (198 \times 0.3 \times \text{fresh weight}).$$

For transmission electron microscopy (TEM) the first true leaves from 17 day old plants were used and the service of the University of Leicester Electron Microscope Laboratory (Faculty of Medicine and Biological Sciences) was employed.

### 3.5.3 Antibody production and immunoblotting

The anti-ALB4 antibody was generated by cloning the coding sequence of the C-terminal 155 amino acids of ALB4 (soluble part) into pQE-30 (Qiagen) using BamHI and PstI. Transformed XL1-Blue cells were grown in the presence of 1% glucose in order to repress the lac operon and avoid leaky expression (see Section 6.2.7). Expression of His-tagged ALB4 C-terminus was induced with 1 mmol/L isopropyl  $\beta$ -D-1-thiogalactopyranoside (IPTG) and the cells were lysed by sonication in lysis buffer (50 mM NaH<sub>2</sub>PO<sub>4</sub>, 300 mM NaCl, 10 mM imidazole, pH 8.0). The lysate was put onto polypropylene columns (Qiagen), washed with wash buffer (50 mM NaH<sub>2</sub>PO<sub>4</sub>, 300 mM NaCl, 20 mM imidazole, pH 8.0) and the proteins were eluted in elution buffer (50 mM NaH<sub>2</sub>PO<sub>4</sub>, 300 mM NaCl, 250 mM imidazole, pH 8.0). Purified protein was sent to Harlan for antibody production and the antiserum was affinity purified using the original antigen. The anti-ALB3 antibody was a gift from Prof. D. Schünemann. The cpSRP and cpFtsY antibodies were a gift from Prof. M. Nakai. Immunoblots were performed using standard methods with 12% polyacrylamide gels and nitrocellulose membranes.

### 3.5.4 Creation of ALB4-FLAG lines

The ALB4 coding sequence without the stop codon was cloned into a C-terminal FLAG vector derived from pEarlyGate 302 (Earley et al., 2006) containing a 35S promoter and spectinomycin and hygromycin resistance using the Gateway® technology (Invitrogen) (see Section 6.2.5). *Agrobacterium* GV3101 was transformed by the freeze-thaw method (Holsters et al., 1978) (see Section 6.1.5) with the plasmids containing the ALB4-FLAG construct and 6-week-old flowering wild-type plants were transformed with *Agrobacterium* by the floral dip method (Clough and Bent, 1998). ALB4-FLAG overex-

pressing T<sub>2</sub> lines were confirmed by immunoblotting with anti-ALB4 and anti-FLAG (Sigma) antibodies.

### **3.5.5 Chloroplast isolation and crosslinking**

Chloroplasts of 2-week-old wild-type plants or plants overexpressing the ALB4-FLAG construct were isolated as described previously (Aronsson and Jarvis, 2002) (see Section 6.4.7). Freshly isolated chloroplasts were counted using a counting chamber (Weber Scientific) and normalised to 100 million chloroplasts in 300 ml HEPES-MES-sorbitol (HMS) buffer (Aronsson and Jarvis, 2002). For crosslinking, 0.5 mM DSP (in DMSO) was added to the chloroplasts and incubated on ice for 15 minutes. The reaction was then quenched with 50 mM glycine for 15 minutes before the chloroplasts were pelleted by centrifugation at maximum speed and 4°C for 30 seconds using an Eppendorf Centrifuge 5417 R with an EL 082 rotor. The supernatant was removed and the pellet was used for immunoprecipitations.

### **3.5.6 FLAG- and co-immunoprecipitation**

Anti-FLAG-immunoprecipitation was performed with 100 million crosslinked chloroplasts from the ALB4-FLAG expressing plant line and an equal number of wild type chloroplasts as control (see Section 6.4.10). The chloroplasts were solubilised in solubilisation buffer (20 mM Tris-HCl, 150 mM NaCl, 1 mM EDTA, 10% glycerol, 1% *n*-dodecyl- $\beta$ -D-maltopyranoside (DDM), pH 7.5) containing 1 $\times$  protease inhibitor cocktail (cOmplete, Mini, EDTA-free, Roche). Following the manufacturers guidelines, 60  $\mu$ l of Anti-FLAG M2 Affinity Gel (Sigma) per sample was pre-equilibrated and the ALB4-FLAG (and control) was immunoprecipitated for 2 hours by rotating at 4°C. The Anti-

FLAG M2 Affinity Gel was then washed six times with wash buffer (20 mM Tris-HCl, 150 mM NaCl, 1 mM EDTA, 10% glycerol, 0.3% DDM, pH 7.5) before 50  $\mu$ l of 2  $\times$  protein sample buffer was added. Per experiment, 18  $\mu$ l of the denatured eluate was loaded. Co-immunoprecipitation was performed with 100 million crosslinked chloroplasts from wild-type plants. The chloroplasts were solubilised as described above and 5  $\mu$ l of anti-ALB4 antibody was added to the lysate (5  $\mu$ l of pre-immune serum to the control) and incubated for 3 hours by rotating at 4°C. 50 mg of Protein A sepharose CL-4B (GE Healthcare) was pre-equilibrated in 200  $\mu$ l sterile water on ice for 30 minutes, then washed 3  $\times$  with water and once with solubilisation buffer. To the samples 100  $\mu$ l of this slurry was added, rotated for 2 hours at 4°C and then washed as described above. Again, 50  $\mu$ l of 2  $\times$  protein sample buffer was added to the slurry and 18  $\mu$ l of the denatured eluate was loaded per experiment.

### 3.6 Figures and Tables

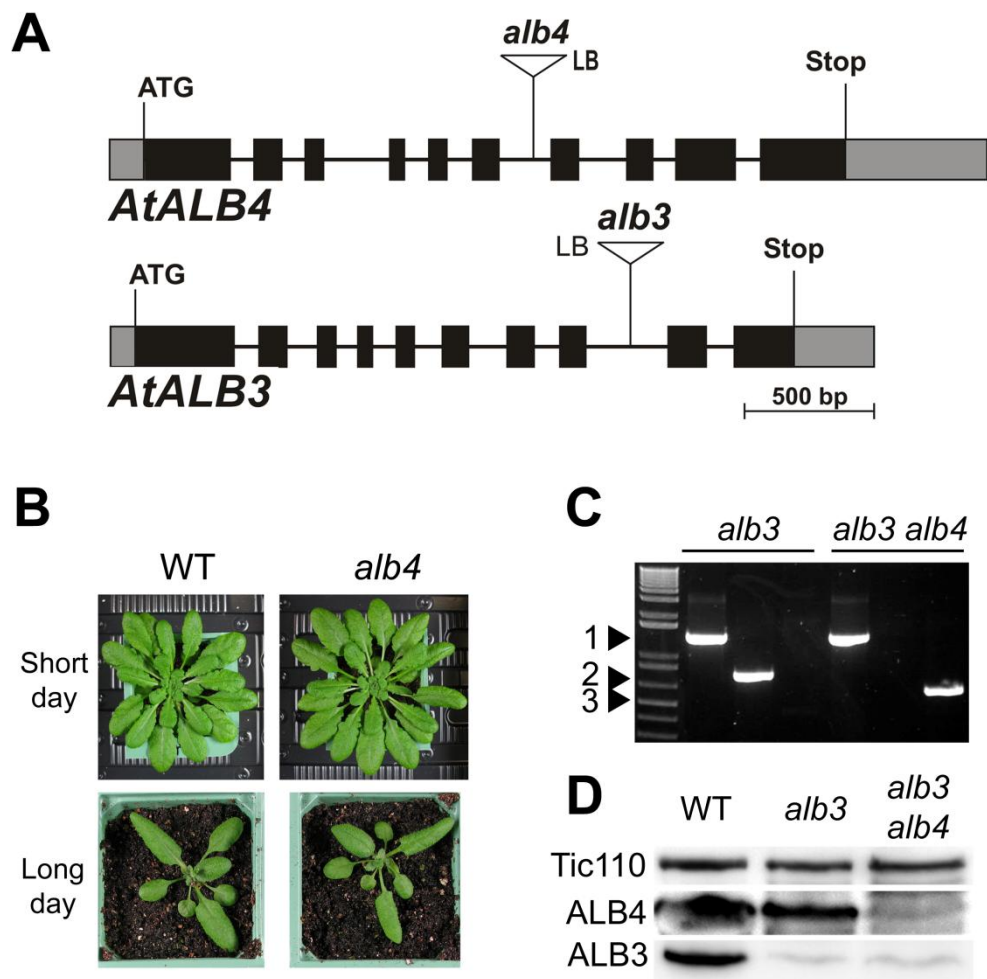


**Figure 3.1:** Analysis of *alb4* and *alb3* single mutants and *alb3 alb4* double mutants. (A) Gene diagrams of ALB4 and ALB3 with the T-DNA insertions of the *alb4* and *alb3* mutant lines. (B) Wild type and *alb4* mutant plants (Salk\_136199) were directly grown on soil under short day (8h light/16h dark) or long day (16h light/8h dark) conditions. Pictures were taken after 7 weeks (short day) and 4 weeks (long day). (C) Agarose gel showing PCR products, with a 1 kb marker on the left. Heterozygous *alb3* mutants (GK\_293B08) and *alb3/+ alb4/alb4* plants were indistinguishable from wild type but both contained the *alb3* T-DNA insertion (1), *alb3/+ alb4/alb4* contained additionally the homozygous *alb4* T-DNA insertion (3) but not the wild type ALB4 allele (2). (D) Immunoblot using equal quantities of total protein from 3 weeks old albino *alb3 alb4* double mutant and *alb3* single mutant seedlings compared to wild type. Tic110 is shown as a loading control. The *alb3 alb4* double contained considerably less ALB4 protein than the *alb3* single mutant. Detection of HRP-linked secondary antibodies with ECL method.

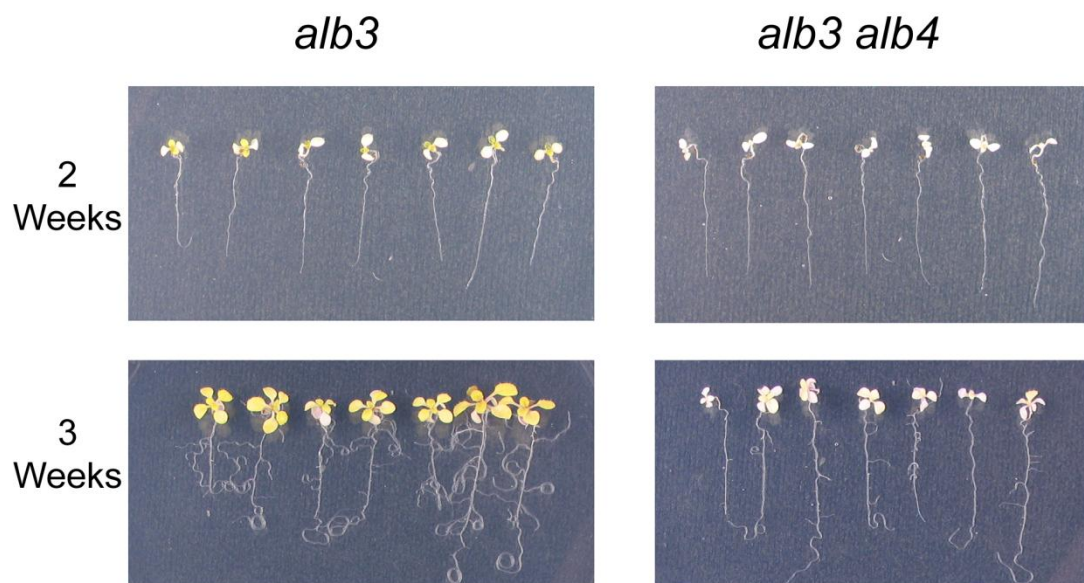


**Figure 3.2:** Phenotype analysis of *alb3 alb4* double mutants.

Albino seedlings from segregating *alb3/+* and *alb3/+ alb4/alb4* plants grown *in vitro* on MS medium supplemented with 0.6% sucrose were transferred to MS medium containing 3% sucrose 2 weeks after germination. Pictures were taken immediately after transfer (2 weeks) or after another week of growth under standard conditions (3 weeks). While *alb3* has yellowish true leaves, the double mutant accumulates fewer pigments and is generally smaller than *alb3*.

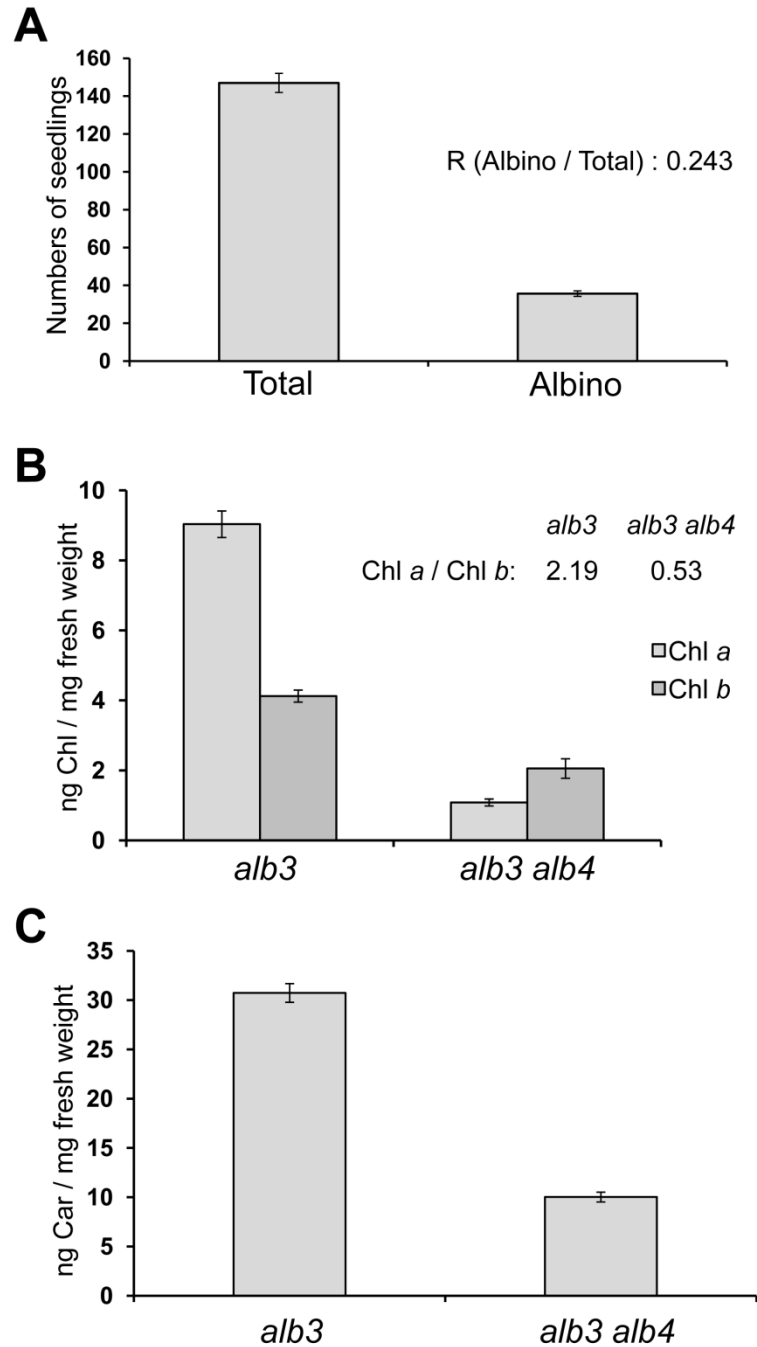


**Figure 3.3:** Segregation analysis and measurement of thylakoid pigments.

(A) Segregation analysis with progeny from three individual *alb3/+ alb4/alb4* (het/hom) plants. Values are averages of the numbers of total seedlings and albino seedlings from each of the three parent plants. R: ratio. (B) Chlorophyll *a* (Chl *a*) and chlorophyll *b* (Chl *b*) were measured in  $\mu\text{g}/\text{mg}$  fresh weight using 3 weeks old seedlings grown *in vitro* on MS medium supplemented with sucrose. The ratio of chlorophyll *a* to chlorophyll *b* (Chl *a*/Chl *b*) is larger than 1 for *alb3* but smaller than 1 for *alb3 alb4*. (C) Total carotenoid (Car) was measured in  $\mu\text{g}/\text{mg}$  fresh weight using 3 weeks old seedlings grown *in vitro* on MS medium supplemented with sucrose. All error bars denote standard errors.

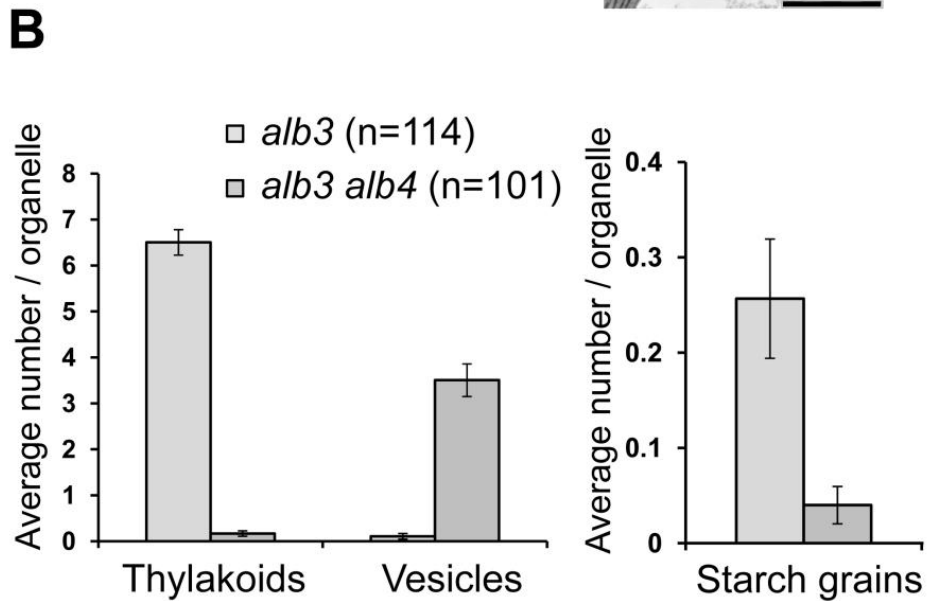
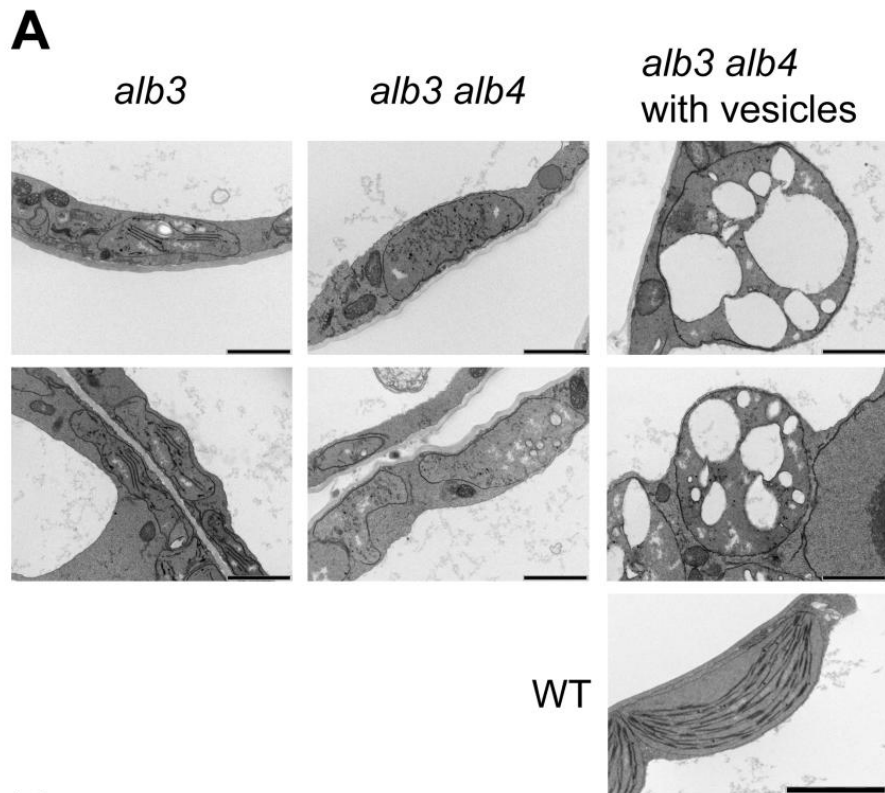


**Figure 3.4:** Transmission electron micrographs of *alb3* single and *alb3 alb4* double mutants. (A) Transmission electron micrograph (TEM) images of mesophyll cell plastids from the first true leaves of 17 days old seedlings grown *in vitro*. All images show plastids at the same scale. The black bar in the lower right corner corresponds to 2  $\mu$ m. The top image of *alb3* shows a starch grain in the middle of the plastid. The *alb3* plastids generally contain a few thylakoid membranes while these lack almost completely in the *alb3 alb4* double mutants. In the *alb3 alb4* double mutants, large round plastids with many vesicles occur roughly at the same frequency as relatively flat plastids without vesicles. (B) Average number of thylakoids, vesicles and starch grains found in plastids from *alb3* single and *alb3 alb4* double mutants. Numbers in brackets denote numbers of plastids used for counting. The plastids came from the TEM images of three biological replicates. Error bars denote standard errors.

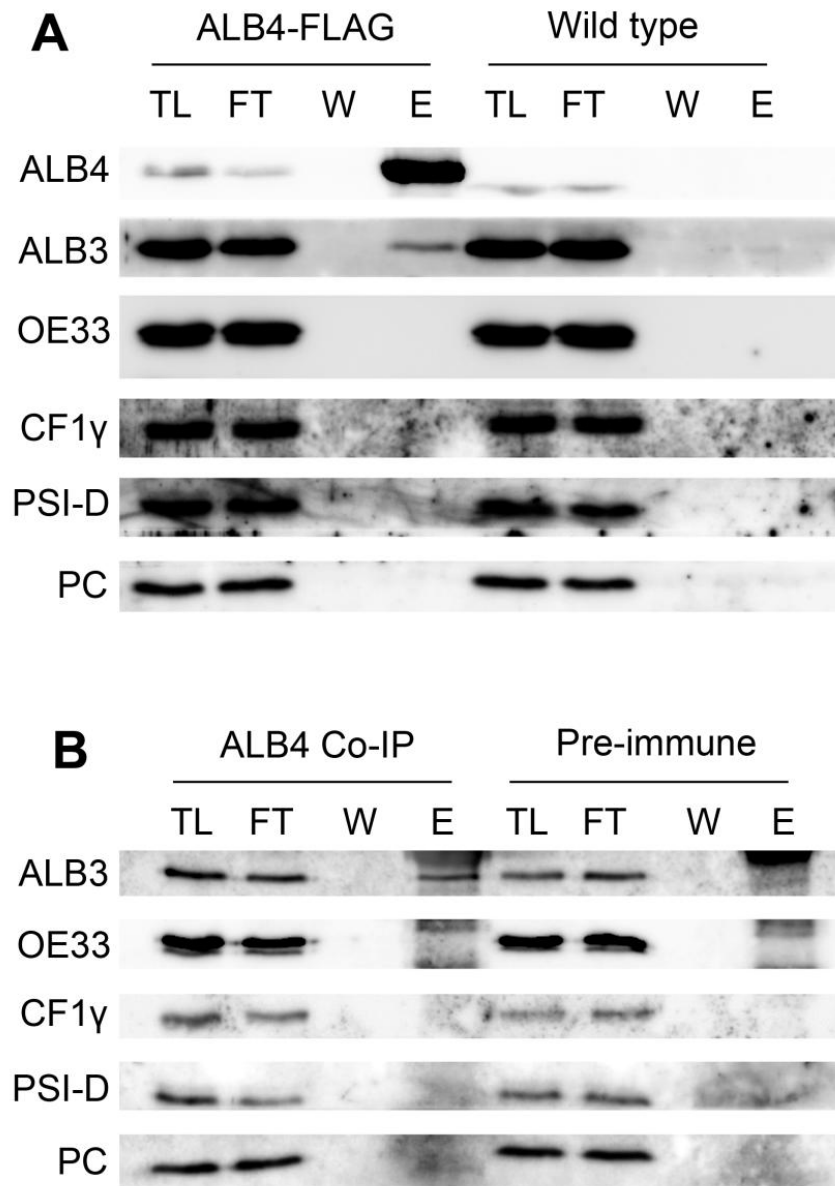


**Figure 3.5:** Interaction between ALB3 and ALB4 *in vivo*.

(A) Immunoprecipitation with anti-FLAG M2 affinity gel using 100 million chloroplasts isolated from 2-weeks-old plants stably overexpressing an N-terminal ALB4-FLAG fusion under the CaMV 35S promoter. Chloroplasts were crosslinked with 0.5mM DSP. TL: total lysate (0.45%), FT: flow-through (0.45%), W: wash (~4.5%), E: elute (36%). ALB4 was detected with anti-ALB4 antibody and HRP-linked secondary antibodies using the ECL method; the size shift of ALB4 in the ALB4-FLAG sample compared to wild type corresponds to the size of the FLAG tag. (B) Co-immunoprecipitation with anti-ALB4 antibody using 100 million chloroplasts isolated from wild type plants. Chloroplasts were crosslinked with 0.5mM DSP. Loading and detection are identical to (A).

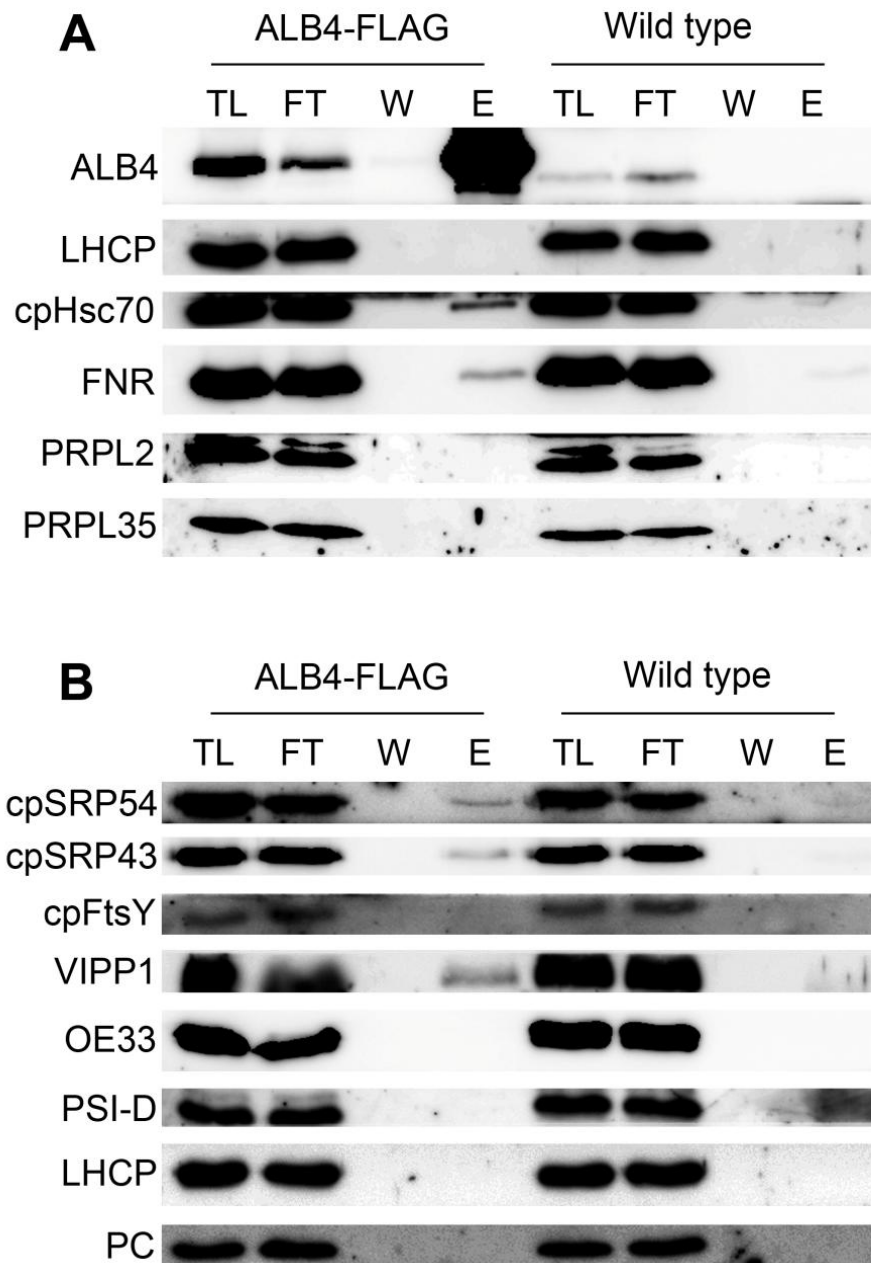


**Figure 3.6:** Interaction of ALB4 with cpHsc70 and chloroplast SRP components.

(A) Immunoprecipitation with anti-FLAG M2 affinity gel using 100 million chloroplasts isolated from 2-weeks-old plants stably overexpressing and N-terminal ALB4-FLAG fusion under the CaMV 35S promoter. Chloroplasts were crosslinked with 0.5mM DSP. TL: total lysate (0.45%), FT: flow-through (0.45%), W: wash (~4.5%), E: elute (36%). Detection of HRP-linked secondary antibodies with ECL method. No interaction between ALB4-FLAG and the plastid ribosomal proteins PRPL2 and PRPL35 (large subunit) could be observed, however ALB4-FLAG interacts with cpHsc70 and ferredoxin-NADP<sup>+</sup> reductase (FNR). (B) Identical to (A) except for the detection with a range of antibodies for chloroplast signal recognition particle (SRP) and other thylakoid components.

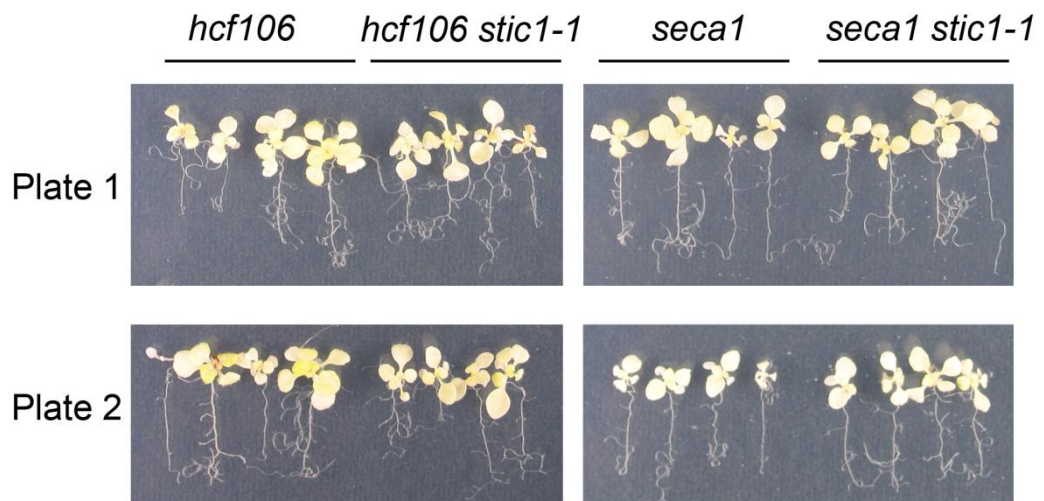


**Figure 3.7:** No genetic interaction between *stic1/alb4* and Sec or Tat components.

Progeny of heterozygous *hcf106/+* and *seca1/+* in the wild-type and *stic1-1* backgrounds segregated to a quarter of albino mutants on half strength MS plates supplemented with 0.6% sucrose. These were transferred two weeks after germination to plates supplemented with 3% sucrose to allow further growth for one week. Photographs from two separate plates are shown in each case.

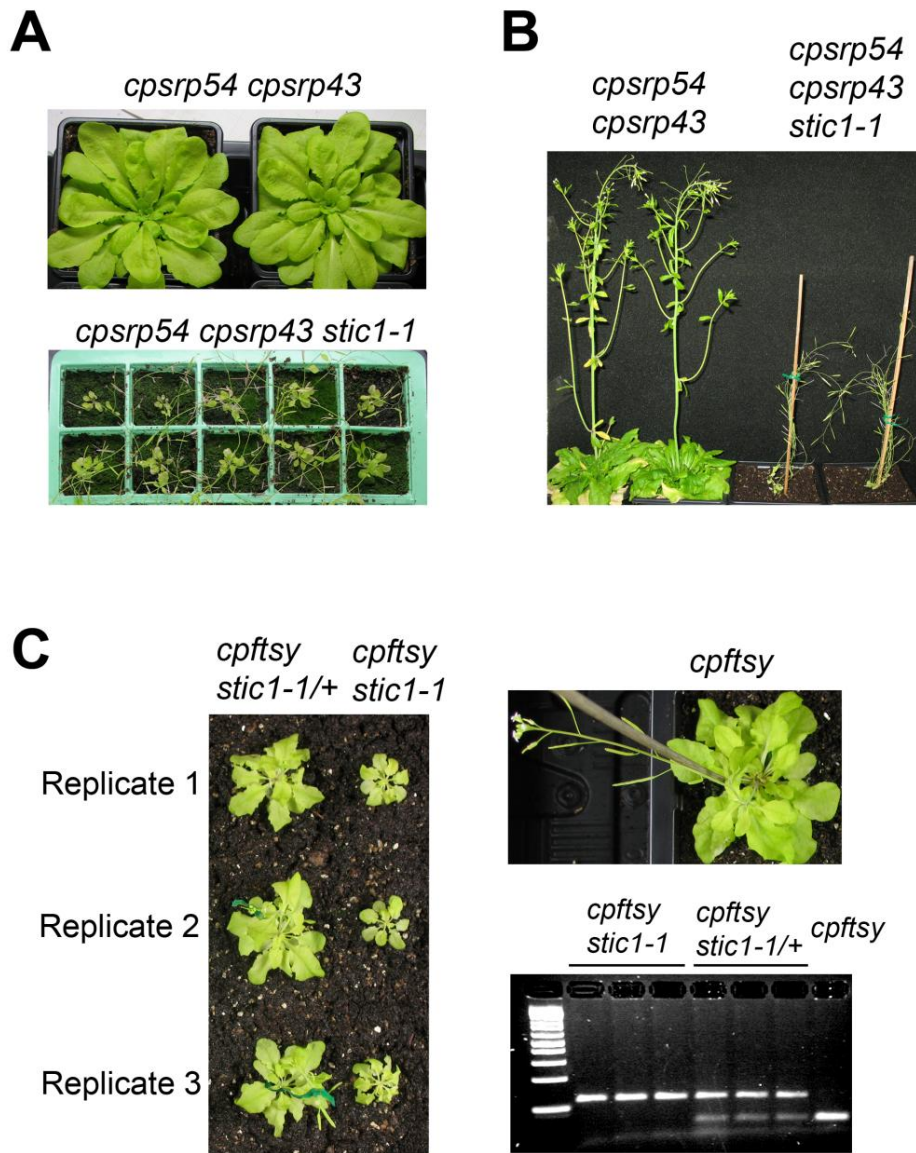


**Figure 3.8:** Genetic interaction between *stic1/alb4* and chloroplast SRP components.

(A,B) Mutants were grown directly on soil and photographed after 10 weeks (A) and 12 weeks (B). The upper and lower panels in (A) are at the same scale. (C) The left panel shows three replicates (individuals) of *cpftsy stic1-1/+* and *cpftsy stic1-1* at the same scale and age (12 weeks) as the *cpftsy* mutant shown on the top right. The bottom right image shows the genotyping (agarose gel) of each of the mutants shown in (C) by dCAPS markers for the *stic1-1* mutation. MnlI cleaves the wild-type allele (resulting in the lower band) but not *stic1-1* (upper band). 1 kb marker shown on the left.

# Chapter 4

## Results III

### The Stromal Processing Peptidase of Chloroplasts Is Essential in *Arabidopsis*, with Knockout Mutations Causing Embryo Arrest after the 16-Cell Stage

This work has been published in PLoS One:

**Trösch, R. and Jarvis, P. (2011).** The Stromal Processing Peptidase of Chloroplasts Is Essential in *Arabidopsis*, with Knockout Mutations Causing Embryo Arrest after the 16-Cell Stage. PLoS One, 6(8): e23039. doi:10.1371/journal.pone.0023039

Author Contributions: Conceived and designed the experiments: PJ. Performed the experiments: RT. Analyzed the data: RT PJ. Wrote the paper: RT PJ.

## 4.1 Abstract

The stromal processing peptidase (SPP), a metalloendopeptidase located in the stroma of chloroplasts, is responsible for the cleavage of transit peptides from pre-proteins upon their import into the organelle. In the present study, two independent mutant *Arabidopsis* lines with T-DNA insertions in the SPP gene (*spp-1* and *spp-2*) were analysed. For both lines, the segregating progeny of *spp* heterozygotes contained heterozygous and wild-type plants in a ratio of 2:1, and no homozygous mutant plants could be detected. The siliques of heterozygous *spp-1* and *spp-2* plants contained aborted seeds at a frequency of ~25%, which suggests embryo lethality of homozygous mutations. By contrast, gametophytic effects could be ruled out since transmission of the *spp* mutations through the male and female gametes was found to be normal. Mutant and wild-type seeds were cleared and analysed by Nomarski microscopy in order to further elucidate the timing of the developmental arrest. Approximately ~25% of the seeds in mutant siliques exhibited delayed embryogenesis compared to those in wild type, with the mutant embryos never progressing normally beyond the 16-cell stage and cell divisions not completing properly thereafter. Furthermore, heterozygous *spp* mutant plants were phenotypically indistinguishable from the wild type, indicating that the *spp* knockout mutations are completely recessive and suggesting that one copy of the SPP gene is able to produce sufficient SPP protein for normal development under standard growth conditions.

## 4.2 Introduction

The chloroplast is a unique plant cell compartment which harbours many essential processes such as photosynthesis, starch metabolism, and the biosynthesis of lipids and secondary metabolites (Lopez-Juez and Pyke, 2005; Nelson and Ben-Shem, 2004). Like all plastids, chloroplasts are derived from an ancient free-living cyanobacterial ancestor that was incorporated into early eukaryotic cells through endosymbiosis (Reyes-Prieto et al., 2007). As a result of this evolutionary origin, modern chloroplasts contain DNA and are able to synthesise roughly one hundred of their own proteins (Timmis et al., 2004). Nonetheless, the bulk of the over 3000 different proteins in chloroplasts are encoded in the nuclear genome and must be imported post-translationally from the cytosol (Keegstra and Cline, 1999; Leister, 2003).

Soon after the emergence of the signal hypothesis to account for the translocation of ER proteins, it was suggested that nucleus-encoded chloroplast proteins are similarly synthesised with a targeting tag that directs them to the organelle (Blair and Ellis, 1973; Blobel and Sabatini, 1971). This tag is an N-terminal extension of the protein called a transit peptide, and it is cleaved off after organellar import, producing a smaller, mature form of the chloroplast protein (Bruce, 2000) (see also Section 1.3.8). Chloroplast transit peptides vary greatly in length and amino acid sequence, and while secondary structural features have been reported in some cases the general significance of such observations remains uncertain (Bruce, 2001; Krimm et al., 1999). Thus, it is not fully understood how different pre-proteins are all targeted quite specifically to the same organelle. Transit peptides do contain slightly more hydroxylated residues and fewer acidic residues than average, giving them a net positive charge, and it has been suggested that a

lack of a secondary structure might be necessary for their targeting properties (von Heijne and Nishikawa, 1991).

The transit peptide is recognised by receptor components at the chloroplast surface, and subsequently the pre-protein is guided through pores in the outer and inner envelope membranes. The multiprotein assemblies responsible for these recognition and translocation events are the TOC and TIC complexes (translocon at the outer/inner envelope membrane of chloroplasts) (Inaba and Schnell, 2008; Jarvis, 2008; Kessler and Schnell, 2006; Li and Chiu, 2010; Soll and Schleiff, 2004). Upon reaching the stromal side of the envelope, the transit peptide is removed by the stromal processing peptidase (SPP), a metalloendopeptidase of the M16 family (members of which include subunit  $\beta$  of the mitochondrial processing peptidase, MPP, and *Escherichia coli* pitrilysin) which has a high specificity for chloroplast transit peptides (Richter and Lamppa, 1998; Richter et al., 2005; VanderVere et al., 1995). The SPP enzyme recognises a stretch of basic residues with weak sequence or physicochemical conservation at the C-terminus of the transit peptide (Emanuelsson et al., 1999; Richter and Lamppa, 2002; Rudhe et al., 2004). Following recognition, it cleaves the transit peptide from the mature sequence using the catalytic activity of its zinc-binding domain, and subsequently proteolyse the C-terminal binding site of the transit peptide which facilitates release of the peptide fragments so that they may be degraded by the pre-sequence protease, PreP (Moberg et al., 2003; Richter and Lamppa, 2002, 2003) (see also Section 1.3.8). Homologues of SPP exist in red and green algae as well as in the malaria parasite, *Plasmodium falciparum*, suggesting that the protein's function is well conserved amongst plastid-containing organisms (Richter et al., 2005). An ancestral activity was probably inherited with the original endosymbiont, as SPP-related sequences even exist in cyanobacteria.

Antisense mediated down-regulation of *SPP* gene expression in *Arabidopsis* or tobacco plants resulted in chlorotic, albino or even a seedling-lethal phenotypes, indicating that the SPP enzyme plays an important role in chloroplast biogenesis (Wan et al., 1998; Zhong et al., 2003). Indeed, the antisense lines displayed reduced numbers of chloroplasts per cell, and those organelles that were present were structurally abnormal. Both *in vitro* import experiments (using isolated chloroplasts and radiolabelled preproteins) and an *in vivo* targeting assay (involving expression of a transit peptide fusion to green fluorescent protein) revealed defects in chloroplast protein import in the antisense lines (Wan et al., 1998; Zhong et al., 2003). Such defects may reflect the fact that most components of the TOC-TIC import machinery are themselves synthesised as pre-proteins (with transit peptides that presumably must be removed before those components can begin to operate), or indicate that transit peptide cleavage is a fully-integrated step of the translocation mechanism. More recently, a hypomorphic *spp* allele was identified in a forward-genetic screen of ethyl methanesulfonate-mutagenised rice plants (Yue et al., 2010). The relevant mutant lacks a conserved glutamate residue in a C-terminal M16 domain of SPP, and it exhibits chlorosis associated with small, under-developed chloroplasts as well as defective root development (see also Section 1.3.8).

The aforementioned *in vivo* studies all analysed the consequences of reduced levels of SPP activity for plant development. To determine the consequences of complete loss of SPP protein, T-DNA knockout mutants were identified and characterised in the *Arabidopsis* background.

## 4.3 Results

### 4.3.1 No homozygous *spp* mutants could be obtained

To further assess the importance of SPP during plant development, two different *Arabidopsis* lines with T-DNA insertions in the *SPP* gene (*AT5G42390*) were obtained from the Nottingham Arabidopsis Stock Centre (NASC). These mutants were called *spp-1* (SALK\_087683) and *spp-2* (SAIL\_242\_H11). Firstly, both T-DNA insertion sites were confirmed by genomic PCR, and by sequencing the T-DNA/gene junctions at one or both sides, as indicated (Fig. 4.1 A). In *spp-1*, the T-DNA disrupts the first exon of the *SPP* gene, whereas in *spp-2* the insertion lies in the nineteenth exon (Fig. 4.1 A).

Next, 30 antibiotic-resistant plants were genotyped for each line in PCR reactions using gene- and T-DNA-specific primers in an attempt to identify homozygous mutant lines in each case. However, it was found that all of the 60 tested plants (30 for each allele) were heterozygous for the relevant T-DNA insertion (Fig. 4.1 B), suggesting that the homozygous genotypes are not viable. Consistent with this notion, when segregation of the antibiotic-resistance marker associated with each T-DNA insertion was analysed (by plating seeds from heterozygous plants on medium containing either kanamycin [*spp-1*] or phosphinothricin [*spp-2*]), significant deviations from standard Mendelian inheritance were observed: only two antibiotic-resistant plants were observed for every one antibiotic-sensitive plant, instead of the more normal 3:1 segregation ratio (Table 4.1). The heterozygous *spp* mutants were visually indistinguishable from wild type and accumulated normal levels of chlorophyll (Fig. 4.2).

### **4.3.2 The *spp* mutation is embryo lethal but not gametophytic lethal**

To investigate the possibility of embryo lethality, the seeds within ripe siliques of heterozygous *spp-1* and *spp-2* plants were carefully examined. Significant numbers of small, aborted seeds were observed in both mutant genotypes (Fig. 4.3 A), but not within wild-type siliques (data not shown). Amongst the fertilised seeds, abortions occurred with a frequency of almost exactly 25% (Fig. 4.3 B), strongly supporting the notion that the homozygous mutant genotypes were responsible for developmental arrest. Small numbers (~3–5%) of what appeared to be failed ovules were also apparent in the *spp* siliques (data not shown), suggesting that there might be an additional effect of the mutations on gametophytic transmission (Kasmati et al., 2011; Kovacheva et al., 2007). To assess this possibility, reciprocal crossing experiments were conducted, between both *spp* alleles and wild-type plants, analysing transmission of the mutations to the resulting F<sub>1</sub> progenies by plating on selective media. However, the results revealed essentially normal transmission of both mutations through both male and female gametes (Fig. 4.3 C) (Howden et al., 1998). This indicated that the *spp*-mediated block in development is exclusively post-fertilisation, occurring during embryogenesis, and that the presumed failed ovules observed in ripe siliques (mentioned earlier) were perhaps very early seed abortions and/or the consequences of environmental stresses.

### **4.3.3 The *spp* mutation leads to embryo arrest at the 16-cell stage**

To precisely determine the stage of embryogenesis during which the *spp* mutations arrest growth, a detailed examination of developing embryos was conducted in both mutants as well as in the wild type, using Nomarski optics microscopy (Table 4.2). Figure 4.4 shows equivalent developmental series for normal (i–iv) and mutant (v–viii) embryos within immature siliques of self-pollinated *spp-1* (Fig. 4.4 A) and *spp-2* (Fig. 4.4 B)

heterozygotes. Typically, when normal embryos were at the 16-cell stage (Fig. 4.4, i panels), mutant embryos were delayed at the 2- to 8-cell stages (Fig. 4.4, v panels). As the normal embryos progressed to the globular and heart stages (Fig. 4.4, ii and iii panels), the mutants were retarded at the 8- to 16-cell stages (Fig. 4.4, vi and vii panels). In fact, the mutant embryos were never seen to develop normally beyond the 16-cell stage, even when the other embryos had reached the torpedo stage (Fig. 4.4, iv and viii panels). Cell boundaries in the most mature mutant embryos were frequently indistinct, and such embryos often had an irregular or swollen appearance. As the normal seeds reached the cotyledon stage, significant numbers of aborted seeds (with degenerated structures containing no discernable embryo) became apparent within the mutant siliques (Table 4.2). In contrast with the situation in *spp* siliques, where two distinct classes of embryos could be observed (normal and mutant; the latter corresponding to ~25% of the total), embryos within individual wild-type siliques rarely spanned more than three consecutive developmental stages (Table 4.2).

#### **4.3.4 Gene expression of *SPP* is more similar to *atTIC110* than to *atTOC75-III***

Interestingly, the aborted seeds of homozygous *spp* mutants (Fig. 4.3 A) were intermediate in size and stage of embryo arrest between those of homozygous *toc75-III* mutants, which arrest embryogenesis at the two-cell stage (Baldwin et al., 2005; Hust and Gutensohn, 2006), and those of homozygous *tic110* mutants, which arrest embryogenesis at the globular stage (Inaba et al., 2005; Kovacheva et al., 2005). Therefore, one may speculate that during embryogenesis maximal *SPP* gene expression might peak at a stage between maximal expression of *atTOC75-III* and *atTIC110*. However, when analysing publicly-available Affymetrix microarray data from the eFP browser (Winter et al., 2007), it seems that *SPP* expression is very similar to *atTIC110* expression, both

genes being expressed at much lower levels than *atTOC75-III* during early embryogenesis and reaching slightly higher expression levels during later embryogenesis (Fig. 4.5).

#### **4.3.5 Analyses of mRNA and protein expression in the *toc75-III*, *tic110* and *spp* heterozygotes**

Even though the gene expression pattern of *SPP* during embryogenesis is more similar to *atTIC110* than to *atTOC75-III*, the *spp* mutation is completely recessive (Fig. 4.2) like the *toc75-III* mutation, while the *tic110* mutation is semi-dominant (Baldwin et al., 2005; Kovacheva et al., 2005). To test if this is caused by higher mRNA expression levels of *SPP* and *atTOC75-III* compared to *atTIC110* at a later stage of development, qPCR was performed on 14 day old seedlings from the green heterozygotes of *spp* and *toc75-III* and the slightly pale heterozygote of *tic110*. It was found that the expression levels of *SPP* and *atTOC75-III* mRNA in the *spp* and *toc75-III* heterozygotes, respectively, were not significantly higher than the expression level of *atTIC110* in the *tic110* heterozygotes (Fig. 4.6 A), arguing against the idea that a lower *atTIC110* mRNA level causes the pale phenotype of the *tic110* heterozygote. Also, the extent of reduction of atToc75-III and atTic110 protein levels in the *toc75-III* and *tic110* heterozygotes compared to wild type did not differ significantly, showing that the semidominant effect of the *tic110* mutation is also not caused by a reduced protein level (Fig. 4.6 B).

## 4.4 Discussion

While it was evident from earlier studies that SPP is an important chloroplast protein, the phenotype of homozygous knockout plants had not previously been reported. In this study, we employed *Arabidopsis* T-DNA insertion lines to demonstrate that SPP is indispensable *in vivo*. Homozygotes were absent from the progeny of plants carrying *spp* mutations, while a quarter of the seeds in the siliques of such plants were aborted, consistent with an embryo lethal phenotype. The mutant embryos exhibited delayed development, with cell divisions not terminating properly after the 16-cell stage. This work further emphasises the importance of plastid functions during seed development, and extends the list of protein transport components known to be essential for plant viability.

It is well documented that the disruption of chloroplast functions can lead to a block in embryogenesis (Bryant et al., 2011). In fact, it has been estimated that a disproportionately large number (~25–30%) of non-redundant, embryo-lethal mutations in *Arabidopsis* affect chloroplast proteins (Hsu et al., 2010; McElver et al., 2001). Prominent amongst the chloroplast functions that lead to embryo arrest, when disrupted, are: plastid gene expression (including RNA and protein synthesis); non-photosynthetic metabolism (including amino acid, vitamin and nucleotide biosynthesis); and, protein modification, transport and degradation (Bryant et al., 2011; Hsu et al., 2010). Of the previous reports linking chloroplast function to embryogenesis, those pertaining to two core components of the chloroplast protein import machinery, atToc75-III and atTic110, are most relevant (Baldwin et al., 2005; Hust and Gutensohn, 2006; Inaba et al., 2005; Kovacheva et al., 2005). The aborted seeds observed in the *spp* mutant siliques (Fig. 4.3 A) appeared to be somewhat larger than those in *toc75-III* (Baldwin et al., 2005), and

smaller in size than those in *tic110* siliques (Kovacheva et al., 2005), suggesting that the *spp* mutations may affect embryo development at a stage intermediate between *toc75-III* and *tic110*.

The *spp* mutations indeed arrest embryogenesis at a stage (the 16-cell stage) intermediate between those during which *toc75-III* (two-cell stage) and *tic110* (globular stage) block growth (Baldwin et al., 2005; Hust and Gutensohn, 2006; Inaba et al., 2005; Kovacheva et al., 2005). These differences in phenotype severity may partly reflect the differing expression patterns of the genes during embryogenesis: publicly-available microarray data show that *atTOC75-III* expression peaks at a much earlier stage in embryogenesis than that of either *atTIC110* or *SPP* (Fig. 4.5) (Casson et al., 2005; Spencer et al., 2007; Winter et al., 2007). The phenotypic differences may also be linked to the roles of the proteins, as has been discussed (Hsu et al., 2010). Toc75 is the channel component of the outer membrane through which the vast majority of chloroplast proteins gain entry, including many envelope proteins, while Tic110 is thought to play roles in channel formation and/or the coordination of chaperones at the inner membrane, and is likely to be utilised by a smaller subset of chloroplast-destined proteins (Jarvis, 2008; Li and Chiu, 2010). The proteins that are dependent upon SPP for proper targeting may be intermediate in number and/or importance. An alternative explanation is that the differing phenotypes are a reflection of differing stabilities of the proteins, and the extent to which they can persist at functional levels during embryogenesis following the segregative loss of a functional gene. Irrespective of the basis for these differences in severity, the data leave no doubt that all three proteins play crucial roles in protein transport, and that efficient protein transport into plastids is essential during embryogenesis.

While *toc75-III* mutations are completely recessive (Baldwin et al., 2005), heterozygous *tic110* plants are clearly chlorotic with quantifiable defects in chloroplast biogenesis (Kovacheva et al., 2005). In this respect, the *spp* mutations are more similar to *toc75-III*, as *spp* heterozygotes were visibly indistinguishable from wild type throughout development (Fig. 4.2, A and B), and accumulated normal levels of chlorophyll pigment (Fig. 4.2 C). This indicates that a single copy of the *SPP* gene is able to produce sufficient quantities of the peptidase for normal growth under standard conditions. The phenotypic difference between *tic110* heterozygotes and *toc75-III* or *spp* heterozygotes cannot easily be explained in terms of mRNA or protein levels, as quantitative RT-PCR and immunoblot experiments did not reveal more severe deficiencies in *tic110* plants/+ (Fig. 4.6). As was discussed previously (Patel et al., 2008), the greater dosage dependency of the *tic110* mutation may reflect the absence of excess expression capacity for *atTic110* in the wild type.

## 4.5 Materials and Methods

### 4.5.1 Plant growth and chlorophyll analysis

All *Arabidopsis thaliana* plants were of the Columbia-0 ecotype. For *in vitro* growth, seeds were surface sterilised, sown on Murashige and Skoog agar medium containing 0.5% (w/v) sucrose in petri plates, cold treated at 4°C, and thereafter kept in a growth chamber, as described previously (Aronsson and Jarvis, 2002) (see Section 6.1.2). To select for the presence of T-DNA insertions, the following antibiotics were added to the medium: kanamycin monosulfate, 50 µg/ml (*spp-1*); phosphinothricin, 10 µg/ml (*spp-2*). All plants were grown under a long-day cycle (16 h light, 8 h dark). Chlorophyll content was measured using a SPAD-502 meter following the manufacturer's instructions (Konica-Minolta) (see Section 6.1.6.2). Conversion from SPAD units to chlorophyll concentration values (nmol chlorophyll *a+b* per mg fresh weight) was done using a validated calibration curve (Ling et al., 2011).

### 4.5.2 Identification of the *spp* mutants

The *spp-1* mutant was from the Salk Institute Genomic Analysis Laboratory (line number SALK\_087683) (Alonso et al., 2003), while the *spp-2* mutant was from Syngenta (line number SAIL\_242\_H11) (Sessions et al., 2002). Mutant genotypes were assessed by PCR (Fig. 4.1 B). Genomic DNA was extracted from *Arabidopsis* plants using a published protocol (Edwards et al., 1991) (see Section 6.2.9) and PCR was conducted using standard procedures. The primers used were as follows: *spp-1* forward, 5'-CTTCAAACCCTTTGCTACAAA-3'; *spp-1* reverse, 5'-GACGATGGATTAAACCTAACT-3'; *spp-1* T-DNA LB, 5'-GCGTGGACCGCTTGCTGCAACT-3'; *spp-2* forward,

5'-AAACTGTGTATAGGTCTGGTT- 3'; *spp-2* reverse, 5'-GGAGACGAGAGATG-AGTATAGATAATGGGG-3'; *spp-2* T-DNA LB, 5'-TAGCATCTGAATTCATAA-CCAATCTCGATACAC-3'. Amplification products were resolved by agarose gel electrophoresis and stained with SYBR Safe (Invitrogen). The location of each T-DNA insertion was determined precisely (Fig. 4.1 A) by sequencing PCR products spanning both junctions (except in the case of *spp-2*, where only one junction was identified).

#### **4.5.3 Seed and embryo analyses**

The phenotypes of seeds in ripe siliques were determined by dissecting siliques held on double-sided sticky tape using a stereo microscope (Zeiss Stemi 2000). The analysis of cleared wild-type and *spp* mutant embryos using Nomarski optics was performed as described previously (Baldwin et al., 2005; Goubet et al., 2003), using a microscope equipped for differential interference contrast (Nikon Eclipse 80i).

#### **4.5.4 Quantitative RT-PCR analysis of mRNA levels**

Total RNA samples were extracted from ~10–30 whole seedlings that had been grown *in vitro* for 14 days under standard conditions. RNA was isolated using an RNeasy Plant Mini Kit (Qiagen, Hilden, Germany), and was then treated with DNase I (DNA-free; Ambion, Texas, USA). Quantitative RT-PCR was performed using an MJ Research Chromo4 Gradient Cycler (Bio-Rad, Hercules, CA, USA) and SYBR Green Jump Start Taq Ready Mix (Sigma, St. Louis, MO, USA) for high-throughput quantitative PCR. Relative quantification was determined according to published methods (Allen et al., 2006; Pfaffl, 2001) (see also Section 6.3.2). Reactions were characterised by comparing

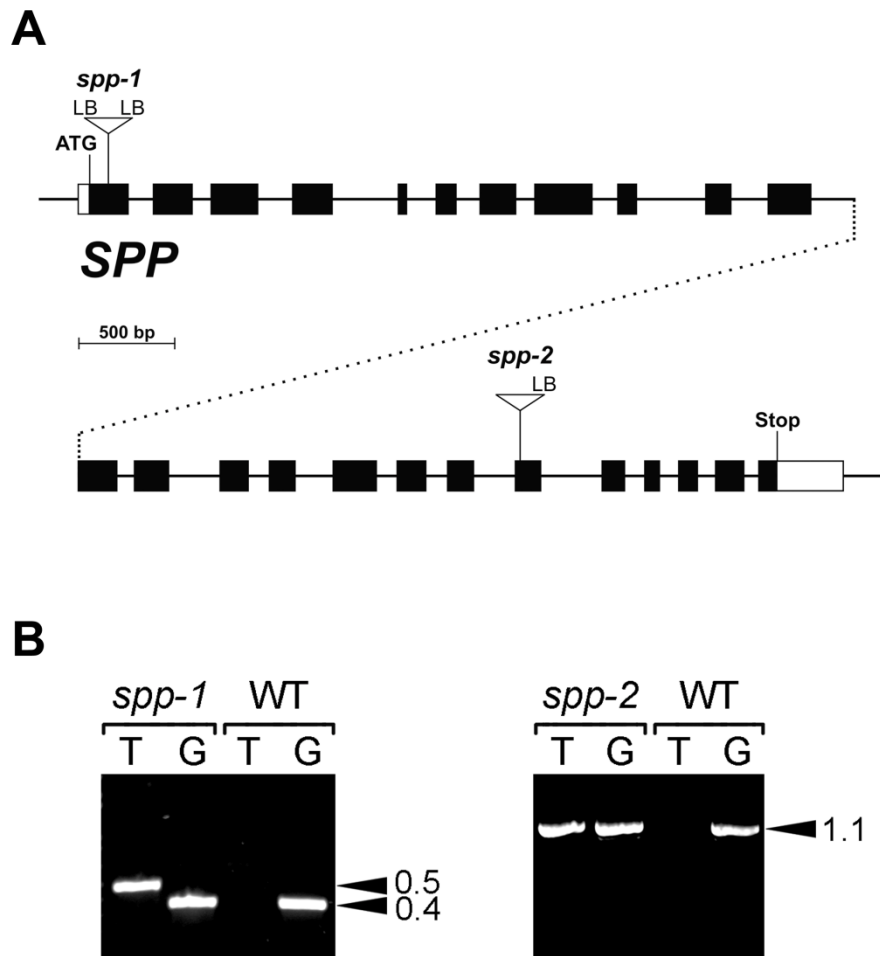
threshold cycle (CT) values; CT is a unit-less value defined as the fractional cycle number at which the sample fluorescence signal passes a fixed threshold. The relative amount of transcript was calculated by subtracting the control gene (*ACTIN 2*; At3g18780) CT-value from the gene-of-interest (*atTOC75-III*, *atTIC110*, *SPP*) CT-value ( $\Delta$ CT). Then,  $\Delta$ CT values for the wild type were subtracted from those for the mutants to yield  $\Delta\Delta$ CT values, and these were used to estimate expression levels as  $2^{-\Delta\Delta CT}$ . Data shown are means ( $\pm$  standard error) derived from four independent amplifications performed on three biological replicates. The *ACTIN2* primers have been described previously (Kasmati et al., 2011); the other primers used were: *atTOC75-III* sense 5'-TCGCATCTCCACTCAATC-3'; *atTOC75-III* antisense, 5'-GTCTCTGTATCTCGGTTA GG-3'; *atTIC110* sense, 5'-CTCCTCAGGTGCCTTATCAGAAG-3'; *atTIC110* antisense, 5'-CGAGCAAGAGCAGCCGAGAAC-3'; *SPP* sense, 5'-AAGC-TAGCCATGATTCTGCAA-3'; *SPP* antisense, 5'-CATCATGAGCAACAGG-AAGTT-3'.

#### **4.5.5 Immunoblot analysis of protein levels**

Total protein was extracted from plant material samples equivalent to those in Section 4.5.4, using previously-described procedures (Kasmati et al., 2011) (see also Section 6.4.1). Three different protein amounts (80, 60 and 40  $\mu$ g) of each genotype were analysed by immunoblotting, as described previously (Kasmati et al., 2011) (see also Section 6.4.6) , using primary antibodies against *atToc75-III*, *atTic110* and the plasma membrane H<sup>+</sup>-ATPase, PMA2 (Aronsson et al., 2010; Kasmati et al., 2011; Morsomme et al., 1998); unfortunately, an *SPP* antibody was not available for this work. The secondary antibody was anti-rabbit IgG conjugated with horseradish peroxidase (Santa

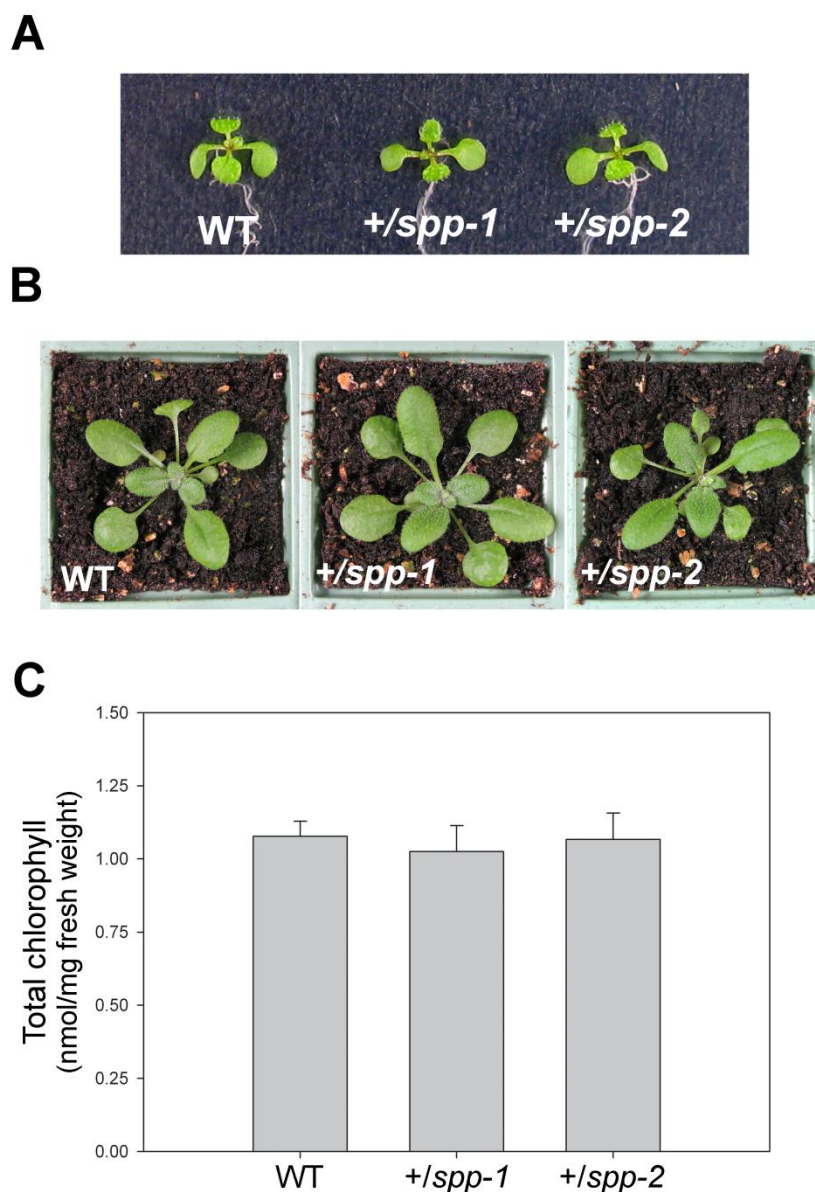
Cruz Biotechnology, Santa Cruz, CA, USA), and the detection reagent was ECL Plus (GE Healthcare, Chalfont St. Giles, UK). Chemiluminescence detection employed a Fujifilm LAS-4000 imager. Quantification of all images was performed using Aida software (Raytest, Straubenhardt, Germany). The atToc75-III and atTic110 data were normalised using equivalent PMA2 data. Values shown are means ( $\pm$  standard error) derived from three independent measurements.

## 4.6 Figures and Tables



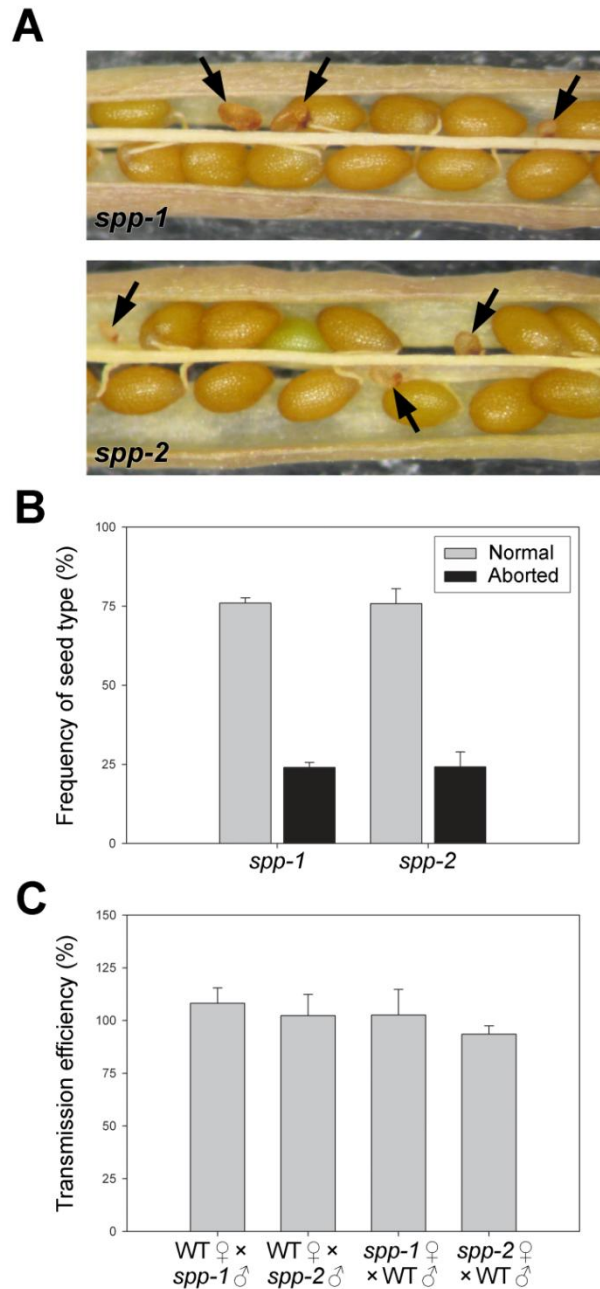
**Figure 4.1.** Molecular characterisation of the *SPP* T-DNA insertion mutants.

(A) Schematic diagram of the *SPP* gene showing the location of each T-DNA insertion. Exons: black boxes; introns: black lines; UTRs: white boxes; ATG: start codon. The gene model shown is based on the RIKEN full-length cDNA clone, RAFL07-08-B09; it is separated over two lines to aid presentation. Positions of T-DNA insertions are indicated precisely, but the insertion sizes are not to scale. (B) Genomic DNA samples extracted from wild-type and mutant plants (*spp-1* and *spp-2*) were analysed by PCR. Appropriate T-DNA- and *SPP*-gene-specific primers were employed in two different combinations: the first (T) comprised one T-DNA primer (LB) and one gene-specific primer (forward for *spp-1*; reverse for *spp-2*); the second (G) comprised two gene-specific primers flanking the T-DNA insertion site. The results shown for *spp-1* and *spp-2* are representative of those obtained for all antibiotic-resistant plants tested; amplification using both T and G indicated the presence of both mutant and wild-type alleles, respectively, and demonstrated that the plants were heterozygous. Amplicon sizes are indicated at right (in kb).



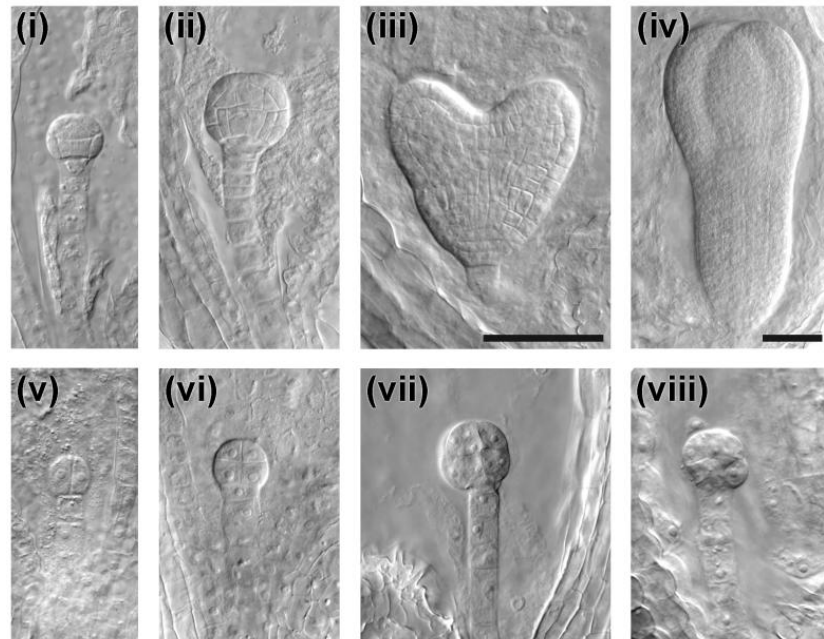
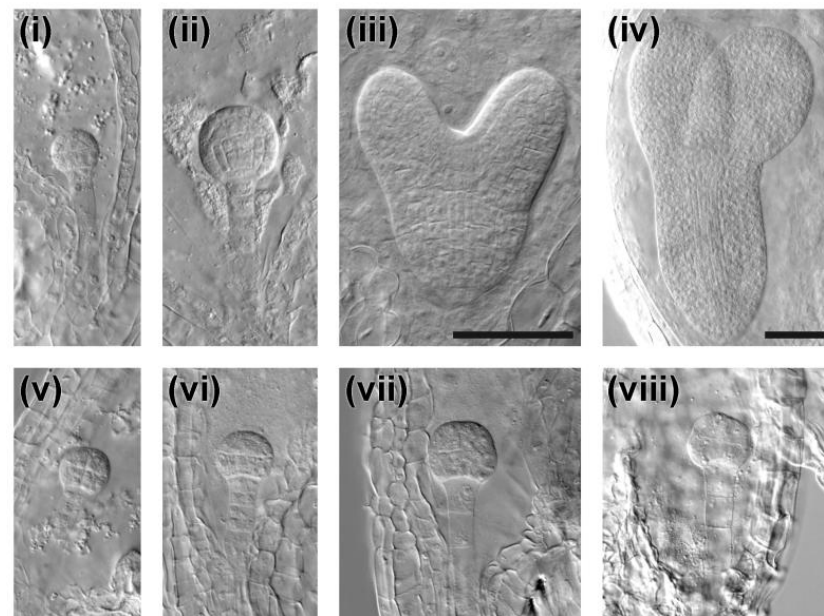
**Figure 4.2.** Phenotypic analysis of the *spp* heterozygotes.

(A,B) Plants of the indicated genotypes were grown *in vitro* on selective medium (non-selective in the case of wild type) for 7 days, and then photographed (A). Additional similar plants were transferred to soil on day 7, and then allowed to grow further until they were 21 days old prior to photography (B). Representative plants are shown in each case. (C) Chlorophyll concentrations in 21-day-old plants grown as described above were determined using a SPAD-205 meter. Values shown are means ( $\pm$  standard error) derived from six independent measurements per genotype, each one taken using a different plant. Units are nmol chlorophyll *a+b* per mg fresh weight of tissue.



**Figure 4.3.** Embryo lethality of the *spp-1* and *spp-2* mutations.

(A) Aborted seeds indicative of embryo lethality (see black arrows) are smaller in size than normal seeds, and have a darker, shriveled appearance. (B) Frequencies of normal and aborted seeds within ripe siliques of *spp-1* and *spp-2* heterozygotes. The data shown are means ( $\pm$  standard error) derived from analyses of six different siliques per genotype, each one from a different plant. Values shown refer to fertilised seeds only. (C) Transmission of the *spp-1* and *spp-2* mutations through the male and female gametes was assessed by crossing heterozygotes of both mutants to wild type, in both directions, multiple times (28-50 crosses per direction and allele). Inheritance of the *spp* mutations in the F<sub>1</sub> progeny was assessed by determining antibiotic resistance of the F<sub>1</sub> plants. Transmission efficiencies were calculated for each plant as described previously (Howden et al., 1998), and then these values were used to derive the means shown ( $\pm$  standard error).

**A****B**

**Figure 4.4.** Analysis of embryo development in the *spp* mutants using Nomarski optics. Equivalent developmental series for normal (i-iv) and mutant (v-viii) embryos within immature heterozygous siliques of *spp-1* (A) and *spp-2* (B). Normal embryos: i, 16-cell stage; ii, early globular stage; iii, heart stage; iv, torpedo stage. Corresponding mutant embryos from the same siliques: v, 2-8 cell stages; vi, 8- to 16-cell stages; vii and viii, arrested or abnormal 16-cell stages. Embryo developmental stage names refer to the cell number or morphology of the embryo proper. Images i-iii and v-viii are all at the same magnification (40× objective); images iv are at lower magnification (20× objective). Bars = 50 μm.

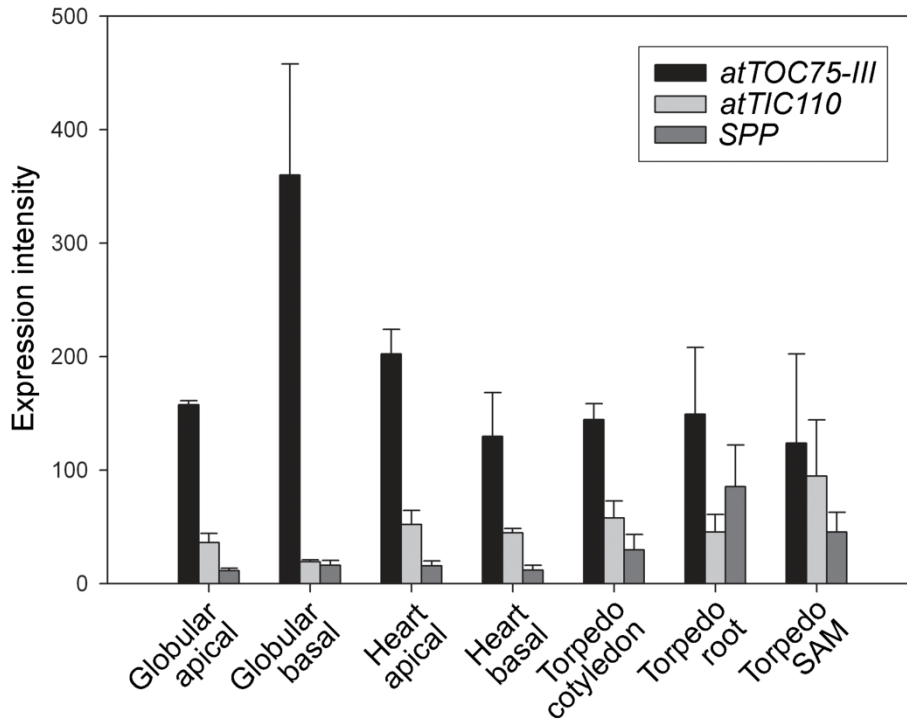


**Figure 4.5.** Expression pattern of *atTOC75-III*, *atTIC110* and *SPP* during embryogenesis. Publicly-available Affymetrix microarray data corresponding to defined tissues and developmental stages of *Arabidopsis* embryogenesis (Casson et al., 2005; Spencer et al., 2007) were accessed using an electronic fluorescent pictograph (eFP) browser online (Winter et al., 2007). Data for the essential chloroplast protein import apparatus genes *atTOC75-III* (*AT3G46740*), *atTIC110* (*AT1G06950*) and *SPP* (*AT5G42390*) are shown. Values are means ( $\pm$  standard error) derived from three or six independent measurements. SAM, shoot apical meristem.

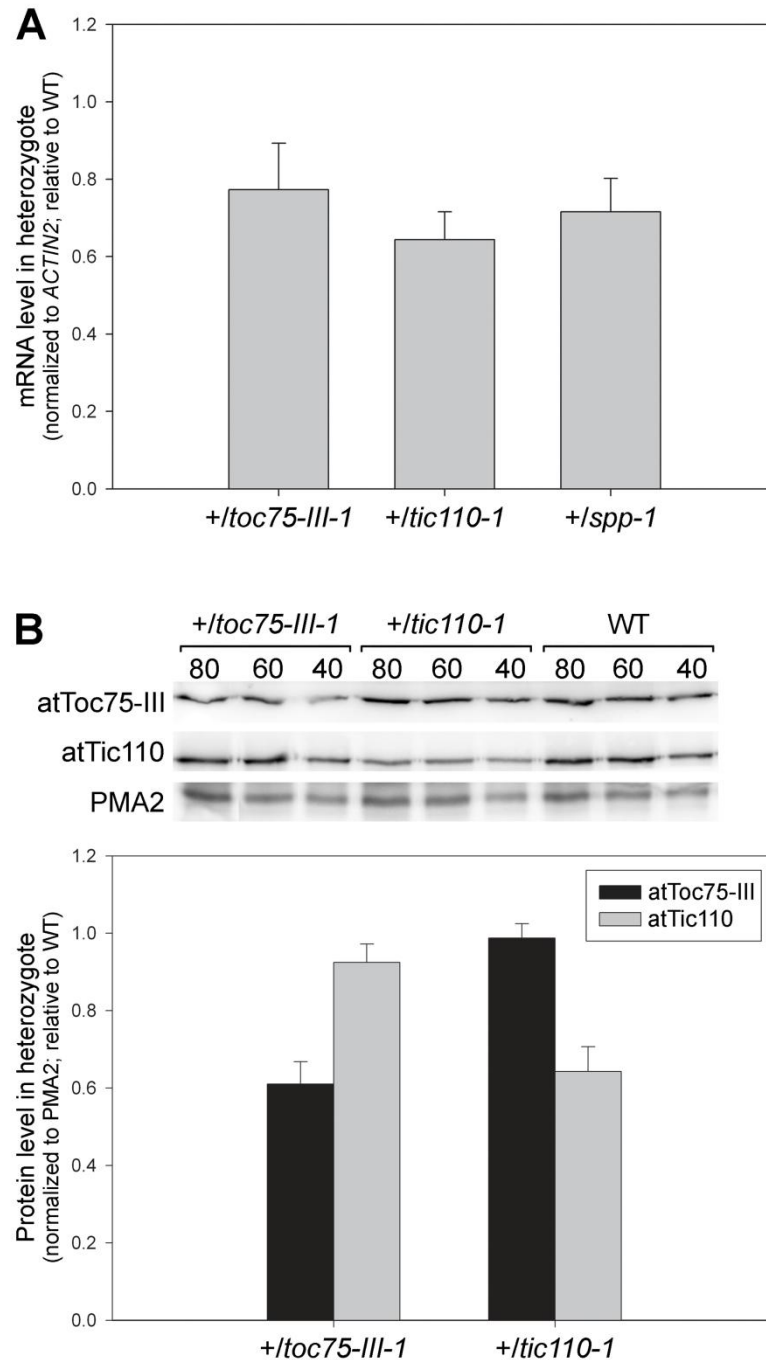


**Figure 4.6.** Expression analyses in the *toc75-III*, *tic110* and *spp* heterozygotes. (A) Quantitative RT-PCR analysis of mRNA levels. The levels of *TOC75-III*, *TIC110* and *SPP* mRNA in 14-days-old seedling of the indicated heterozygous mutants are shown relative to the corresponding mRNA level in wild type (which is assigned the value 1). All values (including for wild type) were first normalised to the values for *ACTIN2* mRNA in all genotypes to account for fluctuations which are caused by other factors than the genotype itself. (B) Immunoblot analysis of protein levels. Of each genotype, 80, 60 and 40  $\mu$ g of total protein extracted from 14-days-old seedlings was loaded. The plasma membrane H<sup>+</sup>-ATPase (PMA2) was used as a loading control. The protein levels are shown relative to wild type and normalised to PMA2, similar as in (A).

Parental genotype	Plant number	Antibiotic	Resistant (R)	Sensitive (S)	R:S ratio	<i>P</i> -value <sup>a</sup>
+/spp-1	1	Kanamycin	87	37	2.35	0.41
	2		82	44	1.86	0.71
	3		99	42	2.36	0.37
	4		69	46	1.50	0.13
	<i>sum</i>		337	169	1.99	0.97
+/spp-2	1	Phosphinothricin	74	38	1.95	0.89
	2		105	43	2.44	0.27
	3		78	43	1.81	0.61
	4		100	45	2.22	0.56
	5		83	40	2.08	0.85
	<i>sum</i>		440	209	2.11	0.54

**Table 4.1.** Segregation of the T-DNA-borne antibiotic resistance markers in the *spp* mutant lines. (a) Goodness of fit of the observed ratios to 2:1 was assessed by  $\chi^2$  analysis. *P*-values are the probabilities that the observed ratios differ from 2:1 due to random chance only.

Genotype / Siliques <sup>b</sup>	1-cell	2-cell	8-cell	16-cell	Aborted seed <sup>c</sup>	EG <sup>a</sup>	LG <sup>a</sup>	EH <sup>a</sup>	Heart	Torpedo	Cotyledon	Total scored	Proportion delayed
<b>WT</b>													
1			9	22		5						36	
2			4			11	23	6				44	
3						4	33	10				47	
4							20	18	9			47	
5								17	33			50	
6									37	18		55	
7									1	19	33	53	
8											53	53	
<b>spp-1</b>													
1	2	15	22	5								44	
2		2	12	25		2						41	
3	1	3	7	17		17						45	
4			3	12		3	15	15				48	0.31
5		2	2	8			5	4	21			42	0.29
6			8	8	8				5	22	2	45	0.36
7			6	6	6					3	26	41	0.29
<b>spp-2</b>													
1		2	11	5								18	
2		2	12	6		4						24	
3			12	11		7	1	1				32	
4			4	6		12	5	3				30	
5			8	2		2	10	13				35	
6			2	5	1	9	5	6	10			38	0.21
7			2	8	2				15	21		48	0.25
8				2	7				2	30		41	0.22
9			1	9	9					6	26	42	0.24

**Table 4.2:** Distribution of the embryo phenotypes in single siliques of wild type and *spp* mutant heterozygotes. (a) Embryo developmental stage names refer to the cell number or morphology of the embryo proper. Abbreviations are defined as follows: EG, early globular; LG, larger globular; EH, early heart. (b) Siliques were numbered consecutively from the top of the inflorescence, such that the oldest siliques have the highest numbers. (c) Aborted seeds were shriveled with no visible embryo or endosperm development.

# Chapter 5

## General Discussion

Plastid protein import is a complex process which takes place at the plastid envelope membranes, and the first key players in this process were discovered and characterised almost 20 years ago (Hirsch et al., 1994; Kessler et al., 1994; Perry and Keegstra, 1994; Schnell et al., 1994). Since then, research on plastid protein import has yielded a rough picture for the function of many TOC and TIC components. However, especially with regard to the TIC components, many uncertainties remain to be resolved by future research. Tic110 and Tic40 are TIC components that are known to form a complex in the inner envelope membrane which also involves chaperones (Chou et al., 2003; Inoue et al., 2013; Stahl et al., 1999; Su and Li, 2010) and, based on their interaction with Toc75 and importing precursor proteins, have been proposed to be integral parts of the TOC/TIC system (Akita et al., 1997; Caliebe et al., 1997; Lubeck et al., 1996; Nielsen et al., 1997). Disagreement on the topology of Tic110 led to the conflicting ideas that Tic110 might form (or form part of) the inner envelope channel of the TIC translocon (Balsera et al., 2009; Heins et al., 2002) or rather a membrane-anchored scaffold for the binding of stromal chaperones (Inaba et al., 2005; Inaba et al., 2003; Jackson et al., 1998; Tsai et al., 2013). Recent research suggest that Tic110 and Tic40 are not part of the TIC channel (Kikuchi et al., 2013), but might rather act at a later stage during protein import (Chou et al., 2006), presumably after pre-proteins have already passed through the channel. It might be speculated that the stromal processing peptidase (SPP), the pre-sequence protease (PreP) and chaperones involved in protein import propulsion form processing-propulsion complexes together with Tic110 and Tic40.

Since the functions of Tic110 and Tic40 are yet unclear, a forward genetic screen has been performed on pale *tic40* mutants (which are more suitable for such genetic analyses than the embryo-lethal *tic110* mutants) and the two suppressor loci *stic1* and *stic2* have been identified. This work achieved the identification of the *ALB4* locus as

the *ALB4* gene, which is mutated in all five *stic1* alleles, and confirmed suppression of *tic40* by the *alb4* mutation with an independent T-DNA insertion mutant, *alb4-1* (see also Section 2.4). Moreover, it excluded the possibility that some ALB4 is localised in the envelopes but rather confirms the localisation in the thylakoids (see Fig. 2.5) as reported previously by Benz et al. (2009). This is intriguing, since it is not evident how the lack of a thylakoid protein can suppress the visual defect of *tic40* mutants. The easiest explanation would be that *stic* mutants accumulate thylakoids non-specifically which would lead to a greener phenotype in most pale mutant backgrounds. However, it could clearly be shown that *stic1* suppresses exclusively the pale *tic40* phenotype, and that neither other *tic* mutants nor unrelated pale chloroplast mutants are suppressed by *stic1* (Fig. 2.3 and 2.4). Additionally, *stic1* also suppresses the protein import defect of *tic40* mutants, suggesting that an indirect signal in *stic* mutants acts directly on the TOC/TIC apparatus.

Interestingly, work by Dr Feijie Wu revealed that the *stic2* mutants have essentially the same properties than the *stic1* mutants (unpublished results). Furthermore, the present work shows clearly that ALB4 and STIC2 interact, and that they most likely share a common function, the abrogation of which suppresses *tic40* by a common response. This is underlined by the finding that *stic1* and *stic2* single mutants have a very similar defect in the thylakoid ultrastructure which includes swollen, more spherical chloroplasts, frequently disrupted and disorganised stromal lamellae and an accumulation of plastoglobules (Fig. 2.8, see also Section 2.4). But what might that common function of ALB4 and STIC2 be?

While STIC2 is a small stromal protein with an as yet unknown function, ALB4 has been described to be involved in the assembly and stabilisation of ATP synthase complexes in the thylakoid membrane (Benz et al., 2009). ALB4 is a paralogue of the

thylakoid protein ALB3 which is involved in the insertion of LHCPs into the thylakoid membranes (Gerdes et al., 2006; Moore et al., 2003; Moore et al., 2000). The absence of two C-terminal motifs in ALB4 account for its inability of LHCP insertion and, hence, for the lack of a visible phenotype defect of *alb4* mutants (Falk et al., 2010). In this study, an interaction of ALB4 with ALB3 as well as cpSRP components and VIPP1 could be shown, partly conflicting with previous reports (Benz et al., 2009). The study of *alb3 alb4* double mutants further supports the idea that ALB3 and ALB4 may contribute differentially but synergistically to the process of protein insertion, potentially of pigment-binding photosystem core subunits (Fig. 3.2 and 3.3). Together with the finding that both ALB4 and STIC2 are able to bind to cpHsc70 and potentially other chaperones, these results suggest that ALB4 and STIC2 play a role in chaperoning or fine-tuning thylakoid protein insertion (see Section 3.4). This would also fit to the absence of a visible phenotype different from wild type of *stic1/alb4* and *stic2* mutants, to the disturbed thylakoid ultrastructure and accumulation of plastoglobules in the *stic1/alb4* and *stic2* mutants as shown in the present study (Fig. 2.8), and to the fact that *alb4* mutants have a changed ratio of large and small ATP synthase complexes (Benz et al., 2009).

Furthermore, genetic analyses support the idea that ALB4 is involved in thylakoid protein insertion. The *alb4 ftsy* double mutants are visibly smaller and more impaired in development than the *ftsyt* single mutants (Fig. 3.8). Similarly, the *alb4 cpsrp43 cpsrp54* triple mutants are much smaller and more impaired in development than the *cpsrp43 cpsrp54* double mutants (Fig. 3.8). Because *alb4* lacks a visible phenotype different from wild type, these double and triple mutant phenotypes are considered more than additive, and a functional overlap becomes apparent. Interestingly, similar to the semi-dominant behaviour of *stic1/alb4* in the suppression of *tic40*, the *alb4* mutation also behaves in a semi-dominant fashion in the homozygous *ftsyt* background, suggesting that

ALB4 protein levels are important for the extent of its functionality. On the other hand, the double mutants *alb4 seca1* and *alb4 hcf106* show no differences to the seedling-lethal *seca1* and *hcf106* single mutants (Fig. 3.7), suggesting that there is no genetic interaction between *ALB4* and *SECA1* and between *ALB4* and *HCF106* and that therefore a functional overlap between ALB4 and the thylakoid Sec or Tat protein targeting systems is unlikely. In summary, the genetic analysis complements the biochemical protein interaction studies and leads to the conclusion that ALB4 (and potentially also STIC2) plays a minor role in thylakoid protein insertion together with ALB3, cpSRP and cpFtsY (see also Section 3.4).

Assumed that both ALB4 and STIC2 play a role in chaperoning or fine-tuning thylakoid membrane protein insertion, how could a defect in such a process suppress the protein import defect of *tic40* mutants? A hint comes from the finding that Tic40, apart from its function in protein import propulsion, was reported to be involved in protein re-insertion into the inner envelope membrane (Chiu and Li, 2008). Since it has been known for a long time that the inner envelope membrane is the central site for plastid lipid biosynthesis (Douce and Joyard, 1990) and that proteins which are essential for thylakoid biogenesis reside in the inner envelope membrane (Garcia et al., 2010; Kobayashi et al., 2007; Kroll et al., 2001), it could be speculated that Tic40 has an influence on plastid membrane biogenesis. Indeed, it was shown that over-expression of Tic40 in the plastid genome leads to an over-accumulation of plastid membranes (Singh et al., 2008), and that in *Brassica napus* the Tic40 homologue BnaC.Tic40 is essential for tapetal maturation which depends on lipid biosynthesis and accumulation in plastids of the tapetal tissue (Dun et al., 2011). If Tic40 is involved in the regulation of thylakoid biosynthesis, it becomes more plausible that a thylakoid membrane defect could sup-

presses *tic40* mutants through feedback regulation. But what factors would such a feedback regulation include?

Microarray expression profiling of *stic1* and *stic2* mutants showed that in both mutants the same gene is up-regulated over 20-fold compared to wild type (Fig. 2.13). It is therefore tempting to speculate that this gene, termed *HINAS1* for highly induced in *Arabidopsis stic* locus 1, is part of such a feedback regulation as described above (see also Section 2.4). To assess this possibility, it will have to be determined if HINAS1 is necessary for suppression (by investigating whether *tic40* is still suppressed in the *stic tic40 hinas1* triple mutant) and if it is sufficient for suppression (by analyzing whether HINAS1 over-expression in *tic40* can suppress *tic40* alone). Apart from *HINAS1*, predominantly genes involved in perception and transduction of auxin and jasmonic acid signals were up-regulated in the *stic* mutants, suggesting that the thylakoid defect caused by *stic1* and *stic2* might induce such a hormonal signal. It might be speculated that *HINAS1* expression is induced as a response to such a hormonal signal and, given that the list of genes that are significantly up-regulated in the *stic* mutants is rather short, that *HINAS1* up-regulation might actually be the defining response of STIC malfunction. The function of the HINAS1 protein is completely unknown, and its localisation is predicted to be nuclear although its *Arabidopsis* paralogue, HINAS2, is predicted to be chloroplast localised by the majority of prediction tools. It will be interesting to determine if HINAS1 localises to the chloroplast inner envelope membrane and is involved in the regulation of chloroplast protein import, potentially under specific conditions of thylakoid disruption. As the suppression of *tic40* by the *stic* mutants is very specific, and no other pale mutant that was tested could be suppressed, one might even speculate that HINAS1 has Tic40-like function and complements the absence of Tic40 in the *stic tic40* suppressors.

Since the knockout of *STIC* genes is a rather artificial situation, the question might arise: Under which natural conditions is *HINAS1* up-regulated? Is it possible that under certain stress conditions *STIC* (or *Tic40*) function is impaired, resulting in disturbed thylakoid biogenesis and thus the need for up-regulation of alternative, stress-induced regulators of thylakoid biogenesis? The present study shows that at least the *STIC* proteins are likely not necessary under specific stress conditions but share a rather constitutive function (see also Section 2.4). It cannot be excluded, though, that the *STIC* proteins become crucial under a certain stress condition that has not been tested in this study. But even if the *STIC function* is rather constitutive, the *STIC malfunction* might still be stress-induced and lead similarly to hormone signals and *HINAS1* induction like the *stic* knockout mutants. This will have to be determined in future by looking directly at *HINAS1* expression under stress conditions. A specific visual phenotype in the *stic* mutants or under such stress conditions might be prohibited by *HINAS1* up-regulation, and therefore it will be fascinating to observe if *stic hinas1* or *tic40 hinas1* double mutants have more severe phenotypes than the respective single mutants.

Presently, it is not known whether the *tic40* phenotype is so mild compared to *tic110* because *Tic40* function is less important than *Tic110* function, or because other proteins (potentially *HINAS1*) can have *Tic40*-like functions. *Tic40* has been shown to be crucial for the release of the transit peptides of importing precursors from *Tic110* and therefore to facilitate precursor processing (Chou et al., 2006). The subsequent steps of precursor processing are cleavage of the transit peptide by the stromal processing peptidase (SPP), degradation of the transit peptide by the pre-sequence protease (PreP) and complete translocation of the precursor into the stroma, potentially by the action of *Hsp93* (Kovacheva et al., 2007; Moberg et al., 2003; Richter and Lamppa, 2002, 2003). Therefore, one might speculate that SPP acts on pre-proteins at a similar stage to *Tic40*

and Tic110. In this study, it was shown that *SPP* is an essential gene, and that knockout mutants abort embryo development at the 16-cell stage (Fig. 4.4, see also Section 4.4). This is intermediate to knockout mutants of *toc75-III* and *tic110*, suggesting that either Toc75-III is essential at an earlier stage in embryogenesis than SPP and Tic110, or that parent-derived Toc75-III protein is less stable and degraded sooner in the early embryo than parent-derived SPP and Tic110. Like for *toc75-III/+*, the heterozygous *spp/+* mutants had no visible defect (Fig. 4.2), suggesting that both mutations are recessive and the observed reduction in mRNA levels (and for Toc75-III also protein levels) in the heterozygotes do not impair function. This is in contrast to the semi-dominant *tic110/+* heterozygotes where the reduced mRNA and protein levels caused a visibly paler phenotype than wild type and impaired efficiency in chloroplast protein import (Kovacheva et al., 2005). Thus, it seems that Tic110 function is dependent on abundant availability of Tic110 protein, which might not be the case for SPP.

# Chapter 6

## General Materials and Methods

## **6.1 Growth of *Arabidopsis* plants and basic handling techniques**

### **6.1.1 Preparation of Murashige and Skoog medium plates**

For half-strength Murashige and Skoog (MS) medium with 0.5% (w/v) sucrose and 0.6% plant agar, 17.2 g of MS basal salt mixture (Duchefa), 20 g of sucrose (Fisher), and 2 g of 2-(N-morpholino)ethanesulfonic acid (MES, Melford) were mixed in 2 liters of purified water (Elgastat Option 2) and the pH was adjusted to 5.7 with KOH. In each of five 500 ml Duran bottles, 2.4 g of phyto agar (Duchefa, 950-1050 g/cm<sup>3</sup>) and 400 ml of the MS solution were added. The bottles were autoclaved at 120°C for one hour in a Boxer autoclave and stored at room temperature for further use. For plates, an MS bottle was heated in a microwave in cycles of 90 seconds at 950 W with few second breaks. Molten MS was either directly poured in plastic Petri dishes (Sterilin, 9 cm diameter) placed in the laminar flow hood (Bassaire) or first supplemented with sterile antibiotics or salts according to the experimental requirements. Poured plates (ca. 16 per 400 ml medium) were dried for at least 1 hour in the laminar flow hood and then stored at 4°C in plastic bags for further use.

### **6.1.2 Growth of *Arabidopsis thaliana* plants on plates**

*Arabidopsis thaliana* seeds were sterilised as follows: Seeds were aliquoted in micro-centrifuge tubes to an approximate volume of 20-50 µl. To each aliquot, 500 µl of 70% ethanol containing 0.05% Triton X-100 was added. The tubes were closed and incubated vertically at 250 revolutions per minute on an orbital shaker (SO1, Stuart Scientific) for 10 minutes. Then they were quickly centrifuged in an Eppendorf centrifuge (5415 D, rotor EL 082) at low speed to collect the seeds at the bottom of the tube. The superna-

tant was removed and replaced with 500  $\mu$ l of 100% ethanol. The tubes were again incubated on the orbital shaker for 10 minutes. For each aliquot of seeds, a Whatman filter paper (circles, 70 mm diameter) was folded in the middle and opened again to leave a groove for the seeds to be easily dispersed on the plates. The filter papers were soaked with industrial methylated spirits (IMS, Fisher Scientific) in a laminar flow hood and let dry. The seeds were centrifuged and pipetted onto the middle of the dry filter paper with a cut blue (1 ml) tip. The seeds were left to dry for ~30 minutes and then dispersed on the plates to a density of roughly 100-150 seeds per plate. Plates were sealed with Micropore tape (3M) and stratified at 4°C for 2-3 days. Stratified plates were put into Percival growth cabinets with white fluorescent light of approximately 120  $\mu$ E/m<sup>2</sup>/s and a constant temperature of 20°C at a classical long day cycle (8h dark, 16h light).

### **6.1.3 Growth of *Arabidopsis* plants on soil**

*Arabidopsis* seeds were put into microcentrifuge tubes and covered with ~500  $\mu$ l of water. The tubes were stratified at 4°C for 2-3 days. Soil (Seed and Modular Compost Plus Sand, Levington) was mixed with vermiculite at a ratio of approximately 10:1 and filled into pots of variable sizes. Trays with pots were soaked with water containing 1 ml of Gnat Off (Hydrogarden) per litre of water as a biological pest control against larvae from sciarid flies. To the stratified seeds, 500  $\mu$ l of top agar (0.05% phyto agar) was added and mixed to achieve a homogeneous suspension of seeds. The seeds were distributed evenly on the soaked soil with a pipette using a cut blue (1 ml) tip. Alternatively, 14-day-old seedlings from plates were transferred onto soil using forceps, taking care that the roots remained intact and were completely covered in soil to prevent the seedlings from dehydrating. The trays were put into growth cabinets (Percival or

Snijders Scientific) at 22°C, 60% relative humidity, with a classical long day cycle and an average of about 150  $\mu\text{E}/\text{m}^2/\text{s}$  of fluorescent white light for experiments, or in a greenhouse for seed bulking. They were covered with a plastic lid for 2 days at high humidity, then the lid was removed and the trays were watered regularly.

#### **6.1.4 Crossing of *Arabidopsis* plants**

Plants were grown on soil as described above. Desired genotypes were assigned to the female acceptor and the male donor. Usually, homozygous mutants with a clear, recessive phenotype were used as female acceptors because self-pollinated progeny could be easily eliminated in the  $F_1$  based on the mutant phenotype. Mutants containing resistance markers were used as male donors because in this case selection could be used in the  $F_1$  to eliminate self-pollinated progeny. From 2-3 branches of the acceptor genotype per cross, all siliques and opened flowers were removed. From the 3-4 largest unopened flower buds of these branches, all sepals, petals and stamens were removed with forceps (INOX, Dumont). The remaining pistils were left to recover over night. The branches were labelled with the donor genotype and open donor flowers were used to pollinate the stigmata using forceps. The stigmata were re-pollinated after one day and the developing siliques allowed to reach maturity.

#### **6.1.5 Transformation of *Arabidopsis* plants using *Agrobacterium tumefaciens***

Plants were grown on soil as described above. When the plants reached a height of approximately 5 cm, the primary shoots were clipped in order to promote the formation of a higher number of secondary branches. The plants were left to grow secondary branches for approximately one week.

### **6.1.5.1 Freeze-thaw transformation of *Agrobacterium***

This method was adapted from a method described previously (Weigel and Glazebrook, 2006). About 1  $\mu$ l of the desired plasmid was added to 50  $\mu$ l of *Agrobacterium* stock suspension (GV3101 cells) and mixed. The tube was frozen in liquid nitrogen and subsequently thawed by incubating at 37°C in a water bath for 5 minutes. To the cells 1 ml of LB medium (see Section 6.2.1) was added and they were incubated at 28°C for 2-4 hours, shaking at 240 rounds per minute (rpm) (Temperature Controlled Shaker Cabinet, Gallenkamp). After 30 seconds centrifugation at 5000 rpm (Eppendorf centrifuge, 5415 D, rotor EL 082) the pellet was resuspended in 50-100  $\mu$ l of LB medium and spread on LB plates containing gentamycin (7.15  $\mu$ g/ml) against growth of other bacteria plus a plasmid-specific antibiotic for selection of transformed agrobacteria. The plates were put at 28°C for 2-3 days. Then, a single resistant colony was put into 5 ml of LB medium containing the required antibiotic using a sterile yellow pipette tip, leaving the tip in the medium. The culture was incubated at 28°C over-night, shaking at 240 rpm. Then, 1 ml of the over-night culture was transferred into 300 ml LB medium containing the required antibiotic in a 1 litre Erlenmeyer flask. The culture was incubated at 28°C over-night, shaking at 240 rpm.

### **6.1.5.2 Floral-dip transformation of *Arabidopsis***

This method is adapted from a method described previously (Clough and Bent, 1998). Over-night *Agrobacterium* culture (250 ml) was centrifuged at 5000 rpm for 10 minutes in 250 ml Nalgene tubes using a Sorvall RC6 centrifuge (using the Swinging Bucket Rotor 7500 6445). The pellet was resuspended in approximately 50 ml of 5% (w/v) sucrose containing 300  $\mu$ l/l Silwet L-77 (Lehle Seeds) and further diluted in su-

crose/Silwet solution until the suspension reached an optical density (OD) between 0.7 and 0.8 at 600 nm wavelength. All siliques and open flowers of the *Arabidopsis* plants were removed and the above-ground parts were dipped into the *Agrobacterium* suspension with gentle swirling for 20-30 seconds. The plants were covered with a plastic dome for one day to retain high humidity and then watered as usual from ~5 days after transformation until full maturity. Mature seeds were sown on MS plates containing 200 µg/l cefotaxime (against growth of *Agrobacterium* on the plates) and an additional selection agent for the specific T-DNA-borne plant resistance marker.

### **6.1.6 Chlorophyll measurements**

Plants were grown on plates to an age of 10-14 days or on soil to an age of 3-4 weeks as described above. Amounts of chlorophyll in these plant samples were measured in two different ways.

#### **6.1.6.1 Chlorophyll measurements of plants grown on plates**

Samples of whole seedlings were weighed in microcentrifuge tubes to a total of 15-30 mg depending on phenotype. To the seedlings 1 ml of dimethylformamide (DMF) was added and the tubes were wrapped in aluminium foil and incubated over-night on an orbital shaker (SSM1, Stuart) at 4°C and 30 rpm. Wild-type-like samples were diluted 1:5 in DMF before measurement. The absorbance of each sample was measured for the wavelengths 646.8 nm and 663.8 nm in the fume hood relative to a blank (DMF) using a spectrophotometer (Ultrospec 100 Pro Visible, Amersham) and a 200 µl quartz cuvette. The cuvette was rinsed with DMF between the reads. The readout of the absorbance should ideally be between 0.01 and 0.8; if it exceeded 0.8 the sample was further

diluted in DMF. Amounts of chlorophyll in nmol per mg of fresh weight were calculated as follows (Porra et al., 1989):

Chlorophyll  $a = ((13.43 \times A_{663.8}) - (3.47 \times A_{646.8}) \times \text{dilution factor}) / \text{fresh weight}$

Chlorophyll  $b = (22.9 \times A_{646.8}) - (5.38 \times A_{663.8}) \times \text{dilution factor} / \text{fresh weight}$

Chlorophyll  $a+b = (19.43 \times A_{646.8}) + (8.05 \times 663.8) \times \text{dilution factor} / \text{fresh weight}$

#### **6.1.6.2 Chlorophyll measurements of plants grown on soil**

Individual leaves per sample were measured using the SPAD-502 chlorophyll meter (Konica Minolta) according to the manufacturer's guidelines. The readout  $A$  was converted into nmol of total chlorophyll ( $a + b$ ) per mg of fresh weight using the following formula (Ling et al., 2011):

Chlorophyll  $a+b = 0.0007 \times A^2 + 0.023 \times A + 0.0544 \text{ nmol/mg}$

## **6.2 Bacterial work, cloning and DNA-related techniques**

### **6.2.1 Preparation of LB medium**

For liquid medium, 25 g of lysogeny broth (LB, Melford) was dissolved in 1 litre of purified water. The broth was aliquoted into 500 ml Duran bottles and autoclaved for 1 hour at 120°C. For plates, 50 g of lysogeny broth was dissolved in 2 litres of purified water and aliquoted 5 × 400 ml into five 500 ml Duran bottles containing 7 g of agar (ForMedium) each. The bottles were autoclaved for 1 hour at 120°C and let cool to hand temperature before any antibiotics were added according to the experimental requirements. The medium was poured into plates in a flow hood and let dry for at least one hour.

### **6.2.2 PCR, agarose gel and gel band purification**

Polymerase chain reaction (PCR) was performed using Biometra Thermocycler T1 or T3 devices and standard reaction mixtures (10 mM Tris-HCl pH 8.3, 50 mM KCl, 50 mM MgCl, 0.05% Tween® 20, 200 µM of each dNTP, 125 nM of each primer) with differences based on protocols for different DNA polymerases. DNA polymerases were mostly used at 0.5 units per 20 µl reaction, or otherwise depending on the user guide. Primers were designed based upon the PrimerSelect program from the Lasergene Core Suite of DNASTAR and ordered at Sigma-Aldrich. Agarose gels were prepared with 1% (standard) to 3% (CAPS and dCAPS) agarose (Melford) in 0.5× TBE (44.5 mM Tris, 44.5 mM boric acid, 1 mM EDTA) containing 1× SYBR safe DNA gel stain (Invitrogen). Samples were loaded in 1× Orange G loading buffer (0.1% Orange G, 50% glycerol), next to a DNA marker (mostly 1 Kb Plus DNA Ladder from Invitrogen) and

run in tanks ((Wide) Mini-Sub® Cell GT, Bio-Rad) containing 0.5× TBE at ~10 V/cm. Finally, the bands were visualised using GeneFlash (Syngene). If the PCR product was to be retrieved, the gel band was cut on a UV dual intensity transilluminator (UVP) at low intensity and processed using the QIAquick Gel Extraction kit (Qiagen) following exactly the manufacturer's guidelines.

### **6.2.3 *E.coli* heat shock transformation and plasmid preparations**

Competent DH5α *Escherichia coli* cells (Alpha-Select Silver Efficiency, Bioline) (25 µl) were thawed on ice. About 10-50 ng (or according to purpose) of plasmid was added to the cells and the tubes were incubated on ice for 30 minutes with flicking every 5-10 minutes. The cells were heat-shocked for 45 seconds at 42°C (this was done in a Thermomixer or a water bath) and then left on ice for 2 minutes. Liquid LB medium (450 µl), pre-warmed at 37°C, was added and the tubes were incubated at 37°C for 2 h, with shaking at 240 rpm. Aliquots (50 µl and 200 µl) of each transformation were streaked on LB plates containing a plasmid-specific antibiotic, and the plates were incubated at 37°C over-night. Individual colonies were picked with yellow pipette tips and the whole tips were put in 5 ml of liquid LB containing the plasmid-specific antibiotic. The culture was incubated at 37°C over night with shaking at 240 rpm. *E. coli* stocks were prepared with a 1:1 mixture of over-night culture and sterile 50% glycerol and stored at -80°C. Minipreps were performed with the over-night culture using the QIAprep Spin Miniprep kit (Qiagen) or the ISOLATE Plasmid Mini kit (Bioline) following exactly the manufacturer's guidelines. For midi-preps, 500 µl of the over-night culture was diluted in 50 ml of liquid LB medium containing the plasmid-specific antibiotic. The 50 ml culture was grown at 37°C over-night and midi-preps were performed

with the culture using the QIAfilter Plasmid Midi kit (Qiagen) or GenElute Plasmid Midiprep kit (Sigma-Aldrich) following exactly the manufacturer's guidelines. Plasmid DNA was quantified using a NanoDrop 2000 spectrophotometer (Thermo Scientific).

#### **6.2.4 Restriction digestion and CAPS/dCAPS markers**

Restriction enzymes (mostly from NEB) were used to cleave DNA at specific sites. Plasmid and genomic DNA sequences were first digested *in silico*, mostly using the online program NEBcutter (NEB), in order to choose restriction enzymes for specific experiments. Restriction digestions were performed with specific buffers and at specific temperatures which depended on the enzyme that was used. Digested fragments were visualised on 1% (cut vectors), 2% (CAPS markers), or 3% (dCAPS markers) agarose gels. Cleaved amplified polymorphic sequence (CAPS) markers were chosen based on differences in the DNA sequence between two genotypes that give rise to differential restriction patterns (Konieczny and Ausubel, 1993). CAPS primers were designed on both sides of the marker, and PCR-amplified fragments were digested with the specific restriction enzyme that gives rise to the differential pattern. Analysis of the pattern on a 2% agarose gel allowed a higher resolution of fragments with similar size than on 1% gels, and allowed assignment of the DNA sequence to one or the other genotype. In cases where a restriction enzyme recognition site was incomplete, a long primer was designed that covered the restriction site and contained sequence alterations that led to a full recognition site in the PCR product of one genotype but not in the other. This long designed CAPS (dCAPS) primer was made in a way such that at least 20 nucleotides could be cleaved off by the restriction enzyme, and a second primer was designed at the opposite side so that the total length of the PCR product was around 100 nucleotides

(Neff et al., 1998). The cleavage by digestion would lead to two bands of approximately 20 and 80 base pairs which could be visualised on a 3% agarose gel.

### **6.2.5 Cloning of a DNA sequence using the Gateway® technology**

Primers for the DNA sequence to be cloned were designed based on sequence information in The Arabidopsis Information Resource 8 (TAIR 8) database ([www.arabidopsis.org](http://www.arabidopsis.org)). The forward primer was given the 5'-addition 5'-AAAAGCAGGCTCC-3' and the reverse primer was given the 5'-addition 5'-AGAAAGCTGGGT-3'. PCR was always performed using either HiFi Platinum Taq polymerase (Invitrogen) or Phusion High-Fidelity DNA polymerase (NEB). A second PCR was performed (annealing temperature 55°C) using 10 µl of the primary PCR product in a 50 µl reaction and the primers AttB1: 5'-GGGGACAAGTTTGTACAAAAAAGCAGGCT-3' and AttB2: 5'-GGGGACCACTTTGTACAAGAAAGCTGGGT-3' which bind to the 5'-additions that were introduced into the primary PCR product with the first primers. The secondary PCR product was run on a standard 1% agarose gel and retrieved using the QIAquick Gel Extraction kit.

#### **6.2.5.1 BP reaction**

Approximately 100 ng of gel-purified secondary PCR product was mixed with ~100 ng of pDONR 207 vector (Invitrogen) and 1 µl of BP clonase (Invitrogen) per 5 µl reaction. The reaction was incubated at 25°C for 1 hour or overnight and terminated with 0.5 µl of proteinase K (Invitrogen) at 37°C for 10 minutes. *E. coli* DH5α cells were transformed with the reaction as described in Section 6.2.3, and streaked on LB plates con-

taining the antibiotic gentamycin (7.15 µg/ml) which selects for pDONR 207. Plasmid from positive colonies was collected by mini-prep as described in Section 6.2.3, and tested by a restriction digestion in a way such that the fragment pattern seen could distinguish between empty pDONR 207 vectors and plasmids containing the PCR product. Plasmids containing the PCR product were sequenced using the pDONR-specific primers pDONR-F: 5'-TCGCGTTAACGCTAGCATGGATCTC-3' and pDONR-R: 5'-GTAACATCAGAGATTTTGAGACAC-3'. Only plasmids with the correct PCR insertion and sequence were used for LR reactions.

#### **6.2.5.2 LR reaction**

Approximately 100 ng of the entry clone (pDONR 207 containing PCR product) and ~100 ng of destination vector (depending on the experiment) were mixed with 1 µl of LR clonase (Invitrogen) per 5 µl reaction. The reaction was incubated at 25°C for 1 hour and terminated with 0.5 µl of proteinase K (Invitrogen) at 37°C for 10 minutes. *E. coli* DH5α cells were transformed with the reaction as described in Section 6.2.3 and streaked on LB plates containing the destination vector-specific antibiotic. Mini-preps were extracted from resistant clones and the plasmid was tested by restriction digestion as described in Sections 6.2.3 and 6.2.4, respectively. For stable expression of the constructs in *Arabidopsis*, *Agrobacterium tumefaciens* was transformed with the plasmid using the freeze-thaw method and plants were transformed with *Agrobacterium* using the floral-dip method as described in Sections 6.1.5.1 and 6.1.5.2.

### **6.2.6 Cloning for bimolecular fluorescence complementation**

For bimolecular fluorescence complementation (BiFC), the vectors pSAT4(A)-nEYFP-N1 and pSAT4(A)-cEYFP-N1 containing the genetic information for the N- and C-terminal halves of yellow fluorescent protein (YFP), respectively, were used (Tzfira et al., 2005). Primers were designed in order to amplify the target gene without the stop codon such that the YFP fragments could be attached C-terminally to the protein. Primer extensions were designed with restriction sites such that restriction digestion of the PCR product and the plasmids would allow an unambiguous ligation of the PCR product into the vector, and that the 5' ends of the YFP sequences would be in frame with the gene of interest. Digested vectors were phosphatase treated in order to prevent re-circularisation as follows: 1 µl of Calf Intestine Alkaline Phosphatase (CIAP, Fermentas) was added to each 50 µl reaction; the reaction was incubated at 37°C for 30 minutes and terminated at 85°C for 15 minutes. Ligation was performed with T4 DNA ligase and ligation buffer (NEB) following the manufacturers guidelines. The ligation was transformed into *E. coli* DH5α as described in Section 6.2.3, and colonies resistant to the plasmid-specific antibiotic were screened for positive insertions by colony PCR with one primer in the vector and the other in the inserted sequence (Ward, 1992). Plasmid DNA from colonies with positive insertions was collected using the mini-prep method, subjected to a control restriction digestion, and sequenced, as described above in Section 6.2.5.

### 6.2.7 Cloning for antigen expression and antibody production

For antigen expression, the pQE-30 vector system (Qiagen), which encodes a C-terminal 6×His tag, was used. Primers were designed to amplify just the soluble, C-terminal part of ALB4 in order to avoid problems with solubility during expression. Primer extensions again contained restriction sites for an unambiguous ligation of the PCR product into the vector and were designed such that the 3' region encoding the 6×His tag was in frame with the target gene. Phosphatase treatment and ligation were performed as described in Section 6.2.6. The ligation was transformed into *E. coli* XL1-Blue (a high *lacI* expressor) which was grown in presence of 1% glucose in order to repress expression of the construct via the lac operon in pQE-30. This prevents leaky expression during cloning and ensures optimal growth in case the protein is toxic to the bacterium. Colonies resistant to the plasmid-specific antibiotic were again tested by colony PCR, restriction digestion and sequencing as described above in Sections 6.2.5 and 2.6.

For induction of recombinant protein expression, positive clones were grown in 5 ml LB cultures containing the plasmid-specific antibiotic and 1% glucose over-night at 37°C, and then diluted 1:100 in 500 ml LB (again containing antibiotic and glucose). This culture was grown for 2-3 hours at 37°C until it reached an OD<sub>600</sub> of approximately 0.6. Then, 1 mmol/l isopropyl-β-D-thiogalactopyranosid (IPTG) was added and the culture was grown at 28°C over night. The optimal concentration of IPTG was found by conducting a test induction with a range of different IPTG concentrations followed by western blotting using an anti-His antibody. Cells were harvested by centrifugation at 5000 g and resuspended in 15 ml of lysis buffer (2-5 ml per gram of pellet; 50 mM NaH<sub>2</sub>PO<sub>4</sub>, 300 mM NaCl, 10 mM imidazole, pH 8.0). After sonication of the lysate (6×10 seconds with 10 second intervals) and centrifugation at 10,000 g, the supernatant

was collected and 2 ml of 50% Ni-NTA slurry (Qiagen) was added in order to bind the His-tagged proteins. The supernatant-slurry mixture was transferred onto a column (Vivaspin, Sartorius) and washed twice with 8 ml wash buffer (50mM NaH<sub>2</sub>PO<sub>4</sub>, 300mM NaCl, 20mM imidazole, pH 8.0) by gravity flow. The bound His-tagged protein was eluted in six fractions by adding 6×0.5ml elution buffer (50 mM NaH<sub>2</sub>PO<sub>4</sub>, 300 mM NaCl, 250 mM imidazole, pH 8.0) and the individual fractions were tested for abundance and purity of the antigen protein by SDS-PAGE and Coomassie staining (see Section 6.4.4). The identity of the antigen protein was confirmed by MALDI-TOF using the Leicester University on-campus Protein Nucleic Acid Chemistry Laboratory (PNAACL) service and sent to Harlan for antibody production.

### **6.2.8 DNA precipitation**

In case a higher concentration of DNA was needed than was initially available, the DNA was precipitated and resuspended in a smaller volume. To the DNA sample, 0.1 volumes of 3 M sodium acetate and 2 volumes of 100% ethanol were added. The sample was vortexed and incubated at -20°C for at least one hour (or overnight). The sample was then centrifuged at maximum speed in a microcentrifuge at 4°C for 30 minutes; the supernatant was decanted and the remaining liquid removed from the tube walls with a paper towel. The pellet was washed with 300 µl of 70% ethanol by flicking the tube several times, and then the sample was centrifuged again at maximum speed and 4°C for 10 minutes. The supernatant was decanted, the remaining liquid removed with a paper towel, and the pellet air dried before resuspension in the desired volume of sterile water.

### 6.2.9 DNA extraction from plant leaves and genotyping

One medium-sized leaf per sample was put into a 1.5 ml microcentrifuge tube containing a glass bead (BDH Prolabo, 2.5-3.5 mm) and flash-frozen in liquid nitrogen. The leaf tissue was disrupted by using a Qiagen TissueLyser for 30 seconds (maximum frequency), and then 0.5 ml of DNA extraction buffer (200 mM Tris-HCl, pH 7.5, 250 mM NaCl, 25 mM EDTA, 0.5% SDS) was added to the tissue powder. The samples were again mixed using the TissueLyser for one minute (at maximum frequency) and then centrifuged at maximum speed and 4°C for 5 minutes in an Eppendorf 5417 R microcentrifuge. The supernatant was transferred to a fresh tube and 450 µl of isopropanol was added to precipitate the DNA. The samples were incubated at -20°C for at least 1 hour and then centrifuged at maximum speed and 4°C for 6 minutes. The supernatant was discarded, the pellets were washed with 70% ethanol by vortexing, and the samples were again centrifuged at maximum speed and 4°C for 5 minutes. The supernatant was discarded completely and the pellets were dried in a vacuum desiccator (Kartell) for 15-20 minutes. Dried DNA pellets were resuspended in 50 µl of sterile water (or depending on pellet size).

For genotyping, *Arabidopsis* mutants with T-DNA insertions were grown on half-strength MS medium containing the selection according to the T-DNA type as described in Section 6.1.2. In case the resistance marker was silenced, plants were directly grown on soil (see Section 6.1.3). Resistant plants were transferred to soil two weeks after germination and DNA extraction was performed with 4-weeks-old plants as described above. Primers flanking the T-DNA insertion site (as specified in TAIR 8) were designed and PCR was performed on the sample DNA as described in Section 6.2.2. PCR on DNA from heterozygous (and wild-type) plants will yield a product, but the large T-DNA insertion in both alleles of the homozygous plant will prevent a product. In order

to confirm the presence of the T-DNA insertion in homozygous plants, a T-DNA-specific primer (according to the type of T-DNA) was used together with either the forward or reverse primer depending on the orientation of the T-DNA insertion. Homozygous plants were used for further analysis or crosses (see Section 6.1.4).

## 6.3 RNA-related techniques

### 6.3.1 RNA extraction and semi-quantitative RT-PCR

Samples (100 mg) of 2-week-old *Arabidopsis* seedlings grown on plates (Section 6.1.2) were harvested into 1.5 ml microcentrifuge tubes and flash-frozen in liquid nitrogen. A sterile pellet pestle (Sigma) was used to grind the plant material to fine powder. RNA isolation from the ground plant material was performed with the Spectrum™ Plant Total RNA Kit (Sigma), following exactly the manufacturer's guidelines. Extracted RNA was DNase I treated using the DNA Free kit (Ambion) and then quantified using a NanoDrop 2000 spectrophotometer. For reverse transcription, about 5 µg of RNA was added to 1 µl of the oligo-dT primer (50 µM stock) and 1 µl of 10mM dNTP mix in a 13 µl reaction and incubated at 65°C for 5 minutes followed by a quick chill on ice. Then, 4 µl of 5× first strand buffer (Invitrogen), 2 µl of 100 mM DTT and 1 µl of RNase inhibitor was added to reach a total reaction volume of 20 µl. After two minutes of incubation at 42°C, 1 µl of SuperScript™ reverse transcriptase (Invitrogen) was added and the reaction was incubated at 42°C for a further 50 minutes; the enzyme was inactivated by heating to 70°C for 15 minutes. Complementary DNA (cDNA) was quantified using a NanoDrop 2000, and then diluted 4-8 times to reach equal concentrations among a sample set. Semi-quantitative RT-PCR was performed using primers for the target gene and the control primers eIF4E1-F: 5'-AAACAATGGCGGTAGAAGACACTC-3' and eIF4E1-R: 5'-AAGATTTGAGAGG-TTCAAGCGGTGTAAG-3' for the eukaryotic initiation factor 4E1 (*eIF4E1*, AT4G18040 (Rodriguez et al., 1998)), cDNA of equal concentration, and a lower number of PCR cycles (20-25 cycles). The bands of the gel image were then quantified *in silico* using AIDA Image Analyser soft-

ware (Raytest) by drawing boxes of equal size around each band, quantifying pixel intensity, and normalizing these values to the values for the control bands.

### 6.3.2 qPCR

For quantitative PCR (qPCR), cDNA was produced as described above (Section 6.3.1), and primers specific for the target that produce a ~200 bp product and anneal at 58-60°C were designed. In a 20 µl total reaction volume, 10 µl of SYBR Green JumpStart™ *Taq* ReadyMix™ (Sigma), 200nM of each primer, 1 µl cDNA (an equal concentration of each sample) were mixed. The samples were transferred into a 96-well ABgene PCR plates (Thermo Scientific) and analysed with an MJ Research PTC-200 thermal cycler coupled to the Chromo4 detector (Bio-Rad). A threshold was arbitrarily set above the background fluorescence and the  $C_{\tau}$  values (fractional number of cycles at which the sample fluorescence reaches the threshold) were determined for each sample. The expression level of the target in each sample was determined using the comparative  $C_{\tau}$  method (Livak and Schmittgen, 2001).

$$\text{Normalised expression} = 2^{-\Delta\Delta C_{\tau}}$$

$$\Delta\Delta C_{\tau} = ((C_{\tau, \text{sample}} - C_{\tau, \text{reference}})_{\text{mutant}} - (C_{\tau, \text{sample}} - C_{\tau, \text{reference}})_{\text{wt}})$$

## **6.4 Biochemical and protein-related techniques**

### **6.4.1 Total protein extraction from *Arabidopsis* plants**

Plant material (leaf or seedlings) was harvested into a 1.5 µl microcentrifuge tube and flash-frozen in liquid nitrogen. To 980 µl of protein extraction buffer (100 mM Tris-HCl, pH 6.8, 10% glycerol, 0.5% SDS, 0.1% Triton X-100, 5 mM EDTA), 10 µl of 1 M dithiothreitol (DTT) and 5 µl of 200× protease inhibitor cocktail (cOmplete mini, Roche) were added freshly. The plant material was ground with a pellet pestle (Sigma) and 200 µl of protein extraction buffer containing DTT and protease inhibitors were added per sample to the ground powder. The powder was homogenised in the extraction buffer using the pestle, and the sample was subsequently centrifuged at maximum speed and 4°C for 10 minutes in a microcentrifuge. About 150 µl of the supernatant per sample was transferred to a fresh tube and stored at -20°C (short time) or -80°C (long time), or used for downstream experiments.

### **6.4.2 Protein quantification using BioRad microassay**

Bovine serum albumin (BSA) (10 µg/µl, NEB) was diluted 1:10 in sterile water and a standard curve was generated by adding 0, 1, 2, 4, 6, 8 and 10 µl of 1 µg/µl BSA to sterile water to reach a total volume of 799 µl each. Then, 1 µl of protein extraction buffer was added to compensate for its absorption. For the actual samples, 1 µl of protein (in extraction buffer) was added to 799 µl of sterile water. After adding 200 µl of Bio-Rad Protein Assay (Bio-Rad), the samples were vortexed, incubated for 5 minutes at room temperature, and then the absorbances were measured at a wavelength of 595 nm using

a DU 730 UV/Vis spectrophotometer (Beckman Coulter) and disposable cuvettes (Semimicro, Fisherbrand). The control absorbance values were plotted against the BSA concentrations in Excel (Microsoft) and the equation of a linear approximation was used to calculate the concentrations of all other samples by inputting their absorbance values.

### **6.4.3 Protein precipitation**

When a higher concentration of protein was required than was available in a sample, the proteins were precipitated and subsequently resuspended in a smaller volume. An equal volume of 20% trichloroethanoic acid (TCA) was added to the sample which then was incubated on ice for 30 minutes. The sample was centrifuged at maximum speed and 4°C for 30 minutes in a microcentrifuge, and then the supernatant was decanted and the remaining liquid on the tube walls removed with a paper towel. The pellet was washed with 500 µl of pre-chilled 100% acetone by vortexing and then centrifuged again at maximum speed and 4°C for 5 minutes. The supernatant was decanted and the pellet air dried over-night. The dried pellet was then resuspended in the desired volume of protein extraction buffer (see Section 6.4.1).

### **6.4.4 SDS-PAGE and Coomassie staining**

Polyacrylamide resolving gels containing 375 mM Tris-HCl, pH 8.8 and 0.1% SDS were generally prepared with acrylamide concentrations between 10% (lower resolution, shorter running time) and 15 % (higher resolution, longer running time). A 30% acrylamide stock containing 0.8% bis-acrylamide (ProtoGel) was diluted in a Tris-SDS buffer to reach the required concentrations. The stacking gel always contained 125mM Tris-HCl, pH 6.8, 0.1% SDS and 5% acrylamide. Before pouring, 50 µl of 10% ammo-

niium persulfate (AP) and 5  $\mu$ l tetramethylethylenediamine (TEMED) were added in order to polymerise the acrylamide. To pour and run the gels, the Mini-PROTEAN 3 Cell gel system (Bio-Rad) was used. The resolving gels were poured first to a height of approximately 1.5 cm below the top edge of the glass chamber and layered with 500  $\mu$ l of isopropanol before polymerisation to maintain a flat surface and aid polymerisation by excluding air. After polymerisation of the resolving gel, the isopropanol was decanted and remaining droplets were removed with a filter paper before the stacking gel was poured and a comb was inserted to form the loading wells. Fully polymerised polyacrylamide gels were fitted into the Mini-PROTEAN gel chamber which was filled with 1 $\times$ TGS (25 mM Tris, 250 mM glycine, 0.1% SDS) buffer to cover both electrodes. Then the comb was removed and the wells were washed with TGS buffer to avoid gel pieces blocking them. Prior to sample loading, all protein samples were diluted in an equal volume of 2 $\times$  protein loading buffer (4% SDS, 20% glycerol, 120 mM Tris-HCl, pH 6.8 and 0.02% bromophenol blue) (Laemmli, 1970); DTT was added freshly to reach a concentration of 50 mM, and the samples were heated to 95°C for 5 minutes in order to denature the proteins. Denatured protein samples were loaded into the wells of the gel alongside 3  $\mu$ l of a protein ladder (Precision Plus Protein™ All Blue Standards, Bio-Rad) as a standard. Gels were run at 150 V using a Power Pac 300 station (Bio-Rad) until the bromophenol blue dye front reached the bottom of the resolving gel. Then, gels were either directly used for immunoblotting or Coomassie stained for 30 minutes (0.25% Coomassie Brilliant Blue R-250, 45% methanol, 10% acetic acid) and subsequently de-stained (40% methanol, 10% acetic acid) over-night.

#### **6.4.5 Silver staining of SDS gels**

For silver staining, SDS gels were incubated in 50% methanol and 5% acetic acid for 20 minutes. Then, the gels were rinsed with 50% methanol for 10 minutes and subsequently twice with purified water for 10 minutes each. Gels were sensitised with 0.02% sodium thiosulfate for 1 minute and then again rinsed twice with purified water for 1 minute each. The sensitised gels were incubated in 0.2% silver nitrate containing 0.125% freshly-added formalin (35% formaldehyde) for 20 minutes, and then rinsed twice with purified water for 1 minute each. To develop the gels, they were incubated in 3% potassium carbonate containing 1.25% sodium thiosulfate and 0.125% freshly-added formalin (35% formaldehyde) until the protein bands were clearly visible. The development was stopped with a solution containing 4% Tris and 2% acetic acid before the background turned brown. After 30 minutes in the stop solution, the gel was rinsed twice with purified water for 30 minutes each, and then scanned or photographed.

#### **6.4.6 Immunoblotting and amido black staining**

Protein transfer from polyacrylamide gels onto Amersham Hybond-ECL nitrocellulose membranes (GE Healthcare) was performed using the Mini Trans-Blot Cell system (Bio-Rad). The transfer “sandwich” consisted of a sponge (cathode side), two filter papers (7×10 cm), the polyacrylamide gel, the nitrocellulose membrane (6×9 cm), again two filter papers (7×10 cm), and another sponge (anode side). All layers were pre-wet in cold transfer buffer (0.6% Tris, 2.88% glycine, 0.1% SDS and 20% methanol). The transfer sandwich was placed inside the tank along with an ice block and a magnetic stirrer to keep the buffer homogeneously cold during transfer. Then the tank was filled with transfer buffer and the transfer was run at 400 mA for one hour.

After the transfer, the membrane was cut into slices that contained the proteins of interest with the help of the coloured protein ladder (see Section 6.4.4). All membrane slices were then blocked with TBS-Tween (10 mM Tris-HCl, pH 8.0, 150 mM NaCl, 0.05% Tween 20) containing 5% non-fat milk powder (Marvel Original) for 30 minutes. The blocked membranes were then transferred to specific primary antibodies diluted in TBS-Tween with 5% milk powder and incubated at 4°C over-night. The concentrations of the antibodies varied considerably and were found by trial and error. Then, the membranes were washed three times with TBS-Tween for 10 minutes each and subsequently incubated in secondary antibody diluted in TBS-Tween with 5% milk powder for one hour at room temperature. Before detection, the membranes were again washed three times with TBS-Tween, as before. The secondary antibody needed to recognise the IgG of the host organism in which the primary antibody was raised so that it could bind to the primary antibody and thus indirectly to the protein of interest. It could be alkaline phosphatase (AP)- or horseradish peroxidase (HRP)-linked for detection. AP-linked antibodies were detected by incubating the membranes in cold AP buffer (100 mM Tris-HCl, pH 9.5, 100 mM NaCl, 5 mM MgCl<sub>2</sub>) for 10 minutes and then in 15 ml of AP buffer containing 100 µl of nitro-blue tetrazolium chloride (NBT, 50 mg/µl in 70% DMF) and 2.5 mg 5-bromo-4-chloro-3'-indolyphosphate p-toluidine (BCIP). HRP-linked antibodies were detected using the EZ-ECL Chemiluminescence Detection Kit (BI) following the manufacturer's guidelines. The chemiluminescence was visualised and recorded using a LAS-4000 image analyser (Fujifilm).

For quick visualisation of total protein amounts bound to the nitrocellulose membranes prior to immunodetection, amido black staining was performed. The washed membrane was incubated in amido black solution (0.5% amido black 10B, 50% methanol, 7% acetic acid) for a few seconds. Amido black solution was poured back for later

re-use. The stained membrane was washed with purified water for several minutes to remove background.

#### **6.4.7 Chloroplast isolation**

This method was adapted from a method described previously (Aronsson and Jarvis, 2002). *Arabidopsis* seedlings were grown on plates, at a density of roughly 200 seedlings per plate, for 14 days (see Section 6.1.2). Per isolation experiment, 10-40 plates were used depending on the phenotype (more plant material was necessary for pale genotypes like *tic40* mutants). Seedlings were harvested directly from the plates and put into a beaker containing 100 ml of ice-cold chloroplast isolation buffer (CIB, 0.3 M sorbitol, 5 mM MgCl<sub>2</sub>, 5 mM EGTA, 5 mM EDTA, 20 mM HEPES-KOH, 10 mM NaHCO<sub>3</sub>, pH 8.0). The seedlings were mixed for 3-5 seconds at low speed in portions of 20 ml CIB using a Polytron PT 10-35 (Kinematica) with a PTA 20 S rotor and subsequently filtered through a double layer of Miracloth (EMD Millipore). The filtrate (usually 100-200 ml) was centrifuged in 250 ml Nalgene tubes and a SLA1500 rotor in an RC-6 centrifuge (Sorvall) at 3000 rpm and 4°C for 6 minutes. The supernatant was discarded and the chloroplast pellet was resuspended in the remaining buffer by gentle rotation on ice.

Percoll gradients were prepared by mixing 13 ml of 2×CIB and 13 ml of Percoll (GE Healthcare) with ~5 mg of reduced glutathione (Duchefa) in 30 ml Nalgene tubes. The gradient was formed by centrifugation at 19,000 rpm and 4°C for 30 minutes using a HB-6 rotor with Nalgene tube adaptors (Sorvall). The deceleration rate was reduced in this case in order not to disturb the gradient during deceleration. The resuspended chloroplasts were loaded on the gradients which were again centrifuged using the HB-6 ro-

tor at 7000 rpm and 4°C for 10 minutes, again with a reduced deceleration rate. After centrifugation, the lower band (which corresponded to the intact and therefore denser chloroplasts) was harvested into a separate 30 ml Nalgene tube and was diluted with ~25 ml of ice-cold HMS buffer (50 mM HEPES-KOH, 3 mM MgSO<sub>4</sub>, 0.3 M sorbitol, pH 8.0) in order to wash the Percoll from the chloroplasts. The chloroplasts were again pelleted using the HB-6 rotor at 2000 rpm and 4°C for 5 minutes and, after decanting the supernatant, resuspended in the remaining buffer on ice by gentle rotation. Depending on the pellet size, the chloroplast suspension was further diluted with 200-500 µl of HMS for counting.

For counting, 5 µl of homogeneous chloroplast suspension was diluted in 495 µl of ice-cold HMS buffer. Approximately 60 µl of this dilution was pipetted with a cut tip between a counting chamber (Weber Scientific) and a microscope cover slip. The number of intact chloroplasts was counted on 5 large squares of the chamber and then multiplied by 5 to get an average number on 25 squares which cover a volume of 0.1 µl. In order to calculate the number of chloroplasts per ml, the average number on 25 squares was therefore multiplied by 10<sup>6</sup>, taking also into account the dilution factor used for the counting.

#### **6.4.8 Chloroplast protein import assays**

This method was adapted from a method described previously (Aronsson and Jarvis, 2002). A plasmid containing the *Arabidopsis* cDNA for RuBisCO small subunit isoform 1A (*SSU*) under a T7 promoter was used as a template to amplify the chimeric *SSU* gene by PCR with standard M13 primers. The amplified product was *in-vitro* translated by mixing 40 µl of T<sub>N</sub>T<sup>®</sup> T7 PCR Quick Master Mix (Promega), 5 µl of [<sup>35</sup>S]-

methionine, and 5  $\mu$ l of the transcript (100-800 ng), and incubating the mixture at 30°C for 90 minutes. Of the resulting precursor SSU (pSSU), 5  $\mu$ l was added to 1 $\times$ HMS buffer, 20 mM K-gluconic acid, 10 mM NaHCO<sub>3</sub>, 0.2% BSA, 5 mM MgATP and 10 mM methionine. Chloroplasts were isolated and counted as described above (Section 6.4.7), and 10<sup>7</sup> freshly-isolated chloroplasts per import reaction and time point were added. For the reaction itself, the tube was placed in a water bath at 26°C in front of a light source, and after defined time intervals equal volumes of sample were transferred into equal volumes of stop solution (50 mM EDTA, 0.3 M sorbitol, 50 mM HEPES-KOH, pH 8.0). Before each transfer the tube was flicked to mix the chloroplasts so that equal numbers of chloroplasts (ideally  $\sim$ 10<sup>7</sup>) were removed per time point. The tubes containing the chloroplasts in stop solution were centrifuged for 30 seconds at maximum speed; in each case the supernatant was completely discarded and the pellet was resuspended in 30  $\mu$ l of protein loading buffer. The samples were then heated to 95°C for 2 minutes, and then centrifuged for 1 minute at maximum speed in a microcentrifuge prior to storage at -20°C until later analysis. The radiolabeled protein samples were run on 15% polyacrylamide gels as described in Section 6.4.4. The gels were dried on pre-wet filter paper using a gel dryer (Bio-Rad). Dried gels were put on a storage phosphor screen (GE healthcare) for several days before the radio image was scanned with the Storm 860 imager (Molecular Dynamics).

#### **6.4.9 Chloroplast subfractionation**

This method was adapted from a method described previously (Perry et al., 1991). Chloroplasts were isolated as described above (see Section 6.4.7). The chloroplast pellet was resuspended in 1 ml of 25 mM HEPES-KOH, pH 8.0, containing 1× protease inhibitor cocktail. The chloroplasts were burst by pipetting up and down several times followed by rotation at 4°C for one hour. In order to test if the lysis was complete, 50 µl of the lysate was loaded on a 40% Percoll/1× HMS cushion and centrifuged at 3000 g and 4°C for 6 minutes using the HB-6 rotor (Sorvall). Lysis was complete when after centrifugation through 40% Percoll no pellet was visible. Then, 700 µl of 25mM HEPES-KOH, pH 8.0, containing 0.6 M sucrose and 4 mM MgCl<sub>2</sub> was added to the lysate and mixed. Gradients were prepared by layering 0.9 ml of 1.2 M, 1.0 M and 0.46 M sucrose, each in 25 mM HEPES-KOH, pH 8.0, into 5 ml ultracentrifuge tubes so that the interfaces between the different sucrose concentrations were clearly visible. The lysate was then layered onto the gradients and centrifuged at 200,000 g and 4°C for 1 hour in a Discovery M120 SE ultracentrifuge (Sorvall, Thermo Scientific). After centrifugation, the supernatant was collected as the stromal fraction, the yellowish band at the interface of 0.46 M and 1.0 M sucrose was collected as the envelope fraction, and the greenish band at the interface of 1.0 M and 1.2 M sucrose was collected as the thylakoid fraction. The envelope and thylakoid fractions were washed by adding 2 volumes of 25 mM HEPES-KOH, pH 8.0, and subsequently pelleted by centrifugation at 48,000 g and 4°C for one hour in the ultracentrifuge. The envelope and thylakoid pellets were resuspended in 50-100 µl of 25 mM HEPES-KOH, pH 8.0, and further used for SDS-PAGE analysis. The stromal fraction was first precipitated (see Section 6.4.3) from the supernatant and then directly resuspended in 50-100 µl of 2× protein loading buffer for further analysis with SDS-PAGE.

#### **6.4.10 Co-immunoprecipitation and anti-FLAG-immunoprecipitation**

For co-immunoprecipitation, 50 mg of Protein A Sepharose CL-4B (GE Healthcare) was soaked in 200  $\mu$ l of sterile water by pipetting with a cut yellow tip, and left on ice for 30 minutes. The sepharose was washed three times with 1 ml of sterile water and then once with 1 ml of solubilisation buffer (20 mM Tris-HCl, 150 mM NaCl, 1 mM EDTA, 10% glycerol, 1% *n*-dodecyl  $\beta$ -D-maltoside (DDM), 1 $\times$  protease inhibitor cocktail, pH 7.5) and pelleted at 500 *g* and 4°C for 1 minute in an Eppendorf centrifuge (5415 D, rotor EL 082). To the soaked sepharose, 200  $\mu$ l of solubilisation buffer (SB buffer) was added to reach a total volume of ~500-600  $\mu$ l. Freshly-isolated chloroplasts were either directly pelleted by a short spin at maximum speed in a microcentrifuge, or first crosslinked with dithiobis(succinimidyl propionate) (DSP) for 15 minutes and then quenched with 50mM glycine for 15 minutes on ice before pelleting. Chloroplast pellets were solubilised in 2 ml of SB buffer and rotated at 4°C for 20 minutes. The total lysate fraction (TL) was collected after solubilisation. Then, 30  $\mu$ l of the Protein A Sepharose slurry was added to the lysate and rotated at 4°C for 30 minutes in order to remove proteins that bind to the sepharose non-specifically. The samples were then centrifuged at maximum speed and 4°C for 10 minutes in an Eppendorf centrifuge (5415 D, rotor EL 082) and the supernatant transferred to a fresh tube. An arbitrary volume of antibody (usually 5-10  $\mu$ l, depending on the antibody efficiency) was added and the samples were rotated at 4°C for 2-5 hours. Then, 100  $\mu$ l of the Protein A Sepharose slurry was added with a cut tip and rotated at 4°C for 2 hours. The sepharose was pelleted at 6000 rpm and 4°C for 30 seconds in an Eppendorf centrifuge (5415 D, rotor EL 082) and the flow-through fraction (FT) was collected from the supernatant. The Protein A Sepharose pellet was washed six times with wash buffer (20 mM Tris-HCl, 150 mM NaCl, 1 mM EDTA, 10% glycerol, 0.3% DDM, 1 $\times$  protease inhibitor, pH 7.5), and after

the last wash the wash fraction (W) was collected from the supernatant; the remaining supernatant was removed from the Protein A Sepharose pellet which formed the elute fraction (E). All fractions were diluted in 2× protein loading buffer and further analysed by SDS-PAGE and immunoblotting.

For anti-FLAG-immunoprecipitation, 60 µl of Anti-Flag M2 Affinity Gel (Sigma) was washed with 100 µl of TBS buffer (10 mM Tris-HCl, pH 8.0, 150 mM NaCl) and centrifuged at 6000 rpm and 4°C for 30 seconds in an Eppendorf centrifuge (5415 D, rotor EL 082). Then, the pellet was washed three times with 60 µl of 0.1 M glycine-HCl, pH 3.5, five times with 200 µl TBS buffer, and twice with 400 µl SB buffer. The resin was centrifuged at 6000 rpm and 4°C for 30 seconds in an Eppendorf centrifuge (5415 D, rotor EL 082) and the pellet stored on ice. The chloroplast pellet was solubilised as described above, the TL fraction was collected, and the complete affinity gel pellet was added to the sample, followed by rotation at 4°C for 2 hours. The following steps were performed just like for co-immunoprecipitation.

#### **6.4.11 Protoplast isolation, transfection and microscopy**

This method was based on a method described previously (Power and Davey, 1990). About 6-10 *Arabidopsis* leaves (age 3-4 weeks) were peeled using the tape-*Arabidopsis* sandwich method (Wu et al., 2009). Pealed leaves were incubated in 20 ml of enzyme solution (1% cellulase, 0.25% maceroenzyme, 0.4 M mannitol, 10 mM CaCl<sub>2</sub>, 20 mM KCl, 0.1% BSA, 20 mM MES-KOH, pH 5.7) for 2 hours at room temperature on a shaker at lowest speed. The released protoplasts were transferred into a 50 ml Falcon tube and pelleted at 60 g and 4°C for 5 minutes using a Legend RT centrifuge (Sorvall). The pellet was washed twice with 25 ml of ice-cold W5 buffer (154 mM NaCl, 125 mM

CaCl<sub>2</sub>, 5 mM KCl, 5 mM glucose, 2 mM MES-KOH, pH 5.7). The protoplasts were pelleted at 40 g and 4°C for 4 minutes and then resuspended in 2 ml of W5 buffer and left on ice for 20 minutes. Protoplasts were counted using a counting chamber as described in Section 6.4.7. After counting, the protoplasts were pelleted at 40 g and 4°C for 4 minutes and the pellet was resuspended in  $N \times 20 \mu\text{l}$  of ice-cold MMg buffer (0.4 M mannitol, 15 mM MgCl<sub>2</sub>, 4 mM MES-KOH, pH 5.7), where  $N$  is the number of protoplasts counted per 25 squares of the counting chamber.

For protoplast transfection, the required plasmid was prepared using a midi-prep procedure as described in Section 6.2.3. PEG solution (40% PEG-4000, 100 mM Ca(NO<sub>3</sub>)<sub>2</sub>, 200 mM mannitol) was prepared by melting the PEG in the solution by microwaving for 15 seconds, mixing, and then cooling to room temperature. Plasmid DNA (10  $\mu\text{g}$  or 10  $\mu\text{g}$  each for BiFC; see Section 6.2.6) was diluted in 10  $\mu\text{l}$  of sterile water in a 2 ml microcentrifuge tube. Protoplast suspension (100  $\mu\text{l}$ , in MMg buffer) was added to the plasmid using a cut yellow tip, and immediately thereafter 110  $\mu\text{l}$  of PEG solution was added; this was then mixed by flicking and incubated at room temperature for 5 minutes. Then, twice 750  $\mu\text{l}$  of W5 at room temperature was added, sequentially, and the mixture was incubated for 5 and 2 minutes at room temperature, respectively. The protoplasts were then washed twice with 1.5 ml of W5 at room temperature, and pelleted at 40 g and room temperature for 2 minutes. The pellet was resuspended in 500  $\mu\text{l}$  of W5 at room temperature, transferred to a 6-well cell culture plate using a cut blue tip, and incubated over-night at room temperature in the dark. Fluorescence microscopy was then performed on the transfected protoplasts with an Eclipse TE2000-E fluorescence microscope (Nikon) using filters for YFP (exciter HQ500/20x, emitter HQ535/30m) and

for chlorophyll autofluorescence (exciter D480/30x, emitter D660/50m) (Chroma Technologies).

## 7 Bibliography

- Abdallah, F., Salamini, F., and Leister, D. (2000).** A Prediction of the Size and Evolutionary Origin of the Proteome of Chloroplasts of *Arabidopsis*. *Trends Plant Sci.* 5, 141-142.
- Abe, Y., Shodai, T., Muto, T., Mihara, K., Torii, H., Nishikawa, S., Endo, T., and Kohda, D. (2000).** Structural Basis of Presequence Recognition by the Mitochondrial Protein Import Receptor Tom20. *Cell* 100, 551-560.
- Adl, S.M., Simpson, A.G., Farmer, M.A., Andersen, R.A., Anderson, O.R., Barta, J.R., Bowser, S.S., Brugerolle, G., Fensome, R.A., Fredericq, S., et al. (2005).** The New Higher Level Classification of Eukaryotes with Emphasis on the Taxonomy of Protists. *J. Eukaryot. Microbiol.* 52, 399-451.
- Akita, M., Nielsen, E., and Keegstra, K. (1997).** Identification of Protein Transport Complexes in the Chloroplastic Envelope Membranes via Chemical Cross-linking. *J. Cell Biol.* 136, 983-994.
- Aldridge, C., Storm, A., Cline, K., and Dabney-Smith, C. (2012).** The Chloroplast Twin Arginine Transport (Tat) Component, Tha4, Undergoes Conformational Changes Leading to Tat Protein Transport. *J. Biol. Chem.* 287, 34752-34763.
- Allen, T., Ingles, P.J., Praekelt, U., Smith, H., and Whitelam, G.C. (2006).** Phytochrome-mediated Agravitropism in *Arabidopsis* Hypocotyls Requires GIL1 and Confers a Fitness Advantage. *Plant J.* 46, 641-648.
- Alonso, J.M., Stepanova, A.N., Leisse, T.J., Kim, C.J., Chen, H., Shinn, P., Stevenson, D.K., Zimmerman, J., Barajas, P., Cheuk, R., et al. (2003).** Genome-wide Insertional Mutagenesis of *Arabidopsis thaliana*. *Science* 301, 653-657.
- Amin, P., Sy, D.A., Pilgrim, M.L., Parry, D.H., Nussaume, L., and Hoffman, N.E. (1999).** *Arabidopsis* Mutants Lacking the 43- and 54-Kilodalton Subunits of the Chloroplast Signal Recognition Particle Have Distinct Phenotypes. *Plant Physiol.* 121, 61-70.
- Aronsson, H., Boij, P., Patel, R., Wardle, A., Topel, M., and Jarvis, P. (2007).** Toc64/OEP64 Is Not Essential for the Efficient Import of Proteins into Chloroplasts in *Arabidopsis thaliana*. *Plant J.* 52, 53-68.
- Aronsson, H., Combe, J., Patel, R., Agne, B., Martin, M., Kessler, F., and Jarvis, P. (2010).** Nucleotide Binding and Dimerization at the Chloroplast Pre-protein Import Receptor, atToc33, Are Not Essential *in vivo* But Do Increase Import Efficiency. *Plant J.* 63, 297-311.
- Aronsson, H., and Jarvis, P. (2002).** A Simple Method for Isolating Import-competent *Arabidopsis* Chloroplasts. *FEBS Lett.* 529, 215-220.
- Aronsson, H., and Jarvis, P. (2011).** Dimerization of TOC Receptor GTPases and its Implementation for the Control of Protein Import into Chloroplasts. *Biochem. J.* 436, e1-2.
- Asakura, Y., Hirohashi, T., Kikuchi, S., Belcher, S., Osborne, E., Yano, S., Terashima, I., Barkan, A., and Nakai, M. (2004).** Maize Mutants Lacking Chloroplast FtsY Exhibit Pleiotropic Defects in the Biogenesis of Thylakoid Membranes. *The Plant cell* 16, 201-214.
- Asakura, Y., Kikuchi, S., and Nakai, M. (2008).** Non-identical Contributions of two Membrane-bound cpSRP Components, cpFtsY and Alb3, to Thylakoid Biogenesis. *Plant J.* 56, 1007-1017.

- Austin, J.R., 2nd, Frost, E., Vidi, P.A., Kessler, F., and Staehelin, L.A. (2006).** Plastoglobules are Lipoprotein Subcompartments of the Chloroplast that are Permanently Coupled to Thylakoid Membranes and Contain Biosynthetic Enzymes. *The Plant cell* *18*, 1693-1703.
- Baldwin, A., Wardle, A., Patel, R., Dudley, P., Park, S.K., Twell, D., Inoue, K., and Jarvis, P. (2005).** A Molecular-genetic Study of the *Arabidopsis* Toc75 Gene Family. *Plant Physiol.* *138*, 715-733.
- Balsera, M., Goetze, T.A., Kovacs-Bogdan, E., Schurmann, P., Wagner, R., Buchanan, B.B., Soll, J., and Bolter, B. (2009).** Characterization of Tic110, a Channel-forming Protein at the Inner Envelope Membrane of Chloroplasts, Unveils a Response to Ca(2+) and a Stromal Regulatory Disulfide Bridge. *J. Biol. Chem.* *284*, 2603-2616.
- Bannenberg, G., Martinez, M., Hamberg, M., and Castresana, C. (2009).** Diversity of the Enzymatic Activity in the Lipoxygenase Gene Family of *Arabidopsis thaliana*. *Lipids* *44*, 85-95.
- Bauer, J., Chen, K., Hiltbunner, A., Wehrli, E., Eugster, M., Schnell, D., and Kessler, F. (2000).** The Major Protein Import Receptor of Plastids is Essential for Chloroplast Biogenesis. *Nature* *403*, 203-207.
- Bauer, J., Hiltbrunner, A., Weibel, P., Vidi, P.A., Alvarez-Huerta, M., Smith, M.D., Schnell, D.J., and Kessler, F. (2002).** Essential Role of the G-domain in Targeting of the Protein Import Receptor atToc159 to the Chloroplast Outer Membrane. *J. Cell Biol.* *159*, 845-854.
- Beale, S.I. (1990).** Biosynthesis of the Tetrapyrrole Pigment Precursor, delta-Aminolevulinic Acid, from Glutamate. *Plant Physiol.* *93*, 1273-1279.
- Becker, T., Hritz, J., Vogel, M., Caliebe, A., Bukau, B., Soll, J., and Schleiff, E. (2004).** Toc12, a Novel Subunit of the Intermembrane Space Preprotein Translocon of Chloroplasts. *Mol. Biol. Cell* *15*, 5130-5144.
- Bedard, J., Kubis, S., Bimanadham, S., and Jarvis, P. (2007).** Functional Similarity between the Chloroplast Translocon Component, Tic40, and the Human Co-chaperone, Hsp70-interacting Protein (Hip). *J. Biol. Chem.* *282*, 21404-21414.
- Bellafiore, S., Ferris, P., Naver, H., Gohre, V., and Rochaix, J.D. (2002).** Loss of Albino3 Leads to the Specific Depletion of the Light-harvesting System. *The Plant cell* *14*, 2303-2314.
- Benz, M., Bals, T., Gugel, I.L., Piotrowski, M., Kuhn, A., Schunemann, D., Soll, J., and Ankele, E. (2009).** Alb4 of *Arabidopsis* Promotes Assembly and Stabilization of a Non Chlorophyll-binding Photosynthetic Complex, the CF1CF0-ATP Synthase. *Mol. Plant* *2*, 1410-1424.
- Berghofer, J., and Klosgen, R.B. (1999).** Two Distinct Translocation Intermediates Can Be Distinguished During Protein Transport by the TAT (Deltaph) Pathway across the Thylakoid Membrane. *FEBS Lett.* *460*, 328-332.
- Bhushan, S., Kuhn, C., Berglund, A.K., Roth, C., and Glaser, E. (2006).** The Role of the N-terminal Domain of Chloroplast Targeting Peptides in Organellar Protein Import and Miss-sorting. *FEBS Lett.* *580*, 3966-3972.
- Bhushan, S., Lefebvre, B., Stahl, A., Wright, S.J., Bruce, B.D., Boutry, M., and Glaser, E. (2003).** Dual Targeting and Function of a Protease in Mitochondria and Chloroplasts. *EMBO Rep.* *4*, 1073-1078.
- Bischof, S., Baerenfaller, K., Wildhaber, T., Troesch, R., Vidi, P.A., Roschitzki, B., Hirsch-Hoffmann, M., Hennig, L., Kessler, F., Gruissem, W., et al. (2011).** Plastid Proteome Assembly without Toc159: Photosynthetic Protein Import and

- Accumulation of N-acetylated Plastid Precursor Proteins. *The Plant cell* 23, 3911-3928.
- Blair, G.E., and Ellis, R.J. (1973).** Protein Synthesis in Chloroplasts. I. Light-driven Synthesis of the Large Subunit of Fraction I Protein by Isolated Pea Chloroplasts. *Biochim. Biophys. Acta* 319, 223-234.
- Blobel, G., and Dobberstein, B. (1975).** Transfer of Proteins Across Membranes. I. Presence of Proteolytically Processed and Unprocessed Nascent Immunoglobulin Light Chains on Membrane-bound Ribosomes of Murine Myeloma. *J. Cell Biol.* 67, 835-851.
- Blobel, G., and Sabatini, D.D. (1971).** Ribosome-membrane Interactions in Eukaryotic Cells. Manson, L.A. editor, *Biomembranes*. New York: Plenum., pp. 193–195. .
- Block, M.A., Dorne, A.J., Joyard, J., and Douce, R. (1983).** Preparation and Characterization of Membrane Fractions Enriched in Outer and Inner Envelope Membranes from Spinach Chloroplasts. II. Biochemical Characterization. *J. Biol. Chem.* 258, 13281-13286.
- Boij, P., Patel, R., Garcia, C., Jarvis, P., and Aronsson, H. (2009).** *In vivo* Studies on the Roles of Tic55-related Proteins in Chloroplast Protein Import in *Arabidopsis thaliana*. *Mol. Plant* 2, 1397-1409.
- Bolter, B., May, T., and Soll, J. (1998).** A Protein Import Receptor in Pea Chloroplasts, Toc86, Is only a Proteolytic Fragment of a Larger Polypeptide. *FEBS Lett.* 441, 59-62.
- Brix, J., Dietmeier, K., and Pfanner, N. (1997).** Differential Recognition of Preproteins by the Purified Cytosolic Domains of the Mitochondrial Import Receptors Tom20, Tom22, and Tom70. *J. Biol. Chem.* 272, 20730-20735.
- Bruce, B.D. (1998).** The Role of Lipids in Plastid Protein Transport. *Plant Mol. Biol.* 38, 223-246.
- Bruce, B.D. (2000).** Chloroplast Transit Peptides: Structure, Function and Evolution. *Trends Cell Biol.* 10, 440-447.
- Bruce, B.D. (2001).** The Paradox of Plastid Transit Peptides: Conservation of Function Despite Divergence in Primary Structure. *Biochim. Biophys. Acta* 1541, 2-21.
- Bryant, N., Lloyd, J., Sweeney, C., Myouga, F., and Meinke, D. (2011).** Identification of Nuclear Genes Encoding Chloroplast-localized Proteins Required for Embryo Development in *Arabidopsis*. *Plant Physiol.* 155, 1678-1689.
- Caliebe, A., Grimm, R., Kaiser, G., Lubeck, J., Soll, J., and Heins, L. (1997).** The Chloroplastic Protein Import Machinery Contains a Rieske-type Iron-sulfur Cluster and a Mononuclear Iron-binding Protein. *EMBO J.* 16, 7342-7350.
- Casson, S., Spencer, M., Walker, K., and Lindsey, K. (2005).** Laser Capture Microdissection for the Analysis of Gene Expression During Embryogenesis of *Arabidopsis*. *Plant J.* 42, 111-123.
- Chaddock, A.M., Mant, A., Karnauchov, I., Brink, S., Herrmann, R.G., Klosgen, R.B., and Robinson, C. (1995).** A New Type of Signal Peptide: Central Role of a Twin-arginine Motif in Transfer Signals for the Delta pH-dependent Thylakoidal Protein Translocase. *EMBO J.* 14, 2715-2722.
- Chen, K., Chen, X., and Schnell, D.J. (2000).** Initial Binding of Preproteins Involving the Toc159 Receptor Can be Bypassed During Protein Import into Chloroplasts. *Plant Physiol.* 122, 813-822.
- Chen, L.J., and Li, H.M. (1998).** A Mutant Deficient in the Plastid Lipid DGD is Defective in Protein Import into Chloroplasts. *Plant J.* 16, 33-39.

- Chen, X., Smith, M.D., Fitzpatrick, L., and Schnell, D.J. (2002).** *In vivo* Analysis of the Role of atTic20 in Protein Import into Chloroplasts. *The Plant cell* *14*, 641-654.
- Chew, O., and Whelan, J. (2004).** Just Read the Message: a Model for Sorting of Proteins between Mitochondria and Chloroplasts. *Trends Plant Sci.* *9*, 318-319.
- Chini, A., Fonseca, S., Fernandez, G., Adie, B., Chico, J.M., Lorenzo, O., Garcia-Casado, G., Lopez-Vidriero, I., Lozano, F.M., Ponce, M.R., et al. (2007).** The JAZ family of Repressors is the Missing Link in Jasmonate Signalling. *Nature* *448*, 666-671.
- Chiu, C.C., Chen, L.J., and Li, H.M. (2010).** Pea Chloroplast DnaJ-J8 and Toc12 Are Encoded by the Same Gene and Localized in the Stroma. *Plant Physiol.* *154*, 1172-1182.
- Chiu, C.C., and Li, H.M. (2008).** Tic40 Is Important for Reinsertion of Proteins from the Chloroplast Stroma into the Inner Membrane. *Plant J.* *56*, 793-801.
- Chotewutmontri, P., Reddick, L.E., McWilliams, D.R., Campbell, I.M., and Bruce, B.D. (2012).** Differential Transit Peptide Recognition During Preprotein Binding and Translocation into Flowering Plant Plastids. *The Plant cell* *24*, 3040-3059.
- Chou, M.L., Chu, C.C., Chen, L.J., Akita, M., and Li, H.M. (2006).** Stimulation of Transit-peptide Release and ATP Hydrolysis by a Cochaperone During Protein Import into Chloroplasts. *J. Cell Biol.* *175*, 893-900.
- Chou, M.L., Fitzpatrick, L.M., Tu, S.L., Budziszewski, G., Potter-Lewis, S., Akita, M., Levin, J.Z., Keegstra, K., and Li, H.M. (2003).** Tic40, a Membrane-anchored Co-chaperone Homolog in the Chloroplast Protein Translocon. *EMBO J.* *22*, 2970-2980.
- Chua, N.H., and Schmidt, G.W. (1978).** Post-translational Transport into Intact Chloroplasts of a Precursor to the Small Subunit of Ribulose-1,5-bisphosphate Carboxylase. *Proc. Natl. Acad. Sci. U. S. A.* *75*, 6110-6114.
- Cline, K., Ettinger, W.F., and Theg, S.M. (1992).** Protein-specific Energy Requirements for Protein Transport across or into Thylakoid Membranes. Two Luminal Proteins Are Transported in the Absence of ATP. *J. Biol. Chem.* *267*, 2688-2696.
- Cline, K., and Mori, H. (2001).** Thylakoid Delta pH-dependent Precursor Proteins Bind to a cpTatC-Hcf106 Complex Before Tha4-dependent Transport. *J. Cell Biol.* *154*, 719-729.
- Cline, K., Werner-Washburne, M., Andrews, J., and Keegstra, K. (1984).** Thermolysin Is a Suitable Protease for Probing the Surface of Intact Pea Chloroplasts. *Plant Physiol.* *75*, 675-678.
- Cline, K., Werner-Washburne, M., Lubben, T.H., and Keegstra, K. (1985).** Precursors to Two Nuclear-encoded Chloroplast Proteins Bind to the Outer Envelope Membrane Before Being Imported into Chloroplasts. *J. Biol. Chem.* *260*, 3691-3696.
- Clough, S.J., and Bent, A.F. (1998).** Floral Dip: a Simplified Method for *Agrobacterium*-mediated Transformation of *Arabidopsis thaliana*. *Plant J.* *16*, 735-743.
- Constan, D., Froehlich, J.E., Rangarajan, S., and Keegstra, K. (2004a).** A Stromal Hsp100 Protein is Required for Normal Chloroplast Development and Function in *Arabidopsis*. *Plant Physiol.* *136*, 3605-3615.
- Constan, D., Patel, R., Keegstra, K., and Jarvis, P. (2004b).** An Outer Envelope Membrane Component of the Plastid Protein Import Apparatus Plays an Essential Role in *Arabidopsis*. *Plant J.* *38*, 93-106.

- Creighton, A.M., Hulford, A., Mant, A., Robinson, D., and Robinson, C. (1995).** A Monomeric, Tightly Folded Stromal Intermediate on the Delta pH-dependent Thylakoidal Protein Transport Pathway. *J. Biol. Chem.* 270, 1663-1669.
- Croce, R., Morosinotto, T., Castelletti, S., Breton, J., and Bassi, R. (2002).** The Lhca Antenna Complexes of Higher Plants Photosystem I. *Biochim. Biophys. Acta* 1556, 29-40.
- Czarnecki, O., Peter, E., and Grimm, B. (2011).** Methods for analysis of photosynthetic pigments and steady-state levels of intermediates of tetrapyrrole biosynthesis. *Methods Mol. Biol.* 775, 357-385.
- Dabney-Smith, C., and Cline, K. (2009).** Clustering of C-terminal Stromal Domains of Tha4 Homo-oligomers During Translocation by the Tat Protein Transport System. *Mol. Biol. Cell* 20, 2060-2069.
- Dabney-Smith, C., Mori, H., and Cline, K. (2006).** Oligomers of Tha4 Organize at the Thylakoid Tat Translocase During Protein Transport. *J. Biol. Chem.* 281, 5476-5483.
- DellaPenna, D. (2005).** A Decade of Progress in Understanding Vitamin E Synthesis in Plants. *J. Plant Physiol.* 162, 729-737.
- Deschamps, P., Moreau, H., Worden, A.Z., Dauvillee, D., and Ball, S.G. (2008).** Early Gene Duplication within Chloroplastida and its Correspondence with Relocation of Starch Metabolism to Chloroplasts. *Genetics* 178, 2373-2387.
- Di Cola, A., Bailey, S., and Robinson, C. (2005).** The Thylakoid Delta pH/delta Psi Are Not Required for the Initial Stages of Tat-dependent Protein Transport in Tobacco Protoplasts. *J. Biol. Chem.* 280, 41165-41170.
- Dobberstein, B., Blobel, G., and Chua, N.H. (1977).** *In vitro* Synthesis and Processing of a Putative Precursor for the Small Subunit of Ribulose-1,5-bisphosphate Carboxylase of *Chlamydomonas reinhardtii*. *Proc. Natl. Acad. Sci. U. S. A.* 74, 1082-1085.
- Dorrell, R.G., and Howe, C.J. (2012).** What Makes a Chloroplast? Reconstructing the Establishment of Photosynthetic Symbioses. *J. Cell Sci.* 125, 1865-1875.
- Dorrell, R.G., and Smith, A.G. (2011).** Do Red and Green Make Brown?: Perspectives on Plastid Acquisitions within Chromalveolates. *Eukaryot. Cell* 10, 856-868.
- Douce, R., and Joyard, J. (1990).** Biochemistry and Function of the Plastid Envelope. *Annu. Rev. Cell Biol.* 6, 173-216.
- Dun, X., Zhou, Z., Xia, S., Wen, J., Yi, B., Shen, J., Ma, C., Tu, J., and Fu, T. (2011).** BnaC.Tic40, a Plastid Inner Membrane Translocon Originating from *Brassica oleracea*, is Essential for Tapetal Function and Microspore Development in *Brassica napus*. *Plant J.* 68, 532-545.
- Dunschede, B., Bals, T., Funke, S., and Schunemann, D. (2011).** Interaction Studies between the Chloroplast Signal Recognition Particle Subunit cpSRP43 and the Full-length Translocase Alb3 Reveal a Membrane-embedded Binding Region in Alb3 Protein. *J. Biol. Chem.* 286, 35187-35195.
- Duy, D., Wanner, G., Meda, A.R., von Wiren, N., Soll, J., and Philippar, K. (2007).** PIC1, an Ancient Permease in Arabidopsis Chloroplasts, Mediates Iron Transport. *The Plant cell* 19, 986-1006.
- Earley, K.W., Haag, J.R., Pontes, O., Opper, K., Juehne, T., Song, K., and Pikaard, C.S. (2006).** Gateway-compatible vectors for plant functional genomics and proteomics. *Plant J.* 45, 616-629.
- Eckart, K., Eichacker, L., Sohrt, K., Schleiff, E., Heins, L., and Soll, J. (2002).** A Toc75-like Protein Import Channel Is Abundant in Chloroplasts. *EMBO Rep.* 3, 557-562.

- Economou, A., and Wickner, W. (1994).** SecA Promotes Preprotein Translocation by Undergoing ATP-driven Cycles of Membrane Insertion and Deinsertion. *Cell* 78, 835-843.
- Edwards, K., Johnstone, C., and Thompson, C. (1991).** A Simple and Rapid Method for the Preparation of Plant Genomic DNA for PCR Analysis. *Nucleic Acids Res.* 19, 1349.
- Emanuelsson, O., Nielsen, H., Brunak, S., and von Heijne, G. (2000).** Predicting Subcellular Localization of Proteins Based on Their N-terminal Amino Acid Sequence. *J. Mol. Biol.* 300, 1005-1016.
- Emanuelsson, O., Nielsen, H., and von Heijne, G. (1999).** ChloroP, a Neural Network-based Method for Predicting Chloroplast Transit Peptides and Their Cleavage Sites. *Protein Sci.* 8, 978-984.
- Ertel, F., Mirus, O., Bredemeier, R., Moslavac, S., Becker, T., and Schleiff, E. (2005).** The Evolutionarily Related Beta-barrel Polypeptide Transporters from *Pisum sativum* and *Nostoc* PCC7120 Contain Two Distinct Functional Domains. *J. Biol. Chem.* 280, 28281-28289.
- Eugeni Piller, L., Abraham, M., Dormann, P., Kessler, F., and Besagni, C. (2012).** Plastid Lipid Droplets at the Crossroads of Prenylquinone Metabolism. *J. Exp. Bot.* 63, 1609-1618.
- Falk, S., Ravaud, S., Koch, J., and Sinning, I. (2010).** The C Terminus of the Alb3 Membrane Insertase Recruits cpSRP43 to the Thylakoid Membrane. *J. Biol. Chem.* 285, 5954-5962.
- Ferreira, K.N., Iverson, T.M., Maghlaoui, K., Barber, J., and Iwata, S. (2004).** Architecture of the Photosynthetic Oxygen-evolving Center. *Science* 303, 1831-1838.
- Finazzi, G., Chasen, C., Wollman, F.A., and de Vitry, C. (2003).** Thylakoid Targeting of Tat Passenger Proteins Shows No Delta pH Dependence *in vivo*. *EMBO J.* 22, 807-815.
- Flores-Perez, U., Sauret-Gueto, S., Gas, E., Jarvis, P., and Rodriguez-Concepcion, M. (2008).** A Mutant Impaired in the Production of Plastome-encoded Proteins Uncovers a Mechanism for the Homeostasis of Isoprenoid Biosynthetic Enzymes in *Arabidopsis* plastids. *The Plant cell* 20, 1303-1315.
- Franklin, A.E., and Hoffman, N.E. (1993).** Characterization of a Chloroplast Homologue of the 54-kDa Subunit of the Signal Recognition Particle. *J. Biol. Chem.* 268, 22175-22180.
- Friedman, A.L., and Keegstra, K. (1989).** Chloroplast Protein Import : Quantitative Analysis of Precursor Binding. *Plant Physiol.* 89, 993-999.
- Fulgosi, H., Gerdes, L., Westphal, S., Glockmann, C., and Soll, J. (2002).** Cell and Chloroplast Division Requires ARTEMIS. *Proc. Natl. Acad. Sci. U. S. A.* 99, 11501-11506.
- Garcia, C., Khan, N.Z., Nannmark, U., and Aronsson, H. (2010).** The Chloroplast Protein CPSAR1, Dually Localized in the Stroma and the Inner Envelope Membrane, Is Involved in Thylakoid Biogenesis. *Plant J.* 63, 73-85.
- Gentle, I., Gabriel, K., Beech, P., Waller, R., and Lithgow, T. (2004).** The Omp85 Family of Proteins Is Essential for Outer Membrane Biogenesis in Mitochondria and Bacteria. *J. Cell Biol.* 164, 19-24.
- Gentle, I.E., Burri, L., and Lithgow, T. (2005).** Molecular Architecture and Function of the Omp85 Family of Proteins. *Mol. Microbiol.* 58, 1216-1225.

- Gerard, F., and Cline, K. (2006).** Efficient Twin Arginine Translocation (Tat) Pathway Transport of a Precursor Protein Covalently Anchored to its Initial cpTatC Binding Site. *J. Biol. Chem.* *281*, 6130-6135.
- Gerdes, L., Bals, T., Klostermann, E., Karl, M., Philippar, K., Hunken, M., Soll, J., and Schunemann, D. (2006).** A Second Thylakoid Membrane-localized Alb3/OxaI/YidC Homologue Is Involved in Proper Chloroplast Biogenesis in *Arabidopsis thaliana*. *J. Biol. Chem.* *281*, 16632-16642.
- Glaser, E., Nilsson, S., and Bhushan, S. (2006).** Two Novel Mitochondrial and Chloroplastic Targeting-peptide-degrading Peptidasomes in *A. thaliana*, AtPreP1 and AtPreP2. *Biol. Chem.* *387*, 1441-1447.
- Glaser, S., van Dooren, G.G., Agrawal, S., Brooks, C.F., McFadden, G.I., Striepen, B., and Higgins, M.K. (2012).** Tic22 Is an Essential Chaperone Required for Protein Import into the Apicoplast. *J. Biol. Chem.* *287*, 39505-39512.
- Glick, B.S., and Von Heijne, G. (1996).** *Saccharomyces cerevisiae* Mitochondria Lack a Bacterial-type Sec Machinery. *Protein Sci.* *5*, 2651-2652.
- Gohre, V., Ossenbuhl, F., Crevecoeur, M., Eichacker, L.A., and Rochaix, J.D. (2006).** One of Two Alb3 Proteins Is Essential for the Assembly of the Photosystems and for Cell Survival in *Chlamydomonas*. *The Plant cell* *18*, 1454-1466.
- Goubet, F., Misrahi, A., Park, S.K., Zhang, Z., Twell, D., and Dupree, P. (2003).** AtCSLA7, a Cellulose Synthase-like Putative Glycosyltransferase, Is Important for Pollen Tube Growth and Embryogenesis in *Arabidopsis*. *Plant Physiol.* *131*, 547-557.
- Gould, S.G., Keller, G.A., and Subramani, S. (1987).** Identification of a Peroxisomal Targeting Signal at the Carboxy Terminus of Firefly Luciferase. *J. Cell Biol.* *105*, 2923-2931.
- Grabowski, B., Cunningham, F.X., Jr., and Gantt, E. (2001).** Chlorophyll and Carotenoid Binding in a Simple Red Algal Light-harvesting Complex Crosses Phylogenetic Lines. *Proc. Natl. Acad. Sci. U. S. A.* *98*, 2911-2916.
- Grabowski, E., Miao, Y., Mulisch, M., and Krupinska, K. (2008).** Single-stranded DNA-binding Protein Whirly1 in Barley Leaves Is Located in Plastids and the Nucleus of the Same Cell. *Plant Physiol.* *147*, 1800-1804.
- Gupta, R.S., Mukhtar, T., and Singh, B. (1999).** Evolutionary Relationships Among Photosynthetic Prokaryotes (*Heliobacterium chlorum*, *Chloroflexus aurantiacus*, Cyanobacteria, *Chlorobium tepidum* and Proteobacteria): Implications Regarding the Origin of Photosynthesis. *Mol. Microbiol.* *32*, 893-906.
- Halpin, C., Elderfield, P.D., James, H.E., Zimmermann, R., Dunbar, B., and Robinson, C. (1989).** The Reaction Specificities of the Thylakoidal Processing Peptidase and *Escherichia coli* Leader Peptidase Are Identical. *EMBO J.* *8*, 3917-3921.
- Harwood, J.L. (1988).** Fatty Acid Metabolism. *Ann. Rev. Plant Physiol. Plant Mol. Biol.* *39*, 101-138.
- Heins, L., Mehrle, A., Hemmler, R., Wagner, R., Kuchler, M., Hormann, F., Sveshnikov, D., and Soll, J. (2002).** The Preprotein Conducting Channel at the Inner Envelope Membrane of Plastids. *EMBO J.* *21*, 2616-2625.
- Hell, K., Herrmann, J.M., Pratje, E., Neupert, W., and Stuart, R.A. (1998).** Oxa1p, an Essential Component of the N-tail Protein Export Machinery in Mitochondria. *Proc. Natl. Acad. Sci. U. S. A.* *95*, 2250-2255.

- Hell, K., Neupert, W., and Stuart, R.A. (2001).** Oxa1p Acts as a General Membrane Insertion Machinery for Proteins Encoded by Mitochondrial DNA. *EMBO J.* 20, 1281-1288.
- Hernandez-Pinzon, I., Ross, J.H., Barnes, K.A., Damant, A.P., and Murphy, D.J. (1999).** Composition and Role of Tapetal Lipid Bodies in the Biogenesis of the Pollen Coat of *Brassica napus*. *Planta* 208, 588-598.
- Highfield, P.E., and Ellis, R.J. (1978).** Synthesis and Transport of the Small Subunit of Chloroplast Ribulose Bisphosphate Carboxylase. *Nature* 271, 420-424.
- Hiltbrunner, A., Grunig, K., Alvarez-Huerta, M., Infanger, S., Bauer, J., and Kessler, F. (2004).** AtToc90, a New GTP-binding Component of the *Arabidopsis* Chloroplast Protein Import Machinery. *Plant Mol. Biol.* 54, 427-440.
- Hinnah, S.C., Hill, K., Wagner, R., Schlicher, T., and Soll, J. (1997).** Reconstitution of a Chloroplast Protein Import Channel. *EMBO J.* 16, 7351-7360.
- Hinnah, S.C., Wagner, R., Sveshnikova, N., Harrer, R., and Soll, J. (2002).** The Chloroplast Protein Import Channel Toc75: Pore Properties and Interaction with Transit Peptides. *Biophys. J.* 83, 899-911.
- Hirabayashi, Y., Kikuchi, S., Oishi, M., and Nakai, M. (2011).** *In vivo* Studies on the Roles of Two Closely Related *Arabidopsis* Tic20 Proteins, AtTic20-I and AtTic20-IV. *Plant Cell Physiol.* 52, 469-478.
- Hirsch, S., Muckel, E., Heemeyer, F., von Heijne, G., and Soll, J. (1994).** A Receptor Component of the Chloroplast Protein Translocation Machinery. *Science* 266, 1989-1992.
- Holsters, M., de Waele, D., Depicker, A., Messens, E., van Montagu, M., and Schell, J. (1978).** Transfection and transformation of *Agrobacterium tumefaciens*. *Mol. Gen. Genet.* 163, 181-187.
- Hou, B., Frielingsdorf, S., and Klosgen, R.B. (2006).** Unassisted Membrane Insertion as the Initial Step in Delta pH/Tat-dependent Protein Transport. *J. Mol. Biol.* 355, 957-967.
- Howden, R., Park, S.K., Moore, J.M., Orme, J., Grossniklaus, U., and Twell, D. (1998).** Selection of T-DNA-tagged Male and Female Gametophytic Mutants by Segregation Distortion in *Arabidopsis*. *Genetics* 149, 621-631.
- Howe, C.J., Barbrook, A.C., Nisbet, R.E., Lockhart, P.J., and Larkum, A.W. (2008).** The Origin of Plastids. *Philos. Trans. R. Soc. Lond. B. Biol. Sci.* 363, 2675-2685.
- Hsu, S.C., Belmonte, M.F., Harada, J.J., and Inoue, K. (2010).** Indispensable Roles of Plastids in *Arabidopsis thaliana* Embryogenesis. *Curr. Genomics* 11, 338-349.
- Hsu, S.C., and Inoue, K. (2009).** Two Evolutionarily Conserved Essential Beta-barrel Proteins in the Chloroplast Outer Envelope Membrane. *Biosci. Trends* 3, 168-178.
- Huang, S., Taylor, N.L., Whelan, J., and Millar, A.H. (2009).** Refining the Definition of Plant Mitochondrial Presequences Through Analysis of Sorting Signals, N-terminal Modifications, and Cleavage Motifs. *Plant Physiol.* 150, 1272-1285.
- Huang, W., Ling, Q., Bedard, J., Lilley, K., and Jarvis, P. (2011).** *In vivo* Analyses of the Roles of Essential Omp85-related Proteins in the Chloroplast Outer Envelope Membrane. *Plant Physiol.* 157, 147-159.
- Hust, B., and Gutensohn, M. (2006).** Deletion of Core Components of the Plastid Protein Import Machinery Causes Differential Arrest of Embryo Development in *Arabidopsis thaliana*. *Plant Biol. (Stuttg.)* 8, 18-30.
- Hutin, C., Havaux, M., Carde, J.P., Kloppstech, K., Meierhoff, K., Hoffman, N., and Nussaume, L. (2002).** Double Mutation cpSRP43--/cpSRP54-- Is Necessary

- to Abolish the cpSRP Pathway Required for Thylakoid Targeting of the Light-harvesting Chlorophyll Proteins. *Plant J.* 29, 531-543.
- Hynds, P.J., Robinson, D., and Robinson, C. (1998).** The Sec-independent Twin-arginine Translocation System Can Transport Both Tightly Folded and Malfolded Proteins across the Thylakoid Membrane. *J. Biol. Chem.* 273, 34868-34874.
- Inaba, T., Alvarez-Huerta, M., Li, M., Bauer, J., Ewers, C., Kessler, F., and Schnell, D.J. (2005).** *Arabidopsis* Tic110 Is Essential for the Assembly and Function of the Protein Import Machinery of Plastids. *The Plant cell* 17, 1482-1496.
- Inaba, T., Li, M., Alvarez-Huerta, M., Kessler, F., and Schnell, D.J. (2003).** atTic110 Functions as a Scaffold for Coordinating the Stromal Events of Protein Import into Chloroplasts. *J. Biol. Chem.* 278, 38617-38627.
- Inaba, T., and Schnell, D.J. (2008).** Protein Trafficking to Plastids: One Theme, Many Variations. *Biochem. J.* 413, 15-28.
- Infanger, S., Bischof, S., Hiltbrunner, A., Agne, B., Baginsky, S., and Kessler, F. (2011).** The Chloroplast Import Receptor Toc90 Partially Restores the Accumulation of Toc159 Client Proteins in the *Arabidopsis thaliana* *ppi2* Mutant. *Mol. Plant* 4, 252-263.
- Inoue, H., and Akita, M. (2008a).** Three Sets of Translocation Intermediates Are Formed During the Early Stage of Protein Import into Chloroplasts. *J. Biol. Chem.* 283, 7491-7502.
- Inoue, H., and Akita, M. (2008b).** The Transition of Early Translocation Intermediates in Chloroplasts Is Accompanied by the Movement of the Targeting Signal on the Precursor Protein. *Arch. Biochem. Biophys.* 477, 232-238.
- Inoue, H., Li, M., and Schnell, D.J. (2013).** An Essential Role for Chloroplast Heat Shock Protein 90 (Hsp90C) in Protein Import into Chloroplasts. *Proc. Natl. Acad. Sci. U. S. A.* 110, 3173-3178.
- Inoue, K., and Potter, D. (2004).** The Chloroplastic Protein Translocation Channel Toc75 and its Paralog OEP80 Represent Two Distinct Protein Families and Are Targeted to the Chloroplastic Outer Envelope by Different Mechanisms. *Plant J.* 39, 354-365.
- Ivanova, Y., Smith, M.D., Chen, K., and Schnell, D.J. (2004).** Members of the Toc159 Import Receptor Family Represent Distinct Pathways for Protein Targeting to Plastids. *Mol. Biol. Cell* 15, 3379-3392.
- Jackson-Constan, D., and Keegstra, K. (2001).** *Arabidopsis* Genes Encoding Components of the Chloroplastic Protein Import Apparatus. *Plant Physiol.* 125, 1567-1576.
- Jackson, D.T., Froehlich, J.E., and Keegstra, K. (1998).** The Hydrophilic Domain of Tic110, an Inner Envelope Membrane Component of the Chloroplastic Protein Translocation Apparatus, Faces the Stromal Compartment. *J. Biol. Chem.* 273, 16583-16588.
- Jarvis, P. (2008).** Targeting of Nucleus-encoded Proteins to Chloroplasts in Plants. *New Phytol.* 179, 257-285.
- Jarvis, P., Chen, L.J., Li, H., Peto, C.A., Fankhauser, C., and Chory, J. (1998).** An *Arabidopsis* Mutant Defective in the Plastid General Protein Import Apparatus. *Science* 282, 100-103.
- Jaynes, M., and Vernon, L. (1982).** The Cyanelle of *Cyanophora paradoxa*: Almost a Cyanobacterial Chloroplast. *Trends in Biochemical Sciences* 7, 22-24.
- Jelic, M., Soll, J., and Schleiff, E. (2003).** Two Toc34 Homologues with Different Properties. *Biochemistry* 42, 5906-5916.

- Jelic, M., Sveshnikova, N., Motzkus, M., Horth, P., Soll, J., and Schleiff, E. (2002).** The Chloroplast Import Receptor Toc34 Functions as Preprotein-regulated GTPase. *Biol. Chem.* 383, 1875-1883.
- Jia, L., Dienhart, M., Schramp, M., McCauley, M., Hell, K., and Stuart, R.A. (2003).** Yeast Oxa1 Interacts with Mitochondrial Ribosomes: the Importance of the C-terminal Region of Oxa1. *EMBO J.* 22, 6438-6447.
- Jia, L., Dienhart, M.K., and Stuart, R.A. (2007).** Oxa1 Directly Interacts with Atp9 and Mediates its Assembly into the Mitochondrial F1Fo-ATP Synthase Complex. *Mol. Biol. Cell* 18, 1897-1908.
- Jiang, F., Yi, L., Moore, M., Chen, M., Rohl, T., Van Wijk, K.J., De Gier, J.W., Henry, R., and Dalbey, R.E. (2002).** Chloroplast YidC Homolog Albino3 Can Functionally Complement the Bacterial YidC Depletion Strain and Promote Membrane Insertion of Both Bacterial and Chloroplast Thylakoid Proteins. *J. Biol. Chem.* 277, 19281-19288.
- Jonas-Straube, E., Hutin, C., Hoffman, N.E., and Schunemann, D. (2001).** Functional Analysis of the Protein-interacting Domains of Chloroplast SRP43. *J. Biol. Chem.* 276, 24654-24660.
- Jordan, P., Fromme, P., Witt, H.T., Klukas, O., Saenger, W., and Krauss, N. (2001).** Three-dimensional Structure of Cyanobacterial Photosystem I at 2.5 Å Resolution. *Nature* 411, 909-917.
- Kalanon, M., and McFadden, G.I. (2008).** The Chloroplast Protein Translocation Complexes of *Chlamydomonas reinhardtii*: a Bioinformatic Comparison of Toc and Tic Components in Plants, Green Algae and Red Algae. *Genetics* 179, 95-112.
- Kalderon, D., Roberts, B.L., Richardson, W.D., and Smith, A.E. (1984).** A Short Amino Acid Sequence Able to Specify Nuclear Location. *Cell* 39, 499-509.
- Karimi, M., De Meyer, B., and Hilson, P. (2005).** Modular Cloning in Plant Cells. *Trends Plant Sci.* 10, 103-105.
- Karimi, M., Inze, D., and Depicker, A. (2002).** GATEWAY Vectors for *Agrobacterium*-mediated Plant Transformation. *Trends Plant Sci.* 7, 193-195.
- Kasmati, A.R., Topel, M., Khan, N.Z., Patel, R., Ling, Q., Karim, S., Aronsson, H., and Jarvis, P. (2013).** Evolutionary, Molecular and Genetic Analyses of Tic22 Homologues in *Arabidopsis thaliana* Chloroplasts. *PloS one* 8, e63863.
- Kasmati, A.R., Topel, M., Patel, R., Murtaza, G., and Jarvis, P. (2011).** Molecular and Genetic Analyses of Tic20 Homologues in *Arabidopsis thaliana* Chloroplasts. *Plant J.* 66, 877-889.
- Keegstra, K., and Cline, K. (1999).** Protein Import and Routing Systems of Chloroplasts. *The Plant cell* 11, 557-570.
- Keeling, P.J. (2010).** The Endosymbiotic Origin, Diversification and Fate of Plastids. *Philos. Trans. R. Soc. Lond. B. Biol. Sci.* 365, 729-748.
- Kessler, F., and Blobel, G. (1996).** Interaction of the Protein Import and Folding Machineries of the Chloroplast. *Proc. Natl. Acad. Sci. U. S. A.* 93, 7684-7689.
- Kessler, F., Blobel, G., Patel, H.A., and Schnell, D.J. (1994).** Identification of two GTP-binding Proteins in the Chloroplast Protein Import Machinery. *Science* 266, 1035-1039.
- Kessler, F., and Schnell, D.J. (2006).** The Function and Diversity of Plastid Protein Import Pathways: a Multilane GTPase Highway into Plastids. *Traffic (Copenhagen, Denmark)* 7, 248-257.
- Kikuchi, S., Bedard, J., Hirano, M., Hirabayashi, Y., Oishi, M., Imai, M., Takase, M., Ide, T., and Nakai, M. (2013).** Uncovering the Protein Translocon at the Chloroplast Inner Envelope Membrane. *Science* 339, 571-574.

- Kikuchi, S., Oishi, M., Hirabayashi, Y., Lee, D.W., Hwang, I., and Nakai, M. (2009).** A 1-Megadalton Translocation Complex Containing Tic20 and Tic21 Mediates Chloroplast Protein Import at the Inner Envelope Membrane. *The Plant cell* *21*, 1781-1797.
- Kleffmann, T., Russenberger, D., von Zychlinski, A., Christopher, W., Sjolander, K., Gruissem, W., and Baginsky, S. (2004).** The *Arabidopsis thaliana* Chloroplast Proteome Reveals Pathway Abundance and Novel Protein Functions. *Curr. Biol.* *14*, 354-362.
- Klimyuk, V.I., Persello-Cartieaux, F., Havaux, M., Contard-David, P., Schuenemann, D., Meierhoff, K., Gouet, P., Jones, J.D., Hoffman, N.E., and Nussaume, L. (1999).** A Chromodomain Protein Encoded by the *Arabidopsis* CAO Gene Is a Plant-specific Component of the Chloroplast Signal Recognition Particle Pathway that Is Involved in LHCP Targeting. *The Plant cell* *11*, 87-99.
- Klosgen, R.B., Brock, I.W., Herrmann, R.G., and Robinson, C. (1992).** Proton Gradient-driven Import of the 16 kDa Oxygen-evolving Complex Protein as the Full Precursor Protein by Isolated Thylakoids. *Plant. Mol. Biol.* *18*, 1031-1034.
- Klostermann, E., Droste Gen Helling, I., Carde, J.P., and Schuenemann, D. (2002).** The Thylakoid Membrane Protein ALB3 Associates with the cpSecY-Translocase in *Arabidopsis thaliana*. *Biochem. J.* *368*, 777-781.
- Ko, K., and Cashmore, A.R. (1989).** Targeting of Proteins to the Thylakoid Lumen by the Bipartite Transit Peptide of the 33 kd Oxygen-evolving Protein. *EMBO J.* *8*, 3187-3194.
- Kobayashi, K., Kondo, M., Fukuda, H., Nishimura, M., and Ohta, H. (2007).** Galactolipid Synthesis in Chloroplast Inner Envelope Is Essential for Proper Thylakoid Biogenesis, Photosynthesis, and Embryogenesis. *Proc. Natl. Acad. Sci. U. S. A.* *104*, 17216-17221.
- Kogata, N., Nishio, K., Hirohashi, T., Kikuchi, S., and Nakai, M. (1999).** Involvement of a Chloroplast Homologue of the Signal Recognition Particle Receptor Protein, FtsY, in Protein Targeting to Thylakoids. *FEBS Lett.* *447*, 329-333.
- Konieczny, A., and Ausubel, F.M. (1993).** A Procedure for Mapping *Arabidopsis* Mutations Using Co-dominant Ecotype-specific PCR-based Markers. *Plant J.* *4*, 403-410.
- Kouranov, A., Chen, X., Fuks, B., and Schnell, D.J. (1998).** Tic20 and Tic22 Are New Components of the Protein Import Apparatus at the Chloroplast Inner Envelope Membrane. *J. Cell Biol.* *143*, 991-1002.
- Kouranov, A., and Schnell, D.J. (1997).** Analysis of the Interactions of Preproteins with the Import Machinery over the Course of Protein Import into Chloroplasts. *J. Cell Biol.* *139*, 1677-1685.
- Kovacheva, S., Bedard, J., Patel, R., Dudley, P., Twell, D., Rios, G., Koncz, C., and Jarvis, P. (2005).** *In vivo* Studies on the Roles of Tic110, Tic40 and Hsp93 During Chloroplast Protein Import. *Plant J.* *41*, 412-428.
- Kovacheva, S., Bedard, J., Wardle, A., Patel, R., and Jarvis, P. (2007).** Further *in vivo* Studies on the Role of the Molecular Chaperone, Hsp93, in Plastid Protein Import. *Plant J.* *50*, 364-379.
- Kovacs-Bogdan, E., Benz, J.P., Soll, J., and Bolter, B. (2011).** Tic20 Forms a Channel Independent of Tic110 in Chloroplasts. *BMC Plant Biol.* *11*, 133.
- Krebs, R.A., and Feder, M.E. (1997).** Deleterious Consequences of Hsp70 Overexpression in *Drosophila melanogaster* Larvae. *Cell stress & chaperones* *2*, 60-71.

- Krimm, I., Gans, P., Hernandez, J.F., Arlaud, G.J., and Lancelin, J.M. (1999).** A Coil-helix Instead of a Helix-coil Motif Can Be Induced in a Chloroplast Transit Peptide from *Chlamydomonas reinhardtii*. *Eur. J. Biochem.* *265*, 171-180.
- Kroll, D., Meierhoff, K., Bechtold, N., Kinoshita, M., Westphal, S., Vothknecht, U.C., Soll, J., and Westhoff, P. (2001).** VIPP1, a Nuclear Gene of *Arabidopsis thaliana* Essential for Thylakoid Membrane Formation. *Proc. Natl. Acad. Sci. U. S. A.* *98*, 4238-4242.
- Kubis, S., Baldwin, A., Patel, R., Razzaq, A., Dupree, P., Lilley, K., Kurth, J., Leister, D., and Jarvis, P. (2003).** The *Arabidopsis ppil* Mutant Is Specifically Defective in the Expression, Chloroplast Import, and Accumulation of Photosynthetic Proteins. *The Plant cell* *15*, 1859-1871.
- Kubis, S., Patel, R., Combe, J., Bedard, J., Kovacheva, S., Lilley, K., Biehl, A., Leister, D., Rios, G., Koncz, C., et al. (2004).** Functional Specialization Amongst the Arabidopsis Toc159 Family of Chloroplast Protein Import Receptors. *The Plant cell* *16*, 2059-2077.
- Kugelmann, M. (2010).** Analyse von *Arabidopsis thaliana* Mutanten mit Defekten im plastidären Protein-Transport. Dissertation.
- Kuhn, A., Stuart, R., Henry, R., and Dalbey, R.E. (2003).** The Alb3/Oxa1/YidC Protein Family: Membrane-localized Chaperones Facilitating Membrane Protein Insertion? *Trends Cell Biol.* *13*, 510-516.
- Laemmli, U.K. (1970).** Cleavage of Structural Proteins During the Assembly of the Head of Bacteriophage T4. *Nature* *227*, 680-685.
- Laidler, V., Chaddock, A.M., Knott, T.G., Walker, D., and Robinson, C. (1995).** A SecY Homolog in *Arabidopsis thaliana*. Sequence of a Full-length cDNA Clone and Import of the Precursor Protein into Chloroplasts. *J. Biol. Chem.* *270*, 17664-17667.
- Lam, H.M., Coschigano, K., Schultz, C., Melo-Oliveira, R., Tjaden, G., Oliveira, I., Ngai, N., Hsieh, M.H., and Coruzzi, G. (1995).** Use of *Arabidopsis* Mutants and Genes to Study Amide Amino Acid Biosynthesis. *The Plant cell* *7*, 887-898.
- Lee, D.W., Lee, S., Lee, G.J., Lee, K.H., Kim, S., Cheong, G.W., and Hwang, I. (2006).** Functional Characterization of Sequence Motifs in the Transit Peptide of *Arabidopsis* Small Subunit of Rubisco. *Plant Physiol.* *140*, 466-483.
- Lee, D.W., Lee, S., Oh, Y.J., and Hwang, I. (2009).** Multiple Sequence Motifs in the Rubisco Small Subunit Transit Peptide Independently Contribute to Toc159-dependent Import of Proteins into Chloroplasts. *Plant Physiol.* *151*, 129-141.
- Lee, E.J., Matsumura, Y., Soga, K., Hoson, T., and Koizumi, N. (2007).** Glycosyl Hydrolases of Cell Wall Are Induced by Sugar Starvation in *Arabidopsis*. *Plant Cell Physiol.* *48*, 405-413.
- Lehenty, E.A., and Theg, S.M. (1994).** Apparent Inhibition of Chloroplast Protein Import by Cold Temperatures Is Due to Energetic Considerations Not Membrane Fluidity. *The Plant cell* *6*, 427-437.
- Leister, D. (2003).** Chloroplast Research in the Genomic Age. *Trends Genet.* *19*, 47-56.
- Leustek, T., and Saito, K. (1999).** Sulfate Transport and Assimilation in Plants. *Plant Physiol.* *120*, 637-644.
- Levy-Rimler, G., Bell, R.E., Ben-Tal, N., and Azem, A. (2002).** Type I Chaperonins: Not All Are Created Equal. *FEBS Lett.* *529*, 1-5.
- Lewis, N.E., Marty, N.J., Kathir, K.M., Rajalingam, D., Kight, A.D., Daily, A., Kumar, T.K., Henry, R.L., and Goforth, R.L. (2010).** A Dynamic cpSRP43-Albino3 Interaction Mediates Translocase Regulation of Chloroplast Signal

- Recognition Particle (cpSRP)-targeting Components. *J. Biol. Chem.* 285, 34220-34230.
- Li, H.M., and Chiu, C.C. (2010).** Protein Transport into Chloroplasts. *Annu. Rev. Plant Biol.* 61, 157-180.
- Li, H.M., and Teng, Y.S. (2013).** Transit Peptide Design and Plastid Import Regulation. *Trends Plant Sci.* 18, 360-366.
- Li, X., Henry, R., Yuan, J., Cline, K., and Hoffman, N.E. (1995).** A Chloroplast Homologue of the Signal Recognition Particle Subunit SRP54 Is Involved in the Posttranslational Integration of a Protein into Thylakoid Membranes. *Proc. Natl. Acad. Sci. U. S. A.* 92, 3789-3793.
- Ling, Q., Huang, W., Baldwin, A., and Jarvis, P. (2012).** Chloroplast biogenesis is regulated by direct action of the ubiquitin-proteasome system. *Science* 338, 655-659.
- Ling, Q., Huang, W., and Jarvis, P. (2011).** Use of a SPAD-502 Meter to Measure Leaf Chlorophyll Concentration in *Arabidopsis thaliana*. *Photosynth. Res.* 107, 209-214.
- Liu, D., Gong, Q., Ma, Y., Li, P., Li, J., Yang, S., Yuan, L., Yu, Y., Pan, D., Xu, F., et al. (2010).** cpSecA, a Thylakoid Protein Translocase Subunit, Is Essential for Photosynthetic Development in *Arabidopsis*. *J. Exp. Bot.* 61, 1655-1669.
- Liu, Z., Yan, H., Wang, K., Kuang, T., Zhang, J., Gui, L., An, X., and Chang, W. (2004).** Crystal Structure of Spinach Major Light-harvesting Complex at 2.72 Å Resolution. *Nature* 428, 287-292.
- Livak, K.J., and Schmittgen, T.D. (2001).** Analysis of Relative Gene Expression Data Using Real-time Quantitative PCR and the  $2^{-\Delta\Delta C(T)}$  Method. *Methods (San Diego, Calif.)* 25, 402-408.
- Long, D., Martin, M., Sundberg, E., Swinburne, J., Puangsomlee, P., and Coupland, G. (1993).** The Maize Transposable Element System Ac/Ds as a Mutagen in *Arabidopsis*: Identification of an Albino Mutation Induced by Ds Insertion. *Proc. Natl. Acad. Sci. U. S. A.* 90, 10370-10374.
- Lopez-Juez, E., and Pyke, K.A. (2005).** Plastids Unleashed: Their Development and Their Integration in Plant Development. *Int. J. Dev. Biol.* 49, 557-577.
- Lubeck, J., Soll, J., Akita, M., Nielsen, E., and Keegstra, K. (1996).** Topology of IEP110, a Component of the Chloroplastic Protein Import Machinery Present in the Inner Envelope Membrane. *EMBO J.* 15, 4230-4238.
- Ma, Y., Kouranov, A., LaSala, S.E., and Schnell, D.J. (1996).** Two Components of the Chloroplast Protein Import Apparatus, IAP86 and IAP75, Interact with the Transit Sequence During the Recognition and Translocation of Precursor Proteins at the Outer Envelope. *J. Cell Biol.* 134, 315-327.
- Margulis, L. (1970).** Origin of Eukaryotic Cells. New Haven, CT: Yale University Press.
- Marin, B., Nowack, E.C., and Melkonian, M. (2005).** A Plastid in the Making: Evidence for a Second Primary Endosymbiosis. *Protist* 156, 425-432.
- Marques, J.P., Schattat, M.H., Hause, G., Dudeck, I., and Klosgen, R.B. (2004).** *In vivo* Transport of Folded EGFP by the Delta pH/TAT-dependent Pathway in Chloroplasts of *Arabidopsis thaliana*. *J. Exp. Bot.* 55, 1697-1706.
- Marshall, J.S., DeRocher, A.E., Keegstra, K., and Vierling, E. (1990).** Identification of Heat Shock Protein Hsp70 Homologues in Chloroplasts. *Proc. Natl. Acad. Sci. U. S. A.* 87, 374-378.
- Martin, W., Rujan, T., Richly, E., Hansen, A., Cornelsen, S., Lins, T., Leister, D., Stoebe, B., Hasegawa, M., and Penny, D. (2002).** Evolutionary Analysis of

- Arabidopsis*, Cyanobacterial, and Chloroplast Genomes Reveals Plastid Phylogeny and Thousands of Cyanobacterial Genes in the Nucleus. Proc. Natl. Acad. Sci. U. S. A. 99, 12246-12251.
- Martoglio, B., and Dobberstein, B. (1998).** Signal Sequences: More than Just Greasy Peptides. Trends Cell Biol. 8, 410-415.
- Marty, N.J., Rajalingam, D., Kight, A.D., Lewis, N.E., Fologea, D., Kumar, T.K., Henry, R.L., and Goforth, R.L. (2009).** The Membrane-binding Motif of the Chloroplast Signal Recognition Particle Receptor (cpFtsY) Regulates GTPase Activity. J. Biol. Chem. 284, 14891-14903.
- Masclaux-Daubresse, C., Daniel-Vedele, F., Dechorgnat, J., Chardon, F., Gaufichon, L., and Suzuki, A. (2010).** Nitrogen Uptake, Assimilation and Remobilization in Plants: Challenges for Sustainable and Productive Agriculture. Ann. Bot. 105, 1141-1157.
- Matilsky, M.B., and Jacobs, W.P. (1983).** Accumulation of Amyloplasts on the Bottom of Normal and Inverted Rhizome Tips of *Caulerpa prolifera* (Forsskål) Lamouroux. Planta 159, 189-192.
- McElver, J., Tzafrir, I., Aux, G., Rogers, R., Ashby, C., Smith, K., Thomas, C., Schetter, A., Zhou, Q., Cushman, M.A., et al. (2001).** Insertional Mutagenesis of Genes Required for Seed Development in *Arabidopsis thaliana*. Genetics 159, 1751-1763.
- McFadden, G.I. (2001).** Chloroplast Origin and Integration. Plant Physiol. 125, 50-53.
- Michl, D., Robinson, C., Shackleton, J.B., Herrmann, R.G., and Klosgen, R.B. (1994).** Targeting of Proteins to the Thylakoids by Bipartite Presequences: C<sub>F</sub>OII Is Imported by a Novel, Third Pathway. EMBO J. 13, 1310-1317.
- Miras, S., Salvi, D., Piette, L., Seigneurin-Berny, D., Grunwald, D., Reinbothe, C., Joyard, J., Reinbothe, S., and Rolland, N. (2007).** Toc159- and Toc75-independent Import of a Transit Sequence-less Precursor into the Inner Envelope of Chloroplasts. J. Biol. Chem. 282, 29482-29492.
- Moberg, P., Stahl, A., Bhushan, S., Wright, S.J., Eriksson, A., Bruce, B.D., and Glaser, E. (2003).** Characterization of a Novel Zinc Metalloprotease Involved in Degrading Targeting Peptides in Mitochondria and Chloroplasts. Plant J. 36, 616-628.
- Moore, M., Goforth, R.L., Mori, H., and Henry, R. (2003).** Functional Interaction of Chloroplast SRP/FtsY with the ALB3 Translocase in Thylakoids: Substrate Not Required. J. Cell Biol. 162, 1245-1254.
- Moore, M., Harrison, M.S., Peterson, E.C., and Henry, R. (2000).** Chloroplast Oxa1p Homolog Albino3 Is Required for Post-translational Integration of the Light Harvesting Chlorophyll-binding Protein into Thylakoid Membranes. J. Biol. Chem. 275, 1529-1532.
- Mori, H., and Cline, K. (2001).** Post-translational Protein Translocation into Thylakoids by the Sec and Delta pH-dependent Pathways. Biochim. Biophys. Acta 1541, 80-90.
- Mori, H., and Cline, K. (2002).** A Twin Arginine Signal Peptide and the pH Gradient Trigger Reversible Assembly of the Thylakoid [Delta]pH/Tat Translocase. J. Cell Biol. 157, 205-210.
- Mori, H., Summer, E.J., Ma, X., and Cline, K. (1999).** Component specificity for the thylakoidal Sec and Delta pH-dependent protein transport pathways. J. Cell Biol. 146, 45-56.
- Morsomme, P., Dambly, S., Maudoux, O., and Boutry, M. (1998).** Single Point Mutations Distributed in 10 Soluble and Membrane Regions of the *Nicotiana*

- plumbaginifolia* Plasma Membrane PMA2 H<sup>+</sup>-ATPase Activate the Enzyme and Modify the Structure of the C-terminal Region. *J. Biol. Chem.* 273, 34837-34842.
- Mould, R.M., and Robinson, C. (1991).** A Proton Gradient Is Required for the Transport of Two Lumenal Oxygen-evolving Proteins across the Thylakoid Membrane. *J. Biol. Chem.* 266, 12189-12193.
- Nada, A., and Soll, J. (2004).** Inner Envelope Protein 32 Is Imported into Chloroplasts by a Novel Pathway. *J. Cell Sci.* 117, 3975-3982.
- Nakai, M., Goto, A., Nohara, T., Sugita, D., and Endo, T. (1994).** Identification of the SecA Protein Homolog in Pea Chloroplasts and its Possible Involvement in Thylakoidal Protein Transport. *J. Biol. Chem.* 269, 31338-31341.
- Nambara, E., and Marion-Poll, A. (2005).** Abscisic Acid Biosynthesis and Catabolism. *Annu. Rev. Plant Biol.* 56, 165-185.
- Nanjo, Y., Oka, H., Ikarashi, N., Kaneko, K., Kitajima, A., Mitsui, T., Munoz, F.J., Rodriguez-Lopez, M., Baroja-Fernandez, E., and Pozueta-Romero, J. (2006).** Rice Plastidial N-Glycosylated Nucleotide Pyrophosphatase/phosphodiesterase Is Transported from the ER-Golgi to the Chloroplast Through the Secretory Pathway. *The Plant cell* 18, 2582-2592.
- Neff, M.M., Neff, J.D., Chory, J., and Pepper, A.E. (1998).** dCAPS, a Simple Technique for the Genetic Analysis of Single Nucleotide Polymorphisms: Experimental Applications in *Arabidopsis thaliana* Genetics. *Plant J.* 14, 387-392.
- Nelson, N., and Ben-Shem, A. (2004).** The Complex Architecture of Oxygenic Photosynthesis. *Nat. Rev. Mol. Cell. Biol.* 5, 971-982.
- Neuhaus, H.E., and Emes, M.J. (2000).** Nonphotosynthetic Metabolism in Plastids. *Annu. Rev. Plant Physiol. Plant Mol. Biol.* 51, 111-140.
- Nielsen, E., Akita, M., Davila-Aponte, J., and Keegstra, K. (1997).** Stable Association of Chloroplastic Precursors with Protein Translocation Complexes that Contain Proteins from Both Envelope Membranes and a Stromal Hsp100 Molecular Chaperone. *EMBO J.* 16, 935-946.
- Nilsson Cederholm, S., Backman, H.G., Pesaresi, P., Leister, D., and Glaser, E. (2009).** Deletion of an Organellar Peptidosome PreP Affects Early Development in *Arabidopsis thaliana*. *Plant Mol. Biol.* 71, 497-508.
- Nilsson, R., Brunner, J., Hoffman, N.E., and van Wijk, K.J. (1999).** Interactions of Ribosome Nascent Chain Complexes of the Chloroplast-encoded D1 Thylakoid Membrane Protein with cpSRP54. *EMBO J.* 18, 733-742.
- Nishiyama, K., Hanada, M., and Tokuda, H. (1994).** Disruption of the Gene Encoding p12 (SecG) Reveals the Direct Involvement and Important Function of SecG in the Protein Translocation of *Escherichia coli* at Low Temperature. *EMBO J.* 13, 3272-3277.
- Nomura, H., Komori, T., Uemura, S., Kanda, Y., Shimotani, K., Nakai, K., Furuichi, T., Takebayashi, K., Sugimoto, T., Sano, S., *et al.* (2012).** Chloroplast-mediated Activation of Plant Immune Signalling in *Arabidopsis*. *Nat. Commun.* 3, 926.
- Obayashi, T., Kinoshita, K., Nakai, K., Shibaoka, M., Hayashi, S., Saeki, M., Shibata, D., Saito, K., and Ohta, H. (2007).** ATTED-II: a Database of Co-expressed Genes and Cis Elements for Identifying Co-regulated Gene Groups in *Arabidopsis*. *Nucleic Acids Res.* 35, D863-869.
- Ohlrogge, J., and Browse, J. (1995).** Lipid Biosynthesis. *The Plant cell* 7, 957-970.
- Olsen, L.J., and Keegstra, K. (1992).** The Binding of Precursor Proteins to Chloroplasts Requires Nucleoside Triphosphates in the Intermembrane Space. *J. Biol. Chem.* 267, 433-439.

- Olsen, L.J., Theg, S.M., Selman, B.R., and Keegstra, K. (1989).** ATP Is Required for the Binding of Precursor Proteins to Chloroplasts. *J. Biol. Chem.* *264*, 6724-6729.
- Oreb, M., Hofle, A., Koenig, P., Sommer, M.S., Sinning, I., Wang, F., Tews, I., Schnell, D.J., and Schleiff, E. (2011).** Substrate Binding Disrupts Dimerization and Induces Nucleotide Exchange of the Chloroplast GTPase Toc33. *Biochem. J.* *436*, 313-319.
- Ossenbuhl, F., Gohre, V., Meurer, J., Krieger-Liszkay, A., Rochaix, J.D., and Eichacker, L.A. (2004).** Efficient Assembly of Photosystem II in *Chlamydomonas reinhardtii* Requires Alb3.1p, a Homolog of *Arabidopsis* ALBINO3. *The Plant cell* *16*, 1790-1800.
- Pal, D., Fite, K., and Dabney-Smith, C. (2013).** Direct Interaction between a Precursor Mature Domain and Transport Component Tha4 During Twin Arginine Transport of Chloroplasts. *Plant Physiol.* *161*, 990-1001.
- Palmieri, L., Picault, N., Arrigoni, R., Besin, E., Palmieri, F., and Hodges, M. (2008).** Molecular Identification of Three *Arabidopsis thaliana* Mitochondrial Dicarboxylate Carrier Isoforms: Organ Distribution, Bacterial Expression, Reconstitution into Liposomes and Functional Characterization. *Biochem. J.* *410*, 621-629.
- Pasch, J.C., Nickelsen, J., and Schunemann, D. (2005).** The Yeast Split-ubiquitin System to Study Chloroplast Membrane Protein Interactions. *Applied microbiology and biotechnology* *69*, 440-447.
- Patel, R., Hsu, S.C., Bedard, J., Inoue, K., and Jarvis, P. (2008).** The Omp85-related Chloroplast Outer Envelope Protein OEP80 Is Essential for Viability in *Arabidopsis*. *Plant Physiol.* *148*, 235-245.
- Perry, S.E., and Keegstra, K. (1994).** Envelope Membrane Proteins that Interact with Chloroplastic Precursor Proteins. *The Plant cell* *6*, 93-105.
- Perry, S.E., Li, H.M., and Keegstra, K. (1991).** *In vitro* Reconstitution of Protein Transport into Chloroplasts. *Methods Cell Biol.* *34*, 327-344.
- Pesaresi, P., Varotto, C., Meurer, J., Jahns, P., Salamini, F., and Leister, D. (2001).** Knock-out of the Plastid Ribosomal Protein L11 in *Arabidopsis*: Effects on mRNA Translation and Photosynthesis. *Plant J.* *27*, 179-189.
- Pfaffl, M.W. (2001).** A New Mathematical Model for Relative Quantification in Real-time RT-PCR. *Nucleic Acids Res.* *29*, e45.
- Pilgrim, M.L., van Wijk, K.J., Parry, D.H., Sy, D.A., and Hoffman, N.E. (1998).** Expression of a Dominant Negative Form of cpSRP54 Inhibits Chloroplast Biogenesis in *Arabidopsis*. *Plant J.* *13*, 177-186.
- Porra, R.J., Thompson, W.A., and Kriedemann, P.E. (1989).** Determination of Accurate Extinction Coefficients and Simultaneous Equations for Assaying Chlorophylls *a* and *b* Extracted with Four Different Solvents: Verification of the Concentration of Chlorophyll Standards by Atomic Absorption Spectroscopy. *Biochim. Biophys. Acta* *975*, 384-394.
- Power, J.B., and Davey, M.R. (1990).** Protoplasts of Higher and Lower Plants : Isolation, Culture, and Fusion. *Methods Mol Biol.* *6*, 237-259.
- Prihoda, J., Tanaka, A., de Paula, W.B., Allen, J.F., Tirichine, L., and Bowler, C. (2012).** Chloroplast-mitochondria Cross-talk in Diatoms. *J. Exp. Bot.* *63*, 1543-1557.
- Qbadou, S., Becker, T., Bionda, T., Reger, K., Ruprecht, M., Soll, J., and Schleiff, E. (2007).** Toc64--a Preprotein-receptor at the Outer Membrane with Bipartite Function. *J. Mol. Biol.* *367*, 1330-1346.

- Radhamony, R.N., and Theg, S.M. (2006).** Evidence for an ER to Golgi to Chloroplast Protein Transport Pathway. *Trends Cell Biol.* *16*, 385-387.
- Rahim, G., Bischof, S., Kessler, F., and Agne, B. (2009).** *In vivo* Interaction between atToc33 and atToc159 GTP-binding Domains Demonstrated in a Plant Split-ubiquitin System. *J. Exp. Bot.* *60*, 257-267.
- Raines, C.A. (2011).** Increasing Photosynthetic Carbon Assimilation in C3 Plants to Improve Crop Yield: Current and Future Strategies. *Plant Physiol.* *155*, 36-42.
- Rassow, J., Dekker, P.J., van Wilpe, S., Meijer, M., and Soll, J. (1999).** The Preprotein Translocase of the Mitochondrial Inner Membrane: Function and Evolution. *J. Mol. Biol.* *286*, 105-120.
- Ratnayake, R.M., Inoue, H., Nonami, H., and Akita, M. (2008).** Alternative Processing of *Arabidopsis* Hsp70 Precursors During Protein Import into Chloroplasts. *Biosci. Biotechnol. Biochem.* *72*, 2926-2935.
- Rawsthorne, S. (2002).** Carbon Flux and Fatty Acid Synthesis in Plants. *Prog. Lipid Res.* *41*, 182-196.
- Reddick, L.E., Vaughn, M.D., Wright, S.J., Campbell, I.M., and Bruce, B.D. (2007).** *In vitro* Comparative Kinetic Analysis of the Chloroplast Toc GTPases. *J. Biol. Chem.* *282*, 11410-11426.
- Rensink, W.A., Schnell, D.J., and Weisbeek, P.J. (2000).** The Transit Sequence of Ferredoxin Contains Different Domains for Translocation across the Outer and Inner Membrane of the Chloroplast Envelope. *J. Biol. Chem.* *275*, 10265-10271.
- Reyes-Prieto, A., and Moustafa, A. (2012).** Plastid-localized Amino Acid Biosynthetic Pathways of Plantae Are Predominantly Composed of Non-cyanobacterial Enzymes. *Sci. Rep.* *2*, 955.
- Reyes-Prieto, A., Weber, A.P., and Bhattacharya, D. (2007).** The Origin and Establishment of the Plastid in Algae and Plants. *Annu. Rev. Genet.* *41*, 147-168.
- Richter, S., and Lamppa, G.K. (1998).** A Chloroplast Processing Enzyme Functions as the General Stromal Processing Peptidase. *Proc. Natl. Acad. Sci. U. S. A.* *95*, 7463-7468.
- Richter, S., and Lamppa, G.K. (1999).** Stromal Processing Peptidase Binds Transit Peptides and Initiates Their ATP-dependent Turnover in Chloroplasts. *J. Cell Biol.* *147*, 33-44.
- Richter, S., and Lamppa, G.K. (2002).** Determinants for Removal and Degradation of Transit Peptides of Chloroplast Precursor Proteins. *J. Biol. Chem.* *277*, 43888-43894.
- Richter, S., and Lamppa, G.K. (2003).** Structural Properties of the Chloroplast Stromal Processing Peptidase Required for its Function in Transit Peptide Removal. *J. Biol. Chem.* *278*, 39497-39502.
- Richter, S., Zhong, R., and Lamppa, G. (2005).** Function of the Stromal Processing Peptidase in the Chloroplast Import Pathway. *Physiol. Plant.* *123*, 362-368.
- Robert, H.S., Quint, A., Brand, D., Vivian-Smith, A., and Offringa, R. (2009).** BTB and TAZ Domain Scaffold Proteins Perform a Crucial Function in *Arabidopsis* Development. *Plant J.* *58*, 109-121.
- Rodriguez, C.M., Freire, M.A., Camilleri, C., and Robaglia, C. (1998).** The *Arabidopsis thaliana* cDNAs Coding for eIF4E and eIF(iso)4E Are Not Functionally Equivalent for Yeast Complementation and Are Differentially Expressed During Plant Development. *Plant J.* *13*, 465-473.
- Roise, D., and Schatz, G. (1988).** Mitochondrial Presequences. *J. Biol. Chem.* *263*, 4509-4511.

- Rosenbaum Hofmann, N., and Theg, S.M. (2005).** Toc64 Is Not Required for Import of Proteins into Chloroplasts in the Moss *Physcomitrella patens*. *Plant J.* *43*, 675-687.
- Row, P.E., and Gray, J.C. (2001).** The Effect of Amino Acid-modifying Reagents on Chloroplast Protein Import and the Formation of Early Import Intermediates. *J. Exp. Bot.* *52*, 57-66.
- Rudhe, C., Clifton, R., Chew, O., Zemam, K., Richter, S., Lamppa, G., Whelan, J., and Glaser, E. (2004).** Processing of the Dual Targeted Precursor Protein of Glutathione Reductase in Mitochondria and Chloroplasts. *J. Mol. Biol.* *343*, 639-647.
- Rudolf, M., Machettira, A.B., Gross, L.E., Weber, K.L., Bolte, K., Bionda, T., Sommer, M.S., Maier, U.G., Weber, A.P., Schleiff, E., et al. (2013).** *In vivo* Function of Tic22, a Protein Import Component of the Intermembrane Space of Chloroplasts. *Mol. Plant* *6*, 817-829.
- Rutschow, H., Ytterberg, A.J., Friso, G., Nilsson, R., and van Wijk, K.J. (2008).** Quantitative Proteomics of a Chloroplast SRP54 Sorting Mutant and its Genetic Interactions with CLPC1 in *Arabidopsis*. *Plant Physiol.* *148*, 156-175.
- Samaniego, R., Jeong, S.Y., Meier, I., and de la Espina, S.M. (2006).** Dual Location of MAR-binding, Filament-like Protein 1 in *Arabidopsis*, Tobacco, and Tomato. *Planta* *223*, 1201-1206.
- Samuelson, J.C., Chen, M., Jiang, F., Moller, I., Wiedmann, M., Kuhn, A., Phillips, G.J., and Dalbey, R.E. (2000).** YidC Mediates Membrane Protein Insertion in Bacteria. *Nature* *406*, 637-641.
- Sanchez-Pulido, L., Devos, D., Genevrois, S., Vicente, M., and Valencia, A. (2003).** POTRA: a Conserved Domain in the FtsQ Family and a Class of Beta-barrel Outer Membrane Proteins. *Trends Biochem. Sci.* *28*, 523-526.
- Sato, S., Nakamura, Y., Kaneko, T., Asamizu, E., and Tabata, S. (1999).** Complete Structure of the Chloroplast Genome of *Arabidopsis thaliana*. *DNA Res.* *6*, 283-290.
- Sauret-Gueto, S., Botella-Pavia, P., Flores-Perez, U., Martinez-Garcia, J.F., San Roman, C., Leon, P., Boronat, A., and Rodriguez-Concepcion, M. (2006).** Plastid Cues Posttranscriptionally Regulate the Accumulation of Key Enzymes of the Methylerythritol Phosphate Pathway in *Arabidopsis*. *Plant Physiol.* *141*, 75-84.
- Schein, A.I., Kissinger, J.C., and Ungar, L.H. (2001).** Chloroplast Transit Peptide Prediction: a Peek Inside the Black Box. *Nucleic Acids Res.* *29*, E82.
- Schirmer, E.C., Glover, J.R., Singer, M.A., and Lindquist, S. (1996).** HSP100/Clp Proteins: a Common Mechanism Explains Diverse Functions. *Trends Biochem. Sci.* *21*, 289-296.
- Schnell, D.J., Blobel, G., Keegstra, K., Kessler, F., Ko, K., and Soll, J. (1997).** A Consensus Nomenclature for the Protein-import Components of the Chloroplast Envelope. *Trends Cell Biol.* *7*, 303-304.
- Schnell, D.J., Kessler, F., and Blobel, G. (1994).** Isolation of Components of the Chloroplast Protein Import Machinery. *Science* *266*, 1007-1012.
- Schopf, J.W. (1993).** Microfossils of the Early Archean Apex Chert: New Evidence of the Antiquity of Life. *Science* *260*, 640-646.
- Schuenemann, D., Amin, P., Hartmann, E., and Hoffman, N.E. (1999a).** Chloroplast SecY Is Complexed to SecE and Involved in the Translocation of the 33-kDa but Not the 23-kDa Subunit of the Oxygen-evolving Complex. *J. Biol. Chem.* *274*, 12177-12182.

- Schuenemann, D., Amin, P., and Hoffman, N.E. (1999b).** Functional Divergence of the Plastid and Cytosolic Forms of the 54-kDa Subunit of Signal Recognition Particle. *Biochem. Biophys. Res. Commun.* 254, 253-258.
- Schuenemann, D., Gupta, S., Persello-Cartieaux, F., Klimyuk, V.I., Jones, J.D., Nussaume, L., and Hoffman, N.E. (1998).** A Novel Signal Recognition Particle Targets Light-harvesting Proteins to the Thylakoid Membranes. *Proc. Natl. Acad. Sci. U. S. A.* 95, 10312-10316.
- Scotti, P.A., Urbanus, M.L., Brunner, J., de Gier, J.W., von Heijne, G., van der Does, C., Driessen, A.J., Oudega, B., and Luirink, J. (2000).** YidC, the *Escherichia coli* Homologue of Mitochondrial Oxa1p, Is a Component of the Sec Translocase. *EMBO J.* 19, 542-549.
- Seedorf, M., Waegemann, K., and Soll, J. (1995).** A Constituent of the Chloroplast Import Complex Represents a New Type of GTP-binding Protein. *Plant J.* 7, 401-411.
- Serek, J., Bauer-Manz, G., Struhalla, G., van den Berg, L., Kiefer, D., Dalbey, R., and Kuhn, A. (2004).** *Escherichia coli* YidC Is a Membrane Insertase for Sec-independent Proteins. *EMBO J.* 23, 294-301.
- Sessions, A., Burke, E., Presting, G., Aux, G., McElver, J., Patton, D., Dietrich, B., Ho, P., Bacwaden, J., Ko, C., et al. (2002).** A High-throughput *Arabidopsis* Reverse Genetics System. *The Plant cell* 14, 2985-2994.
- Shang, Y., Yan, L., Liu, Z.Q., Cao, Z., Mei, C., Xin, Q., Wu, F.Q., Wang, X.F., Du, S.Y., Jiang, T., et al. (2010).** The Mg-Chelatase H Subunit of *Arabidopsis* Antagonizes a Group of WRKY Transcription Repressors to Relieve ABA-Responsive Genes of Inhibition. *The Plant cell* 22, 1909-1935.
- Shanklin, J., DeWitt, N.D., and Flanagan, J.M. (1995).** The Stroma of Higher Plant Plastids Contain ClpP and ClpC, Functional Homologs of *Escherichia coli* ClpP and ClpA: an Archetypal Two-component ATP-dependent Protease. *The Plant cell* 7, 1713-1722.
- Shi, L.X., and Theg, S.M. (2010).** A Stromal Heat Shock Protein 70 System Functions in Protein Import into Chloroplasts in the Moss *Physcomitrella patens*. *The Plant cell* 22, 205-220.
- Singh, N.D., Li, M., Lee, S.B., Schnell, D., and Daniell, H. (2008).** *Arabidopsis* Tic40 Expression in Tobacco Chloroplasts Results in Massive Proliferation of the Inner Envelope Membrane and Upregulation of Associated Proteins. *The Plant cell* 20, 3405-3417.
- Sivaraja, V., Kumar, T.K., Leena, P.S., Chang, A.N., Vidya, C., Goforth, R.L., Rajalingam, D., Arvind, K., Ye, J.L., Chou, J., et al. (2005).** Three-dimensional Solution Structures of the Chromodomains of cpSRP43. *J. Biol. Chem.* 280, 41465-41471.
- Skalitzky, C.A., Martin, J.R., Harwood, J.H., Beirne, J.J., Adamczyk, B.J., Heck, G.R., Cline, K., and Fernandez, D.E. (2011).** Plastids Contain a Second Sec Translocase System with Essential Functions. *Plant Physiol.* 155, 354-369.
- Smeekens, S., Bauerle, C., Hageman, J., Keegstra, K., and Weisbeek, P. (1986).** The Role of the Transit Peptide in the Routing of Precursors Toward Different Chloroplast Compartments. *Cell* 46, 365-375.
- Smith, M.D., Hiltbrunner, A., Kessler, F., and Schnell, D.J. (2002).** The Targeting of the atToc159 Preprotein Receptor to the Chloroplast Outer Membrane Is Mediated by its GTPase Domain and Is Regulated by GTP. *J. Cell Biol.* 159, 833-843.

- Smith, M.D., Rounds, C.M., Wang, F., Chen, K., Afithile, M., and Schnell, D.J. (2004).** atToc159 Is a Selective Transit Peptide Receptor for the Import of Nucleus-encoded Chloroplast Proteins. *J. Cell Biol.* *165*, 323-334.
- Sohrt, K., and Soll, J. (2000).** Toc64, a New Component of the Protein Translocon of Chloroplasts. *J. Cell Biol.* *148*, 1213-1221.
- Soll, J., and Schleiff, E. (2004).** Protein Import into Chloroplasts. *Nat. Rev. Mol. Cell Biol.* *5*, 198-208.
- Sommer, M., Rudolf, M., Tillmann, B., Tripp, J., Sommer, M.S., and Schleiff, E. (2013).** Toc33 and Toc64-III Cooperate in Precursor Protein Import into the Chloroplasts of *Arabidopsis thaliana*. *Plant Cell Environ.* *36*, 970-983.
- Spence, E., Bailey, S., Nenninger, A., Moller, S.G., and Robinson, C. (2004).** A Homolog of Albino3/Oxa1 Is Essential for Thylakoid Biogenesis in the Cyanobacterium *Synechocystis* sp. PCC6803. *J. Biol. Chem.* *279*, 55792-55800.
- Spencer, M.W., Casson, S.A., and Lindsey, K. (2007).** Transcriptional Profiling of the *Arabidopsis* Embryo. *Plant Physiol.* *143*, 924-940.
- Stahl, T., Glockmann, C., Soll, J., and Heins, L. (1999).** Tic40, a New "Old" Subunit of the Chloroplast Protein Import Translocon. *J. Biol. Chem.* *274*, 37467-37472.
- Stanga, J.P., Boonsirichai, K., Sedbrook, J.C., Otegui, M.S., and Masson, P.H. (2009).** A Role for the TOC Complex in *Arabidopsis* Root Gravitropism. *Plant Physiol.* *149*, 1896-1905.
- Su, P.H., and Li, H.M. (2008).** *Arabidopsis* Stromal 70-kD Heat Shock Proteins Are Essential for Plant Development and Important for Thermotolerance of Germinating Seeds. *Plant Physiol.* *146*, 1231-1241.
- Su, P.H., and Li, H.M. (2010).** Stromal Hsp70 Is Important for Protein Translocation into Pea and *Arabidopsis* Chloroplasts. *The Plant cell* *22*, 1516-1531.
- Sun, Q., Emanuelsson, O., and van Wijk, K.J. (2004).** Analysis of Curated and Predicted Plastid Subproteomes of *Arabidopsis*. Subcellular Compartmentalization Leads to Distinctive Proteome Properties. *Plant Physiol.* *135*, 723-734.
- Sun, Y.J., Forouhar, F., Li Hm, H.M., Tu, S.L., Yeh, Y.H., Kao, S., Shr, H.L., Chou, C.C., Chen, C., and Hsiao, C.D. (2002).** Crystal Structure of Pea Toc34, a Novel GTPase of the Chloroplast Protein Translocon. *Nat. Struct. Biol.* *9*, 95-100.
- Sundberg, E., Slagter, J.G., Fridborg, I., Cleary, S.P., Robinson, C., and Coupland, G. (1997).** ALBINO3, an *Arabidopsis* Nuclear Gene Essential for Chloroplast Differentiation, Encodes a Chloroplast Protein that Shows Homology to Proteins Present in Bacterial Membranes and Yeast Mitochondria. *The Plant cell* *9*, 717-730.
- Sveshnikova, N., Soll, J., and Schleiff, E. (2000).** Toc34 Is a Preprotein Receptor Regulated by GTP and Phosphorylation. *Proc. Natl. Acad. Sci. U. S. A.* *97*, 4973-4978.
- Swinkels, B.W., Gould, S.J., Bodnar, A.G., Rachubinski, R.A., and Subramani, S. (1991).** A Novel, Cleavable Peroxisomal Targeting Signal at the Amino-terminus of the Rat 3-Ketoacyl-CoA Thiolase. *EMBO J.* *10*, 3255-3262.
- Szyrach, G., Ott, M., Bonnefoy, N., Neupert, W., and Herrmann, J.M. (2003).** Ribosome Binding to the Oxa1 Complex Facilitates Co-translational Protein Insertion in Mitochondria. *EMBO J.* *22*, 6448-6457.
- Tamura, T., and Akutsu, T. (2007).** Subcellular Location Prediction of Proteins Using Support Vector Machines with Alignment of Block Sequences Utilizing Amino Acid Composition. *BMC bioinformatics* *8*, 466.

- Tanz, S.K., Castleden, I., Hooper, C.M., Vacher, M., Small, I., and Millar, H.A. (2013).** SUBA3: a Database for Integrating Experimentation and Prediction to Define the SUBcellular Location of Proteins in *Arabidopsis*. *Nucleic Acids Res.* *41*, D1185-1191.
- Teixeira, P.F., and Glaser, E. (2013).** Processing Peptidases in Mitochondria and Chloroplasts. *Biochim. Biophys. Acta* *1833*, 360-370.
- Teng, Y.S., Su, Y.S., Chen, L.J., Lee, Y.J., Hwang, I., and Li, H.M. (2006).** Tic21 Is an Essential Translocon Component for Protein Translocation across the Chloroplast Inner Envelope Membrane. *The Plant cell* *18*, 2247-2257.
- Thines, B., Katsir, L., Melotto, M., Niu, Y., Mandaokar, A., Liu, G., Nomura, K., He, S.Y., Howe, G.A., and Browse, J. (2007).** JAZ Repressor Proteins Are Targets of the SCF(COI1) Complex During Jasmonate Signalling. *Nature* *448*, 661-665.
- Timmis, J.N., Ayliffe, M.A., Huang, C.Y., and Martin, W. (2004).** Endosymbiotic Gene Transfer: Organelle Genomes Forge Eukaryotic Chromosomes. *Nat. Rev. Genet.* *5*, 123-135.
- Tranel, P.J., Froehlich, J., Goyal, A., and Keegstra, K. (1995).** A Component of the Chloroplastic Protein Import Apparatus Is Targeted to the Outer Envelope Membrane via a Novel Pathway. *EMBO J.* *14*, 2436-2446.
- Tripp, J., Hahn, A., Koenig, P., Flinner, N., Bublak, D., Brouwer, E.M., Ertel, F., Mirus, O., Sinning, I., Tews, I., *et al.* (2012).** Structure and Conservation of the Periplasmic Targeting Factor Tic22 Protein From Plants and Cyanobacteria. *J. Biol. Chem.* *287*, 24164-24173.
- Tsai, J.Y., Chu, C.C., Yeh, Y.H., Chen, L.J., Li, H.M., and Hsiao, C.D. (2013).** Structural Characterizations of the Chloroplast Translocon Protein Tic110. *Plant J.*
- Tsakazaki, T., Mori, H., Echizen, Y., Ishitani, R., Fukai, S., Tanaka, T., Perederina, A., Vassilyev, D.G., Kohno, T., Maturana, A.D., *et al.* (2011).** Structure and Function of a Membrane Component SecDF that Enhances Protein Export. *Nature* *474*, 235-238.
- Tu, C.J., Peterson, E.C., Henry, R., and Hoffman, N.E. (2000).** The L18 Domain of Light-harvesting Chlorophyll Proteins Binds to Chloroplast Signal Recognition Particle 43. *J. Biol. Chem.* *275*, 13187-13190.
- Tu, C.J., Schuenemann, D., and Hoffman, N.E. (1999).** Chloroplast FtsY, Chloroplast Signal Recognition Particle, and GTP Are Required to Reconstitute the Soluble Phase of Light-harvesting Chlorophyll Protein Transport into Thylakoid Membranes. *J. Biol. Chem.* *274*, 27219-27224.
- Tu, S.L., Chen, L.J., Smith, M.D., Su, Y.S., Schnell, D.J., and Li, H.M. (2004).** Import Pathways of Chloroplast Interior Proteins and the Outer-membrane Protein OEP14 Converge at Toc75. *The Plant cell* *16*, 2078-2088.
- Tzfira, T., Tian, G.W., Lacroix, B., Vyas, S., Li, J., Leitner-Dagan, Y., Krichevsky, A., Taylor, T., Vainstein, A., and Citovsky, V. (2005).** pSAT Vectors: a Modular Series of Plasmids for Autofluorescent Protein Tagging and Expression of Multiple Genes in Plants. *Plant molecular biology* *57*, 503-516.
- Tzvetkova-Chevolleau, T., Hutin, C., Noel, L.D., Goforth, R., Carde, J.P., Caffarri, S., Sinning, I., Groves, M., Teulon, J.M., Hoffman, N.E., *et al.* (2007).** Canonical Signal Recognition Particle Components Can Be Bypassed for Posttranslational Protein Targeting in Chloroplasts. *The Plant cell* *19*, 1635-1648.
- van der Laan, M., Bechtluft, P., Kol, S., Nouwen, N., and Driessen, A.J. (2004).** F1F0 ATP Synthase Subunit c Is a Substrate of the Novel YidC Pathway for Membrane Protein Biogenesis. *J. Cell Biol.* *165*, 213-222.

- Van Ree, K., Gehl, B., Chehab, E.W., Tsai, Y.C., and Braam, J. (2011).** Nitric Oxide Accumulation in *Arabidopsis* Is Independent of NOA1 in the Presence of Sucrose. *Plant J.* 68, 225-233.
- VanderVere, P.S., Bennett, T.M., Oblong, J.E., and Lamppa, G.K. (1995).** A Chloroplast Processing Enzyme Involved in Precursor Maturation Shares a Zinc-binding Motif with a Recently Recognized Family of Metalloendopeptidases. *Proc. Natl. Acad. Sci. U. S. A.* 92, 7177-7181.
- Vickers, C.E., Gershenzon, J., Lerdau, M.T., and Loreto, F. (2009).** A Unified Mechanism of Action for Volatile Isoprenoids in Plant Abiotic Stress. *Nat. Chem. Biol.* 5, 283-291.
- Villarejo, A., Buren, S., Larsson, S., Dejardin, A., Monne, M., Rudhe, C., Karlsson, J., Jansson, S., Lerouge, P., Rolland, N., et al. (2005).** Evidence for a Protein Transported Through the Secretory Pathway *en route* to the Higher Plant Chloroplast. *Nat. Cell Biol.* 7, 1224-1231.
- Vojta, A., Alavi, M., Becker, T., Hormann, F., Kuchler, M., Soll, J., Thomson, R., and Schleiff, E. (2004).** The Protein Translocon of the Plastid Envelopes. *J. Biol. Chem.* 279, 21401-21405.
- von Heijne, G., and Nishikawa, K. (1991).** Chloroplast Transit Peptides. The Perfect Random Coil? *FEBS Lett.* 278, 1-3.
- von Heijne, G., Steppuhn, J., and Herrmann, R.G. (1989).** Domain Structure of Mitochondrial and Chloroplast Targeting Peptides. *Eur. J. Biochem.* 180, 535-545.
- Waegemann, K., and Soll, J. (1991).** Characterization of the Protein Import Apparatus in Isolated Outer Envelopes of Chloroplast. *Plant J.* 1, 149-159.
- Wallas, T.R., Smith, M.D., Sanchez-Nieto, S., and Schnell, D.J. (2003).** The Roles of Toc34 and Toc75 in Targeting the Toc159 Preprotein Receptor to Chloroplasts. *J. Biol. Chem.* 278, 44289-44297.
- Wan, J., Bringloe, D., and Lamppa, G. (1998).** Disruption of Chloroplast Biogenesis and Plant Development upon Down-regulation of a Chloroplast Processing Enzyme Involved in the Import Pathway. *Plant J.* 15, 459-468.
- Wang, Z., and Benning, C. (2012).** Chloroplast Lipid Synthesis and Lipid Trafficking Through ER-Plastid Membrane Contact Sites. *Biochem. Soc. Trans.* 40, 457-463.
- Ward, A.C. (1992).** Rapid Analysis of Yeast Transformants Using Colony-PCR. *BioTechniques* 13, 350.
- Weibel, P., Hiltbrunner, A., Brand, L., and Kessler, F. (2003).** Dimerization of Toc-GTPases at the Chloroplast Protein Import Machinery. *J. Biol. Chem.* 278, 37321-37329.
- Weigel, D., and Glazebrook, J. (2006).** Transformation of *Agrobacterium* Using the Freeze-thaw Method. *CSH Protoc.* 2006.
- Weiss, C., Bonshtien, A., Farchi-Pisanty, O., Vitlin, A., and Azem, A. (2009).** Cpn20: Siamese Twins of the Chaperonin World. *Plant Mol. Biol.* 69, 227-238.
- Weiss, J.B., Ray, P.H., and Bassford, P.J., Jr. (1988).** Purified SecB Protein of *Escherichia coli* Retards Folding and Promotes Membrane Translocation of the Maltose-binding Protein *in vitro*. *Proc. Natl. Acad. Sci. U. S. A.* 85, 8978-8982.
- Whatley, J.M., John, P., and Whatley, F.R. (1979).** From Extracellular to Intracellular: the Establishment of Mitochondria and Chloroplasts. *Proc. R. Soc. Lond. B. Biol. Sci.* 204, 165-187.
- Wiedemann, N., Frazier, A.E., and Pfanner, N. (2004).** The Protein Import Machinery of Mitochondria. *J. Biol. Chem.* 279, 14473-14476.

- Wienk, H.L., Wechselberger, R.W., Czisch, M., and de Kruijff, B. (2000).** Structure, Dynamics, and Insertion of a Chloroplast Targeting Peptide in Mixed Micelles. *Biochemistry* 39, 8219-8227.
- Winter, D., Vinegar, B., Nahal, H., Ammar, R., Wilson, G.V., and Provart, N.J. (2007).** An "Electronic Fluorescent Pictograph" Browser for Exploring and Analyzing Large-scale Biological Data Sets. *PloS one* 2, e718.
- Wolfe, G.R., Cunningham, F.X., Durnfordt, D., Green, B.R., and Gantt, E. (1994).** Evidence for a Common Origin of Chloroplasts with Light-harvesting Complexes of Different Pigmentation. *Nature* 367, 566-568.
- Woolhead, C.A., Thompson, S.J., Moore, M., Tissier, C., Mant, A., Rodger, A., Henry, R., and Robinson, C. (2001).** Distinct Albino3-dependent and -independent Pathways for Thylakoid Membrane Protein Insertion. *J. Biol. Chem.* 276, 40841-40846.
- Wu, C., Seibert, F.S., and Ko, K. (1994).** Identification of Chloroplast Envelope Proteins in Close Physical Proximity to a Partially Translocated Chimeric Precursor Protein. *J. Biol. Chem.* 269, 32264-32271.
- Wu, F.H., Shen, S.C., Lee, L.Y., Lee, S.H., Chan, M.T., and Lin, C.S. (2009).** Tape-*Arabidopsis* Sandwich - a Simpler *Arabidopsis* Protoplast Isolation Method. *Plant methods* 5, 16.
- Yang, Z., Tian, L., Latoszek-Green, M., Brown, D., and Wu, K. (2005).** *Arabidopsis* ERF4 Is a Transcriptional Repressor Capable of Modulating Ethylene and Abscisic Acid Responses. *Plant Mol. Biol.* 58, 585-596.
- Yeh, Y.H., Kesavulu, M.M., Li, H.M., Wu, S.Z., Sun, Y.J., Konozy, E.H., and Hsiao, C.D. (2007).** Dimerization Is Important for the GTPase Activity of Chloroplast Translocon Components atToc33 and psToc159. *J. Biol. Chem.* 282, 13845-13853.
- Yi, L., and Dalbey, R.E. (2005).** Oxal/Alb3/YidC System for Insertion of Membrane Proteins in Mitochondria, Chloroplasts and Bacteria (Review). *Mol. Membr. Biol.* 22, 101-111.
- Young, M.E., Keegstra, K., and Froehlich, J.E. (1999).** GTP Promotes the Formation of Early-import Intermediates but Is Not Required During the Translocation Step of Protein Import into Chloroplasts. *Plant Physiol.* 121, 237-244.
- Yu, B., Gruber, M.Y., Khachatourians, G.G., Zhou, R., Epp, D.J., Hegedus, D.D., Parkin, I.A., Welsch, R., and Hannoufa, A. (2012).** *Arabidopsis* cpSRP54 Regulates Carotenoid Accumulation in *Arabidopsis* and *Brassica napus*. *J. Exp. Bot.* 63, 5189-5202.
- Yuan, J., Henry, R., McCaffery, M., and Cline, K. (1994).** SecA Homolog in Protein Transport within Chloroplasts: Evidence for Endosymbiont-derived Sorting. *Science* 266, 796-798.
- Yue, R., Wang, X., Chen, J., Ma, X., Zhang, H., Mao, C., and Wu, P. (2010).** A Rice Stromal Processing Peptidase Regulates Chloroplast and Root Development. *Plant Cell Physiol.* 51, 475-485.
- Zeeman, S.C., Smith, S.M., and Smith, A.M. (2007).** The Diurnal Metabolism of Leaf Starch. *Biochem J.* 401, 13-28.
- Zhang, L., and Aro, E.M. (2002).** Synthesis, Membrane Insertion and Assembly of the Chloroplast-encoded D1 Protein into Photosystem II. *FEBS Lett.* 512, 13-18.
- Zhong, R., Wan, J., Jin, R., and Lamppa, G. (2003).** A Pea Antisense Gene for the Chloroplast Stromal Processing Peptidase Yields Seedling Lethals in *Arabidopsis*: Survivors Show Defective GFP Import *in vivo*. *Plant J.* 34, 802-812.

**Zrenner, R., Stitt, M., Sonnewald, U., and Boldt, R. (2006).** Pyrimidine and Purine Biosynthesis and Degradation in Plants. *Annu. Rev. Plant Biol.* 57, 805-836.